ЖУРНАЛ
ПРИКЛАДНОЙ ХИМИИ

Vol. 31 No. 3

March 1958

JOURNAL OF
APPLIED CHEMISTRY
OF THE USSR

(ZHURNAL PRIKLADNOI KHIMII)

IN ENGLISH TRANSLATION

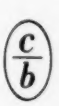

CONSULTANTS BUREAU, INC.

Chemistry Collections

IN ENGLISH TRANSLATION

Consultants Bureau's chemistry collections, a unique venture in the translation-publishing field, consist of articles on specialized subjects, culled by specialists in each field, from Soviet chemical journals published in translation by CB. These collections are then presented in symposium form.

Periodically we shall issue new collections taken from the latest issues of our journals, not only on subjects already covered but also on those which prove most valuable to current scientific research. The following is one of the most recent additions to our list of collections (information on forthcoming titles available on request).

SOVIET RESEARCH IN FUSED SALTS (1956)

42 papers taken from the following Soviet chemistry journals, 1956: Soviet Journal of Atomic Energy; Journal of General Chemistry; Journal of Applied Chemistry; Bulletin of the Academy of Sciences, USSR, Division of Chemical Sciences; Proceedings of the Academy of Sciences, USSR, Chemistry Section. The entire collection consists of one volume, in two section:

I Systems (23 papers)	$30.00
II Electrochemistry: Aluminum and Magnesium, Corrosion, Theoretical; Thermodynamics, Slags, Mattes (19 papers)	20.00
THE COMPLETE COLLECTION	$40.00

also available in translation . . .

SOVIET RESEARCH IN FUSED SALTS (1949-55)

125 papers taken from the following Soviet chemistry journals, 1949-55: Journal of General Chemistry; Journal of Applied Chemistry; Bulletin of Academy of Sciences, USSR, Div. Chemical Sciences; Journal of Analytical Chemistry. Sections of this collection may be purchased separately as follows:

Structure and Properties (100 papers)	$110.00
Electrochemistry (8 papers)	20.00
Thermodynamics (6 papers)	15.00
Slags and Mattes (6 papers)	15.00
General (5 papers)	12.50
THE COMPLETE COLLECTION	$150.00

NOTE: Individual papers from each of the above collections are available at $7.50 each. Tables of contents sent upon request.

CB collections are translated by bilingual scientists, and include all photographic, diagrammatic and tabular material integral with the text. Reproduction is by multilith process from "cold" type; books are staple bound in durable paper covers.

CONSULTANTS BUREAU, INC.

227 WEST 17TH STREET, NEW YORK 11, N. Y

Vol. 31 No. 3

March 1958

JOURNAL OF
APPLIED CHEMISTRY
OF THE USSR

(ZHURNAL PRIKLADNOI KHIMII)

A publication of the Academy of Sciences of the USSR

IN ENGLISH TRANSLATION

Year and issue of first translation:
vol. 23, no. 1 January 1950

	U. S. and Canada	*Foreign*
Annual subscription	*$60.00*	*$65.00*
Annual subscription for libraries of non-profit academic institutions	*20.00*	*25.00*
Single issue	*7.50*	*7.50*

Copyright 1959

CONSULTANTS BUREAU INC.
227 W. 17th ST., NEW YORK 11, N. Y.

Editorial Board
(ZHURNAL PRIKLADNOI KHIMII)

P.P. Budnikov, S.I. Vol'fkovich, A.F. Dobrianskii,
O.E. Zviagintsev, N.I. Nikitin (Editor in Chief),
G.V. Pigulevskii, M.E. Pozin, L.K. Simonova
(Secretary), S.N. Ushakov, N.P. Fedot'ev

NOTE: The sale of photostatic copies of any portion of this copyright translation is expressly prohibited by the copyright owners.

Printed in the United States

JOURNAL OF APPLIED CHEMISTRY OF THE USSR

Volume 31, No. 3 March, 1958

CONTENTS

CONTENTS (continued)

THE CHLORINE METHOD FOR THE COMPOSITE TREATMENT OF SILICATE ORES OF METALS OF THE IRON GROUP

D. P. Bogatskii and G. G. Urazov

H. S. Kurnakov Institute of General and Inorganic Chemistry Academy of Sciences USSR

In previous investigations [1-5] the experimental and theoretical bases of new methods for the composite chemical-metallurgical treatment and concentration of polymetallic iron ores were developed.

The object of the present investigation was to resolve the problem, of great importance to industry, whether it is possible, in principle, to subject silicate-oxide polymetallic iron ores to efficient composite chemical processing according to a system proposed as a result of the experimental and theoretical investigation of processes for the direct reduction and chlorination of nickelous oxide and garnierite [6, 7]. The tasks of the investigation also included the determination of the principal optimum conditions for the technology of carrying out oxidation – reduction processes on an intensified scale by this new system. Since it is of particular importance for industry to resolve the problem of finding efficient methods of concentrating and treating uncleaned waste silicate-oxide iron-nickel-cobalt ores, attention was mainly devoted to studying the possibility and effective use of the proposed method for treating these particular waste ores which are not normally utilized. Waste silicate-oxide ore of the type which cannot be cleaned by existing industrial methods was supplied by industry for the purpose of the investigations.

Numerous experiments were carried out to study the relationship between the intensity of the proposed process of reductive chlorination, the degree of volatilization and condensation of extractable valuable metals and also their behavior in this process and the following basic technical factors: 1) the temperature of the chlorination process, 2) its duration, 3) the consumption of reducing agent, 4) the influence of activators and other alternative conditions reducing the temperature of the investigated process. In addition, experiments were made to show the fundamental possibility of condensing distilled chlorides and obtaining oxide concentrates from them by various methods. The conditions for the experimental investigation of the process of the chlorination of the ore from the point of view of its intensity in regard to apparatus were identical with the conditions for investigating the chlorination process of nickelous oxide and garnierite [6, 7]. Special installations, shown diagrammatically in Fig. 1 and 2, were used for carrying out these investigations by the method of chlorination with condensation of the chlorides on an enlarged laboratory scale.

The principal results of the investigations carried out are characterized by the graphical data given in Fig. 3-9. The reduction of the nickel content in the waste ore during its chlorination is represented by the lower curves and the reduction of the iron content by the upper curves in Fig. 3-5. The degree of chlorination of the nickel of the investigated waste ore during its chlorination is characterized by the curves in the upper part of Fig. 6 and 7 while the lower part of these graphs show curves representing the variation of the degree of chlorination of the iron of the same ore in relationship to the conditions of the chlorination process.

The experimental data obtained in the investigation of the process of chlorination of the investigated difficultly-cleanable waste ore show the considerably high efficiency of this process compared to chlorination roasting of the same ore in the temperature region of 300-600°. As follows from the data given, the chlorination of this ore by the proposed method proceeds without any difficulties, practically all the nickel being converted into chloride, which is completely volatilized under the appropriate conditions. Under the conditions of practically complete extraction of nickel the degree of chlorination of iron is also fairly high (as much as 90-96%).

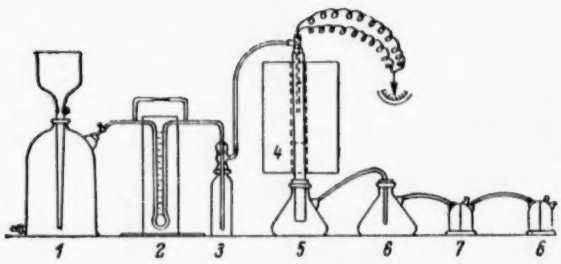

Fig. 1. Diagram of the installation for the chlorination of ore with composite condensation of the chlorides. 1) Gas holder; 2) rheometer; 3) Drexel bottle with concentrated sulfuric acid; 4) electric oven; 5) and 6) condensers; 7) and 8) Tishchenko bottles with caustic soda solution used for reference purposes.

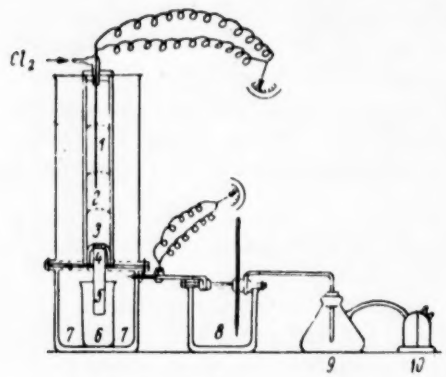

Fig. 2. Diagram of the installation for the chlorination of ore with selective condensation of the chlorides. 1)-5) Points at which check samples were taken for analysis; 4)-8) points at which check samples of the condensates were taken for analysis; 6)-9) condensers; 10) Tishchenko reference bottle with caustic soda solution.

Specially conducted experiments on an enlarged laboratory scale showed that in this process the cobalt is almost completely extracted from the ore. A high extraction of valuable metals is also obtained under the appropriate conditions independently of the degree of crushing of the ore within the investigated limits (from 100 to 6 mesh). The proposed process under the investigated conditions is very highly efficient and intensive independently of the degree of crushing of the ore; this ensures that its practical application soon produces good results as regards maximum yields in the extraction of the metals even when difficulty-cleanable waste ores are treated.

An investigation of the influence of various conditions for the chlorination process on its efficiency, carried out to obtain the maximum reduction of the temperature of the process, showed that the temperature could be reduced to 700° and the consumption of low-grade coal fines to 5% of the weight of treated ore without reducing the extraction of the nickel and without increasing the duration of the process. A favorable influence on the chlorination process in this respect was obtained by the use of carbon tetrachloride and a pyrite-carbon filter as activators of the process and also the introduction of other sulfides (particularly pyrite) into the charge undergoing chlorination. The use of carbon tetrachloride as an activator is a practical step because this chemical can be obtained fairly readily from industrial and natural gases containing methane and other hydrocarbons. Where the processes of direct reduction of the ore and its chlorination take place in the same apparatus the use of this activator can take place directly in the process of reduction and chlorination, which increases its activating influence still further. The influence of sulfur chloride vapor in gaseous chlorine on the intensity of the chlorination process was studied at the same time as the investigation of the activating influence of carbon tetrachloride vapor. Despite the fact that sulfur chloride is obtained as a by-product in the production of carbon tetrachloride, i.e., that both these activators can be produced simultaneously thus lowering their cost, other more simple means of obtaining them were also employed. Since sulfur chloride is formed by the action of gaseous chlorine on metallic sulfides the introduction of the vapor of this activator in gaseous chlorine was carried out by passing it through a pyrite-carbon filter heated to various temperatures in a tubular oven. Chlorination experiments were also carried out in which the sulfur chloride vapor was obtained directly in the reaction zone by introducing pyrite into the ore to be chlorinated. This has more practical significance from the industrial point of view if cobalt-containing pyrite tailings from preparation plants are used as the sulfur-containing addition agent for the ore undergoing chlorination. In this case the process of obtaining the activator is combined with the extraction of the cobalt from the pyrite tailings; this considerably increases the efficiency and economy of the process. Although the degree of chlorination of the nickel is almost complete at a temperature of 700° complete distillation of the nickel chloride at this temperature is far from being always obtainable. The optimum temperature of the process must, therefore, be taken as 800°.

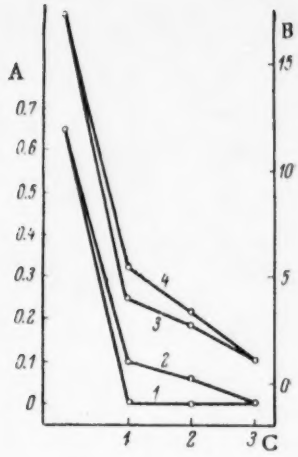

Fig. 3. Reduction of the Ni and Fe content during the process of chlorination of the ore. Degree of crushing of the ore 100 mesh. A) Reduction of the Ni content (as %); B) reduction of the Fe content (as %); C) time (in hours). 1,2) Nickel, 3,4) iron. Temperature (in °C). 1,3) 900; 2,4) 800.

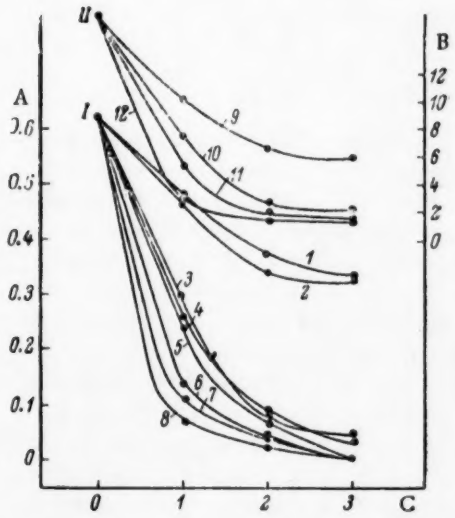

Fig. 5. Reduction of the Ni and Fe content during the process of chlorination of waste Khalilov ore in relationship to the temperature and duration of the process. Degree of crushing of the ore – 35, 10 and 6 mesh. A) Reduction of the Ni content (as %). B) reduction of the Fe content (as %). C) time (in hours). I) Nickel, II) iron. Temperature (as °C) and degree of crushing (mesh), respectively: 1) 700, 10; 2) 700, 35; 3) 800, 35; 4) 800, 10; 5) 800, 6; 6) 900, 6; 7) 900, 10; 8) 900, 35; 9) 700, 10; 10) 800, 6; 11) 800, 10; 12) 900, 10.

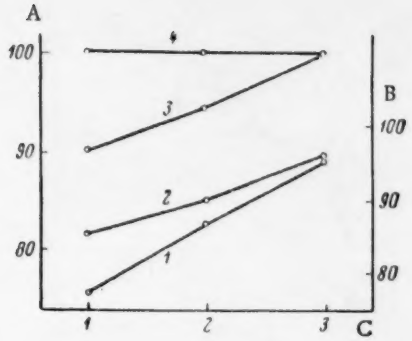

Fig. 4. Relationship between the degree of chlorination of Ni and Fe and the duration of the process. Degree of crushing of the ore 100 mesh. A) Degree of chlorination of Ni (as %); B) degree of chlorination of Fe (as %); C) time (in hours). 1,2) Iron, 3,4) nickel. Temperature (in °C): 1,3) 800; 2,4) 900.

The investigations carried out showed not only the practical possibility of the complete distillation of nickel, cobalt and iron chlorides from the ore but also that there were no essential difficulties in condensing them. This justifies the conclusion that there would also be no real difficulties with regard to the nature of the apparatus for this process. The practical realization of the process of fractional selective condensation of distilled chlorides was, as shown by the investigation, rather more difficult. Being quite insufficiently studied, this problem is under investigation and will, therefore, not be dealt with here. Nevertheless, qualitative investigations carried out have already made it possible to condense the nickel chloride and nickel-cobalt concentrates separately, and these are then converted to the oxides.

The oxide concentrates were obtained by hydrometallurgical and pyrometallurgical methods. The hydrometallurgical preparation of oxide nickel-cobalt concentrates consisted in the precipitation of the corresponding hydroxides from solutions of the chlorides under conditions studied in detail by other investigators [8, 9]. Solutions of caustic soda and milk of lime were used to precipitate the hydroxides from the solutions of the chlorides obtained. The use of caustic soda is of practical value because it is produced as a by-product in the production of chlorine; this production should be organized at plants producing nickel and cobalt either by our proposed method or by existing methods. The use of milk of lime as a precipitation agent for hydroxides is also due to the extensive possibilities of its practical employment. An original method was used for the pyrometallurgical preparation of oxide nickel-cobalt concentrates from their chloride condensates.

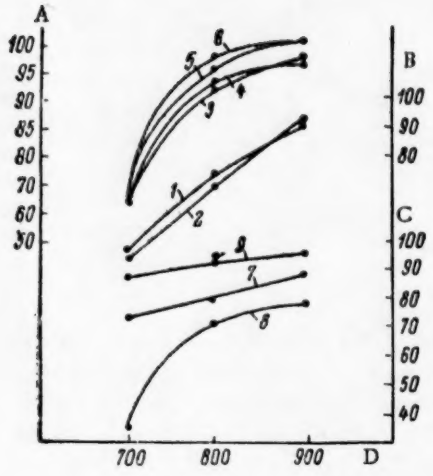

Fig. 6. Relationship between the degree of chlorination of waste Khalilov ore and the temperature of the process. Degree of crushing of the ore 35 and 10 mesh. A) Degree of chlorination of nickel (as %); B) degree of chlorination of nickel in 1 hour (as %); C) degree of chlorination of iron (as %); D) temperature (°C). Time (in hours) and degree of crushing (mesh), respectively: 1) 1, 10; 2) 1, 35; 3) 2, 10; 4) 2, 35; 5) 3, 10; 6) 3, 35; 7) 1, 10; 8) 1, 35; 9) 3, 35.

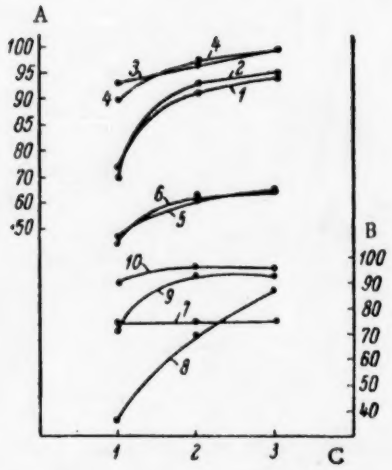

Fig. 7. Relationship between the degree of chlorination of waste Khalilov ore and the duration of the process. Degree of crushing of the ore 35 and 10 mesh. A) Degree of chlorination of Ni (as %); B) degree of chlorination of Fe (as %); C) time (in hours). Temperature (°C) and degree of crushing (mesh), respec- 1) 800, 10; 2) 800, 35; 3) 900, 10; 4) 900, 35; 5) 700, 10; 6) 700, 35; 7) 700, 10; 8) 700, 35; 9) 800, 35; 10) 900, 10.

To ensure maximum simplicity and economy a process was proposed and investigated for the oxidative roasting of chloride nickel-cobalt condensates in air. As was shown by the results of the investigations carried out, complete oxidation of the chloride condensate in air was obtained in a period of 5-6 hours at a temperature of 500° and in 3-4 hours at a temperature of 550°. As a result of the experiments made on the hydrometallurgical and pyrometallurgical preparation of oxide nickel-cobalt concentrates from their chloride concentrates it was established that these processes are practical possibilities and can be carried out very simply. Oxide nickel-cobalt concentrates which contained 12.02 -34.85% nickel, 0.70-4.82% cobalt and 2.73-32.12% iron were obtained from the chloride nickel-cobalt condensates containing 5.85-8.35% nickel, 0.44-0.78% cobalt, 12.63-18.93% iron, 1.97-3.52% chromium and 0.35-0.58% manganese prepared by the chlorination of the investigated waste ore. From the point of view of the nickel and cobalt contents the oxide nickel-cobalt concentrates can by no means be considered as optimum values because of the quite inadequate study of this problem. Their nickel and cobalt contents can be very substantially increased by the distillation of the iron chloride, the practical possibility of which we have proven experimentally. Virtually complete distillation of iron chloride from the nickel-cobalt chloride condensates is obtained by roasting the nickel-cobalt condensate to be refined for 3-5 hours in a current of chlorine at temperatures of 350-400°. As a result of the distillation of iron chloride from nickel-cobalt chloride condensates under these conditions their nickel content was increased from 5.35 to 7.14-8.15% and their cobalt content from 0.44 to 0.77%. These very approximate qualitative data show that the practical application of the process of chlorine refining of nickel-cobalt condensates, which is undergoing closer investigation is, in principle, possible and easy.

The investigations carried out showed that the proposed method for the chemical-metallurgical treatment of lean and waste silicate-oxide iron-nickel-cobalt ores by reducing and chlorinating them at the same place and time is an extremely efficient and very intensive composite process which ensures the almost complete extraction of iron, nickel, cobalt and other valuable metals from these ores. Under optimum conditions for the

proposed process the degree of chlorination of the iron, nickel and cobalt is 100%. In the investigations carried out almost complete extraction of the iron, nickel and cobalt was already obtained at a temperature from 700 to 850-900° even in the case of difficultly-cleanable waste silicate ore. The optimum duration of this process (which is also a sufficient one) is the retention of the ore undergoing reduction and chlorination for 3 hours under the above-mentioned temperature conditions. Under these conditions practically all the iron, nickel, and cobalt chlorides are readily distilled from the treated ore. The complete possibility of the composite and fractional condensation of the distilled chlorides was experimentally proven. A collective nickel-cobalt chloride concentrate was obtained with a nickel content of 5.85% and a cobalt content of 0.44%. The degree of concentration of nickel in the nickel-cobalt chloride concentrate obtained was 9.3, the degree of concentration of cobalt being 17.6. A selective nickel chloride concentrate, containing 31.21% nickel, was obtained, corresponding to a degree of concentration of nickel of 49.5. The detailed study of the behavior of iron and nickel during the process of the chlorination of the investigated difficultly-cleanable waste silicate-oxide nickel ore by the proposed method showed that the degree of chlorination of the iron and nickel varies in a certain direct proportion with the temperature and duration of the process within the investigated limits. Practically complete extraction of nickel during the process of chlorination of the investigated difficultly-cleanable waste ore was obtained at temperatures of 700, 800 and 900°. The necessary duration of the chlorination process to give practically complete extraction of the nickel from this ore varies in a certain inverse proportion with the temperature of the process. Practically complete extraction of the nickel from the investigated ore is obtained with a duration of 1 to 3 hours for the process, depending on the other conditions under which the process is carried out. The necessary temperature and duration of the chlorination process for the practically complete extraction of the nickel from the ore vary in a certain inverse proportion with the composition of the carbon reducing agent under the investigated conditions. It is sufficient to use an amount of low-grade anthracite fines corresponding to 5 to 7% of the weight of the investigated difficultly-cleanable waste ore, depending on other conditions for carrying out the chlorination process. Practically complete extraction of the nickel from the ore during the chlorination process is obtained irrespective of its degree of crushing. Under the investigated conditions no clearly expressed law governing the relationship between the extraction of the nickel and the degree of crushing of the ore was established. The necessary temperature and duration of the chlorination process for the complete chlorination of the nickel vary in a rather poorly expressed inverse proportion with the degree of crushing of the ore within the investigated limits. The investigated influence of different activators on the intensity of the chlorination process indicates methods for its further simplification and intensification as a result of the reduction of the temperature and duration of this process. In particular, in this connection the possibility and advantages of the secondary efficient treatment of pyrite cobalt-containing tailings and other sulfide materials by the proposed method are shown. The technological conditions for the complete distillation of the iron, nickel and cobalt were established; after this the ore, completely chlorinated under the investigated conditions, is waste and does not receive any further treatment, thus resulting in the greater simplicity of the developed method of treatment. The possibility of obtaining oxide nickel-cobalt concentrates by the proposed method was experimentally checked, practically complete extraction of the nickel and cobalt being obtained by the precipitation of these concentrates from the corresponding solutions. In consequence, the extraction of valuable metals in the oxide concentrate practically determines their degree of chlorination and, therefore, the degree of their extraction from the ore during the process of reductive chlorination. The nickel content in the oxide nickel concentrates obtained was raised to 34.85% and their iron content increased from 2.73 to 8.23%. The degree of concentration of the nickel in these oxide concentrates was 55. The cobalt content in the oxide nickel-cobalt concentrates was raised to 4.82% and could be increased still further. The degree of concentration of the cobalt in these oxide concentrates is 188-192. The principal conditions for carrying out the proposed process of pyrometallic preparation of oxide nickel-cobalt concentrates were approximately established. Oxide nickel-cobalt concentrates were obtained by the oxidative roasting of nickel-cobalt chloride concentrates at a temperature of 500° for 5-6 hours. The nickel content in the oxide nickel-cobalt concentrates obtained from the difficultly-cleanable waste ore by the pyrometallurgical method was raised to 12.0-13.15% and could be still further increased by the methods indicated. The degree of concentration of the nickel attained in the oxide nickel-cobalt concentrates prepared by the pyrometallurgical method varies from 19 to 21.

The electrolytic precipitation of valuable metals from chloride solutions [10] with secondary generation of chlorine is more technically efficient than chemical-metallurgical concentration; it ensures the composite preparation of high-grade metals from lean and waste silicate-oxide iron-nickel-cobalt ores.

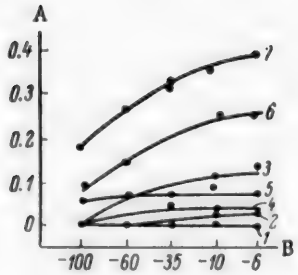

Fig. 8. Reduction of the Ni content in the ore during the process of chlorination in relationship to the degree of crushing of the ore. A) Ni content (as %), B) degree of crushing (mesh). Temperature (in °C) and time (in hours), respectively: 1) 900, 3; 2) 900, 2; 3) 900, 1; 4) 800, 3; 5) 800, 2; 6) 800, 1; 7) 700, 3.

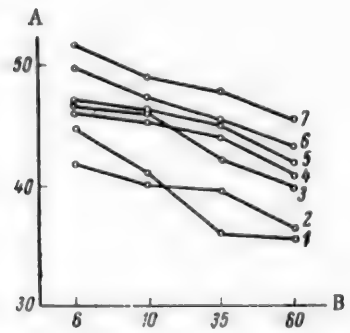

Fig. 9. Relationship between the loss in weight of the charge and the conditions of the chlorination process. A) Loss in weight Δ (as %), B) degree of crushing (mesh). Temperature (in °C) and time (in hours), respectively: 1) 700, 3; 2) 800, 1; 3) 900, 1; 4) 800, 2; 5) 800, 3; 6) 900, 2; 7) 900, 3.

As a result of the investigations carried out the substantial technical and economic advantages of the process developed for the composite chemical treatment and concentration of polymetallic iron ores may be considered as proven, namely: 1) a higher extraction of valuable metals from the ore and a higher efficiency of the process with respect to time than the methods used at Ural plants; 2) the intrinsically composite character of the proposed process and the possibility of the extraction of other metals in addition to iron, nickel and cobalt; 3) it is more simple and compact in comparison with existing industrial systems for the extraction of nickel and cobalt; 4) the applicability of the process for waste silicate-oxide iron-nickel-cobalt ores, not utilized at present because of the absence of an efficient method for concentrating and treating them.

SUMMARY

1. The composite chemical treatment of silicate-oxide polymetallic iron ores by the oxidative-reductive method developed is perfectly possible, rational and of satisfactory efficiency.

2. Even when used for difficultly-cleanable waste (nonprocessed) ores the proposed method is more efficient than existing industrial systems for the partial extraction of nickel and cobalt from richer ores with the loss of the total iron contained in the processed ores.

3. The technological system developed for the proposed process is far more simple, compact and profitable than existing industrial systems for the treatment of richer ores.

4. The use of the process developed for the composite treatment of rich (conditioned) ores allows still higher technical and economic results to be obtained.

5. The proposed method for the reductive-oxidative chlorination of polymetallic iron ores ensures not only the effective composite treatment of lean ores but also the possibility of efficient chemical preparation and treatment of waste and difficultly-cleanable iron-nickel-cobalt ores, not normally utilized because of the absence of sufficiently efficient and profitable methods for cleaning and treating them.

In conclusion the authors wish to express their sincere thanks to I. I. Cherniaev, M. A. Pavlov, I. P. Bardin, I. N. Plaksin, A. A. Zadik'lan, A. A. Mironov, L. G. Berg, G. S. Gritsaenko, Iu. V. Baimakov, V. A. Vaniukov and I. S. Morozov for their active participation in organizing and carrying out our work, for reviewing it and discussing it in the scientific councils of IONKh and the Institute of Metallurgy Academy of Sciences USSR and also in the technical council of MTsM USSR.

LITERATURE CITED

[1] D. P. Bogatskii, Bull. Acad. Sci. USSR, Div. Tech. Sci. 5, 272 (1944).

[2] D. P. Bogatskii, Bull. Acad. Sci. USSR, Div. Tech. Sci. 6, 891 (1946); 12, 1809 (1946).

[3] D. P. Bogatskii, Bull. Acad. Sci. USSR, Div. Tech. Sci. 10, 1512 (1949).

[4] D. P. Bogatskii and G. G. Urazov, Bull. Acad. Sci. USSR, Div. Tech. Sci. 3, 108 (1955).

[5] G. G. Urazov and D. P. Bogatskii, Bull. Acad. Sci. USSR, Div. Chem. Sci. 10 (1956).*

[6] D. P. Bogatskii, Proc. Acad. Sci. USSR, 45, 2, 65 (1944).

[7] D. P. Bogatskii, J. Appl. Chem. 17, 6, 346 (1944).

[8] I. N. Plaksin and D. M. Iukhtanov, Hydrometallurgy (1949).**

[9] A. S. Garnak, Hydrometallurgy of Nickel Ores (1935).**

[10] D. P. Bogatskii and G. G. Urazov, J. Appl. Chem. 31, 2, 203 (1958).*

Received January 12, 1957

*Original Russian pagination. See C. B. Translation.

**In Russian.

THE STABILITY OF THE MINERALS OF PORTLAND CEMENT IN WATER AND SOLUTIONS OF SULFURIC ACID AND CAUSTIC SODA

N. A. Moshchanskii

The different stability of the minerals of Portland cement clinker in water has frequently been the subject of indirect investigations [1]; this problem was, however, only directly studied comparatively recently by Shestoperov and Liubimova [2]. It was established, in particular, that one of the most essential components of Portland cement clinker, tricalcium aluminate, is completely unstable.

The behavior of monomineral cements in solutions of acids and alkalis has, however, been little studied.

The rapid disintegration of mortars and concretes, made from Portland cement, in acid water is well known and is explained by the reaction of the acid with the liberated lime. As a result of this process the calcium hydroxide, which forms the structural element of the cement brick, breaks up and is converted into a softened mass of one of the calcium salts: gypsum if acted on by sulfuric acid, calcium chloride if acted on by hydrochloric acid, etc. It is, however, not adequately explained why these particular salts, which in other instances serve as structural inclusions, lead to the complete decomposition of the cement brick even in weakly-acid water (pH $\cong$ 1 – 4). The calcium salts formed in this instance can evidently only form very porous systems, incapable of setting, in the presence of excess water.

The microscopic character of the formations themselves in this instance has been little studied. The mechanism of the reaction of the aluminates of the cement clinker with acids is also completely unstudied.

Very contradictory data also exist on the problem of the influence of alkaline water on Portland cement. For example, some authoritative foreign authors [3, 4] completely deny the influence of alkalis on cement, while other authors such as Dorsh [5] note a considerable aggressive action of alkaline water on mortars made from Portland cement.

The Soviet investigators of this problem, Budkinov [6], Grigor'ev [7, 8] and Moskvin [9] noted an aggressive action of alkaline solutions on Portland cement brick and concrete. It was assumed that the alkalis can react primarily on the siliceous inclusions of the silicates.

In 1954-1955 we carried out a comprehensive investigation of the action of alkalis on different structural materials with a silicate and aluminosilicate basis and, in particular, on specially synthesized minerals of Portland cement clinker.

The synthesized minerals $3CaO \cdot SiO_2$ (C_3S), $2CaO \cdot SiO_2$ (C_2S), $3CaO \cdot Al_2O_3$ (C_3A), $4CaO \cdot Al_2O_3 \cdot Fe_2O_3$ (C_4AF) were obtained by repeated roasting, carried out by V. V. Koltunova. Table 1 gives the principal data on the chemical composition and stability of the minerals in cement brick. The stability of the mineral cements was determined by tests on compressed 3 cm cubes, one month old.

The minerals obtained were mixed with water until a plastic cement solution was obtained.

The plastic mixtures were placed in the molds of small prisms, 1 × 1 × 3 cm in dimension, they were compacted by means of a shaker and were placed together with the molds over water in desiccators for 2 days. The samples were then freed from the molds and were again kept over water in desiccators for 2 weeks, after which they were immersed in water, a 30% solution of caustic soda and a 1% solution of sulfuric acid.

TABLE 1

Chemical Analysis of Synthesized Minerals of Portland Cement and Their Strength as Shown by the Compression of a Cement Brick, One Month Old (Data of V. V. Koltunova)

Name of mineral / strength (in kg/sq. cm)	Data	Composition (as %)						
		SiO_2	Al_2O_3	Fe_2O_3	CaO	MgO	SO_3	loss on roasting
C_3S	1	26.31	—	—	73.69	—	—	—
566	2	24.4	2.45	0.45	72.5	Traces	Traces	0.87
C_2S	1	34.88	—	—	65.12	—	—	—
83	2	34.3	1.6	0.38	63.8	Traces	Traces	0.33
C_3A	1	—	37.73	—	62.27	—	—	—
57	2	0.72	36.12	0.69	60.14	0.50	0.42	0.63
C_4AF	1	—	20.98	32.86	46.16	—	—	—
135	2	0.02	21.24	32.24	45.6	0.82	0.84	0.14

• 1 — Theoretical data, 2 — analytical data.

The water and the solutions were not changed during the period the samples were kept. The samples were examined periodically once a week and in some cases were photographed; after 1-2 months part of the samples were tested for bending strength.

TABLE 2

Variation of the Strength and Stability of Small Prisms of Monomineral Cements

Expt. No.	Mineral	Medium	Bending strength (in kg/sq. cm)		External appearance of the samples after keeping for	
			30 days	60 days	30 days	60 days
1	C_3S	Water	73.4	79.5	Unchanged	Unchanged
2	C_3S	30% NaOH solution	75.0	83.0	Slight chipping, the surface becomes greasy	Same as after 30 days
3	C_3S	1% H_2SO_4 solution	(56)	—	Considerable swelling	Strong swelling and disintegration
4	C_2S	Water	15.3	22.1	Unchanged	Unchanged
5	C_2S	30% NaOH solution	43.5	50.7	Precipitate formed, the surface becomes greasy (more than No. 2)	Decomposition intensified (see Fig. 2)
6	C_2S	1% H_2SO_4 solution	-	—	Swelling and peeling	Disintegrated but less than No. 3
7	C_3A	Water	9.1	(5)	Unchanged, becomes slightly greasy	Colored
8	C_3A	30% NaOH solution	9.1	—	Flaking at the edges	Crumbled to a powder
9	C_3A	1% H_2SO_4 solution		-	Strong swelling and cracks	—
10	C_4AF	Water	29.0	34.2	Unchanged	Unchanged
11	C_4AF	30% NaOH solution	9.1	(5)	The surface becomes greasy	Slightly colored. Easily broken by hand

After the samples had been kept for 3 months the composition of the solutions was analyzed chemically and they were examined by means of the electron microscope. For this purpose the extracts were further diluted with water 30-50 times. The solutions, applied to a film, were dehydrated in a desiccator over calcium chloride and soda lime (to absorb CO_2). The preparations were examined under a magnification of 5200.

The results of the tests on the bending strength after retention in liquids for 1 and 2 months and the results of the visual examination of the samples are given in Table 2 and also in Fig. 1 and 2. The results of the chemical analysis of the solutions are given in Table 3 and the results of the microscopic examinations in Table 4 and Fig. 3.

TABLE 3

Chemical Composition of the Liquids After Samples of the Minerals of Portland Cement had been Kept in Them

Mineral	Medium in which the samples were kept*	Content of oxides in the liquids (in mg/liter)		
		SiO_2	R_2O_3	CaO
C_3S	Alkali	1230	100	27
	Water	24	20	490
	Acid	96	20	868
C_2S	Alkali	1350	240	27
	Water	132	40	55
C_3A	Alkali	52	1330	88
	Water	12	40	25
	Acid	22	1690	82
C_4AF	Alkali	104	1020	88
	Water	16	140	2750

*Alkali – 30% NaOH solution, acid – 1% H_2SO_4 solution.

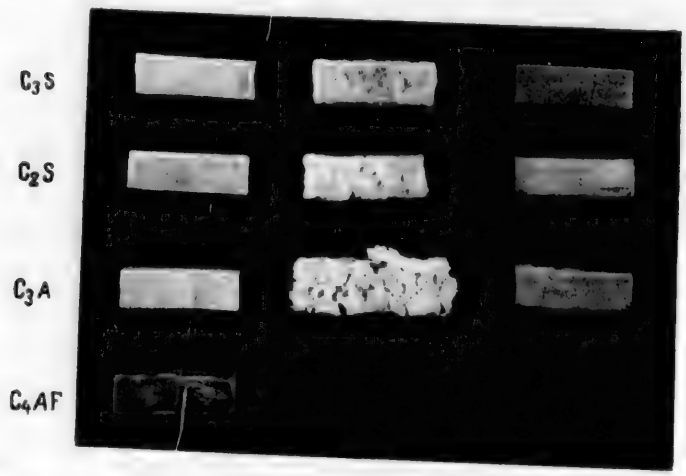

Fig. 1. Microphotographs of small prisms of monomineral cements after retention in water, 30% NaOH and 1% H_2SO_4.

TABLE 4

Description of Electron Microscope Pictures Obtained from Observations of Extracts After Keeping Samples of Monomineral Cements in Them for 3 Months

Name of minerals	Medium		
	30% caustic soda solution	water	1% sulfuric acid solution
C_3S	Sparsely distributed, poorly-shaped formations in the form of spherulites and brushes	Fairly densely distributed. Spherulites of calcium hydroxide and parallelepipeds of calcium carbonate visible.	Very densely distributed. At high dilution many well-shaped crystals of gypsum.
C_2S	More densely distributed than for C_3S. Formations in the form of spherulites with a nucleus and minute accumulations of amorphous particles	Sparsely distributed, but fairly distinct accumulations (concretions) of poorly-shaped particles	Preparations not examined
C_3A	Many large lenticular particles with an aureole and finer, better-shaped particles with an aureole	Dense accumulation of amorphous spheroidal formations	Many well-shaped crystals of gypsum and more fine needles (probably aluminum hydrosulfate). Fine rhomboid crystals also visible
C_4AF	Dense distribution of characteristic spherulites of lime and still more of star-shaped particles	Spherulites of calcium hydroxide and still more parallelepipeds of calcium carbonate are present	Preparations not examined

Retention of nearly all the samples in water up to 2 months strengthened them without any modification of their external appearance or the presence of decomposed particles. Samples of tricalcium aluminate form an exception. Although undamaged as regards their external appearance, the samples had a low strength of the order of 9 kg/cm^2 after they had been kept for one month, and this further decreased by the end of 2 months (the samples were easily broken by hand).

All this again confirms the fact that tricalcium aluminate is by nature an inclusion in Portland cement, which is unstable in water.

As is usually assumed to be the case, dicalcium silicate showed the highest rate of increase of the strength in water, although its absolute strength value was not great.

Chemical analysis of the water above the samples shows the presence of considerable amounts of calcium oxide for C_3S and especially for C_4AF, which is explained by the hydrolysis of these compounds with splitting off of lime; this is also confirmed by the electron microscope determinations. The amount of calcium oxide over C_4AF is even excessively high; this is not fully understandable. The amount of silica and sesquioxides present in the water is relatively small for all the minerals but a considerable number of poorly formed spherulites were noted for C_3A in the electron microscope.

The action of acidic water (1% solution of sulfuric acid) was found to be aggressive for all the minerals, but to a different extent.

The maximum disintegrations in the form of marked fissuration and swelling after keeping for only 3-4 weeks were found in the case of samples of tricalcium aluminate, whereas samples of tri- and dicalcium silicates retained their form (Fig. 1) and had a certain strength. In this connection the concentration of the acid, i.e., after keeping for 2 months, was reduced in the desiccator with samples of C_3S from 10 to 8.4 g/liter, and in the desiccator with samples of C_2S from 10 to 6.0 g/liter.

Fig. 2. Microphotograph of C_2S cement after keeping in 30% caustic soda solution.

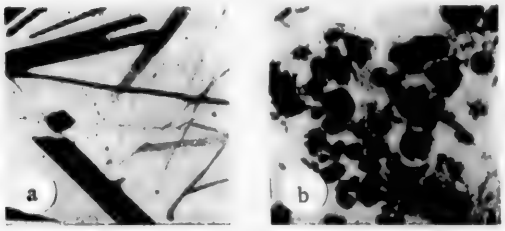

Fig. 3. Electron microscope pictures obtained from the observation of extracts after the samples of cements had been kept in them for 3 months.

The surface of the samples was covered with a layer of firm gypsum. This suggests, therefore, that a new conclusion should be drawn regarding the cause of the low resistance of cement brick to acids (with regard to rate of disintegration), i.e., that this is due to tricalcium aluminate rather than silicates (C_4AF was not tested in H_2SO_4).

The basicity of the silicates evidently also does not play a substantial role in their resistance to acids.

All these considerations, however, require confirmation.

Chemical analysis of the acid solution above the samples shows a high yield of calcium for C_3S and the electron microscope analysis shows that in this instance the calcium is mainly present as gypsum. The analysis of the acid over C_3A shows an increased amount of calcium and, in particular, many sesquioxides (aluminates). The needles of various character visible in the electron microscope must evidently be mainly included in the hydrosulfoaluminate and a relatively small amount of calcium makes it possible to convert it to the low-sulfate form.

The behavior of monomineral cements in a concentrated solution of caustic soda is rather unusual. As in other media, rapid and intensive disintegrations in alkaline solutions with a marked fall in the strength were found for all the samples of tricalcium aluminate. The alkali also acts intensely, however, on tetracalcium aluminoferrite, which is contradictory to Grigor'ev's data [8]. In this connection, after keeping for 5-6 weeks samples from C_3A crumbled to powder, whereas samples from C_4AF still retained their shape to some extent. In a solution of alkali the strength of the samples from C_4AF falls sharply and progressively (Table 2).

After keeping for 1 and 2 months in 30% caustic soda solution the samples from C_3S retained their shape well and showed increased strength even with respect to the standard sample in water, although it was also characterized by a slight disintegration from the surface (the latter becomes greasy and a precipitate is deposited in the solution).

This particular phenomenon – surface decomposition with increased strength – is still more characteristic for samples from C_2S (Fig. 2). In this instance the strength increased from 1 to 2 months exposure by 13% (from 43.5 to 50.7 kg/sq.cm), by 2.5-3 times (from 15.3 to 43.5 kg/sq.cm) compared with the standards in water. There is justification for assuming, however, that with longer exposure to alkalis the strength of calcium silicates would fall.

The fact that the solution of caustic soda reacts with the samples from C_2S is, however, completely evident from the external appearance (Fig. 2) and also from the analysis of the chemical and electron microscope data.

These data indicate considerable precipitations of silica from C_3S and still more from C_2S in the solution, with a small amount of sesquioxides (evidently from mineral impurities). Heavy precipitates of sesquioxides and slight precipitates of silica are characteristic for C_3A and C_4AF (from mineral impurities and possibly from the reaction of the caustic soda solution with the glass of the desiccator).

The electron microscope observations show a low density of coverage (especially for C_3S) of the preparations by amorphous spherulites for silicates, and also by lenticular particles and star-shaped bodies for aluminates. It may be assumed that silica gels and alumina gels intensely dehydrated under vacuum may be observed in this form.

The investigations carried out indicate the presence of a reaction of the alkali both with the silicates and the aluminates of Portland cement.

These conclusions are also confirmed by parallel experiments on the resistance of mortars and concretes to alkalis.

LITERATURE CITED

[1] N. A. Moshchanskii, The Consistency and Stability of Concretes. State Construction Press, 108-122 (1951).*

[2] S. V. Shestoperov and T. Iu. Liubimova, Proc. Acad. Sci. USSR 86, 6 (1952).

[3] R. Grün, Chemische Widerstandfähigkeit von Beton (1928).

[4] R. H. Bogue, The Chemistry of Portland Cement, New York (1955).

[5] K. Dorsh, The Setting and Corrosion of Cements, Div. Sci. Tech. Research (1936).

[6] P. P. Budnikov, Ceramic Technology. ONTVU** Budvidova (1937); P. P. Budnikov and Z. S. Kosyreva. Alkali-resistant Brick Linings. Proceedings of D. I. Mendeleev Institute of Chem. Technol., Symp. 2, 43-52 (1949).

[7] P. N. Grigor'ev and I. M. Doronenkov, Chemically Stable Floors. State Tech. Chem. Press, 61-65 (1951).*

[8] P. N. Grigor'ev and I. M. Doronenkov, The Protection of Buildings from Corrosion. State Chem. Press, 62-67 (1955).*

[9] V. M. Moskvin, The Corrosion of Concrete. State Constr. Press. 158-166 (1952).*

Received June 20, 1956

*In Russian.

**Transliteration of Russian — Publisher's note.

THE LIBERATION OF AMMONIA FROM TECHNICAL SODIUM BICARBONATE

E. M. Mitkevich

Scientific-Research Institute of Basic Chemistry, Khar'kov

At the present time it has been established [1-4] that the combined nitrogen, of which there is ~1% (converted to ammonia) in the technical bicarbonate of the ammonia-soda industry, is contained in the compound sodium carbamate ($NaCO_2NH_2$).

In the literature [5-7] devoted to the problem of calcination the presence of combined nitrogen in moist technical bicarbonate is attributed to the ammonium carbonate salts contained in the precipitate. As is known, these salts are unstable and readily decompose into ammonia and carbon dioxide when heated to 60-65°.

This is evidently responsible for the belief that ammonia is readily liberated from technical bicarbonate.

For example, Gol'dshtein [6] indicates that complete removal of the moisture and ammonia compounds is possible without dissociation of the $NaHCO_3$ by passing carbon dioxide heated to 80° over bicarbonate. Similar opinions are expressed in Avdeeva's work [5].

T'ieh P'ang-Kuo's information [7] is contrary to this. He indicates that in order to avoid losses of ammonia in the soda, oven-calcined soda free from sodium bicarbonate must be used.

In factory practice it is a well known fact that combined nitrogen is present in calcined soda when it gives a low titer.

As may be seen, the information is very contradictory.

The application of new methods for drying and calcining technical sodium bicarbonate (in the suspended state, in the boiling layer, etc.) it met by difficulties associated with the problem of utilizing the nitrogen present in technical bicarbonate.

In view of what has been said, the investigation of this problem was of definite theoretical and practical interest.

Analysis of the literature data [8-10] showed that in order to characterize the behavior of sodium carbamate under the conditions used in processes for drying and calcining technical sodium bicarbonate it was necessary to investigate the possibility of the formation of sodium isocyanate according to the reaction.

$$NaCO_2NH_2 = NaCNO + H_2O \qquad (1)$$

and the kinetics of the reaction of sodium carbamate with water vapor according to the reaction

$$2NaCO_2NH_2 + H_2O = Na_2CO_3 + 2NH_3 + CO_2. \qquad (2)$$

Sodium carbamate of sufficient chemical purity was obtained by the carbonization of sodium chloride in liquid ammonia under atmospheric pressure ($t \approx -30°$).

The method for the analysis of $NaCO_2NH_2$ was based on the following reactions:

$$2NaCO_2NH_2 + 2H_2SO_4 = Na_2SO_4 + (NH_4)_2SO_4 + 2CO_2, \quad (3)$$

$$NaCO_2NH_2 + NaOH = Na_2CO_3 + NH_3. \quad (4)$$

The total alkalinity of the precipitates obtained was determined as a result of carrying out reaction (3). The determination of the nitrogen content according to reaction (4) was carried out by the Kjeldahl method.

The precipitate, washed free from chlorine with liquid ammonia, showed close agreement of the total alkalinity to the half value of the alkalinity of ammonia (according to reactions 3 and 4) and contained 99.1-99.5% $NaCO_2NH_2$. Continued heating of the $NaCO_2NH_2$ under vacuum (for 4 hours at a pressure of 1 mm Hg) at temperatures of 90, 110 and 130° showed that reaction (1) does not take place and that under these conditions sodium carbamate is a completely stable chemical compound.

An investigation of the rate of reaction of sodium carbamate with water vapor was carried out at temperatures obtaining during the calcination of moist technical sodium bicarbonate (100-130°) [11].

In view of the difficulty of measuring small amounts of water vapor the latter was fed together with air for the reaction.

The air-vapor mixture used for the experiments had the composition (in weight %): H_2O 41.2, air 58.7. It was prepared by passing air at a rate of 0.5 liter/min through water, heated to 50°.

The conversion of $NaCO_2NH_2$ with respect to time was determined by the amount of NH_3 liberated.

The laboratory installation is shown in Fig. 1.

The experimental procedure was as follows. A vessel with a weighed sample (1.5 g) of sodium carbamate was placed in an air thermostat. With cock A closed, the vessel was connected to a vacuum pump by means of a three-way cock B and was exhausted (when heated in the isolated state sodium carbamate is chemically stable). The heating current of the air and water thermostats was then switched on. When the thermostats had reached the required temperatures atmospheric pressure was reestablished in the reaction vessel by means of cock B.

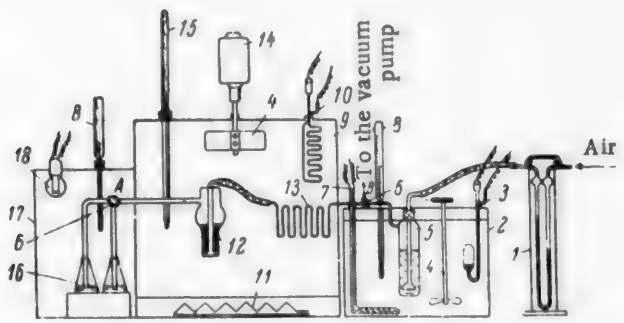

Fig. 1. Diagram of the laboratory installation for investigating the process of the reaction between sodium carbamate and water vapor. 1) Rheometer; 2) water thermostat; 3) toluene thermoregulator; 4) stirrer; 5) vessel for humidifying the air; 6) three-way cocks (A and B); 7) heater; 8) thermometer; 9) air thermostat; 10) mercury thermoregulator; 11) heater; 12) reaction vessel; 13) copper coil; 14) electric motor; 15) decimal-graduated thermometer; 16) conical flask with acid; 17) cupboard; 18) electric light bulb. I) To the vacuum pump, II) air.

The reaction vessel was connected by means of cock A to the small flasks and the blower was then switched on. The air, passing through the rheometer and becoming saturated with water vapor in the flask, located in the water thermostat, entered the copper coil in which the air-vapor mixture was heated to the temperature of the air thermostat and then passed into the reaction vessel. In the latter the air-vapor mixture passed upwards through a layer of sodium carbamate. By turning cock A, the reaction gases formed during this process were fed alternately into conical flasks containing 0.1 N sulfuric acid. The latter were located in a cupboard, heated by an electric light bulb to 60-70° in order to prevent condensation of ammonium carbonate salts from the gas in the feed pipes.

The experimental results are given in Table 1.

TABLE 1

Results of the Investigation of the Process of the Reaction of Sodium Carbamate with Water Vapor

Temperature (in °C)					
100		110		130	
time (min)	conversion of $NaCO_2NH_2$ (as %)	time (min)	conversion of $NaCO_2NH_2$ (as %)	time (min)	conversion of $NaCO_2NH_2$ (as %)
1	5.9	1	8.5	1	16.7
3	13.2	3	24.3	3	45.2
6	30.4	6	47.2	6	71.8
12	57.5	12	73.6	10	86.7
22	78.2	22	88.2	16	95.4
28	84.4	42	94.9	—	—
38	89.2	72	—	—	—
62	94.1	—	—	—	—
112	—	—	—	—	—

Assuming that the rate of the process of the reaction of sodium carbamate with water vapor is determined by the particular rate of this heterogeneous chemical reaction, then the following equation applies:

$$\frac{dx}{d\tau} = K \cdot F \cdot C_{H_2O} \quad B. \qquad (I)$$

Substituting the values

$$F = f_0 \cdot a_0 \cdot (1 - x)^{2/3} \text{ and } B = \frac{D}{a_0 \cdot x}$$

in equation (I), we obtain

$$\frac{dx}{d\tau} = K \cdot f_0 \cdot C_{H_2O} \cdot D \frac{(1 - x)^{2/3}}{x},$$

where $\frac{dx}{d\tau}$ is the rate of variation of the degree of conversion of $NaCO_2NH_2$ into Na_2CO_3 (in parts by weight/min; F is the surface area of the sodium carbamate in the reaction zone at a given moment of time (in sq. m); C_{H_2O} is the concentration (in parts by volume of water vapor in the gas entering the reaction zone; in the experiments this was 0.522); B is the ratio of the number of gram equivalents of water vapor entering the reaction zone per unit of time to the number of gram equivalents of $NaCO_2NH_2$ present in the reaction zone at a given

moment of time; f_0 is the surface area of the particles of a gram equivalent of sodium carbamate (in sq. m g-equiv.); a_0 is the number of g-equiv. of $NaCO_2NH_2$ in the reaction zone before the commencement of the process; $\underline{x}$ is the degree of conversion of $NaCO_2NH_2$ at a given moment of time (in parts by weight); D is the amount of H_2O (in g-equiv.) entering the reaction zone per minute (in the experiments D was 0.0253 g-equiv/min).

Representing the constant value $K \cdot f_0 \cdot C_{H_2O} \cdot D$ in this instance by N and integrating this equation for the initial conditions $\tau = 0$, $x = 0$, we obtain

$$\tau = \frac{(1-x)^{1/3} \cdot \left(\frac{1-x}{4} - 3\right) + 2.75}{N}.$$

The mean values for the constant $K \cdot f_0$ at the temperatures 100, 110 and 130°, determined from the data in Table 1, gave the values 3.18 $\frac{1}{\text{min}}$; 5.18 $\frac{1}{\text{min}}$; 10.05 $\frac{1}{\text{min}}$, respectively.

Figure 2 gives the results of experiments and the theoretical data on the degree of conversion of $NaCO_2NH_2$ into Na_2CO_3 at the given values of the constants $K \cdot f_0$, indicating the correctness of the considerations on which equation (I) was based. It follows, therefore, that the rate of the process of the reaction of sodium carbamate with water vapor increases with the temperature and that under the conditions existing during the process of calcining technical bicarbonate (presence of a considerable amount of water vapor, temperature of the mass 100-130°) sodium carbamate in the free state is a very unstable compound and should be easily converted into Na_2CO_3, according to reaction (2).

The first observations indicate, however, that when moist technical bicarbonate is heated to 100-110° (in the temperature range 100-120° sodium bicarbonate is practically undecomposed [5]) the liberation of the ammonia is of very slight extent and after the evaporation of the free water, when water vapor is present in the gas phase, it ceases completely.

From the point of view of the properties of sodium carbamate (stability when heated in the isolated state and complete instability in the free state in the presence of water [2] and water vapor) these facts can only be explained by assuming that the NH_2COO' carbamate ion is included in the crystalline lattice of technical sodium bicarbonate and is, therefore, protected from the action of water as a chemical reagent. In consequence, the disintegration of the crystalline lattice of technical sodium bicarbonate is a necessary condition for carrying out reaction (2) successfully.

This conclusion was checked experimentally. The disintegration of the crystalline lattice of technical sodium bicarbonate in the presence of water in the vaporous and liquid states at a temperature of the mass of 100-130° in the process of calcination takes place in two stages:

1) During the process of mixing the moist bicarbonate with the calcined soda due to the reaction of the formation of trona ($Na_2CO_3 \cdot NaHCO_3 \cdot 2H_2O$) [11];

2) During the process of dissociation of sodium bicarbonate not converted to trona.

The investigation of the liberation of ammonia from technical bicarbonate during the process of mixing was carried out at the Donets Soda works (DSZ), both on a laboratory and works scale, by analyzing the operation of the mixer of the soda oven.

In the laboratory experiment calcined soda and moist technical bicarbonate were mixed in various weight ratios in a heated-insulated vessel. The weight of the mixture was kept constant in all the experiments, being 200 g.

To determine the amount of ammonia liberated in the gas phase the initial components were analyzed for their content of $NaHCO_3$, Na_2CO_3 and NH_3. The ammonia was determined by the Kjeldahl method. The $NaHCO_3$ was determined by Winkler's method.

It may be pointed out that these analyses which make it possible to determine desired values do not reflect the actual composition of moist technical bicarbonate because the combined nitrogen and part of the alkali, which are calculated as Na_2CO_3 belong to the $NaCO_2NH_2$.

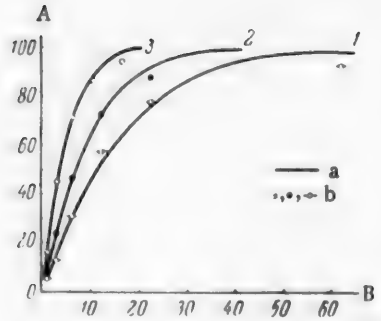

Fig. 2. Rate of the process of the reaction of sodium carbamate with water vapor. A) Degree of conversion of $NaCO_2NH_2$ into sodium carbonate (as %); B) time (in min). Temperature (in °C): 1) 100, 2) 110, 3) 130. a) Theoretical data, b) experimental data.

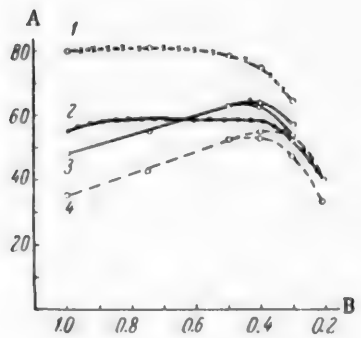

Fig. 3. Liberation of ammonia when calcined soda is mixed with moist (crude) technical sodium bicarbonate. A) Temperature (in °C) and amount of NH_3, liberated in the gas phase (as %); B) weight ratio of soda to moist technical bicarbonate. 1) Heating of the mixtures after mixing for 2 minutes (temperature of the soda 130°), 2) ditto (temperature of the soda 20°), 3) liberation of NH_3 after the soda (temperature 130°) had been mixed 5 and 10 minutes with moist technical bicarbonate, 4) ditto (temperature of the soda 20°).

The calculation of the amount of ammonia liberated was made on the assumption that the Na_2CO_3 and $NaHCO_3$ contained in the initial products did not undergo a loss in weight when mixed.

The initial products had the following composition: calcined soda Na_2CO_3 99.14%; moist technical bicarbonate (as %): in the experiments with cold soda – $NaHCO_3$ 75.28, Na_2CO_3 6.26, NH_3 0.827, H_2O 17.7; in the experiments with hot soda $NaHCO_3$ 75.51, Na_2CO_3 5.94, NH_3 0.859, H_2O 18.0.

The results of the laboratory experiments are given in Fig. 3.

Table 2 gives the results of the examination of the mixer of the soda oven.

From Fig. 3 it is evident that within the range of weight ratios of 1-0.5 for the calcined soda and moist bicarbonate in the mixture the process of liberation of ammonia ceases 5 minutes before the time of mixing. The maximum amount of ammonia liberated in the gas phase corresponds to the ratios 0.5 and 0.4. Commencing with a ratio of 0.5 and below, the amount of ammonia liberated during a mixing time of 5 and 10 minutes becomes different and the curves branch; commencing from a ratio of 0.4 and below, a marked fall in the amount of ammonia liberated and the temperature of warming up of the mass are noted.

The explanation of all these facts lies in the fact that during the process of mixing the sodium carbonate is converted to trona. During this process, as a result of the disintegration of the crystalline lattice of the bicarbonate the bicarbonate ion included in it reacts with the water, according to reaction (2).

In actual fact the coincidence of the curves of the degree of liberation of NH_3 for 5 and 10 minutes mixing within the range of weight ratios of 1-0.5 for the components indicates that the chemical combination of the water in the trona ceases 5 minutes before the mixing time; the process of the reaction of sodium carbamate with water, controlled by this process therefore ceases.

Commencing with a weight ratio of 0.4 and below for the components, free water remains in the mixed mass (this follows from the stoichiometry of the reaction of the formation of trona and the composition of the mixture components), the amount of bicarbonate converted to trona falls markedly and because of this the amount of ammonia liberated and the temperature of the warming up of the mass fall sharply (according to Torgeson's data [12] the thermal effect of the reaction of formation of trona for liquid H_2O is 7760 cal/mole).

The divergence of the curves of liberation of ammonia for 5 and 10 minutes mixing time is the result of the slow progress of reaction (2) as a result of the diffusion of free water inside the crystals of sodium bicarbonate.

TABLE 2

Results of the Examination of the Mixer of the Soda Oven

Substance	Content (in weight %)			Wt. ratio of return soda : moist technical bicarbonate	Temperature (in °C)		NH_3, liberated in gas phase from technical sodium bicarbonate (as %)
	in moist technical bicarbonate	in the return soda	in mixture at entry of soda oven		return soda	mass in mixer	
$NaHCO_3$.	75.14	2.58	47.63				
Na_2CO_3 . .	6.28	96.41	40.14	0.75	130	—	46.13
NH_3 . . .	0.835	0	0.279				
	74.76	0.61	42.31				
Ditto	6.53	98.13	47.47	0.77	134	95	44.36
	0.798	0	0.250				
	75.51	2.58	38.76				
»	6.13	96.41	52.57	1	130	98	42.24
	0.915	0	0.262				
	72.71	0.92	31.50				
»	6.06	97.48	61.47	1.37	131	—	50.7
	0.956	0	0.200				

The maximum amount of liberated ammonia which is close to the maximum possible percentage of conversion of bicarbonate to trona (~ 55%); corresponds to the weight ratio of the components of the mixture, which in turn corresponds to the stoichiometry of the reaction of the formation of trona.

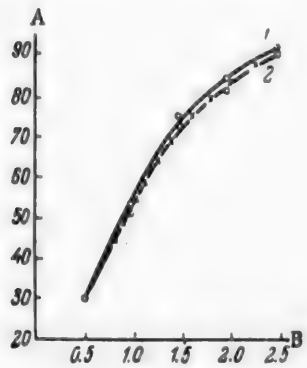

Fig. 4. The reaction of sodium carbamate with water vapor during the process of decomposition of technical sodium bicarbonate. A) Degree of conversion (as %), B) time (in hours). 1) Conversion of $NaCO_2NH_2$ to Na_2CO_3, 2) decomposition of $NaHCO_3$.

From the data of Table 2 it is evident that during the period of mixing of the mass in the soda oven mixer 42 to 51% of the ammonia is liberated from moist technical bicarbonate, which is somewhat less than that obtained under laboratory conditions. This is connected with the fact that the period during which the mass remains in the mixer (~ 30 seconds) is insufficient for the full completion of the process of combination of bicarbonate in trona.

Figure 4 gives the data of the kinetics of the processes of decomposition of $NaHCO_3$ and $NaCO_2NH_2$, contained in technical bicarbonate at a temperature of the reaction volume of 145°. The data were obtained in the following manner.

Equal amounts of air-dry technical bicarbonate with the composition (as %: $NaHCO_3$ 93.00, $NaCO_2NH_2$ 3.1, Na_2CO_3 2.5) were placed in several glass vessels in an air thermostat previously heated to 145°.

During the period of the experiment (at appropriate intervals of time) the vessels were removed in turn from the thermostat. After they had cooled the loss in weight was determined and the contents of $NaHCO_3$, Na_2CO_3 and $NaCO_2NH_2$ were analyzed. The degree of conversion of the components was calculated from the data obtained.

From Fig. 4 it is evident that the amount of reacted sodium carbamate in each section of time is equal to the amount of decomposed sodium bicarbonate, i.e., in this instance the reaction of sodium carbamate with water according to reaction (2) takes place in proportion to the degree of disintegration of the crystalline lattice of sodium bicarbonate.

SUMMARY

1. It was shown that the carbamate ion NH_2COO^- is uniformly distributed in the crystalline lattice of technical sodium bicarbonate. This indicates that technical bicarbonate is a mixture of bicarbonate and sodium carbamate.

2. As a result of the chemical properties of sodium carbamate (stability in the isolated state and complete instability in the presence of water or water vapor) the liberation of ammonia during the process of calcination takes place in proportion to the degree of disintegration of the crystalline lattice of technical bicarbonate: a) during the process of formation of trona when the moist bicarbonate is mixed with calcined soda; b) during the process of dissociation of technical bicarbonate, unconverted to trona.

LITERATURE CITED

[1] E. I. Orlov, Ukr. Chem. J. 1, 14 (1928); 4, 139 (1928).

[2] T. Kuki, S. Niwo and R. Hara, J. Soc. Chem. Ind. Japan, 43, 3, 76 B (1940).

[3] T. Kuki and R. Hara, J. Soc. Chem. Ind. Japan, 43, 4, 118 B (1940).

[4] Z. V. Dolganova, Author's abstract of thesis. Khar'kov, Khar'kov Polytech. Inst. (1950).

[5] A. V. Avdeeva, J. Chem. Ind. 8, 17, 4 (1931).

[6] Ia. R. Gol'dshtein, Production of Calcined Soda, State Chem. Press (1934).*

[7] T'ieh P'ang-Kuo, The Production of Soda, State Chem. Press (1948).*

[8] E. Drechsel, J. pr. Ch. 16, 180 (1877).

[9] B. Joschiki, J. Soc. Chem. Ind. Japan 43, 3, 83 (1940).

[10] V. V. Vasil'ev, Ia. E. Seferovich and V. M. Fridman, J. Appl. Chem. 14, 11-12, 821 (1937).

[11] E. M. Mitkevich, J. Appl. Chem. 31, 2, 158 (1958).**

[12] D. Torgeson, Ind. Eng. Ch. 40, 2, 1152 (1948).

Received June 16, 1956

* In Russian.

** Original Russian pagination. See C. B. Translation.

THE DISSOLUTION APATITE IN PHOSPHORIC ACID PARTIALLY NEUTRALIZED WITH MAGNESIUM (IN SOLUTIONS OF THE SYSTEM $MgO-P_2O_5-H_2O$)

K. S. Krasnov

Ivanov Chemical-Technological Institute

At the present time considerable attention is devoted to the processing of Kara-Tau phosphorites, containing up to 26-28% P_2O_5, for the production of fertilizers. As well as a considerable amount of P_2O_5 these phosphorites contain admixtures – $CaCO_3$, $MgCO_3$ – which cause difficulties when they are used for the production of superphosphate. The presence of $MgCO_3$ reduces the quality of the superphosphate; in particular superphosphate of this type matures very slowly during storage.

Chepelevetskii and Pado [1], showed that the cause of this is as follows. In the initial stage of decomposition of the mineral by sulfuric acid magnesium phosphate $Mg(H_2PO_4)_2$ is formed at the same time as phosphoric acid, its solubility being equal to that of the latter. The liquid phase formed is a buffer mixture H_3PO_4-$Mg(H_2PO_4)_2$, the hydrogen ion concentration of which is less than in free phosphoric acid, depending as a first approximation on the acid/salt ratio, i.e., other circumstances being equal, on the magnesium content in the initial mineral. In the next stage this liquid phase decomposes the remainder of the phosphate mineral (hydroxyapatite) less actively than phosphoric acid, free from the magnesium salt. The decomposition proceeds more slowly and is not fully completed even during storage.

In order to select the most suitable system of processing and storing superphosphate made from Kara-Tau phosphorites it is important to determine to what extent the magnesium content in the liquid phase (and, therefore, in the initial raw material) of the superphosphate influences the rapidity of decomposition of the initial hydroxyapatite. It is this problem which forms the subject of this paper.

To resolve the problem in general outlines the basic equation of the diffusion theory of solution, the Shchukarev-Nernst equation, may be used.

Chepelevetskii showed [2] that the decomposition of apatite by acids can be described within the framework of the diffusion theory of solution; for example, the dissolution of apatite by phosphoric acid, containing 20% P_2O_5, partially neutralized, conforms to the Shchukarev-Nerst equation in the following form:

$$\bar{v} = k \cdot S \cdot \frac{D}{\delta} [H^+], \qquad (1)$$

where $\bar{v}$ is the loss in weight of the apatite, S is the surface of separation of the phases, δ is the thickness of the diffusion layer, D is the coefficient of diffusion, $[H^+]$ is the hydrogen ion concentration. If S, D and δ are constants, the mean specific rate of solution, equal to the amount of dissolved substance from a unit of surface $\bar{v} = \frac{v}{S}$, is expressed by the equation

$$\bar{v} = k' \cdot [H^+], \qquad (2)$$

where $k' = k \frac{D}{\delta}$.

On the basis of Chepelevetskii's work it would be expected that the higher the magnesium content in the liquid phase, the higher will be the percentage of neutralization of the primary H^+ ion of phosphoric acid, the lesser the $[H^+]$ and the slower the process of solution. To pass from qualitative to quantitative inferences it is necessary to know the manner of variation of the diffusion coefficient, depending on the viscosity of the solution and the thickness of the diffusion layer δ with increasing magnesium content in the solution. No such data are to be found in literature. Finally, assuming (without basis) that D and δ are constant it must be made certain that in H_3PO_4 solutions such as are found in industry (approximately 40% P_2O_5) the relationship between the rate $\overline{v}$ and the H^+ ion concentration remains linear, as is the case for the 20% acid. We were not certain on this point and the experiment confirmed our doubts.

We therefore decided to resort to an experiment. The numerical data obtained make it possible to form a direct assessment of the influence of the amount of magnesium in the liquid phase on the rate of solution of apatite and to check the possibility of using equations (1) and (2) for calculating the rate of solution at high concentrations of phosphoric acid.

EXPERIMENTAL

The decomposition of phosphate mineral by phosphoric acid, partially neutralized by magnesium, was studied at a constant temperature of 25 ± 0.1°. The solid phase was formed by particles of selected apatite. A standard sample of 4.000 g has a surface of 42.75 ± 0.25 sq. cm. The liquid phase was phosphoric acid, partially neutralized by magnesium (solutions of the system $MgO-P_2O_5-H_2O$); it was prepared from crystalline phosphoric acid (analytically pure), secondary magnesium phosphate $MgHPO_4 \cdot 3H_2O$ (analytically pure) and distilled water. The total content of P_2O_5 and free acid in these solutions was determined by titration with two indicators.

The solution was thermostatically regulated for 30 minutes in a flat-bottomed cylindrical vessel with a stirrer, after which the weighed sample of apatite was introduced. After 2 hours it was extracted, washed and dried. The mean specific rate of solution $\overline{v}$, expressed in mg of apatite passing into solution from 1 sq. cm of surface per hour (mg/sq.cm · hour), was calculated from the loss in weight of the sample. Each value of $\overline{v}$ was calculated as the mean of two values, obtained in parallel experiments.

The surface of the sample of apatite S was assumed to be constant during the experiment because in the case of maximum loss in weight it did not decrease by more than 8% by the end of the experiment. In the majority of instances the decrease of the surface was insignificant and could be neglected.

The decomposition of apatite was investigated by three series of solutions $MgO-P_2O_5-H_2O$. The total P_2O_5 content for a series was constant, being 45% in the first, 40% in the second and 35% in the third series. The MgO content in each series varied from 1 to 6-7%. To facilitate a comparison the values of the mean specific rate of solution $\overline{v}$, interpolated for contents of 1,2,3,4 and 5% MgO in the liquid phase are given in Tables 1, 2 and 3. These tables also give the values, calculated for these solutions, of the free acidity, the degree of neutralization of the primary H^+ ion of the phosphoric acid Z, the acid/salt ratio, the hydrogen ion concentration $[H^+]$ and the constant k' of equation (2), calculated as $\overline{v}/[H^+]$.

The values of $[H^+]$ were calculated from the formula:

$$[H^+] = -\frac{K_a + [\text{salt}]}{2} + \sqrt{\left\{\frac{K_a + [\text{salt}]}{2}\right\}^2 + K_a [\text{acid}]}, \qquad (3)$$

where K_a is the primary dissociation constant of H_3PO_4, which is $7.52 \cdot 10^{-3}$ at 25°.

In converting percentage concentration to molar concentration, the density of the partially neutralized solution of acid was taken as equal to the density of phosphoric acid solutions with the same P_2O_5 content. This resulted in the introduction of a small but insignificant error.

Graphs, suitable for interpolation (Fig. 1 and 2), were drawn from the data in the Tables.

TABLE 1

The Dissolution of Apatite in Solutions of the System $MgO-P_2O_5-H_2O$, Containing 45% P_2O_5

Name of the characteristic	MgO content (in weight %)					
	0	1	2	3	4	5
Free acidity (in % P_2O_5)	45.00	41.48	37.96	34.44	30.92	27.39
Degree of neutralization Z (as %)	0	7.55	15.65	23.60	31.60	39.60
Acid/salt ratio	—	23.4	10.78	6.53	4.38	3.92
H^+ ion concentration $[H^+]$ (in mole/liter)	0.258	0.127	0.071	0.045	0.033	0.029
Specific rate of solution $\bar{v}$	4.0	2.5	1.6	1.0	0.6	0.3
$k' = \frac{\bar{v}}{[H^+]}$	15.5	19.7	22.6	22.2	18.2	10.2

TABLE 2

The Dissolution of Apatite in Solutions of the System $MgO-P_2O_5-H_2O$, Containing 40% P_2O_5

Name of characteristic	MgO content (in weight %)					
	0	1	2	3	4	5
Free acidity (in % P_2O_5)	40.00	36.48	32.96	29.44	25.92	22.39
Degree of neutralization Z (as %)	0	8.80	17.60	26.60	35.40	44.50
Acid/salt ratio	—	20.75	9.46	5.58	3.68	2.55
H^+ ion concentration $[H^+]$ (in mole/liter)	0.238	0.122	0.063	0.039	0.027	0.019
Specific rate of solution $\bar{v}$	4.9	3.2	2.2	1.5	0.8	0.4
$k = \frac{\bar{v}}{[H^+]}$	20.6	26.2	35.0	38.5	29.6	21.8

TABLE 3

The Dissolution of Apatite in Solutions of the System $MgO-P_2O_5-H_2O$, Containing 35% P_2O_5

Name of characteristic	MgO content (in weight %)					
	0	1	2	3	4	5
Free acidity (in % P_2O_5)	35.00	31.48	27.96	24.44	20.92	17.39
Degree of neutralization Z (as %)	0	10.15	20.30	30.50	40.70	50.80
Acid/salt ratio	—	17.82	7.93	4.62	2.90	2.16
H^+ ion concentration $[H^+]$ (in mole/liter)	0.212	0.099	0.052	0.033	0.022	0.017
Specific rate of solution $\bar{v}$	5.5	4.1	2.57	1.46	0.82	0.35
$k' = \frac{\bar{v}}{[H^+]}$	25.9	41.5	49.5	44.1	37.6	20.4

DISCUSSION OF RESULTS

The data of Tables 1, 2 and 3 indicate that the free acidity, the acid/salt ratio and the hydrogen ion concentration, calculated according to equation (3), decrease with increasing MgO content in the liquid phase. At the same time the value of the specific rate of solution $\bar{v} \cdot [H^+]$ falls and $\bar{v}$ varies symbatically. A linear relationship between $[H^+]$ and $\bar{v}$, corresponding to equation (2) is, however, not found. The value of the velocity constant k' does not remain constant.

The constant $k' = k \frac{D}{\delta}$ depends on the viscosity of the solvent because D is inversely proportional to the viscosity; we neglect the relationship between δ and the viscosity. In Levich's treatise [3] the thickness of the diffusion layer is inversely proportional to the root of the sixth power of the viscosity. For example, when the viscosity is doubled δ decreases by a total of 11%.

There are no data in literature on the viscosity of solutions of the system $MgO-P_2O_5-H_2O$. It is, therefore, impossible to make a quantitative assessment of the relationship between k' and D. Our data on the viscosity of solutions of the system $CaO-P_2O_5-H_2O$ make it possible to assume that with a 3% MgO content in the system the viscosity increases by 75 to 100% compared with phosphoric acid of the same P_2O_5 concentration [4]. It would, therefore, be expected that the value of k' will fall with increasing neutralization of the acid by magnesium because k' is inversely proportional to the viscosity. The experiment was at variance with this assumption. In all the three series of experiments the constant k' increased with increasing MgO content in the solution, reaching a maximum at 2-3% MgO and then commencing to fall. For the solution with a constant P_2O_5 content of 40% the ratio is

$$\frac{k'_{3\%\ MgO}}{k'_{0\%\ MgO}} = \frac{38.5}{20.6} = 1.87.$$

In contrast to k' the constant $\underline{k}$ of equation (1) does not depend on the viscosity and with increasing MgO content in the solution increases still more markedly than k'.

If (by analogy with the system $CaO-P_2O_5-H_2O$) it is assumed that at 3% MgO content in the system with 40% P_2O_5 the viscosity is twice as high as in the free acid with the same P_2O_5 content, it can easily be shown that

$$\frac{k_{3\%\ MgO}}{k_{0\%\ MgO}} = 1.87 \cdot 2 = 3.74.$$

This increase in the velocity constant is of interest and requires an explanation. In this instance the following may be assumed.

a) Equation (1) cannot be employed in the form given; it is possible that the activity should be introduced into the equation instead of the concentration. There is no established opinion in this respect. It was not possible to make a check in this instance because no data were available on activities for the investigated system. If this assumption is correct it could be shown that the activity coefficient of the H^+ ions increases with increasing content of magnesium in the system.

b) It may well be possible that the rate of solution is determined by the hydrogen ion concentration and not by the activity, but Equation (3) cannot be employed for calculation of the $[H^+]$ in solutions containing more than 20-25% P_2O_5 as a result, inter alia, of the modification of the dissociation value K_a in such concentrated solutions.

c) It is possible that the modification of the diffusion coefficient in solutions of considerable ionic strength such as $MgO-P_2O_5-H_2O$ solutions is determined not only by the viscosity but also by the electrostatic reaction of the ions, which is not taken into consideration here.

We have not sufficient data to decide which of these hypotheses is correct. The correctness of hypothesis (a) could be verified by way of the example of the dissolution of apatite in acid whose activity value is accurately known within a wide range of concentrations and where the diffusion is not complicated by a film effect, for example in HCl. From the experiments the conclusion follows that the rate of solution of apatite in solutions of H_2PO_4, partially neutralized by magnesium, cannot be described by equations (1) and (2) if H^+ is calculated from formula (3). The direct experimental data are, therefore, of practical interest.

Data for solutions containing 1, 2, 3, 4 and 5% MgO are given in the Tables. For other concentrations the data can be interpolated from the graph.

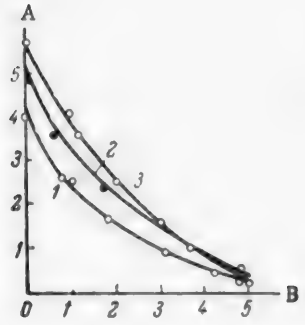

Fig. 1. Relationship between the rate of solution of apatite and the MgO content in the liquid phase. A) Rate of solution of apatite $\bar{v}$, B) MgO content in the liquid phase (as %). P_2O_5 content (as %): 1) 45, 2) 40, 3) 35.

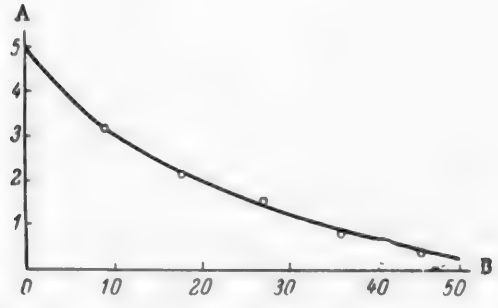

Fig. 2. Rate of solution as a function of the degree of neutralization of acid (40% P_2O_5). A) Rate of solution $\bar{v}$, B) degree of neutralization of acid Z (as %).

A formula may also be proposed, connecting $\bar{v}$ and Z. Figure 2 shows that the greater the rate of solution $\bar{v}$ the more markedly it falls with increasing degree of neutralization. This relationship may be expressed analytically

$$-\frac{d\bar{v}}{dZ} = \beta \cdot \bar{v}, \qquad (4)$$

where β is the coefficient of proportionality.

Hence

$$\bar{v} = v_0 \cdot e^{-\beta z} \qquad (5)$$

or for practical purposes

$$\bar{v} = v_0 \cdot 10^{-0.4343\beta z}.$$

Here $\bar{v}_0$ is the rate of solution where Z = 0, i.e., in free phosphoric acid. The value of β depends on the P_2O_5 content in the solution.

For the series of experiments with P_2O_5 = 45% β = 0.060, for P_2O_5 = 40%, β = 0.0455, for P_2O_5 = 35% β = 0.0463.

The reduction in the solvent action of the acid by the partial neutralization of its primary hydrogen ion may be represented by the value ξ, which signifies the degree of neutralization at which the rate of solution is decreased by half compared with free phosphoric acid. From equation (5)

$$^1/_2\bar{v}_0 = \bar{v}_0 \cdot e^{-\beta\xi},$$

hence we obtain

$$\xi = \frac{\ln 2}{\beta} = \frac{0.692}{\beta}.$$

For acid containing 45, 40 and 35 % P_2O_5, respectively the value of ξ becomes 11.5, 15 and 14.68%. Neutralization evidently reduces the activity of 45% acid more markedly than that of 40 and 35%.

TABLE 4

Relative Rate of Solution of Apatite in Phosphoric Acid, Partially Neutralized by Magnesium

P_2O_5 Content (as %)	Relative rate of solution of apatite at a degree of neutralization Z (as %)										
	0	5	10	15	20	25	30	35	40	45	50
45	1.00	0.75	0.55	0.42	0.30	0.22	0.17	0.12	0.090	0.065	0.050
40	1.00	0.815	0.633	0.505	0.401	0.320	0.254	0.222	0.162	0.129	0.102
35	1.00	0.795	0.630	0.498	0.396	0.312	0.250	0.198	0.157	0.124	0.099

The correctness of Equation (5) can be checked graphically. The relationship between log $\bar{v}$ and Z must be linear. Figure 3 shows that in the region of values of practical importance (from 0 to 30-35%) Equation (5) is valid and may be employed for calculating the rate $\bar{v}$, of the ratio $\frac{\bar{v}}{\bar{v}_0} = \varphi$ of the dimensionless relative rate of solution indicating how much slower apatite dissolves in partially neutralized acid than in free acid (the value of $\bar{v}_0$ where P_2O_5 = 35% must, in accordance with equation (5) be altered from 5.5 to 6.6 mg/sq.cm · ·hour).

Table 4 gives the values of the dimensionless relative rate $\varphi = \frac{\bar{v}}{\bar{v}_0}$, calculated from Equation (5). They are practically convenient values of $\bar{v}$ because the value of $\bar{v}$ depends on the characteristics of the hydrodynamical conditions: mixing, size and shape of the particles, etc. while φ does not depend on them.

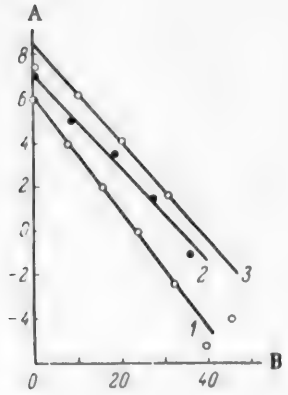

Fig. 3. Verification of the correctness of Equation (5). A) Value of log $\bar{v}$, B) degree of neutralization of acid Z (as %). P_2O_5 content: 1) 45, 2) 40, 3) 35.

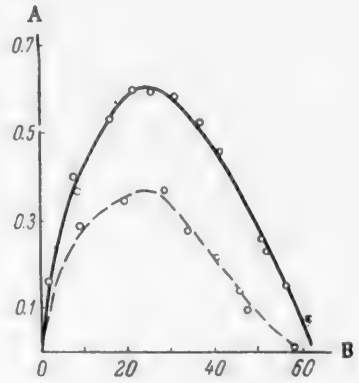

Fig. 4. 25° isotherms of the rate of solution of apatite in phosphoric acid (continuous line) and in acid, partially neutralized by magnesium. Degree of neutralization 18% (dotted line). A) Rate of solution $\bar{v}$, B) P_2O_5 content (as %).

A connection is, therefore, established between the value of the rate of decomposition of apatite and the degree of neutralization of acid. At the same magnesium content in the three series of experiments the rate of solution was greatest in the acid with 35% P_2O_5 and least in that with 45%. This is explained by the intense increase in the viscosity in this region.

In order to determine the influence of the P_2O_5 content on the rate of solution at the same degree of neutralization of acid within a wide range of concentrations experiments were carried out in which the total P_2O_5 content was varied at constant Z = 18%. The results of this series of experiments are given in Table 5.

A graph was drawn (Fig. 4) from the results given in Table 5. The rate of solution was greatest at a P_2O_5 content of 25-30%. Figure 4 also gives a similar curve plotted from our data for the rate of reaction of apatite in free H_3PO_4 at the same temperature 25°. It is evident that the relationship between the rate of solution and the P_2O_5 content in free and partially neutralized acid is the same. The characteristic outline of the curves is explained in previous works. Curves, similar to that represented in Fig. 4, at higher values of the degree of neutralization Z will be flatter, the higher the value of Z. A high value of Z reduces the difference in the solvent action, caused by the different P_2O_5 content in the system. This is noticeable in a comparision of the values of $\bar{v}$ for solutions containing 4-5% MgO. For liquid phases containing 40 and 35% P_2O_5, the difference in the solvent action practically disappears at an MgO content of 3%, i.e., at 26-30% neutralization of the primary H^+ ion of acid.

TABLE 5

Mean Specific Rate of Solution of Apatite in Solutions of Phosphoric Acid, Neutralized by 18% Magnesium

P_2O_5 Content in the solution (as %)	9.33	19.2	28.7	34	40	45.5	48.5	58.3
$\bar{v}$	2.88	3.51	3.66	2.80	2.22	1.40	1.01	0.129

SUMMARY

1. As a result of the investigation of the rate of solution of apatite in solutions of phosphoric acid, partially neutralized by magnesium (in solutions of the system $MgO-P_2O_5-H_2O$) at 25° it was shown that the constant of the rate of solution calculated from the Shchukarev-Nernst equation does not remain constant and depends on the degree of neutralization of the acid, passing through a maximum at an MgO content of 2-3%. Possible explanations of this phenomenon were discussed.

2. An empirical equation, connecting the rate of solution with the degree of neutralization of the solution, was proposed.

3. The relationship between the rate of solution of apatite in solutions with a constant degree of neutralization of acid and the P_2O_5 content was investigated and it was shown that the maximum value of the rate of solution at 25° is attained at a P_2O_5 content of 25-30% in the liquid phase.

LITERATURE CITED

[1] M. L. Chepelevetskii and E. B. Brutskus, The Physicochemical Bases of the Production of Superphosphate, State Chem. Press, Moscow (1958).*

[2] M. L. Chepelevetskii, Trans. Scientific Research Inst. of Fertilizers and Insectifuges, 137 (1937).

[3] V. G. Levich, Physicochemical Hydrodynamics, Acad. Sci. USSR press, Moscow (1952).*

[4] K. S. Krasnov, J. Appl. Chem. 28, 1275 (1955).**

Received July 8, 1956

*In Russian.

**Original Russian pagination. See C. B. Translation.

KINETICS OF THE ABSORPTION OF NITROGEN OXIDES IN CONCENTRATED NITRIC ACID*

V. I. Atroshchenko and V. M. Kaut

The V. I. Lenin Polytechnic Institute, Kharkov

Separation of nitrogen oxides from nitrous gases is one of the principal operations in the production of concentrated nitric acid by direct synthesis. In the technological process, this operation is performed in two steps. The nitrogen oxides are first absorbed in nitric acid, and are then distilled in concentrated form out of the resultant solution (nitrooleum).

The available literature data on the kinetics of absorption of nitrogen oxides in concentrated nitric acid are very scanty and incomplete.

The known investigations include the papers by Pascal and Garnier [1] on the solubility of liquid oxides of nitrogen in concentrated nitric acid, of Klemens and Rupp [2] on density and total vapor pressure in the systems HNO_3-NO_2 and $HNO_3-NO_2-H_2O$, of Klemens and Spiess [3] on the mutual solubility of nitric acid and liquid oxides of nitrogen, of Lowry and Lemon [4] on the system $N_2O_4-H_2O$ in relation to the solution composition and temperature, and of Kuznetsov-Fetisov et al., [5] and of Verkhovskaia and Zhavoronkov [6] on the partial pressures of the components in the gas phase over a solution of NO_2 in nitric acid.

The data of Tikhonov et al., [7] and Pronin et al., [5] on the solubilities of gaseous oxides of nitrogen in concentrated nitric acid are of great interest.

The first investigations on the kinetics of absorption of nitrous gases in concentrated nitric acid were performed by Eidel'man and Atroshchenko [5]. However, low gas velocities and a stationary liquid were used in these investigations.

No data are available in the literature on the variations of the absorption rate with accumulation of nitrogen oxides in the solution, on the influence of the nitric oxide present in the nitrous gases on the rate of the process, etc.

New determinations were performed in order to obtain the data, lacking in the literature, on the kinetics of absorption of nitrogen oxides in concentrated nitric acid, and in order to find experimental conditions approximating to the industrial conditions used in the absorption of nitrogen oxides.

EXPERIMENTAL

The apparatus used for studies of the kinetics of absorption of nitrogen oxides in concentrated nitric acid is shown schematically in Fig. 1.

The main part of the apparatus consisted of trickle tubes (columns) made of laboratory glass and enclosed in thermostats of transparent plastic. The tubes were from 33.5 to 35.0 mm in internal diameter, and 845, 1830, and 2455 mm long. The tube lengths were designed to ensure approximately equal times of contact between the gas and the liquid, so that correct conclusions could be drawn concerning the effect of the linear gas velocity on the absorption process.

*This research forms the basis of Aspirant V. M. Kaut's dissertation.

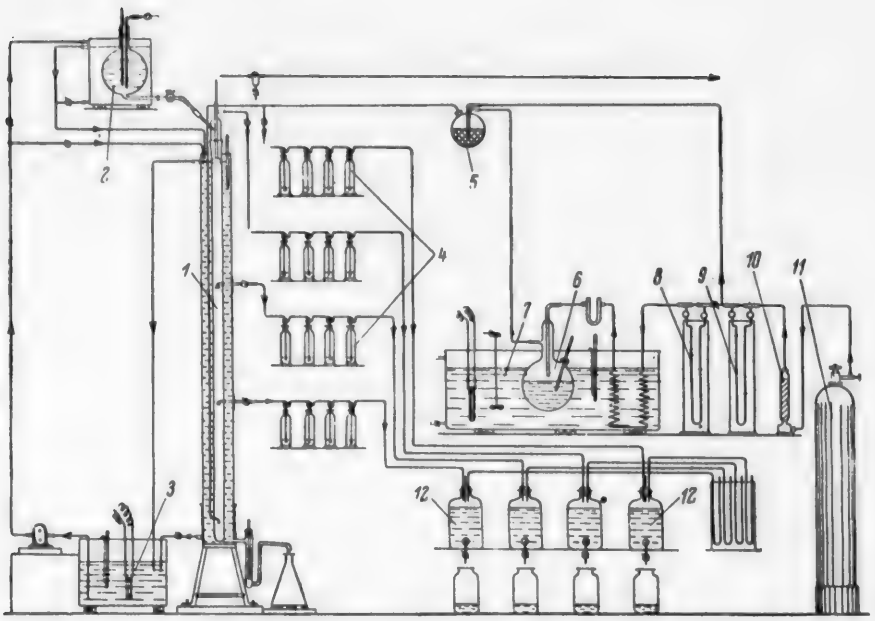

Fig. 1. Absorption apparatus. 1) Absorption column; 2) header; 3) receiver; 4) Dreschel flasks; 5) mixer; 6) evaporator; 7) evaporator thermostat; 8 and 9) flow meters; 10) drying column; 11) nitrogen cylinder; 12) aspirators.

For studies of the absorption mechanism and determination of the mass-transfer coefficients along the course of the gas, gas samples were taken for analysis before entry into the apparatus, at the exit, and along the column.

A definite amount of gas of fixed composition was obtained by the passage of nitrogen through the evaporator with liquid oxides of nitrogen. Highly concentrated nitric acid was prepared by distillation of 96% acid, and liquid nitrogen tetroxide was obtained by distillation of technical 97% nitrogen oxides.

The composition of the nitrous gas at each point of the apparatus was determined by absorption in sulfuric acid. The total nitrogen content in the gas was determined by means of a nitrometer, and the nitrosylsulfuric acid content was determined by oxidation of $HSNO_5$ by potassium permanganate solution.

The acid or nitrooleum were analyzed as follows. A sample of the liquid was collected in an ampoule, and the contents of the ampoule were absorbed in alkali solution. The total acidity was found from the amount of alkali required, and the nitrite content was determined from the amount of potassium permanganate taken for oxidation of $NaNO_2$.

The theoretical considerations of the absorption kinetics of nitrogen oxides were based on the general physical principle that the rate of the process is proportional to the driving force and inversely proportional to the resistance.

Our results show that the kinetics of the absorption process in question is described most correctly by the equation [5] which is written as follows in the integral form:

$$K_1 = \frac{\rho}{\tau}\left[\frac{(p_g^0 - p_g^\tau)}{(p_g^0 - p_i^\tau) - (p_g^\tau - p_i^0)}\right] \ln \frac{p_g^0 - p_i^\tau}{p_g^\tau - p_i^0}, \qquad (1)$$

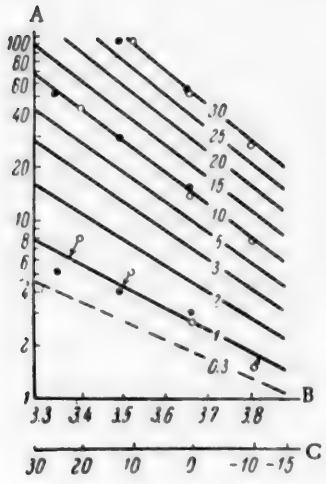

Fig. 2. Vapor pressures p_{NO_2} and $p_{N_2O_4}$ over a solution of nitrogen oxides in highly concentrated nitric acid. A) Pressure of $NO_2 + N_2O_4$ vapors (in mm Hg), B) values of $\frac{1}{T} \cdot 10^3$, C) temperature (°C). The numbers on the lines represent the N_2O_4 contents (in wt. %).

where p_g^0 and p_g^τ are the partial pressures of nitrogen oxides (NO_2 and N_2O_4) in the initial and final gas (in mm Hg); p_i^0 and p_i^τ are the pressures of nitrogen oxides over the acid (in mm Hg); K_1 is the absorption-rate coefficient (in cm/sec); ρ is the mean radius of the packing (in cm), equal to the ratio of the open volume of the packing to its surface, or d/4; d is the internal diameter of the absorption tube (in cm); τ is the absorption time (in seconds).

The following equations were also used for analysis of the experimental data:

$$K_2 = \frac{\rho}{\tau} \ln \frac{p_g^0 - p_i^\tau}{p_g^\tau - p_i^0}, \qquad (2)$$

$$K_3 = \frac{\rho}{\tau} \ln \frac{p_g^0}{p_g^\tau}. \qquad (3)$$

The pressure of nitrogen oxides ($p_{NO_2} + p_{N_2O_4}$) over the solution was found from the data of Klemens and Rupp [2] and of Verkhovskaia and Zhavoronkov [6], plotted in Fig. 2. The vapor pressures of nitric acid and water were taken from Taylor's data [8].

The experimental conditions were such as to exclude the influence of the liquid rate; the liquid rate (calculated for the perimeter of the tube) was 0.5 $cm^3/cm^2 \cdot$second or 18 $m^3/m^2 \cdot$hour.

The main experimental results are summarized in Tables 1-4. It is clear from the data in Table 1 and Fig. 3 that the rate coefficients K_1 and K_2 are roughly constant with between 1.3 and 26% of NO_2 in the original gas.

The small decrease of the absorption-rate coefficient of NO_2 up the column is partially accounted for by the greater turbulence at the entry of the gas into the absorber.

The absorption rate coefficients K_3, calculated from Equation (3), remain roughly constant over the concentration range of 7 to 32% in the initial gas. With less than 7% NO_2 in the gas at the entry into the absorber the values of K_3 diminish.

The rate coefficient is independent of the NO_2 concentration in the gas

$$K \approx f[\%\ NO_2] \approx \text{const}; \qquad (4)$$

consequently the rate of absorption of nitrogen oxides in concentrated nitric acid depends mainly on the driving force of absorption.

It also follows from our results that the presence of some nitric oxide (up to 1.3%) in the original gas has no effect at all on the coefficient of the rate of absorption of nitrogen oxides in nitrooleum of low concentrations. At w = 40 cm/sec, with 98.5% HNO_3, $K_{2\,av}$ is 0.370 at 30°, 0.441 at 15°, and 0.460 at 0°. The oxidation of nitric oxide leads to a decrease of the nitric acid concentration, with an adverse effect on the absorption rate.

$$NO + 2HNO_3 \rightleftarrows 3NO_2 + H_2O \qquad (5)$$

TABLE 1

Effect of Gas Concentration on the Absorption Rate of Nitrogen Oxides (NO_2 and N_2O_4) with Gas Velocity 0.2 m/second, HNO_3 Concentration 98.4% and Temperature 15°

NO_2 conc. in original gas (vol. %)	NO_2 conc. in gas after 1.64 sec. (vol. %)	NO_2 absorption-rate coefficients after 1.64 sec. (cm/sec)			NO_2 conc. in gas after 2.87 sec. (vol. %)	NO_2 absorption-rate coefficients after 2.87 sec. (cm/sec)			NO_2 conc. in gas after 4.01 sec. (vol. %)	NO_2 absorption-rate coefficients after 4.01 sec. (cm/sec)		
		K_1	K_2	K_3		K_1	K_2	K_3		K_1	K_2	K_3
1.3	0.9	0.391	0.365	0.215	0.67	0.378	0.344	0.182	0.55	0.388	0.353	0.172
4.2	2.2	0.413	0.386	0.316	1.4	0.386	0.359	0.301	1.05	0.376	0.351	0.278
7.5	3.6	0.421	0.396	0.358	2.6	0.342	0.321	0.298	1.7	0.359	0.337	0.300
8.7	3.9	0.428	0.405	0.374	2.6	0.374	0.353	0.318	2.0	0.373	0.352	0.317
9.9	4.4	0.429	0.406	0.377	2.7	0.403	0.383	0.357	2.0	0.376	0.356	0.327
26.0	10.8	0.436	0.426	0.413	7.4	0.377	0.368	0.346	4.6	0.380	0.371	0.334

TABLE 2

Effect of Linear Gas Velocity on the Absorption Rate of Nitrogen Oxides (NO_2 and N_2O_4) at 15°

Gas velocity w (in m/sec)	HNO_3 content of solution (wt. %)	NO_2 conc. in original gas (vol. %)	NO_2 conc. in gas after time τ_1 (vol. %)	Contact time τ_1 (sec)	NO_2 absorption-rate coefficient after time τ_1 K_2 (cm/sec)	NO_2 conc. in gas after time τ_2 (vol. %)	Contact time τ_2 (sec)	NO_2 absorption-rate coefficient after time τ_2, K_2 (cm/sec)	NO_2 conc. in gas after time τ_3 (vol. %)	Contact time τ_3 (sec)	NO_2 absorption-rate coefficient after time τ_3, K_2 (sec)
0.6	89.6	9.8	5.5	1.26	0.359	4.0	2.59	0.324	2.3	3.86	0.337
0.4	90.4	9.0	3.9	1.82	0.352	2.8	3.08	0.326	2.0	4.34	0.308
0.2	89.6	10.7	5.7	1.64	0.288	4.7	2.87	0.230	3.4	4.01	0.255
0.6	98.2	10.6	5.3	1.26	0.502	3.1	2.59	0.446	1.7	3.86	0.477
0.4	98.5	10.3	3.6	1.82	0.486	2.3	3.08	0.429	1.4	4.34	0.436
0.2	98.3	9.7	4.7	1.64	0.382	3.0	2.87	0.348	1.8	4.01	0.350

It follows from Table 2 and Fig. 4 that the mass-transfer coefficients increase with increase of the gas velocity.

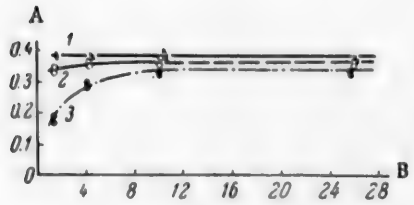

Fig. 3. Effect of gas concentration on the absorption-rate coefficients of nitrogen oxides at linear gas velocity 0.2 m/second and 15°, for 98% HNO_3. A) Coefficient K (cm/sec), B) NO_2 content of gas (vol. %). Coefficients calculated from different equations: 1) K_1, 2) K_2, 3) K_3.

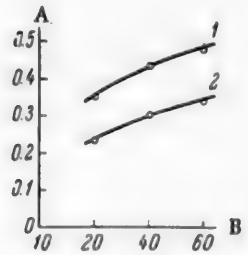

Fig. 4. Effect of linear gas velocity at 15° on the absorption-rate coefficients of nitrogen oxides. A) Absorption-rate coefficient (cm/sec), B) linear gas velocity (cm/sec). Nitric acid concentration (%): 1) 98, 2) 90.

The variation of the absorption-rate coefficient of NO_2 with the linear gas velocity (w) between 0.2 and 0.6 m/sec (or in the range $454 < Re < 1364$) is represented by the equation

$$K_2 = A \cdot Re^a, \qquad (6)$$

where Re is the Reynolds number.

The values of A and a are given below

HNO_3 (wt. %)	98		90	
t (°C)	−10	+15	−10	+15
A	0.0713	0.0619	0.0518	0.0316
a	0.280	0.283	0.317	0.331

For decolorized acid, containing from 90 to 98% HNO_3, $a \approx 0.3$.

The coefficients of the rate of absorption of NO_2 in concentrated nitric acid (within the limits studied) can be found from the equation

$$K'' = K' \left(\frac{w''}{w'}\right)^{0.3} \qquad (7)$$

Our value for the power of the Reynolds number coincides with the findings of Greenwalt [9] and of Hollings and Silver [10] and is close to the results obtained by Malïusov, Malafeev, and Zhavoronkov [11] for the absorption of easily soluble gases.

The absorption of nitrogen oxides increases considerably with increasing concentration of HNO_3 in solution. The variation of the mass-transfer rate coefficients with acid concentration are given in Table 3 and Fig. 5.

The relationship between K_2 and the acid concentration is given by the equation

$$K_2 = B \cdot e^{b \cdot z}, \qquad (8)$$

where e is the base of natural logarithms, and z is the HNO_3 content of the acid (in wt. %).

Values of B and b are given below

w (m/sec)	0.2				0.4			
t (°C)	−10	0	+15	+30	−10	0	+15	+30
B	0.01344	0.01249	0.00538	0.00493	0.01634	0.015350	0.00844	0.00614
b_{av}	0.0343		0.0419		0.0343		0.0419	

In the light of the data of Klemens and Rupp [2] and of the results of this investigation, the mechanism of the absorption of nitrogen oxides in highly concentrated nitric acid may be represented as follows.

TABLE 3

Effects of Acid Concentration and Temperature on the Absorption Rate of Nitrogen Oxides (NO_2 and N_2O_4) with Gas Velocity 0.4 m/second

HNO_3 content of solution (wt.%)	Temperature t (°C)	NO_2 conc. in original gas (vol. %)	NO_2 conc. in gas after time τ_1 (vol. %)	Contact time τ_1 (sec.)	NO_2 absorption-rate coeff. after time τ_1, K_2 (cm/sec)	NO_2 conc. in gas after time τ_2 (vol. %)	Contact time τ_2 (sec.)	NO_2 absorption-rate coeff. after time τ_2, K_2 (cm/sec)	NO_2 conc. in gas after time τ_3 (vol. %)	Contact time τ_3 (sec.)	NO_2 absorption-rate coeff. after time τ_3, K_2 (cm/sec)
98.6	— 9.5	9.7	2.9	2.00	0.513	1.5	3.37	0.506	0.9	4.75	0.470
98.5	+ 0.2	10.2	3.2	1.93	0.511	2.0	3.24	0.453	1.2	4.58	0.450
98.5	+15.3	10.6	3.6	1.82	0.436	2.5	3.08	0.417	1.6	4.36	0.426
98.4	+29.7	10.6	5.0	1.73	0.388	3.8	2.93	0.361	2.7	4.13	0.330
90.5	—10.2	9.7	3.6	2.00	0.416	2.2	3.37	0.403	1.5	4.75	0.357
90.4	0	9.5	3.7	1.93	0.400	2.6	3.24	0.351	1.7	4.58	0.343
90.5	+14.7	9.0	4.1	1.82	0.332	2.8	3.08	0.316	2.0	4.34	0.308
90.4	+29.6	9.8	5.0	1.73	0.278	3.2	2.93	0.257	2.5	4.13	0.260
80.3	—10.3	10.6	5.3	2.00	0.285	4.3	3.37	0.232	2.8	4.75	0.247
80.4	0.4	8.8	4.9	1.93	0.234	4.0	3.24	0.210	2.5	4.58	0.244
80.4	15.5	10.9	6.2	1.82	0.203	5.4	3.08	0.182	3.5	4.34	0.223
80.3	30.3	11.6	7.5	1.73	0.158	6.5	2.93	0.149	5.2	4.13	0.151
70.3	— 9.9	9.9	6.3	2.00	0.185	5.0	3.37	0.175	3.6	4.75	0.187
70.2	0.1	11.1	7.7	1.93	0.162	6.4	3.24	0.150	4.7	4.58	0.166
70.4	14.8	10.0	7.6	1.82	0.134	6.9	3.08	0.121	5.5	4.34	0.130
70.4	30.2	10.1	7.7	1.73	0.100	6.9	2.93	0.096	5.6	4.13	0.106

TABLE 4

Effect of the Contents of Nitrogen Oxides (N_2O_4) in Nitrooleum on the Absorption Rate of Gaseous Nitrogen Oxides (NO_2 and N_2O_4) with Gas Velocity 0.4 cm/second

HNO_3 in solution (wt. %)	N_2O_4 in nitrooleum (wt. %)	Temperature t (°C)	NO_2 conc. in original gas (vol. %)	NO_2 conc. in gas after 2.00 sec. (vol. %)	NO_2 absorption-rate coeff. K_2 (cm/sec.)	NO_2 conc. in gas after 3.37 sec. (vol. %)	NO_2 absorption-rate coeff. K_2 (cm/sec.)	NO_2 conc. in gas after 4.75 sec. (vol. %)	NO_2 absorption-rate coeff. K_2 (cm/sec.)
98.4	0.8	—9.2	11.0	3.3	0.530	1.7	0.495	1.0	0.479
98.4	9.1	—9.0	9.1	3.8	0.460	2.5	0.433	1.8	0.420
98.2	15.6	—9.1	10.2	5.4	0.354	3.7	0.348	3.0	0.323
98.0	22.9	—9.0	9.5	7.4	0.185	6.3	0.171	5.6	0.148
98.2	16.0	+0.2	10.7	8.0	0.235	6.7	0.218	5.9	0.192

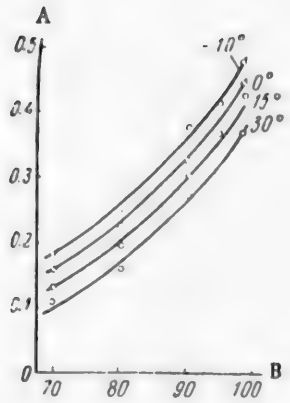

Fig. 5. Effect of acid concentration at gas velocity 0.4 m/second on the absorption-rate coefficient of nitrogen oxides. A) Absorption-rate coefficient (cm/sec), B) HNO_3 content (wt. %).

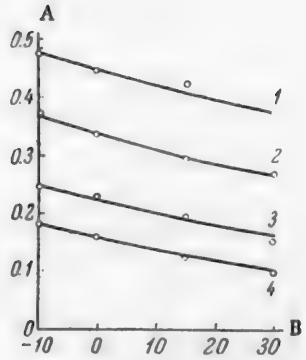

Fig. 6. Effect of temperature at gas velocity 0.4 m/second on the absorption-rate coefficient of nitrogen oxides. A) Absorption-rate coefficient (cm/sec), B) temperature (°C). Concentration of HNO_3 (in wt. %): 1) 98; 2) 90; 3) 80; 4) 70.

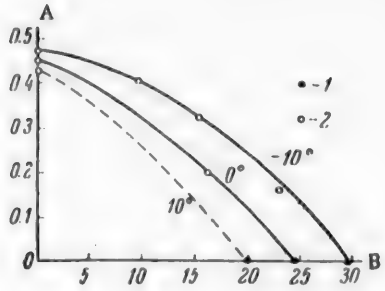

Fig. 7. Effect of the N_2O_4 content of nitrooleum on the absorption-rate coefficient of nitrogen oxides, at gas velocity 0.4 m/second, 98% HNO_3 in the solution, and 10% NO_2 in the gas. A) Absorption-rate coefficient (in cm/sec), B) N_2O_4 content (wt. %). 1) A. V. Tikhonov's data, 2) our data.

Gaseous oxides of nitrogen diffuse through the interface. NO_2 reacts with HNO_3 in the liquid phase to form the compounds $HNO_3 \cdot NO_2$.

Table 3 and Fig. 5 show that the absorption-rate coefficient increases with decrease of temperature. The variations of the absorption-rate coefficient with temperature are represented graphically in Fig. 6.

The relationship between K_2 and temperature in the range studied may be mathematically expressed by the formula

$$K_2 = D \cdot T^d, \qquad (9)$$

where T is the temperature (in °K).

Values of D and d are given below.

HNO_3 (wt. %)	98		90		80		70	
w (m/sec)	0.2	0.4	0.2	0.4	0.2	0.4	0.2	0.4
D	798.7	979.3	589.8	750.8	424.3	500.5	300.4	343.9
d_{av}	—1.37				—1.22			

The influence of the temperature factor increases considerably with increase of the N_2O_4 content in the solution.

It follows from Table 4 and Fig. 7 that the absorption-rate coefficient decreases with increasing content of N_2O_4 in solution.

The relationship between K_2 and the N_2O_4 content of the solution is represented by the formula

$$K_2 = C + a \cdot e^{cx}, \tag{10}$$

where x is the concentration of nitrooleum (in wt. %).

The constants a, C, and c have the following values for nitrooleum containing 98% HNO_3, at gas velocity 0.4 m/second:

t (°C) . . .	−10	0	+10
a	−0.096	−0.363	−0.466
C	0.564	0.812	0.878
c	0.0598	0.0320	0.0315

The factors with the greatest influence on the rate of the process are the acid concentration, the N_2O_4 content of the nitrooleum, the temperature, and the linear velocity of the gas.

The following empirical equations for determination of absorption-rate coefficients were derived.

For acids with low contents of nitrogen oxides

$$\log K_2 = 1.655 + 0.3 \log w - 1.37 \log T + 0.0149 \cdot z \tag{11}$$

or $K_2 = 44.9 \cdot w^{0.3} \cdot T^{-1.37} \cdot e^{0.344} \cdot z$,

where z is the concentration of HNO_3 $85 < z < 98$ wt. %, T is the temperature $263 < T < 283°K$, w is the linear velocity of the gas $0.2 < w < 0.6$ m/second.

For 98% HNO_3 at $t = -10°$ and $w = 0.4$ m/second

$$\log (0.564 - K_2) = 0.0251 \cdot x - 1.018. \tag{12}$$

For 98% HNO_3 at $t = 0°$ and $w = 0.4$ m/second

$$\log (0.812 - K_2) = 0.0139 \cdot x - 0.440, \tag{13}$$

where x is the N_2O_4 content of the acid (wt. %), K_2 is the absorption-rate coefficient (in cm/sec). The values of K_2 (in cm/sec) for the most typical conditions, with $w = 0.4$ m/second are given below.

Temperature (°C)	N_2O_4 Content of 98% nitric acid (in wt. %)					
	0.3	5	10	15	20	25
+10	0.430	0.335	0.240	0.130	—	—
0	0.455	0.385	0.310	0.230	0.125	—
−10	0.480	0.435	0.390	0.330	0.240	0.135

SUMMARY

1. The variations of the coefficients of the absorption rate of nitrogen oxides in concentrated nitric acid with the following principal physicochemical factors have been determined: concentration of nitrogen oxides (NO_2 and N_2O_4) in the gas phase, the content of nitric oxide in the gas, the HNO_3 concentration of the acid, the N_2O_4 content of the solution, and the temperature.

2. The effects of the principal hydrodynamic factors on the absorption-rate coefficients have been demonstrated.

LITERATURE CITED

[1] E. Pascal and E. Garnier, Bull. Soc. chim. France 25, 309 (1919).

[2] A. Klemens and J. Rupp, J. anorg. Ch. 194, 51 (1930).

[3] A. Klemens and T. Spiess, Monatsh. 77, 216 (1947).

[4] T. M. Lowry and J. T. Lemon, J. Chem. Soc. 1 (1936); 6 (1936).

[5] V. I. Atroshchenko and S. I. Kargin, Nitric Acid Technology (Goskhimizdat, 1949).*

[6] Z. I. Verkhovskaia, Candidate's dissertation (MKhTI, 1950).

[7] I. D. Fotinich, Production of Concentrated Nitric Acid (Goskhimizdat, 1952).*

[8] G. B. Taylor, Ind. Eng. Ch. 17, 633 (1925).

[9] C. H. Greenwalt, Ind. Eng. Ch. 18, 1291 (1926).

[10] H. Hollings and L. Silver, Trans. Inst. Chem. Engrs. (London), 12, 49 (1934).

[11] V. A. Mallusov, N. A. Malafeev and N. M. Zhavoronkov, J. Chem. Ind. 4, 110 (1953).

Received October 25, 1956

* In Russian.

ADSORPTION OF NITROGEN OXIDES BY ALUMINOSILICATE SORBENT*

S. N. Ganz

The Dnepropetrovsk Institute of Chemical Technology

The results of a study of the adsorption of nitrogen oxides by a number of granular sorbents were given in the previous communication [1]. Comparison of the adsorptive power and physical properties of the sorbents showed that aluminosilicate is the most suitable sorbent for nitrogen oxides.

The present communication contains more detailed experimental data on the adsorption of nitrogen oxides by aluminosilicate in relation to the NO + NO_2 concentration of the gas, the degree of oxidation of NO, the space velocity, and the moisture content of the gas.

EXPERIMENTAL**

The apparatus used for studying the adsorption of nitrogen oxides by aluminosilicate is shown schematically in Fig. 1. Nitric oxide from the gas holder 1 and air from the gas holder 2 were fed in definite proportions into the mixer 3. The amounts of air and NO were measured by means of the flow meters 4. According to the purpose of the experiment, the gases before mixing were either passed through the vessels 5 containing concentrated sulfuric acid, for drying the gases, or entered the mixer 3 through the by-pass tubes 6.

If moist gases were required, the gases were passed through the vessels 5 filled with distilled water at a definite temperature.

The mixers used were of different dimensions, as they also served as the oxidation vessels. The approximate degree of oxidation of NO before adsorption was estimated from the volume of the mixer. From the mixer, the gas mixture entered the glass adsorption column 7, with a porous bottom d, containing the sorbent s. Before the start of each experiment the gas leaving the mixer was analyzed for total content of nitrogen oxides by the evacuated-bulb method, and for the degree of oxidation of NO. The degree of oxidation was determined iodometrically [2], by absorption of NO_2 in 5% KI solution in the absorption flasks 8.

The total content of NO + NO_2 in the gas after adsorption was also determined by the evacuated-bulb method, and the exhaust nitrogen oxides were absorbed in 10% NaOH solution in the vessels 9 and in $FeSO_4$ solution in vessel 10. Samples of gas for analysis were taken through the tubes 11, and the gas pressures at entry and exit were measured by means of manometers.

The aluminosilicate used was in the form of orange or milk-white balls 3 mm in diameter. Aluminosilicate grains of equal size were selected by means of suitable sieves. The bulk density of the sorbent was 0.72 ton/m^3, the free space in the sorbent was approximately 0.38 m^3/m^3, and the compressive strength of a single grain was ~90 kg.***

The amount of sorbent in the column was 50 cc in all experiments. The height of the sorbent layer was 27.5 cm, and its initial weight was 35.8 g. The amount of nitrogen oxides adsorbed was determined from the formula:

---

*Communication II.

**L. S. Gurevich assisted in the experimental work.

***The composition and method of preparation of the aluminosilicate sorbent are briefly described in the literature [3,4].

$$G = \frac{(V_{NO} + V_{NO_2})_{init} - (V_{NO} + V_{NO_2})_{fin}}{22400} \cdot M_{av}, \quad (1)$$

where $(V_{NO} + V_{NO_2})_{init}$ represents the volumes of NO and NO_2, determined separately and reduced to standard conditions, at entry (in cc); $(V_{NO} + V_{NO_2})_{fin}$ are the corresponding volumes at the exit (in cc); M_{av} is the average molecular weight of NO + NO_2, calculated from the percentage contents of NO + NO_2 in the gas.

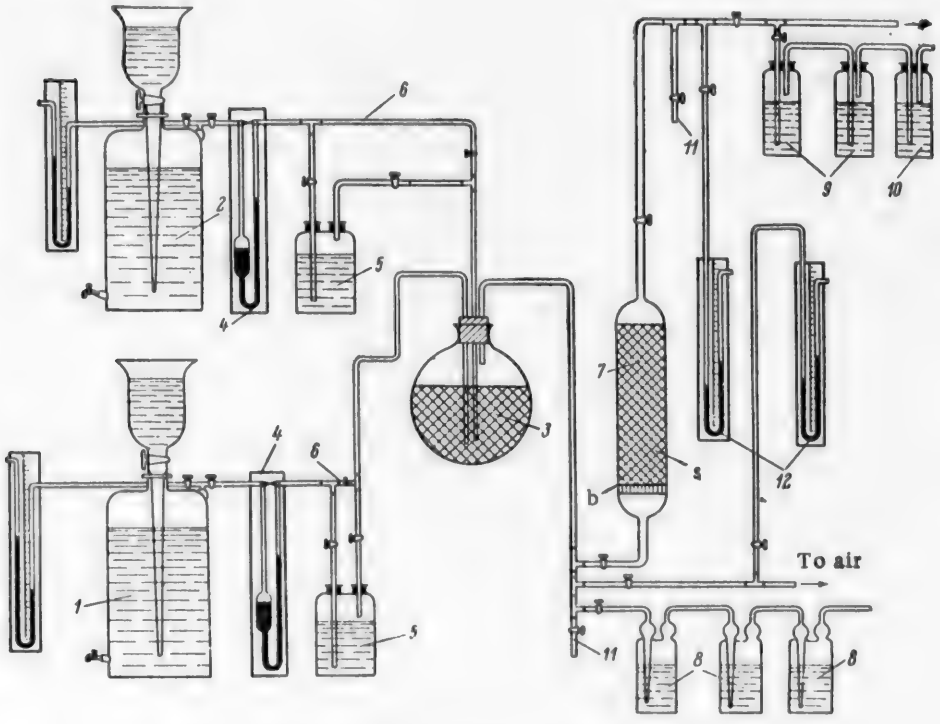

Fig. 1. Diagram of experimental unit. Explanations in text.

The amounts of nitrogen oxides absorbed were also determined by simple weighing of the sorbent on an analytical balance before and after adsorption.

Two oxidation vessels, the smaller of 50 cc and the larger of 2270 cc, were used in experiments on the variations of the rate of adsorption of nitrogen oxides with the degree of oxidation of NO, and on the catalytic effect of the sorbent on the oxidation rate of NO.

Average results obtained under static conditions in the adsorption column 7 are given below; experimental data obtained in a larger unit with moving sorbent are also examined.

Results of the Experiments

In the first series of experiments the variations of the degree and rate of adsorption of nitrogen oxides with their concentration in the gas, the degree of oxidation of NO, and the space velocity were studied. The results of these experiments are plotted in Figs. 2-5.

Figure 2 gives data on the degree of adsorption of nitrogen oxides which passed through the smaller oxidation vessel. The degree of oxidation of NO naturally decreased with increasing space velocity, since the gas was present for a shorter time in the oxidation vessel. The following results were obtained for space velocities $w \approx 1000$-1150 m^3/m^3 sorbent·hour:

Concentration of nitrogen oxides (%)	Degree of oxidation of NO (%)
0.5	5–7
1.06	18–21
1.52	22–25
2.15	30–36

It follows from the data in Fig. 2 that the adsorption of nitrogen oxides increases with increasing concentration and degree of oxidation of the nitrogen oxides in the gas. Increase of space velocity always leads to a decrease of the degree of adsorption of nitrogen oxides because of the decreased time of contact between the gas and the sorbent. Up to space velocities of 400-500 $m^3/m^3 \cdot$hour the degree of adsorption decreases smoothly at a diminishing rate. With further increase of space velocity the adsorption curves descend more steeply.

The adsorption rates of nitrogen oxides were calculated from the experimental data presented in Fig. 2; the values found are plotted in Fig. 3. Figure 3 shows that the yield per unit volume of aluminosilicate sorbent increases with increasing concentration of nitrogen oxides and with the space velocity. The latter, however, is only true up to w = 600-900 $m^3/m^3 \cdot$hour. Further increase of space velocity leads to a decrease of the adsorption rate or, which is the same thing, to a decrease of the sorptive capacity of unit volume of the sorbent per unit time. This also applies to a moving sorbent which travels downward, countercurrent to the gas, through the adsorption zone; under these conditions the saturation of the sorbent with nitrogen oxides did not exceed 60-65% of the equilibrium value. The adsorption coefficients calculated from the experimental data are plotted in Fig. 4.

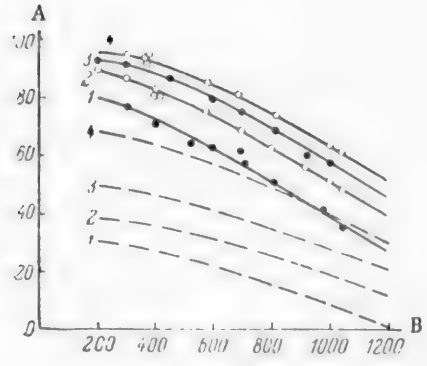

Fig. 2. Variations of the degree of adsorption of nitrogen oxides with the space velocity, the concentration of NO + NO_2 in the gas, and the degree of oxidation of NO; t = 18-20°. A) Degree of adsorption (%), B) space velocity (m^3 gas/m^3 sorbent·hour). Continuous lines – degree of adsorption, dash lines – degree of oxidation of NO. Concentration of NO + NO_2 (in %): 1) 0.5; 2) 1.08; 3) 1.52; 4) 2.15.

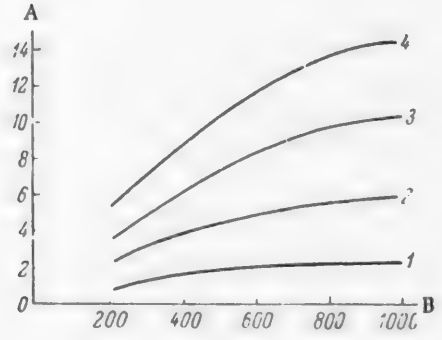

Fig. 3. Rate of adsorption of nitrogen oxides in countercurrent flow of aluminosilicate and gas, at different concentrations of NO + NO_2 and space velocities; t = 18-20°. A) Adsorption rate (kg/$m^3 \cdot$hour), B) space velocity ($m^3/m^3 \cdot$hour). Concentration of NO + NO_2 (%): 1) 0.5; 2) 1.08; 3) 1.52; 4) 2.15.

In calculations of the adsorption coefficients, the driving force was taken to be the logarithmic mean difference of the partial pressures of NO + NO_2 at entry and exit. It follows from Fig. 4 that the maximum adsorption coefficients correspond to space velocities of 600-700 $m^3/m^3 \cdot$hour.

Therefore, the use of space velocities higher (in this instance) than 600-700 $m^3/m^3 \cdot$hour is inexpedient, as the degree and coefficient of adsorption decrease.

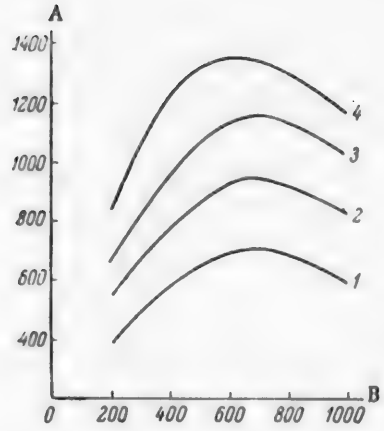

Fig. 4. Variations of the coefficients of adsorption of nitrogen oxides by aluminosilicate with the space velocity and the $NO + NO_2$ concentration, t = 18-20°. A) Adsorption coefficient ($kg/m^3 \cdot hour \cdot atm$), B) space velocity ($m^3/m^3 \cdot hour$). Concentration of $NO + NO_2$ (%): 1) 0.5; 2) 1.08; 3) 1.52; 4) 2.15.

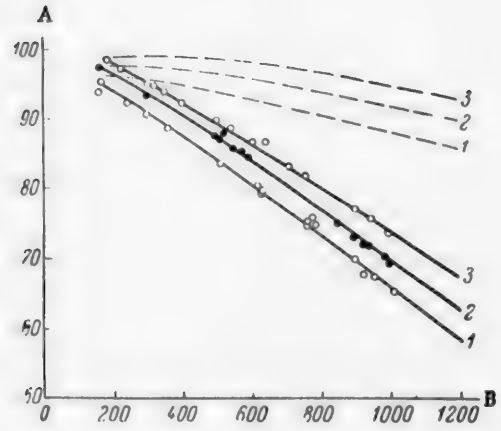

Fig. 5. Variations of the degree of adsorption with the space velocity, concentration of $NO + NO_2$, and the degree of oxidation of NO at t = 22-23°. A) Degree of adsorption (%), B) space velocity ($m^3/m^3 \cdot hour$). Continuous lines — degree of adsorption, dash lines — degree of oxidation of NO. Concentration of $NO + NO_2$ (%): 1) 1.1; 2) 2.08; 3) 2.94.

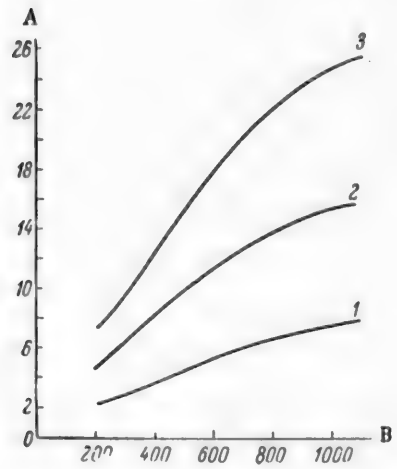

Fig. 6. Variations of adsorption rate with the space velocity and the concentration of $NO + NO_2$, t = 22-23°. A) Adsorption rate (in $kg/m^3 \cdot hour$), B) space velocity ($m^3/m^3 \cdot hour$). Concentration of $NO + NO_2$ (%): 1) 1.1; 2) 2.08; 3) 2.94.

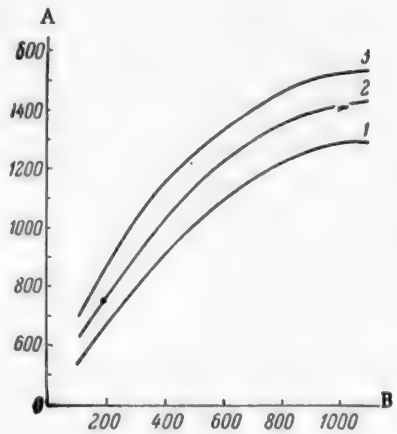

Fig. 7. Variations of the adsorption coefficient with the space velocity and the concentration of $NO + NO_2$. A) Adsorption coefficient ($kg/m^3 \cdot hour \cdot atm$), B) space velocity ($m^3/m^3 \cdot hour$). Concentration of $NO + NO_2$ (%): 1) 1.1; 2) 2.08; 3) 2.94.

Figure 5 shows the effects of the same factors as those shown in Fig. 2 on the degree of adsorption of nitrogen oxides, but in this instance the gas was passed through the larger oxidation vessel (V = 2270 cc), so that the degree of oxidation of NO was considerably higher than before (see Fig. 2).

The curves for the degree of oxidation of NO (dash lines) in Fig. 5 lie considerably higher than in Fig. 2 for similar concentrations of nitrogen oxides. It also follows from Fig. 5 that the degree of adsorption of

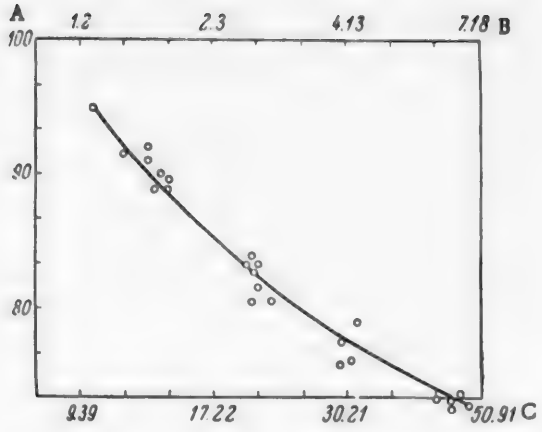

Fig. 8. Variation of the degree of adsorption of nitrogen oxides with the moisture content of the gas (concentration of NO + NO_2 = 1.25-1.28%, w = 500 $m^3/m^3 \cdot$hour). A) Degree of adsorption (%), B) moisture content of gas (%), C) moisture content of gas (in g/m^3).

NO + NO_2 increases with increasing concentration of nitrogen oxides in the gas and with increasing time of contact between the gas and sorbent (i.e., with decreasing w). Comparison of Figs. 2 and 5 suggests that the degree of oxidation of NO has some influence on the degree and rate of adsorption. The degree of adsorption of nitrogen oxides is higher at higher degrees of oxidation of NO. The effect of the degree of oxidation on the rate of adsorption can be found from the general equation for mass transfer.

$$\frac{dx}{d\tau} = k' \cdot x \text{ or } k \cdot \tau = \log \frac{x_0}{x \cdot \tau} = \log \frac{1}{1-\alpha}, \quad (2)$$

where x is the concentration of NO + NO_2 in the gas, k is the adsorption coefficient, and α is the degree of adsorption (in fractions of unity).

For example, at w = 500 $m^3/m^3 \cdot$hour, with 1.1% of NO + NO_2 in the gas, the rates of the two adsorption processes can be represented as the ratio:

$$\log (1 - 0.84) : \log (1 - 0.78) = 1.27,$$

where 0.84 is the degree of adsorption of nitrogen oxides, at 1.1% concentration, with 94% oxidation of NO (see Fig. 5), and 0.78 is the degree of adsorption of nitrogen oxides at the same concentration with 34% oxidation of NO.

Therefore when the degree of oxidation of NO is increased by 60%, the degree of adsorption increases by only 6%, and the adsorption is accelerated 1.27-fold.

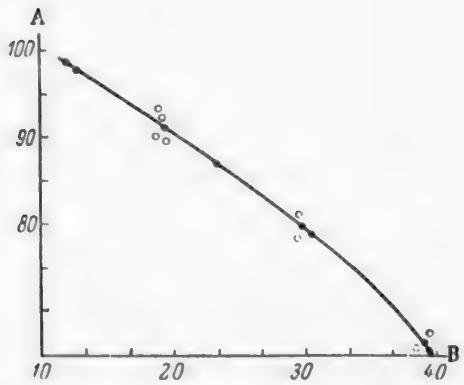

Fig. 9. Variation of the degree of adsorption of nitrogen oxides with the temperature (concentration of NO + NO_2 = 1.35%, degree of oxidation of NO = 98%, w = 500 $m^3/m^3 \cdot$hour). A) Degree of adsorption (%), B) temperature (°C).

This example, which illustrates the general course of the process, leads to the conclusion that aluminosilicate sorbent not only takes up nitrogen oxides, but also acts as a catalyst and accelerates the oxidation of NO. More detailed evidence for this is given below.

The adsorption rates and rate coefficients were calculated from the experimental data. The results are plotted in Figs. 6 and 7. Comparison of these figures with Figs. 3 and 4 shows that the adsorption rates and coefficients are greater at higher degrees of oxidation of NO (Figs. 6 and 7) than at lower. It follows that the sorbent takes up higher oxides of nitrogen.

All the foregoing applies to the adsorption of NO + NO_2 from dried gas.* However, the sorption of NO + NO_2 from moist gases is of great practical interest. For investigation of this, the air of NO entering the mixer were humidified by water vapor in flasks (see Fig. 1) at various temperatures, giving various definite degrees of saturation of the gas with water vapor. The gas temperature varied between 23 and 26°; this could not have

*The water-vapor content of the dried gas was ~8 g/m^3.

any great influence on the degree of oxidation of NO, which was 93-94% in this instance. The initial concentration of NO + NO_2 in the gas was maintained in the range 1.25-1.28%, and the space velocity w was 500 $m^3/m^3 \cdot$hour

The results of these experiments are shown graphically in Fig. 8. It is seen that the degree of adsorption, and therefore the adsorption rate, decreases with increasing concentration of water vapor in the gas.

The adsorption rate likewise decreases with increase of temperature. The following constant conditions were maintained in the 12-42° range: w = 500 $m^3/m^3 \cdot$hour, moisture content of gas 3.1%, NO + NO_2 in gas 1.35%, and degree of oxidation of NO 98-96%. The degree of adsorption fell from 97 to 78%. The results of these experiments are plotted in Fig. 9. It follows from a comparison of Figs. 8 and 9 that increase of the moisture content of the gas has a greater adverse effect on the adsorption of nitrogen oxides than increase of temperature to 40-45°. The degree of adsorption falls rapidly if the temperature is raised above 55-60°.

Desorption of nitrogen oxides and regeneration of the sorbent. Desorption of the nitrogen oxides was performed at 160, 350, and 500°. The sorbent saturated with nitrogen oxides was placed in a closed quartz tube, previously filled with nitrogen of 99.9% purity. The tube was placed in an electric furnace and nitrogen, previously heated to the appropriate temperature in another electric furnace, was blown through.

In passing through the sorbent, the nitrogen was saturated with nitrogen oxides; after leaving the furnace it was cooled in a condenser and passed through absorption vessels. In the first three vessels NO_2 was absorbed in 5% potassium iodide solution, while the next two vessels contained 10% $FeSO_4$ solution (to absorb NO).

For check analyses, the desorbed nitrogen oxides were absorbed in 10% NaOH solution. Analyses of the absorbent solutions and subsequent calculations showed that the desorbed nitrogen oxides were always in a higher state of oxidation than they were before adsorption. Calculation of the time required for oxidation of NO of 0.8-1.5% concentration showed that the oxidation rate of moist nitric oxide• is increased by a factor of 2-2.5 (corresponding to 0.8-1.5% concentrations of NO) in presence of aluminosilicate.

Experiments on the absorption of the desorbed gases in NaOH solution (the desorption temperature being 160°) showed that all the nitrogen oxides taken up by the sorbent are liberated in the form of nitric acid vapor, as their reaction with the absorbent is represented by the equation

$$NaOH + HNO_3 = NaNO_3 + H_2O.$$

In another series of experiments hot nitrous gases were used for the desorption of nitrogen oxides, as the use of this source of heat in the production of nitric acid eliminates additional cost for the heat transfer medium.

The experiments showed that nitrous gases can be successfully used for regeneration of the sorbent at temperatures above 300°. Thus, at t = 500° and a nominal velocity of 0.7 m/second for the nitrous gases in the adsorption column, 96-98% regeneration of the sorbent was effected within 10 minutes. Experiments on the adsorption and regeneration of the same sorbent were repeated 8-10 times; the sorptive capacity of the sorbent was restored almost completely after each regeneration. The physical properties and mechanical strength of the sorbent remained unchanged.

The Practical Use and Feasibility of the Method

Experiments showed that aluminosilicate sorbent has considerable sorption capacity: 1 kg of the sorbent takes up 0.0306 kg of NO_2•• at 20°. Thus, the purification of a gas containing 0.8% NO + NO_2 at a rate of 90,000 m^3/hour, to give 90% purification, requires

$$\frac{90000 \cdot 0.8 \cdot 46}{100 \cdot 22.4 \cdot 0.0306} = 48366 \text{ kg of sorbent}$$

•The moisture content of the gas reached 18.5 g/m^3.

••With 2.5% of water vapor in the gas.

Even with 100% reserve of sorbent, less than 100 tons per hour would be required. Since the sorbent can be regenerated three times per hour and used again for adsorption, the amount present in the system need be only 35-40 tons.

The experimental data obtained with the aid of the adsorption column were verified in a large-scale laboratory with moving sorbent in a three-zone apparatus. The amount of sorbent in the apparatus was 2 liters.

The regenerated sorbent was fed into the top of the column, through which nitrous exit gas was passed in the opposite direction. After the sorption the sorbent passed through pipes into the middle zone, where it met the hot nitrous gas from the contact reactors. The nitrous gas became enriched with nitrogen oxides in the course of desorption; after leaving the desorption zone it was cooled and then passed to the absorbers. The regenerated sorbent then passed through pipes into the lowest, cooling zone, where it was cooled by circulating cold air. Part of this air, containing nitrogen oxides, was fed into the absorption towers for enrichment of the gas with oxygen.

For determination of the economic feasibility of the proposed method, the calculated results obtained with this method were compared with corresponding data on the absorption of nitrogen oxides in milk of lime; the reaction volumes required for the adsorption unit were lower by a factor of 9, capital investment by a factor of 6-7, metal consumption by a factor of 12-13, and electricity consumption by a factor of 3.5-4.

SUMMARY

1. Aluminosilicate is a most effective sorbent for nitrogen oxides, and is very stable in regeneration. Because of its high sorptive capacity, mechanical strength, hardness, and heat resistance, it is very suitable for the adsorption of nitrogen oxides.

2. Aluminosilicate sorbent has a catalytic effect in accelerating the oxidation of NO to nitric acid.

3. With the use of aluminosilicate sorbent a high degree of removal of nitrogen oxides can be achieved, with much lower capital investment and operational costs than in existing methods.

LITERATURE CITED

[1] S. N. Ganz, J. Appl. Chem. 31, 1, 138 (1958).*

[2] N. M. Zhavoronkov, J. Chem. Ind. 7, 419 (1954).

[3] S. N. Obriadchikov, Petroleum Technology, 2 (State Fuel Technology Press, 1952).**

[4] V. P. Oborin, Synthetic Aluminosilicate Catalyst (Groznyi Regional Press, 1948).**

Received July 11, 1956

*Original Russian pagination. See C. B. Translation.

**In Russian.

STUDY OF THE SEPARATION OF CARBON AND OXYGEN ISOTOPES BY FRACTIONAL DISTILLATION OF CARBON MONOXIDE, METHANE, AND MOLECULAR OXYGEN

G. G. Devlatykh, A. D. Zorin, and N. I. Nikolaev

The possibility of using carbon monoxide for concentration of the rare carbon isotope C^{13} was first demonstrated by Johns, Kronberger, and London [1]. They also determined the relative volatilities of heavy-carbon and heavy-oxygen carbon monoxide at a temperature close to the triple point. We determined the relative volatilities of carbon monoxide, with different carbon and oxygen isotopes respectively, in the temperature range between the normal melting point and the normal boiling point. The vapor pressures of the carbon monoxides containing different isotopes were determined by the Rayleigh distillation method. The apparatus and method were the same as in the experiments with methane and molecular oxygen [2]. Liquid nitrogen was used as the refrigerant.

Special Features of Experiments with Liquid Carbon Monoxide

Carbon monoxide was prepared by decomposition of formic acid by hot concentrated sulfuric acid [3]. To remove any impurities present, it was distilled over a column of about 30 theoretical plates. The purity of the carbon monoxide was checked by means of the mass spectrometer. The isotope analysis of carbon monoxide was performed by means of the mass spectrometer, from the peaks of the molecular ions of the $C^{12}O^{16+}$–$C^{13}O^{16+}$ and $C^{12}O^{16+}$–$C^{12}O^{18+}$ isotopic molecules. Carbon monoxide enriched approximately 5-fold with the rare O^{18} isotope was used in most of the experiments. The use of enriched carbon monoxide considerably increased the accuracy of the isotope analysis for content of $C^{12}O^{18}$ molecules, as with carbon monoxide of natural isotopic composition the $C^{12}O^{18+}$ peak is very small in comparison with the $C^{12}O^{16+}$ peak, and it is therefore very difficult to measure with sufficient accuracy. A correction for the content of $C^{12}O^{17}$ molecules in the carbon monoxide was introduced in the mass-spectrum analysis. This correction was based on the assumption that the vapor pressure of $C^{12}O^{17}$ molecules is the geometric mean of the vapor pressures of $C^{12}O^{16}$ and $C^{12}O^{18}$ molecules. No correction for the content of $C^{13}O^{17}$ molecules was applied, as their content in the natural isotopic mixture is very low. The ratio of the densities of liquid and gaseous carbon monoxide was taken from tables [4].

Experimental Results

The results of the determinations of the vapor pressure ratios of isotopic molecules of carbon monoxide are given in Table 1.

The experimental values of the ratios are the arithmetic means of the results of numerous independent determinations. The root mean square error is given for each value of the relative volatility. The temperature–relative volatility relationships for CO molecules containing different carbon and oxygen isotopes may be represented by the equations:

$$\ln \frac{P_{C^{12}O}}{P_{C^{13}O}} = -0.00055 + 0.889/T, \qquad (1)$$

$$\ln \frac{P_{C^{13}O}}{P_{C^{12}O}} = -0.0610 + 5.41/T. \quad (2)$$

These relationships are shown graphically in Fig. 1.

Figure 1 shows that the relative volatility for heavy-oxygen carbon monoxide depends to the greater extent on the temperature. Near the triple point the vapor pressure of heavy-carbon carbon monoxide is greater than that of heavy-oxygen carbon monoxide. The reverse is true at the boiling point. The vapor-pressure difference between the heavy-carbon and ordinary carbon monoxide is the greatest found for any carbon compounds. This suggests that carbon monoxide is one of the best substances for separation of carbon isotopes by means of fractional distillation. The difference between the vapor pressures of CO^{16} and $C^{12}O^{18}$ is also considerable. As is known, oxygen enriched with O^{18} isotope is usually obtained by fractional distillation of water. Single separation factors for isotopic molecules of water and carbon monoxide are compared in Table 2.

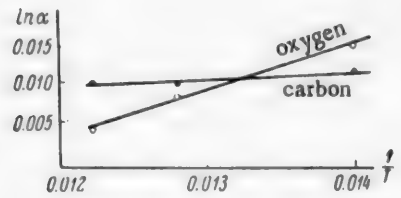

Fig. 1. Relative volatility of heavy-carbon and heavy-oxygen carbon monoxide as a function of the temperature.

TABLE 1

Relative Volatilities of Isotopic Molecules of Carbon Monoxide

Temperature (°K)	$\frac{P_{C^{13}O}}{P_{C^{12}O}}$ experimental	$\frac{P_{CO^{18}}}{P_{CO^{16}}}$ experimental	$\frac{P_{C^{13}O}}{P_{C^{12}O}}$ by Equation (1)	$\frac{P_{CO^{18}}}{P_{CO^{16}}}$ by Equation (2)
68.1 (normal melting point)	—	—	1.0125	1.0186
71.3	1.0120 ± 0.0009	1.0154 ± 0.0019	1.0120	1.0150
78.3	1.0105 ± 0.0017	1.0088 ± 0.0012	1.0109	1.0081
81.8 (normal boiling point)	—	—	1.0104	1.0051
82.1	1.0108 ± 0.0010	1.0043 ± 0.0018	1.0103	1.0049

It follows from the data in Table 2 that the best results should be obtained by fractional distillation of carbon monoxide. However, in practice this process involves great difficulties associated with low-temperature work.

TABLE 2

Relative Volatilities of Isotopic Molecules of Water and Carbon Monoxide

Pressure (mm Hg)	200	400	760	[5]
$P_{H_2O^{16}}/P_{H_2O^{18}}$	1.0060	1.0050	1.0041	[6]
$P_{CO^{16}}/P_{CO^{18}}$	1.0148	1.0094	1.0051	Our determinations

Experiments on the Separation of Carbon and Oxygen Isotopes by Fractional Distillation of Carbon Monoxide

Several experiments were performed on the fractional distillation of carbon monoxide. Glass and metal packed columns were used. The glass column was also used in the purification of methane [2] and carbon monoxide in determinations of the separation factors.

Fractional distillation of carbon monoxide with a glass column. A diagram of the apparatus is given in Fig. 2.

The principal part of the apparatus was the rectification column 1, which was a tube of molybdenum glass. The internal diameter of the tube was 17 mm. The column was filled with packing made from stainless steel wire. The packing was in the form of small spirals 1.5 mm in diameter and 1.5-2 mm long. The diameter of the wire was 0.2 mm. The height of the packing layer was 134 cm. At its lower end the column terminated in a spiral spring and a still. The spring served to compensate the thermal expansion or contraction of the column. The column was insulated by means of a silvered vacuum jacket, and vapor of the spent refrigerant was passed through a rubber tube coiled around the vacuum jacket. At the upper end of the column there was a condenser, of the design described in Fastovskii's book [7]. The condenser 2 was made of sheet copper, 2 mm thick, and consisted of a refrigerant chamber 1 liter in capacity, and a condensation chamber for liquefaction of the vapors of the substance being studied. The column was joined to the condenser by means of a ground-glass joint. Low-temperature grease devised by the Central Scientific Research Institute of Aviation Fuels and Oils was used for this joint. The operation of the column was regulated by means of the droppers 3 and 4. The course of separation of the isotopes was followed by means of analyses of samples, taken at the top and bottom of the column, for their carbon and oxygen isotope contents. Tne average error of the mass spectrum analysis in these experiments was about 1% of the isotope content. This led to 2% relative error in the determinations of the separation factor.

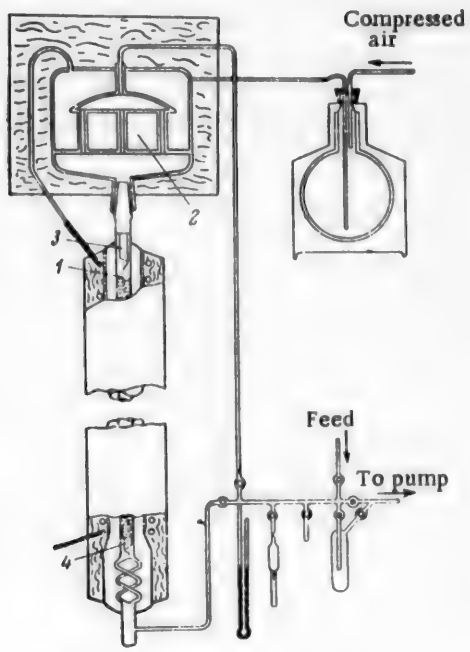

Fig. 2. Glass rectification column. Explanations in text.

The results of experiments on the separation of carbon and oxygen isotopes by fractional distillation of carbon monoxide with the glass column are given in Table 3.

The ratio of the logarithms of the separation factors for oxygen and carbon in distillation of carbon monoxide is about 0.8 when equilibrium is reached in the column. This is in agreement with our determinations of the vapor pressures of isotopic molecules of carbon monoxide, and with the experimental data of Johns, Kronberger and London. The ratio of the separation factors F is shown graphically in Fig. 3.

The lowest HETP (height equivalent to a theoretical plate) in our experiments was 4 cm. In the experiments of the above-named authors HETP was 2.3 cm. The reason for the difference is that, because the column was insufficiently adiabatic, we were compelled to use high liquid flow rates, more than 10 times as high as those in the experiments of Johns, Kronberger, and London. The results obtained in separation of carbon and oxygen isotopes in the form of carbon monoxide in a glass column were used in the design of a metal column.

Experiments with the metal column. The design of the metal column is illustrated in Fig. 4.

TABLE 3

Results of Fractional Distillation of Carbon Monoxide with the Glass Column
Operating pressure in the column 500 mm Hg, liquid flow rate 7 $cm^3/cm^2 \cdot min$

Operating time	Separation factor F for carbon	Separation factor for oxygen	Height equivalent to a theoretical plate (cm)
7 hr.	1.29	—	5.2
2 hr. 45 min.	1.31	1.18	—
3 hr. 45 min.	1.36	1.32	—
5 hr. 30 min.	1.42	1.31	4
7 hr. 30 min.	1.41	1.21	—
9 hr. 30 min.	1.39	1.29	—
11 hr.	1.40	1.37	—

The column 1 itself was a stainless steel tube of 17 mm internal diameter. The wire spirals used for the packing were the same as in the glass column. The height of the packing layer was 370 cm. The outer wall of the column was polished to reduce heat transfer by radiation. The column terminated at the lower end in a glass still 2, with a heater element at its drawn-out end. The still was connected to the column by means of a kovar joint. The upper end of the column terminated in a condenser 3 made of sheet copper. The condenser contained a reservoir, 250 cc in volume, for the distillation liquid. The column, condenser, and still were enclosed in a vacuum jacket 4. The latter was made from steel pipe 134 mm internal diameter. Sight glasses for observation of the liquid level in the still were fitted in the lower end of the jacket. The sight ing the experiments the vacuum jacket was continuously evacuated by means of two TsVL-100 vacuum pumps 5 and 6. The vacuum was measured by means of thermocouple and ionization manometers.

The experiments were performed as follows. The vacuum jacket was evacuated to a high vacuum. Liquid nitrogen was then poured into the condenser and feeding of the carbon monoxide was commenced. About 400 cc of liquid carbon monoxide was put in, and the distillation was commenced. Several experiments were performed; the results of two are given in Tables 4 and 5.

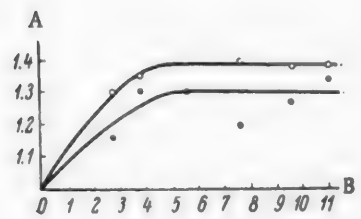

Fig. 3. Results of experiments on the separation of isotopes of carbon (upper curve) and oxygen (lower curve) by fractional distillation of carbon monoxide in a glass column. A) Separation factor, B) time (hours).

First experiment. About 430 cc of liquid carbon monoxide was put into the column. The operating pressure in the column was 527 mm Hg. The pressure drop in the column was about 30 mm Hg. The residual pressure in the jacket was $2\text{-}4 \cdot 10^{-5}$ mm Hg. The experiment was continued for 85 hours. At the end of the experiment 15 liters of gaseous CO, enriched 1.7-fold, was collected. Equilibrium was reached in this experiment; this is shown by the data in Table 4 and the curve in Fig. 5. The equilibrium value of the separation factor was lower than might have been expected from the results of experiments with the glass column (HETP was 5.1 cm, as compared with 4 cm for the glass column). The reason may have been inadequate heat insulation of the column; this is indicated by the fact that the pressure drop in the column was too great. In all probability the column operated under flooding conditions at the upper part. Particular attention was therefore paid to the formation of a higher vacuum in the jacket in the subsequent experiments.

Second experiment. 400 cc of liquid carbon monoxide was put into the column. The pressure of carbon monoxide vapor during the experiment was 510 mm Hg. The pressure difference between the bottom and top of the column was 10-12 mm Hg. The residual pressure in the jacket was $2\text{-}3 \cdot 10^{-6}$ mm Hg. At the end of the experiment this rose to $5\text{-}6 \cdot 10^{-6}$ mm. This led to a decrease of the separation factor. The highest value of the separation factor was 3.62, which corresponded to HETP of 2.7 cm. At the end of the experiment 12 liters of gas with 2.72-fold enrichment with C^{13} isotope, and 12 liters of gas with 2.12-fold enrichment with C^{13*} isotope, was obtained. The results of this experiment are given in Table 5 and Fig. 5.

Fractional distillation of methane was carried out with the glass column only. The results of experiments on the enrichment of carbon with the C^{13} isotope by fractional distillation of methane are given in Table 6.

* As in original — Publisher's note.

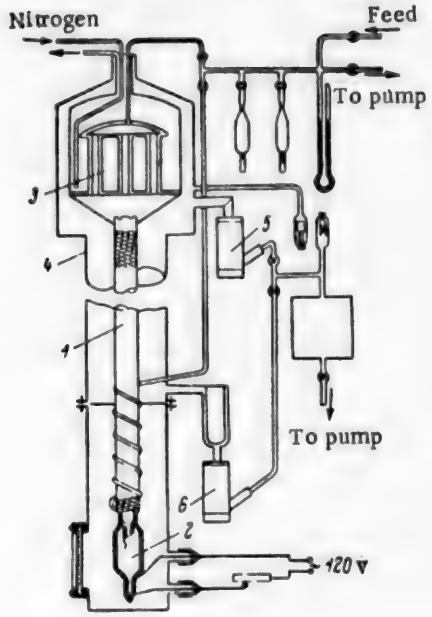

Fig. 4. Metal rectification column. Explanations in text.

The methane samples were analyzed by means of the mass spectrometer, in the form of methane and carbon dioxide. The discrepancy between the separation factors found for CO_2 and CH_4 respectively in the first experiment is due to insufficient purity of the methane. The possible error in determination of the separation factors was estimated in the same way as in the experiments on the determination of the relative volatilities of isotopic methane molecules [2].

Fractional distillation of molecular oxygen was carried out with the glass column only. In these experiments the column was not equipped with a condenser. Oxygen was fed from a 15-liter metal Dewar flask in a thin stream into the top of the column. The upper part of the column was flooded during the experiment. The gaseous oxygen produced during the fractional distillation escaped into the atmosphere. Samples were taken from the lower end of the column and analyzed in the mass spectrometer for O_2^{16} and $O^{16}O^{18}$ molecules. The results of experiments on the separation of oxygen isotopes by fractional distillation of molecular oxygen are given in Table 7.

It is interesting to compare the efficiency of separation of carbon isotopes by fractional distillation of carbon monoxide and methane with the effectiveness of the chemical exchange method. This comparison is presented in Table 8.

TABLE 4

Results of Distillation of Carbon Monoxide with the Metal Column

Operating time	Separation factor for carbon	Separation factor for oxygen	Enrichment with C^{13} at the bottom of the column	Height equivalent to a theoretical plate (cm)
13 hrs.	—	—	1.45	
22 hrs.	—	—	1.82	
30 hrs.	—	—	1.79	
38 hrs.	—	—	1.83	
44 hrs.	2.10	—	2.01	
51 hrs.	2.21	1.67	2.05	5.1
58 hrs.	—	—	2.08	
68 hrs.	2.07	—	2.00	
75hrs. 30 min	—	1.74	2.07	
85hrs. 30 min	—	—	2.04	

It follows from Table 8 that concentration of the rare carbon isotope by fractional distillation of methane and carbon monoxide is considerably more efficient than chemical exchange, based on the isotope exchange reaction between carbon dioxide and the bicarbonate ion, or hydrogen cyanide and the cyanide ion.

TABLE 5

Results of Fractional Distillation of Carbon Monoxide with the Metal Column

Operating time	Separation factor for carbon	Separation factor for oxygen	Operating pressure in column (mm Hg)
7 hrs. 15 min	1.50	1.40	510
12 hrs.	2.70	2.25	
19 hrs.	2.97	2.56	
27 hrs. 15 min	3.22	1.98	
37 hrs.	3.47	2.41	
43 hrs.	3.62	2.32	
51 hrs. 15 min	3.51	2.46	
59 hrs. 30 min	3.16	2.20	
64 hrs. 30 min	3.16	2.44	

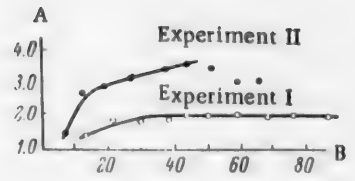

Fig. 5. Results of experiments on the separation of carbon isotopes by fractional distillation of carbon monoxide with the metal column. A) Separation factor; B) time (hours).

TABLE 6

Results of Fractional Distillation of Methane

Operating pressure in column (mm Hg)	Operating time	Gas analyzed	Separation factor	Single separation factor at 200 mm pressure	Height equivalent to a theoretical plate (cm)
260	7 hrs. 36 min	CH_4	1.34	1.0108	4.9
		CO_2	1.25		6.3
220	5 hrs.	CH_4	1.17		9.5
		CO_2	1.176		9
210	6 hrs.	CH_4	1.19		8.4
	10 hr. 30 min	CH_4	1.29		5.5
200	10 hrs.	CH_4	1.24		6.7

TABLE 7

Results of Fractional Distillation of Molecular Oxygen
Operating pressure in column 760 mm Hg

Operating time	Separation factor for O_2^{16} and $O^{16}O^{18}$ molecules	PO_2^{16} / $PO^{16}O^{18}$	Height equivalent to a theoretical plate (cm)
4 hrs.	1.10	1.0045	6.3
3 hrs. 10 min	1.075		8.3
6 hrs.	1.09		7.0
	1.14		4.6
	1.11		5.7

TABLE 8

Comparison of Methods for the Separation of Carbon Isotopes

Method	Reactions and substances used	Single separation factor α	Ht. equiv. to a theoretical plate	Transfer of rare isotope, τ (in g/cm^2·min)	Efficiency factor θ^*	Notes	Literature source
Chemical exchange	$C^{13}O_2$ (gas) + $+ HC^{12}O_3^-$	1.012	458	$2.2 \cdot 10^{-5}$	$5.7 \cdot 10^{-8}$	—	[8]
	$HC^{12}N$ (gas) + $+C^{13}N^-$	1.026	10	$1.8 \cdot 10^{-5}$	$5.2 \cdot 10^{-6}$		[9]
	Carbon monoxide	1.011		$2.6 \cdot 10^{-4}$	$7.3 \cdot 10^{-5}$	Glass column	Our determinations
	Methane	1.0108	4.9	$1.8 \cdot 10^{-4}$	$4.5 \cdot 10^{-5}$	Glass column	Our determinations
Fractional distillation	Carbon monoxide	1.011	2.8	$\sim 1 \cdot 10^{-4}$	$\sim 4 \cdot 10^{-5}$	Metal column	Our determinations
	Carbon monoxide	1.011	2.3	$1.5 \cdot 10^{-5}$	$8.1 \cdot 10^{-6}$	—	[1]

* $\overline{\theta} = (F - 1) \cdot \tau$; where F is the separation factor per unit length of column.

After this work had been completed, a paper was published by Groth et al., [10], dealing with the experimental determination of the temperature variations of the relative volatility of heavy-carbon carbon monoxide. The determinations were performed by means of the differential method. Carbon 10% enriched with the rare C^{13} isotope was used in the experiments. The paper also gives the temperature–relative volatility data for heavy-carbon carbon monoxide determined by Johns and London [11]. We were at that time unaware of the work of Johns and London. The results of the above-named authors are in good agreement with ours.

SUMMARY

1. The Rayleigh distillation method was used to determine the relative volatilities of isotopic molecules of carbon monoxide for carbon and oxygen respectively, in the range from the normal boiling point to the triple point. The results are expressed in the form of Equations (1) and (2).

2. In fractional distillations of liquid carbon monoxide with glass and metal columns, the maximum separation factor for carbon obtained with the metal column was 3.62; this corresponded to 2.8 cm HETP.

3. The efficiency of the methods for the separation of carbon isotopes by fractional distillation of carbon monoxide and methane and by chemical exchange was compared; it was found that fractional distillation of carbon monoxide and methane is the more efficient method for the production of carbon enriched with the rare C^{13} isotope.

In conclusion, we offer our gratitude to the management of the L. Ia. Karpov Physicochemical Institute for the opportunity of performing the experimental part of this investigation, to N. N. Tunitskomuza for valuable advice and discussion, and to M. V. Tikhomirov for assistance in the experimental work.

LITERATURE CITED

[1] T. F. Johns, H. Kronberger and H. London, Mass-spectrometry. London (1952).

[2] G. G. Deviatykh and A. D. Zorin, J. Phys. Chem. 30, 5, 1133 (1956).

[3] Iu. V. Karlakin, Pure Chemical Reagents (Goskhimizdat, Moscow, 1947). •

[4] Chemist's Reference Book, 1 (Goskhimizdat, 1951).•

[5] D. R. Stull, Ind. Eng. Chem. 39, 517 (1947).

[6] I. Kirshenbaum, Heavy Water (Russian translation) (IL, Moscow 1953).

[7] V. G. Fastovskii, Separation of Gas Mixtures (State Tech. Press, 1947); p. 308.

[8] A. F. Reid and H. C. Urey, J. Chem. Phys. 11, 411 (1943).

[9] C. A. Hutchison, D. W. Stewart and H. C. Urey, J. Chem. Phys. 8, 536 (1940).

[10] W. Groth, H. Jhle and A. Murrenholf, Z. Naturforschung 9, 805 (1954).

[11] T. F. Johns and H. London, A.E.R.E. Report, Harwell (1951).

Received January 25, 1956

• In Russian.

INVESTIGATION OF THE FUNDAMENTAL PERFORMANCE CHARACTERISTICS OF THE INJECTION EXTRACTOR AND COMPARATIVE EFFICIENCY OF EXTRACTORS

V. V. Kafarov and S. A. Zhukovskaia

Liquid extraction as a process for separation of the components of mixtures has come into increasing use during recent years. This has made it necessary to devise extraction equipment with maximum turbulence of the phase streams, and therefore with the best mass-transfer conditions. Extractors of this kind, designed recently and becoming more widely used in various branches of industry, include pulsation and vibration columns, packed columns, and centrifugal extractors.

The purpose of the present investigation was to study the possibility of using the energy of a free jet, produced in an apparatus of the ejection-pump type, for intensification of the extraction process. The extensive interphase area which develops in this process, with exceptionally high turbulence of the liquids, creates suitable conditions for intensive mass transfer; the time during which the particles remain in an extractor of this type is the same for all the particles, and is reduced to a minimum because no longitudinal mixing of the streams occurs, and therefore the diffusion pressure is greater than in a mechanical mixer. Because of this, the principle of injection mixing of liquid phases is particularly significant for the extraction of labile substances such as antibiotics.

No information is available in the literature on the operating conditions and calculation methods for ejectors used as extractor-mixers; most of the investigations in this field are devoted to the development of calculation methods relating to ejector pumps [1-15]. All these publications deal with the ejection of homogeneous liquids; nothing is to be found in the literature on the question of streams of two nonmixing liquids. The sole exception is a paper by Gel'perin [16], which contains a reference to the greater efficiency of the injection extractor.

In view of the fact that the problems of the ejection pumping of liquids and of jet mixing require a fundamentally different approach, we undertook a study of the performance of the ejector when used as an extractor-mixer, in order to determine the relationships between the principal hydrodynamic characteristics of jet mixing and to determine the efficiency to mass transfer in a jet extractor.

Investigation of the Hydrodynamics of the Jet Extractor

With a view to the scale modeling of jet extractors, the experiments were performed with laboratory models (Fig. 1, Table 1) and the results were analyzed by means of the theory of similarity.

We attempted to represent the connection between the principal hydrodynamic characteristics of a one-phase stream in an ejector (in absence of auxiliary liquid), in the form of the relationship:

$$Eu = f(Re, \Gamma), \tag{1}$$

where $Eu = \frac{h_p \cdot g}{w_n^2}$ — is the Euler criterion (2)

$$Re = \frac{w_n \cdot d_{ex} \cdot \gamma}{g \cdot \mu}$$ is the Reynolds criterion (3)

h_p is the pressure loss in the nozzle (in m), γ is the density of the working liquid (in kg/m^3), w_n is the velocity of efflux of the active liquid from the nozzle (in m/sec), d_{ex} is the diameter of the nozzle exit (in m), μ is the viscosity of the working liquid (in kg·sec/m^2), g = 9.81 m/sec^2 is the acceleration due to gravity, and Γ is a geometric group.

TABLE 1

Notation for the Jet Extractor (Fig. 1)

Extractor No.	d_{ex} (mm)	d_n (mm)	d'_{ex} (mm)	d_0 (mm)	L (mm)	$F_1 = \frac{\pi \cdot d_{ex}^2}{4}$ (mm^2)	$F_2 = \frac{\pi \cdot d'^2_{ex}}{4}$ (mm^2)	$F_3 = \frac{\pi \cdot d_n^2}{4}$ (mm^2)	$\frac{F_1}{F_2 - F_3}$	$\frac{d_0^2 - d'^2_{ex}}{L}$
1	1.05	1.96	2.00	17.2	62.5	0.865	3.14	3.02	7.2	0.244
2	2.60	4.20	4.40	19.0	66.5	5.30	15.20	13.8	3.79	0.220
3	2.25	3.40	3.70	18.1	68.2	3.98	10.80	9.05	2.26	0.211
4	1.75	2.90	3.30	18.2	71.8	2.40	8.55	6.6	1.23	0.208
5	1.58	2.48	2.78	17.3	73.0	1.96	6.05	4.83	1.61	0.200
6	1.30	2.40	2.98	17.5	70.1	1.33	6.60	4.53	1.23	0.208

The energy loss in the course of jet mixing is mainly determined by the flow conditions of the working (active) liquid and the geometric characteristics of the ejector. The hydrodynamic losses in the chamber of the ejection apparatus (in absence of the secondary liquid) are mainly due to the sudden expansion of the jet at the exit from the nozzle and the formation of stagnant eddy zones [10, 11]. If the ejected liquid is drawn in by suction, eddy formation in the two-phase stream, and thus the hydrodynamic losses, are compensated by some degree of compression of the liquid jet and decreased losses in the expansion of the active jet as it emerges from the nozzle. Therefore the presence of a secondary stream cannot cause a considerable increase of losses in the ejector chamber relative to the losses in a one-phase stream, while at a certain value of the relative velocity coefficient $q = \frac{V_a}{V_w}$ the value of h_p may become less than the corresponding value for a one-phase stream. (These arguments are valid for the range of q which is of practical significance in extraction: q = 0.2-1.0). Therefore the relationship (1) for a one-phase stream may be used for developing a method for calculations of jet extractor design.

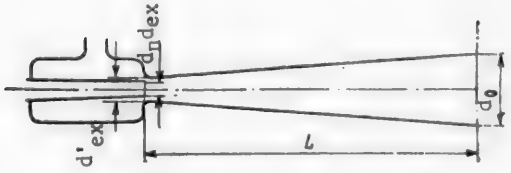

Fig. 1. Principle of the jet extractor. The notation is explained in Table 1.

We also investigated the relationships between the principal geometric parameter of the jet apparatus, the working liquid flow rate, and the limiting relative velocity coefficient q_{lim}:

$$q_{lim} = f\left[\left(\frac{F_1}{F_2 - F_3}\right), \left(\frac{d_0 - d'_{ex}}{L}\right), V_w, \gamma_a\right], \quad (4)$$

where F_1 is the area of the nozzle exit orifice, F_2 is the area of the initial cross section of the mixing chamber, F_3 is the cross-sectional area (external) of the nozzle, γ_a is the density of the auxiliary liquid (in kg/m^3), V_w is the flow rate of the working liquid (in liters/hour).

An experimental unit (Fig. 2) was assembled for investigations of these relationships. The working liquid from the bottle 1 was fed by the pump 2 into the nozzle of the jet extractor 3. The auxiliary liquid from bottle 4 was pumped by the pump 5 into the header bottle 6, from which it passed through the buffer vessel 7 into the suction chamber of the jet extractor 3. The emulsion was collected in the bottle 8. The flow rates of the working and auxiliary liquids were measured by means of the rotameters 9 and 10. The pressure drop in the ejector was measured by means of the mercury differential manometer 11, and the pressure of the working liquid before the nozzle was given by the readings of the direct mercury manometer 12. Six glass jet extractors with different geometrical characteristics were investigated (see Fig. 1).

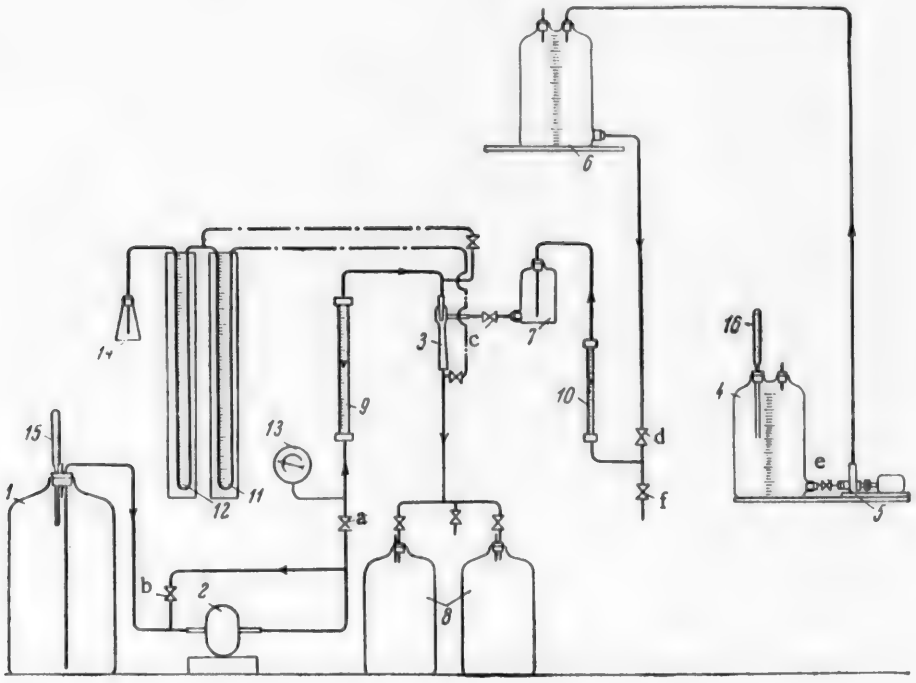

Fig. 2. Layout of apparatus for investigation of stream extractor. Explanation in text.

The hydrodynamics of ejection extractors was investigated in two directions: 1) study of the jet efflux of the working liquid without suction of the second phase, in order to determine the effect of the efflux regime on the pressure drop in the ejector, and 2) study of the hydrodynamics of jet mixing, to determine the influence of the relative quantity of the auxiliary liquid on the pressure drop in the jet extractor, and to establish the relationship between the limiting relative velocity coefficient q_{lim}, the geometric characteristics of the ejector, and the flow rate V_w of the working liquid. In the former case the experimental procedure was as follows. The working liquid was fed by means of the pump 2 into the nozzle of the jet apparatus 3. The flow rate was regulated by means of the valves a and b. A by-pass line to pump 2 was provided to take off excess liquid. After the desired conditions were established, readings of manometers 11, 12, and 13 were taken. The temperature of the working liquid was measured at the same time by means of the thermometers 15 and 16. The working liquids used were water, butyl acetate, benzene, and carbon tetrachloride. Each experimental point for a definite regime of a given ejector represents the average results of 4-5 experiments.

The results of the experiments are shown graphically (Fig. 3) as the relationship $Eu = f(Re, \Gamma)$. The form of this relationship was established from these experimental data:

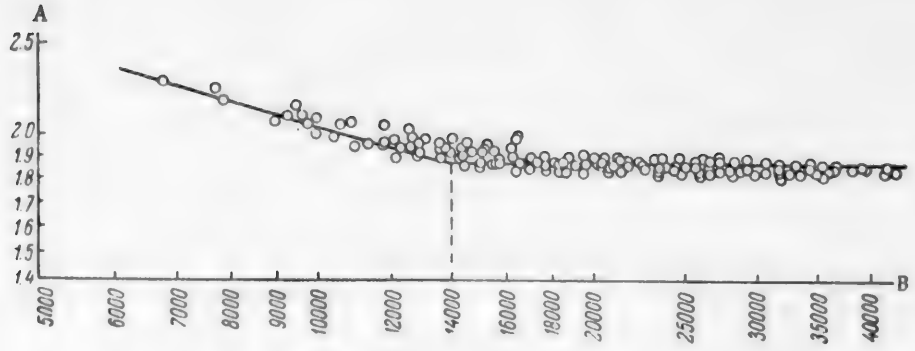

Fig. 3. The Eu = (Re,Γ). A – $Eu \cdot \left[\frac{L \cdot d_{ex}}{(d'_{ex})^2}\right]^{0.74}$, B) values of Re.

The points represent results of experiments with different extractors and different working liquids: water, butyl acetate, benzene, carbon tetrachloride.

$$Eu \cdot \left[\frac{L \cdot d_{ex}}{(d'_{ex})^2}\right]^{0.74} = \frac{2.35}{Re^{0.284}} \qquad (5)$$

$$Re < 14000$$

$$Eu \cdot \left[\frac{L \cdot d_{ex}}{(d'_{ex})^2}\right]^{0.74} = 1.85 \qquad (6)$$

$$Re > 14\,000$$

In the region Re > 14000 the Euler number is independent of the value of the Reynolds number, and the process becomes self-modeling.

For studies of the hydrodynamics of the jet extractor with suction of a second phase, the appropriate regime of the working stream was established. The feed of the auxiliary liquid was regulated by means of the valves c and d, with a constant liquid level in the buffer vessel.

In investigations of the effect of the relative amount of the auxiliary liquids on the pressure drop in the jet extractor, the working liquids used in all the experiments was water, and butyl acetate and carbon tetrachloride were the auxiliary liquids.

The relationship between the pressure drop and the flow rate of the auxiliary liquid at constant V_w is of the same character for all jet extractors, and for different values of V_w. As a rule, introduction of the auxiliary stream into the ejector produces a relatively small increase of Δp up to a certain limit, after which the pressure drop decreases. Evidently a relatively small amount of the auxiliary liquid increases the eddy formation which takes place when the primary jet emerges from the nozzle into the conical mixing chamber. As the flow rate of the auxiliary liquid increases above a certain limit, eddy formation decreases because influx of the auxiliary liquids reduce the zone of stationary eddies. Rolinskii [11] reported a similar effect: when a gas flows into the cylindrical mixing chamber of the jet apparatus, energy losses increase if the influx of the auxiliary gas to the mixing zone becomes less than the suction power of the jet.

It must be pointed out that, at constant flow rate of the working liquid, and with variations of flow rate of the auxiliary liquid from zero to the limiting value, the average changes of the pressure drop did not exceed 10% of the pressure drop in absence of suction at the same values of V_w.

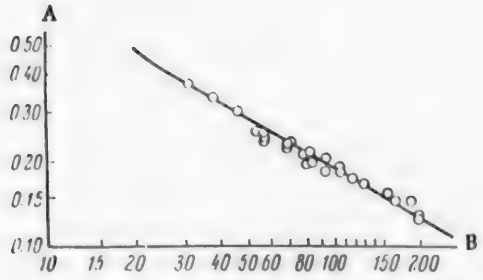

Fig. 4. Relationship between the relative velocity coefficient, the flow rate of the primary (working) liquid, and the geometrical parameters of the jet extractor.

A) $q\left(\frac{F}{F_2-F_3}\right)^{0.5}\cdot\frac{d_0-d'_{ex}}{L}\cdot\left(\frac{\gamma_a}{\gamma_{b.a}}\right)^{0.5}$,

B) V_w (in liters/hour). The points represent experiments with different extractors; butyl acetate was used in five cases, carbon tetrachloride in one, and benzene in one.

Determinations of the limiting relative velocity coefficient $q_{lim}=\frac{V_a}{V_w}$ were carried out with the valve c fully open for each value of V_w; the flow rate of the auxiliary liquid was regulated by means of the valve d so that the liquid level in the buffer vessel 7 remained constant. The manometer readings were taken in each experiment, and the flow rate of the auxiliary liquid was recorded by means of the rotameter 10. The experimental results obtained in these investigations are plotted in Fig. 4. The relationship between the relative velocity coefficient, the geometric characteristics of the jet extractor, and the flow rate of the working liquid can be represented by the expression:

$$q_{lim}\left(\frac{F_1}{F_2-F_3}\right)^{0.5}\cdot\left(\frac{\gamma_a}{\gamma_{b.a}}\right)^{0.5}\cdot\left(\frac{d_0-d'_{ex}}{L}\right)=2.62V_w^{-0.580}, \qquad (7)$$

where $\gamma_{b.a.}$ is the density of butyl acetate.

It was found that the value of q_{lim} is influenced by the density of the auxiliary liquid, and therefore Equation (7) contains the term $\left(\frac{\gamma_a}{\gamma_{b.a.}}\right)^{0.5}$ which takes into account the density of the auxiliary liquid (relative to that of butyl acetate). The results show that the influence of viscosity (in the range of values of μ corresponding to solvents most commonly used in extraction practice) on the coefficient of relative velocity is slight and may be ignored. The Equations (6) and (7), which relate the principal hydrodynamic characteristics of the jet extractor with its geometrical parameters and the physical properties of the liquids used, make an approach to hydrodynamic calculations of jet extractors possible.

To simplify the calculations and to eliminate the laborious simultaneous solution of Equations (6) and (7), we have used suitable data for the construction of a nomogram (Fig. 5), which can be used to find by a graphical method the principal determining dimensions of the jet extractor, d_{ex} and d'_{ex}, for known values of q_{lim}, V_w and h_p.

The values of h_p taken for the calculations is usually based on the pressure obtainable from the pump used for conveying the liquid into the nozzle of the jet apparatus.

The ratio $\frac{d_0-d'_{ex}}{L}$ is usually taken as 0.2, which corresponds to cone angle of the mixing chamber $\alpha\approx10°$. The ratio L/d_0 (ratio of the conical mixing chamber length to the diameter of its outlet orifice) is taken as 4.0.

The nomogram (Fig. 5) can thus be used for determination of all the principal geometrical parameters of the extractor. Limiting values of the relative velocity coefficient, q_{lim}, were used in the construction of the nomogram (Fig. 5). It must be pointed out that the ejector can be used over wide ranges of flow rates of the working and auxiliary liquids. Increase of the flow rate of the working liquid V_w results in an increase

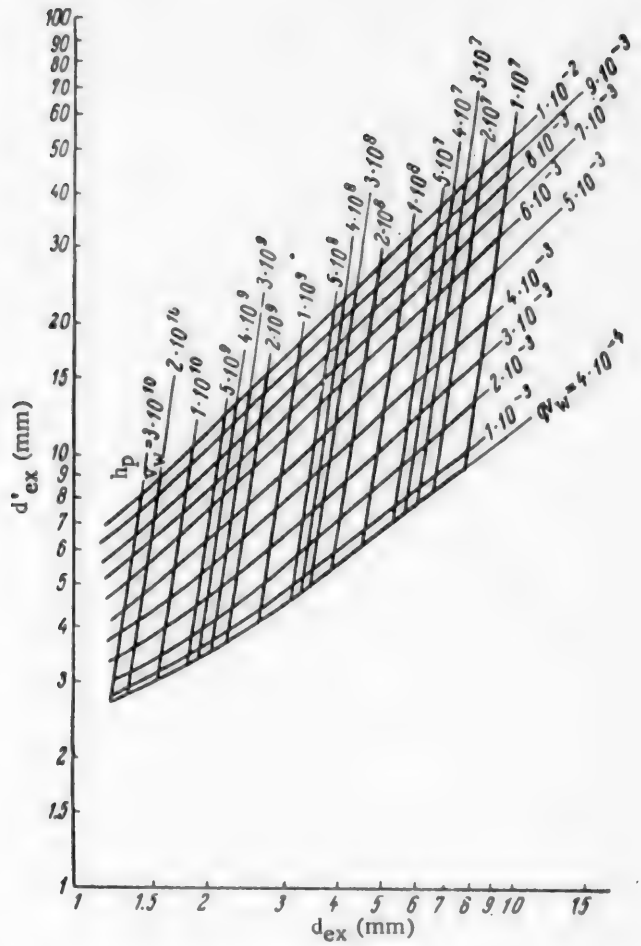

Fig. 5. Nomogram for jet extractor calculations. h_p in m, V_w in m^3/second.

of the pressure drop h_p in the ejector, and therefore when extraction units are planned with jet apparatus as the extractors it is necessary to provide for pumps which can give the necessary pressure of the working liquid before the nozzle, for the range of V_w encountered in the particular process.

Only slight variations of the pressure drop are produced by variations of the flow rate of the auxiliary liquid V_a at constant V_w. As will be shown later, the maximum suction regime is not the most favorable with respect to extractor efficiency, as high values of $q = V_a/V_w$ lead to considerable coalescence of drops in the mixing chamber, observed on decrease of the flow rate at a certain distance from the nozzle.

For evaluation of jet extractor performance with regard to the interface developed in the course of ejection of one liquid phase by another, the dispersity of the emulsion formed in the ejector was studied by the sedimentometric method, with the aid of a special balance for determination of particle size in samples of emulsion taken from the stream.

The methods commonly used in dispersion analysis [17, 18] were applied to the results for evaluation of the dispersity of the emulsions and for comparison of the different regimes.

TABLE 2

Comparative Efficiencies of Different Types of Extraction Equipment

Extractor type	System	Relative efficiency	Literature reference	Notes
Sieve-plate column D_c = 0.915 m, H_p = 0.61 m	Water–acetic acid–ethyl acetate	10.6	[23]	D_c = column diameter, H_p = distance between plates
Sieve-plate column D_c = 0.915 m, H_p = 0.203 m		9.45	[23]	
Sieve-plate column D_c = 0.915 m, H_p = 0.407 m		6.4	[23]	
Packed column D_c = 0.025 m, H_c = 2.9 m, packing–porcelain saddles, 6 mm		1.0	[24]	H_c = height of column
Packed column, emulsification conditions, D_c = 0.040 m, H_c = 1.5 m, packing–6 × 6 rings	Water-phenol–benzene (10% HCl)	5	[25]	
Scheibel column D_c = 0.305 m, H_c = 1.22, n = 400 r.p.m.	Water–acetic acid–methyl isobutyl ketone	8.5	[26]	
Scheibel column, D_c = 0.025 m, n = 1680 r.p.m.		10.7	[27]	
Column with stirrers, D_c = 0.153 m, n = 300-450 r.p.m.		11.2	[28]	
Column with disk rotor, D_c = 0.079 m, n = 1835 r.p.m.		16.5	[29]	
Column with cylindrical rotor, D_c = 0.083 m, H_c = 0.61 m, n = 1300 r.p.m.		7.8	[30]	

The specific surfaces of the disperse phase particles were: for the system water–butyl acetate, from 212 to 742 cm^2/cc, for the system water–benzene, from 456 to 753 cm^2/cc, and for pencillin culture fluid and butyl acetate, from 1010 to 1640 cm^2/cc.

The specific phase-contact area which develops in a jet extractor is considerably greater than in equipment with mechanical stirrers or in tower extractors. In the latter case the specific phase-contact area for the systems: water–(chlorobenzene + toluene) and water–(chlorobenzene + vaseline oil) is from 130 to 500 cm^2/cc, while in equipment with stirrers the specific surface for the water–oil system varies from 133 to 375 cm^2/cc [19].

Investigations of the hydrodynamics of ejection mixing lead to the conclusion that the jet apparatus must be a highly effective extractor, as vigorous turbulent mixing of the working and auxiliary liquids results in the development of a large interfacial area in an extremely short time. Because of the free turbulence (at the interface), mass transfer between the liquids should be very rapid.

Investigation of Mass Transfer in the Jet Extractor

The apparatus shown in Fig. 2 was used for this series of experiments. The following processes were studied: extraction of benzoic acid by water from carbon tetrachloride, extraction of acetic acid by water from carbon tetrachloride, extraction of penicillin by butyl acetate from aqueous solution, and extraction of penicillin by butyl acetate from the culture fluid. The systems had the following characteristics: 1) water–benzoic acid–carbon tetrachloride, $D_{\text{in water}} = 1.31 \cdot 10^{-5}$ cm^2/sec [20] (the diffusion coefficient of the acid in water), K (the distribution coefficient) depends on the concentrations of benzoic acid in the phases, the relationship between the equilibrium concentrations (in g/liter) is given by the expression

$$C_{CCl_4} = 5.59\,C_{H_2O} - 1.025 \qquad (8)$$

TABLE 2 (continued)

Extractor type	System	Relative efficiency	Literature reference	Notes
Pulsation column, D_c = 0.04 m, H_c = 1.22 m, packed with 1/4" Raschig rings, n = 47 cycles/min, a = 6.0 mm	Water–acetic acid–methyl isobutyl ketone	3.79	[31]	n = pulsation frequency, a = pulsation amplitude
Ditto		2.22	[31]	Column operated without pulsation
Sieve-plate column with liquid pulsation, D_c = 0.04 m, H_c = 1.22 m, n = 47 cycles/min, a = 2.5 mm		4.8	[31]	
Luvest extractor, Q = 3.0 m^3/hour, V_d = 0.06 m^3, n = 3800 r.p.m.	Culture fluid–penicillin–butyl acetate (pH = 2.0)	12.1	[32]	Q = total output rate, V_d = drum capacity
Luvest extractor, Q = 0.5 m^3/hour, V_d = 0.003 m^3, n = 3800 r.p.m.	Water–penicillin–butyl acetate (pH = 2.0)	40.5	[32]	
Podbielniak extractor, Q = 9.07 m^3/hour, V_r = 0.034 m^3	Culture fluid–penicillin–butyl acetate (pH = 2.0)	172.0	[33]	V_r = rotor capacity
Jet extractor with separator, d_{ex} = 1.58 mm	Water–benzoic acid–carbon tetrachloride	71.0	–	
a) Q = 0.16 m^3/hour b) Q = 0.15 m^3/hour	Water–acetic acid–carbon tetrachloride	66.0	–	Our data
c) Q = 0.166 m^3/hour	Water–penicillin–butyl acetate (pH = 2.0)	74.7	–	
d) Q = 0.134 m^3/hour	Culture fluid–penicillin–butyl acetate (pH = 2.0)	59.0	–	

in the range of 0.6-2.2 g/liter of benzoic acid in carbon tetrachloride [21]; 2) water–acetic acid–carbon tetrachloride, $D_{\text{in water}} = 1.54 \cdot 10^{-5}$ cm^2/sec [22], $K\ \frac{\text{water}}{CCl_4} = 70$ [23]; 3) water–penicillin–butyl acetate (pH = 2.0), $K\ \frac{\text{water}}{\text{b.a.}} = 65$ (the distribution coefficient of penicillin between water and butyl acetate at pH = 2.0 was determined by us for the concentration range of 200-5000 units/ml of butyl acetate). Water and the culture fluid were used as the working liquids.

For extraction of penicillin, the apparatus was augmented by a device for feeding 5% phosphoric acid into the extractor to bring the pH of the system to 2.0.

The benzoic and acetic acid contents of the samples were determined by titration with alkali in presence of phenolphthalein indicator. The penicillin solutions were analyzed iodometrically (at c > 200 units/ml), and by biological assay. Extractor efficiency under various operating conditions was expressed in percentages of the height equivalent to a theoretical contact stage (HETS)

$$\eta = \frac{c_i - c_f}{c_i - c_{eq}} \cdot 100. \qquad (9)$$

where c_i is the initial concentration, c_f is the concentration in the same phase after extraction; c_{eq} is the equilibrium concentration.

The results of the experiments on mass transfer in the ejection extractor are shown graphically in Fig. 6.

It follows from these results that the nature of the variation of η under constant efflux conditions of the working liquid with variable V_a is the same in all cases. If the feed rate of the working liquid is high enough, η is 100% for all systems and all values of V_a. At lower efflux rates of the working liquid, η increases with increasing V_a up to a certain limit, and then diminishes somewhat. This effect is in full harmony with the hydrodynamics of the mixing of two liquid streams in the jet apparatus. With relatively small amounts of the auxiliary liquid in the eddy zone increases with increasing V_a, but when a definite value of the latter is reached further increase of the auxiliary rate decreases the eddy zone, compressing the primary stream. In this case the phase contact area, and the frequency of its renewal, decrease somewhat. On the other hand, the proportion of the disperse phase in the emulsion then increases, and this leads to coalescence of the disperse-phase droplets at some distance from the nozzle.

However, if the efflux of the working liquid is sufficiently vigorous, the primary stream is so highly turbulent that changes of V_a, while altering the hydrodynamics of mixing, have no practical effect on the extractor efficienty, as η is 100% at all values of V_a; therefore under these conditions the ejection extractor corresponds to one theoretical contact stage (HETS).

For comparison of the efficiencies of different types of extraction equipment, the following expression was used for characterization of extraction columns:

$$I = \frac{w_0}{h_e},$$

where w_0 is the total flow rate of both phases (in $m^3/m^2 \cdot sec$), and h_e is the height equivalent to a theoretical contact stage* (HETS). In its physical meaning this ratio is equivalent to $1/t_c$, where t_c is the time required to attain the theoretical contact stage in an extractor of the given type. Therefore the efficiencies of centrifugal and other types of extractor-mixers may be expressed in terms of

$$I = \frac{1}{t_c} = \frac{w_0}{h_e}, \qquad (10)$$

$$t_c = \frac{t_{ap}}{n}, \qquad (11)$$

where t_{ap} is the holdup time of the liquid in the extractor, and n is the number of theoretical stages in the extractor.

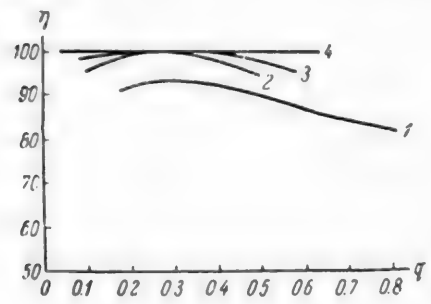

Fig. 6. Variation of extraction efficiency (as % of theoretical contact) with the relative velocity coefficient q for the systems: I) Water–acetic acid–carbon tetrachloride, II) water–benzoic acid–carbon tetrachloride. Curves: 1) System I for V_w = 58 liters/hour; 2) System II for V_w = 82 liters/hour; 3) System II for V_w = 58 liters/hour; 4) System I for V_w = 93 and 106 liters/hour, System II for V_w = 70, 82, and 93 liters/hour.

*The height of a transfer unit may be used as a measure of the length of the contact zone.

The ratio w_0/h_e also represents the output in m^3/sec per unit volume of the reaction zone of the apparatus.

The data of various investigators and our own data for jet extractors, were analyzed; Table 2 presents the results in the form of a comparative evaluation (relative to a packed column operating at far from the optimum conditions) of different extractors, in terms of efficiency expressed as I/I_{pack}.

These results show that the efficiency of the jet extractor is comparable with the efficiencies of centrifugal extractors of the Podbielniak and Luvest types. A combination of the jet extractor with an ordinary centrifugal separator is preferable of the latter, being simpler in design, and convenient and reliable in operation.

SUMMARY

1. The jet (injection) extractor is a highly efficient apparatus for extraction in systems requiring short exposure times.

2. Hydrodynamic calculations relating to jet extractors can be performed on the basis of the relationships derived for one-phase and two-phase streams.

3. A single-stage jet extractor gives a degree of extraction equivalent to one theoretical contact stage.

LITERATURE CITED

[1] K. K. Baulin, Heating and Ventilation, 10 (1931).

[2] K. K. Baulin, Heating and Ventilation, 2 (1933).

[3] M. K. Baranaev, E. N. Teverovskii and K. L. Tregubova, Proc. Acad. Sci. USSR, 84, 5, 821 (1949).

[4] L. D. Berman, Bull. F. Dzerzhinskii All-Union Heat Engineering Inst. 3 (101) (1935).

[5] L. D. Berman, Heat and Power, 8 (1935).

[6] T. Vavakin, Metal Industry Herald, 3 (1928).

[7] P. N. Kamenev, Hydroelevators and Other Jet Equipment (1950).*

[8] P. P. Korolev, "Investigation of the Operation of a Liquid Ejector," Trans. Central Sci. Res. Inst. of Aircraft Engine Construction, 149 (1948).

[9] A. N. Postolenko, Trans. Moscow Electromech. Inst. Eng. Railroad Transport, 22, 88 (1953).

[10] N. A. Rzhanitsyn, Water-jet Pumps (Hydroelevators) (1938).*

[11] V. I. Rolinskii, Candidate's Dissertation (Nikolaev, 1952).

[12] R. G. Folson, Chem. Eng. Progr. 44, 10,765 (1948).

[13] H. Pfotenhauer, Z. Bayerischen Revisonvereins, 16-20 (1913); Gesundheits Ingenieurs 8, 23, 24 (1914).

[14] G. M. Turner and R. W. Moulton, Chem. Eng. Progr. 49, 4, 185 (1953).

[15] G. Zeiner, Das Lokomotiven Blasrohr (1863).

[16] N. I. Gel'perin, Chem. Sci. and Ind. 5 (1956).

[17] W. Clayton, Theory of Emulsions and Their Technical Treatment (Russian translation) (1950).

[18] N. A. Figurovskii, Sedimentometric Analysis (1948).*

[19] F. Vermeulen, G. M. W. Williams and G. E. Langlois, Chem. Eng. Progr. 51, 2, 85 (1955).

[20] Technical Encyclopedia, 7, 259 (1931).*

[21] I. B. Lewis, Chem. Eng. Sci. 3, 6, 260 (1954).

[22] Chemist's Reference Book, 3 (Goskhimizdat, 1952)* p. 301.

[23] F. D. Mayfield and L. Church, Ind. Eng. Ch. 44, 9 (1952).

[24] P. Eaglesfield, B. K. Kelly and J. F. Short, Ind. Chemist. 29, 341, 243 (1953)

[25] V. V. Kafarov and M. A. Planovskaia, J. Appl. Chem. 12 (1951).**

[26] E. G. Scheibel and A. E. Karr, Ind. Eng. Ch. 42, 1048 (1950).

[27] E. G. Scheibel, Chem. Eng. Progr. 44, 681, 771 (1948).

[28] J. Y. Oldshue and J. H. Rushton, Chem. Eng. Progr. 48, 297 (1952).

[29] G. H. Reman, Proceedings of the Third World Petroleum Congress, The Hague, section III, 121 (1951).

[30] J. F. Short and G. H. Twigg, Ind. Eng. Ch. 43, 2932 (1951).

[31] W. A. Chantry, R. L. Von Berg and H. F. Wiegandt, Ind. Eng. Ch. 47, 6, 1153 (1955).

[32] H. Eisenlohr and A. Scharlau, Pharmaz. Ind. 5 (1954).

[33] R. E. Treyval, Liquid extraction, New York (1950).

Received February 11, 1957

*In Russian.
**Original Russian pagination. See C. B. Translation.

EFFECT OF GAS VELOCITY ON MASS TRANSFER IN ABSORPTION UNDER BUBBLING AND FOAM CONDITIONS•

M. E. Pozin and B. A. Kopylev

The Lensoviet Technological Institute, Leningrad

It was shown in the preceding paper [1] that the gas-phase efficiency of absorption in plate columns under bubbling and foam conditions is determined mainly by the solubility of the gas in the liquid. Other factors, such as the linear velocity of the gas and liquid, height of the column of the gas–liquid system, etc., vary the efficiency within definite limits, from ~ 1.0 to 0.5 for easily soluble gases, from ~ 0.5 to 0.05 for gases of moderate solubility, and from ~ 0.05 to 0.001 and less for gases of low solubility. If the variations of efficiency (η) with the linear gas velocity (w) are known, the formula derived earlier [2] can be used to find the absorption coefficient in bubble or foam apparatus with cross flow of the streams on the plates.

Recently the attention of research workers has been drawn to the question of the relationship between the mass-transfer coefficient (K) and the linear gas velocity in bubble and foam equipment. This question has been studied in detail, with reference to the foam regime, by the Department of Inorganic Technology of the Lensoviet Technological Institute, Leningrad [3, 4].

Agarev and Shabalin [5] determined variations of K with the linear gas velocity for bubbling absorption of ammonia and carbon dioxide by water. Kuz'minykh and Koval' [6, 7] studied mass transfer on sieve plates for evaporation of water and desorption of oxygen from water. They found that K for the evaporation of water increases in proportion to the linear gas velocity over the entire range of velocities studied, from 0.2 to 2.0 m/second. The values of K for the desorption of oxygen first increase and then decrease with increasing gas velocity.

The results cited above appear contradictory at first sight. In fact, as is shown below, not only are they not contradictory, but they are mutually supplementary and conform to a general law which characterizes the variations of K with gas velocity for gases of different solubilities.

Analysis of the function $K = f(w, \eta)$. For analysis of the relationship between the efficiency with respect to the gas phase, the absorption coefficient, and the linear gas velocity, we consider the equation derived previously [2], for cross flow.

$$\eta = \frac{2K}{2w + K} \quad . \tag{1}$$

where η is the plate efficiency, K is the absorption coefficient (in m/hour) per 1 m^2 of gas cross section (plate area), with the driving force expressed in units of the gas-phase concentration; w is the linear velocity of the inert (unabsorbable) component of the gas (in m/hour), numerically equal to its flow rate per 1 m^2 of plate area (in $m^3/m \cdot hour$).

Rearrangement of Equation (1) gives

$$K = \frac{2w \cdot \eta}{2 - \eta} \quad . \tag{2}$$

•The experimental data presented in this paper were obtained with the participation of E. Ia. Tarat, N. A. Petrova, V. S. Bogorad, and P. M. Karaseva.

It is evident that $K \to 0$ when $w \to 0^*$, or when $\eta \to 0$, i.e., when $w \to \infty$. When $\underline{w}$ is not 0 or ∞, K has definite numerical values. The values of K pass through a maximum as $\underline{w}$ increases from 0 to ∞.

The existence of an extremal (maximum) point for K as a function of $\underline{w}$ and η can be easily demonstrated if the first and second derivatives of this function are found. For analysis of the function $K = f(w)$, the relationship between η and $\underline{w}$ must be expressed in explicit form.

The nature of the curves for the variation of η with $\underline{w}$ for different gases is illustrated in general form in Fig. 1, on the basis of experimental data obtained earlier [1].

Different cases of the variation of η with $\underline{w}$ may be represented (over a definite range of values of $w > 0$) by a straight line or, in the more general case, in the form of curves described by the equations:

$$\eta = a - b \cdot w^n, \tag{3}$$

where $a \leq 1$, $0 < n \leq 1$

and

$$\eta = C \cdot w^n, \tag{4}$$

where $n < 0$.

If Equations (3) and (4) are substituted into Equation (2) it is easily seen that the function $K = f(w)$ has a maximum.

The general form of the variations of K and η with $\underline{w}$ is shown in Fig. 2.

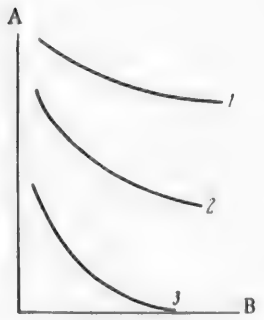

Fig. 1. General form of the relationship between η and the linear gas velocity. A) Efficiency (η), B) linear gas velocity (w). 1) Highly soluble gas, 2) moderately soluble gas, 3) sparingly soluble gas.

The physical meaning of the maximum of the function $K = f(w)$ follows from the differences in the turbulence of the gas and liquid when a gas stream passes through a liquid layer at different velocities. Under otherwise constant conditions (equal height of the original liquid layer on the plate, equal liquid feed rate, the same design characteristics of the plate and the bubbling devices, etc.), variations of the linear gas velocity result in changes in the character of the disperse liquid–gas system with regard to uniformity of the distribution of the gas in the liquid and the degree of dispersion of individual streams. The disperse gas–liquid system exists under bubbling, foam, and spray conditions, according to the linear gas velocity [8]. For a given regime, the structure of the gas–liquid system also varies; accordingly, one distinguishes between individual and mass bubbling conditions; cellular foam of low activity and highly active, continuously renewing mobile foam; gas and liquid streams of different degrees of dispersion; and various intermediate regimes: bubble–foam, bubble–stream, etc. One may therefore assume a continuous variation of the structure of the system, and therefore of the degree of turbulence of the gas and liquid streams, with increase of the gas–liquid ratio.

The turbulence of the gas stream increases over a relatively wider range of linear gas velocities up to velocities at which the gas passes through the liquid in the form of continuous streams, breaking through along liquid "corridors." The maximum value of the absorption coefficient should therefore be found in the transition region between the foam and stream regimes. The liquid phase of the system is less active, and the degree of turbulence of the liquid stream depends to a greater extent on partial changes in the structure of the system.

At the present time there is no method for quantitative characterization of the degree of dispersion or turbulence of the individual phases of a gas–liquid system formed in bubbling or foam apparatus. It is therefore very convenient to use Equation (2) for determination of variations of K with $\underline{w}$ for different gas–liquid

* This is because Equation (1) and (2) are approximate; in reality when $w = 0$ $K \neq 0$ although it is relatively small.

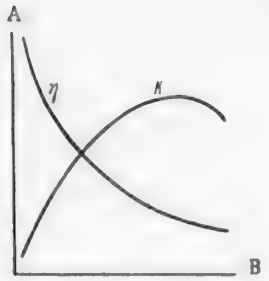

Fig. 2. General form of the relationships between η and K, and the linear gas velocity. A) Efficiency (η) or absorption coefficient (K), B) linear gas velocity (w).

systems. If the influence of changes of $\underline{w}$ on η for gases of different solubilities is approximately known [1], it is possible to determine the relationship between K and $\underline{w}$ over a definite range of gas velocities, and to estimate the degree of turbulence of the individual streams at different values of $\underline{w}$. The range of linear gas velocities is determined by the specific characteristics of the bubbling (0.2-0.5 m/second) and foam (~ 0.7-3.5 m/second) regimes.

EXPERIMENTAL

For experimental determinations of the nature of the variations of K with $\underline{w}$ for gases of different solubilities, and in order to find the values of the linear gas velocity at which K is a maximum, experiments were performed on the absorption, in foaming conditions, of a readily soluble gas – ammonia – by cuprammonium solution, and of a sparingly soluble gas – carbon dioxide – by 1 N sodium carbonate solution. The efficiency over the range of $\underline{w}$ from 0.5 to 3.5 m/second varied between 0.78 and 0.71 in the first case, and between 0.06 and 0.008 in the second. Experiments were also performed on the absorption of carbon dioxide by caustic soda solution. It is known that in this case the resistances of both the gas and the liquid phases have a pronounced influence on the kinetics of the process. In absorption of carbon dioxide by caustic soda solution in a foam apparatus, in the range of $\underline{w}$ between 0.5 and 3.5 m/second, the efficiency varied from 0.3 to 0.08 (analogously to variations of the efficiency in the absorption of a gas of moderate solubility). All the experiments were performed in a single-tray model of the foam apparatus [4]; the plate consisted of a perforated grid with 2 mm openings, spaced 5 mm apart. All the other conditions were chosen so as to be the most typical for the given system. For example, in the experiments on the absorption of ammonia a small weir, 10 mm high, was used to support the liquid, as in this instance it was not necessary to have a high layer of the gas–liquid system. The liquid feed rate was 6 m^3/hour per 1 m of weir width. The initial ammonia content of the gas mixture was about 18 vol.%.

In the absorption of carbon dioxide by caustic soda and sodium carbonate solutions relatively high weirs, 200 and 240 mm respectively, were used to support the liquid, so that a high layer of the gas–liquid system was formed on the plate. The liquid feed rate was 3 $m^3/m \cdot$hour in the experiments with NaOH solution, and 5 $m^3/m \cdot$hour in the experiments with sodium carbonate solution. The gas mixture used in the absorption of carbon dioxide by NaOH solution contained 8-10% CO_2, and in the absorption by sodium carbonate solution, 28-30% CO_2. It is seen that the experimental conditions were chosen so as to ensure mutual compensation of various factors and to obtain the most typical characteristics of each process individually.

Figure 3 shows variations of η and K for a readily soluble gas, based on the experimental data obtained in the absorption of NH_3 by cuprammonium solution in the foam apparatus. It is seen that in this case the absorption coefficient increases continuously over the entire range of gas velocities studied. This means that the maximum of K as a function of η and $\underline{w}$, under these conditions for the given system, is displaced toward higher values of $\underline{w}$ than those used in the foam apparatus. In other words, the maximum value of K for a readily soluble gas in the velocity range studied could only be detected if η varied over a relatively wide range (for example, between 1.0 and 0.5), i.e., under conditions unfavorable for absorption (thin layer of the gas–liquid system, low liquid-feed rate, etc.). Therefore it may be assumed that in the absorption of a readily soluble gas maximum values of K are reached at linear gas velocities above 3.5 m/second.

Changes in the value of η for one shelf of the apparatus have a significant influence on K in this range of linear velocities. The maximum value of K may be found at different gas velocities, according to the change of η. This is associated with the hydrodynamic characteristics of the process and the properties of the gas–liquid system.

As was reported earlier [1], the absorption efficiency for a readily soluble gas decreases little (by a factor of about 1.1-1.3) with increase of the linear gas velocity. In the absorption of a readily soluble gas

a very short time of phase contact is required for high degrees of absorption. The decrease of efficiency caused by a decrease of the phase-contact time (with increasing gas velocity) is counterbalanced to a considerable extent by increased turbulence of the gas phase and a greater contact surface. The greater the turbulence of the system, the less does η change with increase of the gas velocity, and the higher is the gas velocity corresponding to maximum K.

In the absorption of gases of moderate solubility, the efficiency varies roughly between 0.5 and 0.1 in the velocity range of 0.5 to 3.5 m/second. Since the liquid becomes saturated with the gas more slowly in this case than in the absorption of a readily soluble gas, decrease of the phase contact time with increasing $\underline{w}$ begins to influence the value of η considerably sooner, and K reaches its maximum at a lower value of $\underline{w}$ than for a readily soluble gas. This, in its turn, is due to the lower turbulence of the liquid phase relative to the gas phase; in this case the resistance of the liquid phase has a considerable influence on the efficiency and rate of absorption.

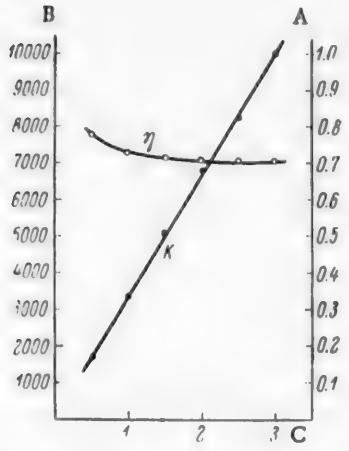

Fig. 3. Values of η and K in the absorption of NH_3 by cuprammonium solution in the foam apparatus. A) Efficiency (η), B) absorption coefficient (K) (m/hour), C) linear gas velocity (w) (m/second).

Figure 4 shows data on variations of η and K in the absorption of carbon dioxide by caustic soda solution in the foam apparatus. It is seen that the maximum value of K is found at gas velocities of about 1.5-2 m/second.

The influence of the phase-contact time on the absorption efficiency is even more pronounced for sparingly soluble gases. To attain high efficiencies in this case, a very long time of phase contact is required, much greater than the time for penetration of the gas through the liquid on the plates of bubbling absorbers, and still more of foam apparatus. In this case the main resistance to absorption is offered by the liquid phase which, as already stated, is considerably less turbulent than the gas phase. Therefore the values for the efficiency obtained in such cases in practice are relatively low. Efficiency varies much more sharply with the linear gas velocity in such cases than in the absorption of readily soluble gases (3 to 5 times as much, and even more). The degree of turbulence attained in the liquid phase is not enough to compensate for the decrease of efficiency with decrease of the phase contact time caused by increase of the gas velocity. Therefore the change of efficiency with the linear gas velocity is a measure of the degree of turbulence of the system. The less turbulent the system, the greater is the decrease of efficiency, and the lower are its absolute values. A distinction must be made between the absorption of sparingly soluble gases in relation to the absolute values of η, and the nature of its variations in the range of linear gas velocities under consideration. When the absorption of a sparingly soluble gas is controlled not only by the resistance of the liquid phase, but partially also by the resistance of the gas phase (for example, in chemisorption or if the concentration of the absorbed component is low), η lies in the approximate range of 0.05-0.01. If the absorption of a sparingly soluble gas is controlled exclusively by the resistance of the liquid phase, η is < 0.01, of the order of 0.001-0.0001 and less. The absorption mechanism is different in the two cases. Therefore, sparingly soluble gases should be classified as sparingly soluble gases ($\eta \approx 0.05$-0.01) and very sparingly soluble gases (η 0.001-0.0001 and less), according to the values of η attained in their absorption on sieve plates under bubbling and foam conditions.

In distinction from the absorption of CO_2 by caustic soda solution, the absorption of CO_2 by sodium carbonate solution must be regarded as the absorption of a sparingly soluble gas, as the efficiency is measured in hundredths of a unit (see Fig. 5). In this case η varies between 0.05 and 0.008 in the range of $\underline{w}$ from 0.5 and 3.5 m/second, and K reaches its maximum at w ~ 1.5 m/second. It should be pointed out that these experiments were performed at relatively high liquid rates. Analogous curves were obtained at lower rates, and the maxima on these curves are also found at gas velocities of about 1.5 m/second, although the $\eta - w$ and $K - w$ curves lie lower because of the lower liquid rates.

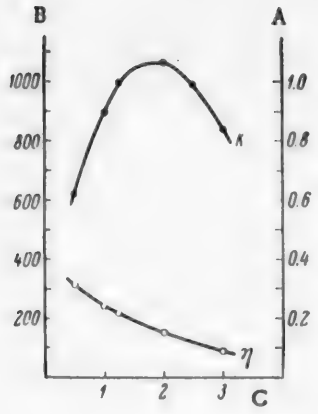

Fig. 4. Variations of η and K with the linear gas velocity in the absorption of CO_2 by 1 N NaOH solution. A) Efficiency (η), B), absorption coefficient (K) (m/hour), C) linear gas velocity (w) (m/second).

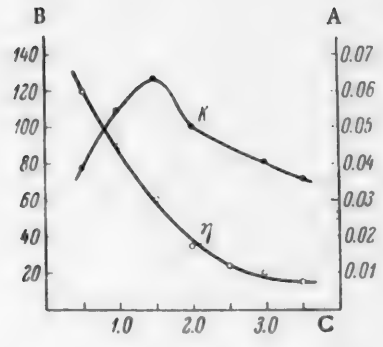

Fig. 5. Variations of η and K with linear gas velocity in the absorption of CO_2 by 1 N Na_2CO_3 solution. A) Efficiency η, B), absorption coefficient (K) (m/hour), C) linear gas velocity $\underline{w}$ (m/second).

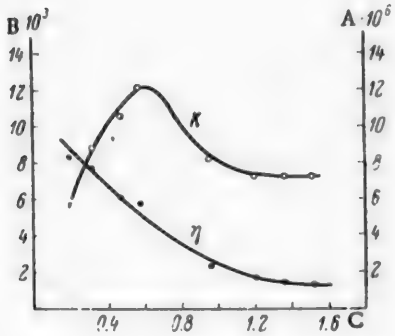

Fig. 6. Values of η and K for desorption of oxygen from aqueous solutions (from the data of Kuz'minykh and Koval'). A) Efficiency η, B) absorption coefficient (K) (m/hour), C) linear gas velocity (w) (m/second).

The absorption of carbon dioxide by caustic soda or sodium carbonate solutions is a chemisorption process, the rate of which depends not only on the resistance of the liquid phase, but also to some extent on the resistance of the gas phase.

If the absorption is controlled exclusively by the resistance of the liquid phase (i.e., in the case of very sparingly soluble gases), the maximum on the K–w curve shifts further toward lower values of $\underline{w}$, since the process is independent of the gas phase, which is easily made turbulent. This applies to the physical absorption of pure gases such as oxygen, nitrogen, and hydrogen, by water, and to the desorption of these gases from aqueous solutions.

Kuz'minykh and Koval' [6, 7] studied the desorption of oxygen from its aqueous solutions, on sieve plates over a wide range of linear gas velocities. Their values of the liquid-phase mass-transfer coefficient K_L were used by us to calculate the gas-phase coefficients K (from the expression $HK = K_L$, on the assumption that for the system water–oxygen at 30° $H = 3.6 \cdot 10^7$ atm/mole fraction). The values of K for a plate with 3 mm openings, with 4.07% open section, are plotted in Fig. 6. The K–w curve in Fig. 6 has a maximum for a linear gas velocity of 0.6 m/second. For a plate with 0.9 mm openings, maximum K corresponds to a velocity of 0.5 m/second, and with increase of the open section of the plate, to 0.7-0.8 m/second. It follows that the maximum value of K for mass-transfer processes controlled exclusively by liquid-phase resistance corresponds to gas velocities of ~ 0.5-0.8 m/second. The values of η calculated by Equation (1) are then very small; with variation of the gas velocity from 0.2 to 1.5 m/second they vary from $0.1 \cdot 10^{-6}$ to $1.3 \cdot 10^{-6}$, i.e., approximately 6-fold.*

The foregoing analysis of bubbling and foam absorption makes it possible to estimate the conditions for intensive absorption of various gases. It is now generally accepted that the absorption of readily soluble gases is many times more rapid in bubbling and foam equipment than in packed towers. The process is, in turn,

*As in original – Publisher's note.

considerably more rapid under foam conditions than under the bubbling regime. However, it follows from the above data that increase of the linear gas velocity up to a definite limit is a factor which intensifies the absorption of moderately and even sparingly soluble gases. Absorption and desorption of these gases in foam conditions take place at fairly high rates, greater than under other conditions at which the necessary linear velocities are not attained. Even in the absorption of very sparingly soluble gases, such as oxygen, nitrogen, etc., which depends exclusively on the resistance of the liquid phase, the process takes place with maximum intensity at velocities of ~ 0.5-0.8 m/second, which are characteristic of the boundary between the bubbling and foam regimes.

It is obvious that in every individual case the optimum gas velocities must be chosen in relation to the properties of the gas involved.

The foregoing data characterize mass transfer in bubbling and foam equipment with cross flow of gas and liquid, in relation to the solubility and linear velocity of the gas. They can be used for a calculated approach to investigations of the process under concrete conditions, and to selection of the optimum process conditions.

SUMMARY

1. The variations of the absorption coefficients in bubbling and foam apparatus with cross flow of gas and liquid with the linear gas velocity have been determined for gases of different solubilities.

2. The absorption coefficient K increases to a definite maximum with increasing linear velocity for all gases; this maximum is situated in different velocity ranges which depend on the properties of the gas. The highest plate efficiency, under otherwise optimum operating conditions (a sufficient liquid layer, correct design parameters, etc.), corresponds to the gas velocity at which K is a maximum.

3. For readily soluble gases, the rate of absorption of which is determined by the gas-phase resistance, the maximum value of K is found at gas velocities beyond the range of the highest velocities used in the foam regime (> 3.5 m/second).

4. For gases of moderate and low solubility, the rate of absorption of which is determined by the resistances of both the gas and the liquid phases, the maximum values of K correspond to linear gas velocities of about 1.5-2.0 m/second; for very sparingly soluble gases, when only the liquid phase determines absorption, they correspond to about 0.5-0.8 m/second. These results determine the optimum conditions for absorption in bubbling and foam apparatus.

5. The above results show that absorption and desorption processes in foam equipment are fairly intensive not only for readily soluble gases, but also for moderately and sparingly soluble gases. The absorption and desorption of very sparingly soluble gases proceed with the highest intensity at linear gas velocities of about 0.5-0.8 m/second, which is the boundary velocity between the bubbling and foam regimes.

LITERATURE CITED

[1] M. E. Pozin and B. A. Kopylev, J. Appl. Chem. 30, 3, 362 (1957).*

[2] M. E. Pozin, J. Appl. Chem. 25, 10, 1032 (1952).*

[3] M. E. Pozin, I. P. Mukhlenov, E. S. Tumarkina and E. Ia. Tarat, J. Appl. Chem. 27, 1, 12 (1954).*

[4] M. E. Pozin, I. P. Mukhlenov, E. S. Tumarkina and E. Ia. Tarat, The Foam Method for the Treatment of Gases and Liquids (Goskhimizdat, 1955).**

[5] L. I. Agarev and K. N. Shaballn, J. Chem. Ind. 8, 136 (1952).

[6] I. N. Kuz'minykh and Zh. A. Koval', et al., J. Chem. Ind. 2 (1954).

[7] I. N. Kuz'minykh and Zh. A. Koval', J. Appl. Chem. 28, 1, 21 (1955).*

[8] M. E. Pozin, I. P. Mukhlenov and E. Ia. Tarat, J. Appl. Chem. 30, 1, 45 (1957).*

Received July 16, 1956

*Original Russian pagination. See C. B. Translation.

**In Russian.

STRUCTURE AND PROPERTIES OF COPPER–GRAPHITE MIXTURES

P. S. Livshits

Methods for the preparation of electrical-carbon materials with definite properties have been studied in a number of investigations [1-5]. In these researches, materials of the required properties were prepared by suitable selection of the components and by variations of the relative proportions of these components. Graphite, carbon black, coke, and pitch are the components chosen for the purpose. However, there are other methods for regulating the properties of such materials.

One such method, used in the electrical-carbon industry, is by the addition of various amounts of metal powders, usually copper, to the carbon mixtures. The mixtures so obtained belong to the so-called copper–graphite system. Members of this system have a number of structural and physicomechanical characteristics which make them suitable for special technical uses.

The literature contains data on the production of different members of the copper–graphite system, and information on some of their properties [6-12]. However, these systems have never been systematically studied in the light of the requirements of the electrical-carbon industry. The purpose of the present investigation is to fill this gap in studies of the copper–graphite group of electrode carbon materials, to describe the structure of members of this group, and to make a quantitative evaluation of the variations in their properties in relation to the composition.

EXPERIMENTAL

The different materials were prepared according to the procedure generally used in the electrical-carbon industry; this consists of preparation of the molding powders, molding, and baking. The compositions of the molding powders, with the optimum amounts of binders, are given in Table 1. The characteristics of the principal raw materials used are given in Tables 2-5. The values in Table 3 apply to crude (natural) graphite. In some of the compositions studied, this graphite was used after an enrichment process in which it was heated at temperatures of the order of 2000-2200°, so that the maximum ash content fell to 0.50%.

TABLE 1

Composition of the Mixtures Used

Contents of components in dry part of mixture				Contents of components in the whole mixture (wt. %)			
wt. %		vol. %				binder	
copper	graphite	copper	graphite	copper	graphite	pitch	tar
0	100*	0	100.0	0	78.4	15.7	5.9
25	75	7.6	92.4	20.8	62.5	11.1	5.6
54	46	24.8	75.2	49.0	41.8	0	9.2
74	26	45.0	55.0	70.2	24.7	0	5.1
82	18	52.6	47.4	82.0	18.0	0	0
86	14	68.0	32.0	86.0	14.0	0	0

*This mixture contained 10% carbon black (by weight).

TABLE 2

Characteristics of PN Copper Powder

Values	Contents (%)		Bulk density (g/cc)	Calcined residue after nitric acid treatment (%)	Particle-size composition (%)			
	copper	iron			passes through sieve No. 0105	residue on sieve No. 0085	residue on sieve No. 0075	passes through sieve No. 0045
Average	99.69	0.005	1.45	0.014	99.94	0.95	2.34	73.08
Extreme	99.40—100.0	0.000—0.030	1.25—1.65	0.000—0.040	99.86—99.96	0.20—4.60	1.00—5.80	65—80

TABLE 3

Characteristics of ZUT-P Graphite from Taiga

Values	Contents (%)					Particle-size composition (%)	
	ash	sulfur	volatiles	moisture	iron	residue on sieve No. 0075	passes through sieve No. 0042
Average	3.8	0.10	0.8	0.24	0.61	2.55	82.8
Extreme	1.8—7.3	0.01—0.25	0.3—1.3	0.08—0.47	0.18—1.04	0.80—7.00	65.0—89.0

TABLE 4

Characteristics of Coal-Tar Pitch

Values	Contents (%)				Coke yield (%)	Melting point (°C)
	ash	volatiles	free carbon	sulfur		
Average	0.13	65	19.8	0.40	35	71.2
Extreme	0.06—0.22	61—69	12.0—26.0	0.2—0.5	31—38	63.0—77.0

TABLE 5

Characteristics of Coal Tar

Values	Contents (%)			Density (g/cc)
	ash	volatiles	free carbon	
Average	0.08	80.5	5.47	1.17
Extreme	0.02—0.16	69.0—91.0	3.0—11.0	1.10—1.20

The components mixed in the proportions indicated in Table 1 were molded and baked. The molding pressure was 2600 kg/cm^2.

The materials were baked at 800-850° in periodic-action electric furnaces. The only exception was the composition at the extreme left of the system, i.e., with 0% of copper. This mixture was baked in annular flame furnaces at temperatures of the order of 1060-1200°.

The structure of the materials so formed, made with the use of natural graphite, is shown in Fig. 1.

TABLE 6

Reliability (β) of the Values Obtained, for Error ϵ (%)

Components in the dry part of the mixture (wt. %)		Characteristics				
		ρ	$\sigma_{comp.}$	$2\Delta U$	μ	Δh
copper	graphite	$\epsilon = \pm 3\%$	$\epsilon = \pm 3\%$	$\epsilon = \pm 3\%$	$\epsilon = \pm 3\%$	$\epsilon = \pm 10\%$
Mixtures with natural graphite						
0	100	1.000	1.000	0.952	0.599	0.937
25	75	0.995	0.984	0.890	0.663	0.948
54	46	1.000	1.000	0.948	0.697	0.988
74	26	0.999	1.000	0.989	0.951	0.996
82	18	1.000	—	0.599	0.796	0.888
86	14	1.000	—	0.861	0.984	0.949
Mixtures with enriched graphite						
0	100	1.000	0.997	0.874	0.630	0.993
25	75	0.999	0.999	0.832	0.698	0.832
54	46	1.000	0.999	0.999	0.983	1.000
74	26	0.850	0.999	0.895	1.000	1.000

Samples of the finished materials were then tested. To conform to the particular requirements of the electrical-carbon industry, the following properties were determined: the electrical resistivity ρ (ohms·mm²/m), compressive strength σ_{comp} (kg/cm²), contact drop of potential between two specimens when a current was passed through them, $2\Delta U$ (in v), the coefficient of friction against a copper surface μ, and the abrasion (in mm) Δh after 50 hours of use of the specimen in an electrical sliding contact.

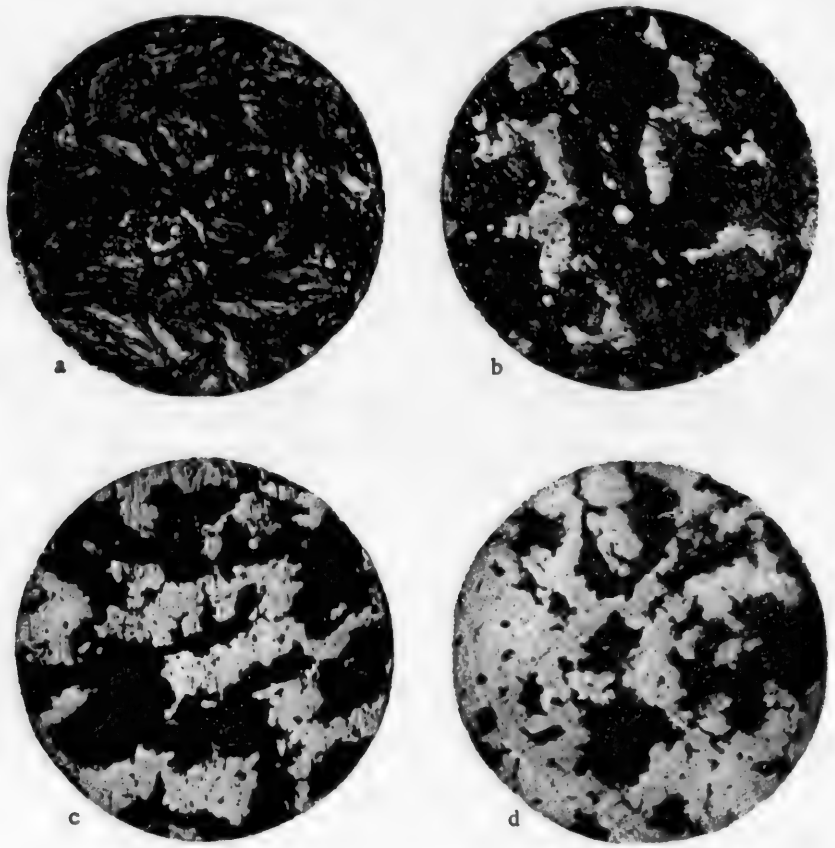

Fig. 1. Microstructure of compositions in the copper–graphite system. Contents of copper and graphite respectively (%): a) 0, 100; b) 54, 46; c) 74, 26; d) 86, 14.

The manner in which these tests were performed on the specimen is shown schematically in Fig. 2. The test methods have been described in detail earlier [13]. Since the results given by these methods are insufficiently accurate, and the technological process of the preparation of electrical carbon materials involves inevitable fluctuations (variations in the properties of the raw materials, temperature and pressure fluctuations, etc.), the numerical values of the properties as given by the tests were scattered around their mean values. As this scatter was very considerable, a specially careful approach to the analysis of the experimental data was necessary.

In order to avoid the possibility of the errors in the interpretation of the results, of the kind described by Blanter [14], the experimental work was so organized as to ensure sufficient accuracy, with a high reliability of the data used in the subsequent analysis. A quantitative evaluation of the accuracy is presented in Table 6, which gives the values of the reliability β in relation to a given error ϵ of the experimental data. The methods used for the calculations of reliability for a given degree of error are described elsewhere [15-17]. It follows from the data in Table 6 that the experimental data are satisfactorily reliable, and the conclusions drawn from them are free from any incidental errors.

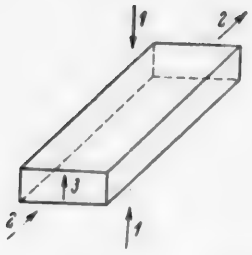

Fig. 2. Testing scheme. 1) Direction of applied compressive force and removal of load in determination of σ_{comp}; 2) direction of current in determinations of ρ and $2\Delta U$, and direction in which Δh is determined; 3) plane in which the abrading surface moves; this plane becomes abraded and μ is determined relative to it.

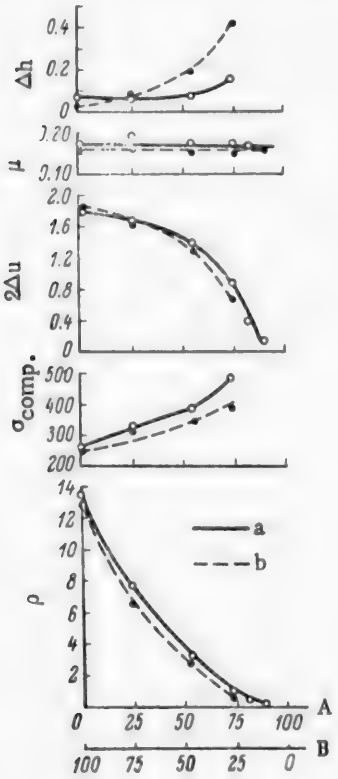

Fig. 3. Variations of the properties of the system copper–graphite with the composition of the type of graphite used. A) Copper content (wt. %), B) graphite content (wt. %). Graphite: a) crude, b) enriched.

DISCUSSION OF RESULTS

Variations of the numerical values of the properties of the copper–graphite system are presented in Fig. 3;* it is seen that these values are consecutively and regularly related to the composition. The coefficient of friction is the only exception. The values of μ remain almost constant over the entire composition range. A possible explanation is that even small quantities of graphite are enough to determine the frictional properties of the sliding surface. Further increases of the graphite content do not alter the frictional properties.

The form of the curves in Fig. 3 indicates that the structure of the consecutive members of the system changes more or less progressively, and no critical points leading to abrupt changes in the properties are found in the system. This is in good agreement with microstructure of the individual members of the system as shown in Fig. 1; it is seen that with increasing metal content the graphite framework of the material is progressively disrupted by inclusions of copper.

In addition to revealing the influence of composition on the properties, the curves in Fig. 3, show the existence of definite relationships between these properties. For example, a comparison of the ρ and σ_{comp} curves shows that ρ decreases and σ_{comp} increases in the transition from a graphite structure to a copper structure. The observed increase of compressive strength does not lead to a decrease of abrasion, but on the contrary, is accompanied by increased abrasion. The two purely electrical characteristics, the resistivity and the contact potential difference, change in the same direction.

Since the value of μ remains constant, it follows that the variation of the abrasion is not connected with this property. An additional experimental investigation of this fact gave the results presented in Fig. 4. These results show the results of tests on a composition containing 54% copper and 46% graphite. Among the 571 specimens of this composition tested, there were a few frictional coefficients deviating from the nominal value of $\mu = 0.15$. This variation was accompanied by variation of the abrasion values, but the latter were grouped more or less symmetrically around the nominal value $\Delta h = 0.20$.

Correlation of the abrasion characteristics and the contact potential drop is of some interest in relation to the compositions studied. It follows from Fig. 3 that Δh increases with decrease of $2\Delta U$. Figure 5, in which the results of 229 tests on specimens of the same composition (54% copper, 46% graphite) are given, indicates

*The values of $2\Delta U$, μ, and Δh for different members of the system were determined at somewhat different current densities in the sliding contact (Fig. 3). However, the results depend mainly on the formulation.

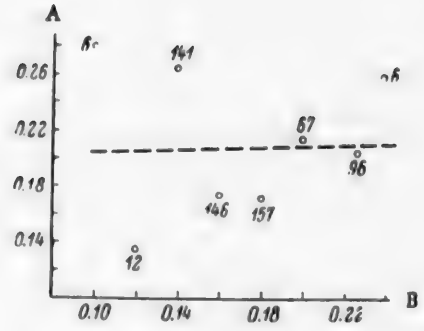

Fig. 4. Scattering of experimental points in determinations of the influence of μ or Δh. A) Abrasion (in mm in 50 hours of testing), B) coefficient of friction. The numbers at the different points indicate the number of tests performed in determinations of each point.

that this relationship is a general one for the systems studied. The scatter of the experimental point confirms that the relationship is valid not only for the system as a whole, but also for each of its members individually.

The foregoing relationships between the technical characteristics of the copper–graphite system refer to all the compositions indicated in Fig. 3; i.e., those with crude (natural) and with low-ash (enriched) graphite. The effect of each of these types of graphite on the properties of the system is of great practical interest; this effect can be determined from Fig. 3. This effect can be estimated quantitatively in terms of the ratios between the numerical values of the properties of systems with enriched graphite and crude graphite respectively. Values of these ratios N are plotted in Fig. 6; it is seen that the use of enriched graphite in copper–graphite compositions leads to some decrease (10-20%) in the values of ρ, σ_{comp} and $2\Delta U$, and a highly peculiar variation of Δh. This peculiarity lies in the fact that wear decreases sharply in compositions with zero metal content, and increases even more sharply with increasing copper content.

Since both the nature and the quantitative aspects of this effect proved to be correlated with the composition of the mixtures (as shown by the intersection of the continuous and dash lines in Fig. 3, and the intersection of the lines for N with the line for N = 1 in Fig. 6), it seemed possible that in pure carbon compositions (without metal) the influence of the kind of graphite might be opposite to its influence in copper–graphite compositions. An experimental test of this hypothesis, performed with carbon specimens composed of graphite and carbon black, gave the results presented in Table 7.

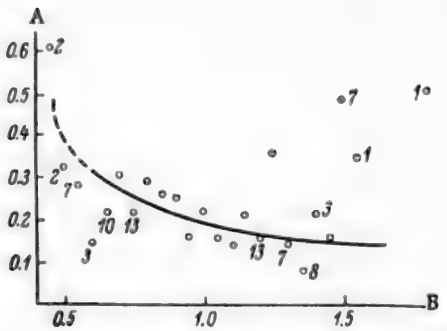

Fig. 5. Scatter of experimental points in determinations of the influence of $2\Delta U$ or Δh. A) Abrasion (in mm in 50 hours of testing), B) contact drop of potential (v).

Calculated values of N are given for carbon mixtures, each of which was prepared with natural and enriched graphite. These results show that the use of enriched graphite in the carbon mixtures results in decreases of ρ, σ_{comp}, μ and Δh, and some increase of $2\Delta U$.

A comparison of this result with the influence, described earlier, of enriched graphite on the properties of mixtures in the copper–graphite system, which may be regarded as graphite systems in which graphite is replaced either by copper or by other carbonaceous materials, suggests that the numerical values of such characteristics as electrical resistivity and compressive strength decrease with replacement of natural by enriched graphite. The direction of the variations of the contact drop of potential and abrasion depends on the nature of the replacing material. If other carbonaceous materials (carbon black in this instance) are used, $2\Delta U$ increases by 10-16% with the use of enriched graphites, while Δh decreases by a factor of 2.0-2.4. The introduction of copper powder as the replacing material reverses the effects produced by the use of enriched graphite. The result is of 10-20% decrease of $2\Delta U$, and almost a 3-fold increase of Δh.

In our opinion, this influence of the type of graphite on the properties of the system may be attributed to the fact that, if natural graphite is used in purely carbonaceous mixtures, which are then baked at temperatures

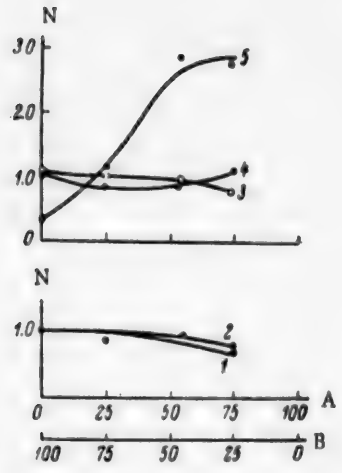

Fig. 6. Influence of the type of graphite on the properties of copper–graphite systems. N) Ratio of properties of compositions containing enriched and natural graphite respectively. A) Copper content (wt. %); B) graphite content (wt. %), 1) Electrical resistivity, 2) compressive strength 3) $2\Delta U$, 4) μ, 5) Δh.

of the order of 1060-1200°, the ash present in the graphite undergoes decomposition. This decomposition causes structural changes which result in increases of ρ and Δh. If thermally-enriched, i.e., low-ash graphite is used in the carbonaceous mixtures, the baking does not result in structural changes such as the above. The values of the two characteristics are therefore lower in such materials.

The situation is essentially different in systems containing metal. The baking temperature in such cases is of the order of 800-850°. This is below the temperatures at which decomposition of the ash may take place. No structural changes therefore take place in natural graphite, and the compositions made with such graphite have higher abrasion resistance. The lower abrasion resistance of compositions made with the use of enriched graphite may be attributed to structural changes in the graphite caused by heat treatment during its enrichment.

It may be noted that the explanation offered may at first sight appear somewhat unconvincing in relation to the simultaneous increase of ρ and σ_{comp}, as it is generally assumed that increase of the former (ρ) must be accompanied by decrease of the latter (σ_{comp}). This contradication is resolved if Fig. 2 is examined; it will be seen that the two-characteristics apply to two mutually perpendicular planes of the specimen.

TABLE 7

Values of N for Carbon Mixtures Without Metallic Components

Composition of mixture (wt. %)					Properties				
graphite	carbon black	coke	pitch	tar	ρ	$\sigma_{comp.}$	$2\Delta u$	μ	Δh
62.0	7.5	0	22.2	8.3	0.98	0.73	1.10	1.00	0.50
49.1	8.4	7.1	28.4	7.0	0.82	0.87	1.16	0.77	0.43

SUMMARY

1. Changes of the composition in the system copper–graphite result in corresponding changes of structure and properties. Micrographs of a number of individual members of the system are presented, and numerical values of their electrical resistivity, compressive strength, contact drop of potential, coefficient of friction, and abrasion are given; the laws governing the variations of these characteristics with the composition of the system are determined.

2. A study of the structural and mechanical properties of different members of the system showed an absence of any extremal points in the variations of their properties.

3. Natural (unenriched) graphite should be used in copper–graphite compositions in order to increase their abrasion resistance. The abrasion resistance is lower if thermally enriched graphite is used.

4. If copper is replaced by other carbonaceous materials, the effect of thermally enriched graphite on the abrasion properties is reversed. In consequence, purely carbonaceous systems containing enriched graphite have higher abrasion resistance.

LITERATURE CITED

[1] G. Ia. Tarasov and A. S. Fialkov, J. Appl. Chem. 27, 12, 1290 (1954).*

[2] G. Ia. Tarasov and A. S. Fialkov, J. Appl. Chem. 27, 12, 1296 (1954).*

[3] G. Ia. Tarasov and A. S. Fialkov, J. Appl. Chem. 29, 1, 53 (1956).*

[4] V. N. Krylov, J. Appl. Chem. 28, 10, 1063 (1955).*

[5] V. N. Krylov, J. Appl. Chem. 28, 11, 1179 (1955).*

[6] V. A. Ivensen, J. Tech. Phys. 20, 12, 1483 (1950).

[7] V. A. Ivensen, J. Tech. Phys. 20, 12, 1490 (1950).

[8] V. A. Ivensen, J. Tech. Phys. 22, 4, 677 (1952).

[9] M. Iu. Bal'shin, J. Tech. Phys. 22, 4, 686 (1952).

[10] V. I. Likhtman and A. T. Nazarov, J. Tech. Phys. 22, 4, 696 (1952).

[11] M. Iu. Bal'shin, Powder Metallography (Metallurgy Press, Moscow, 1948).**

[12] M. Iu. Bal'shin, Powder Metallurgy (State Sci.-Tech. Machine Construction Lit. Press, 1948).**

[13] M. D. Belkin and G. S. Shtykhnov, Brushes for Electrical Machines, Their Production and Uses (Gosenergoizdat, Moscow–Leningrad, 1952).**

[14] M. E. Blanter, Methods of Metal Investigation and Analysis of Experimental Data (Metallurgy Press, Moscow, 1952).**

[15] V. I. Romanovskii, Use of Mathematical Statistics in Experimentation (State United Tech. Press, Moscow, 1947).**

[16] A. M. Dlin, Mathematical Statistics in Technology (Soviet Science, Moscow, 1951).**

[17] I. V. Dunin-Brakovskii and N. V. Smirnov, Theory of Probability and Mathematical Statistics in Technology (General Section) (State Tech. Press, Moscow, 1955).**

Received September 19, 1956

*Original Russian pagination. See C. B. Translation.

**In Russian.

INFLUENCE OF CERTAIN ORGANIC SUBSTANCES ON THE PALLADIUM-PLATING PROCESS

V. V. Ostroumov

The influence of additions of organic substances to the electrolytes on the formation and properties of electrolytic palladium deposits has not been studied sufficiently, although the problem is considered in a number of papers [1-3].

Several substances were tested as additives; of these, only two were selected – furfural and protalbinic acid, which increased the luster of palladium deposits in preliminary trials. This paper deals with a study of the action of these two substances.

Method. Phosphate electrolytes containing 1.2, 5, and 20 g of palladium per liter were mainly used for the deposition. The other components had the following constant concentrations (in g/liter): disodium hydrogen phosphate 100, diammonium hydrogen phosphate 20, ammonium chloride 25.

The hydrogen-ion concentration of the electrolyte was varied between pH 9 and pH 5 by removal of ammonia by boiling.

The metal was deposited on plane polished surfaces of massive bronze and brass cathodes, previously coated with thin layers (0.2 μ) of electrolytic nickel; the reverse sides of the cathodes were insulated with nitrocellulose lacquer. The reflecting power of the palladium coatings deposited on these surfaces was measured by means of a selenium photocell in a beam of white light.

The mechanical stresses in the electrolytic palladium coatings were determined with the aid of a flexible stainless-steel cathode as described previously [4].

It was found that no contact deposition of palladium takes place at the cathodes, even in acid electolytes at pH = 5.

EXPERIMENTAL

Only dull deposits of palladium with low reflectivity coefficients are formed in the electrolyte containing 1.2 g of palladium per liter, at pH = 5.6 (current density 1 ma/cm^2). The addition of a few drops of aqueous saturated furfural solution to this electrolyte appreciably increases the luster of the deposits (Fig. 1). The effects of furfural on solutions of higher pH are shown in Fig. 2. The tests also showed that the deposits become increasingly dull at higher current densities, while if the electrolyte is stirred higher current densities are needed for the formation of bright deposits.

The cathode polarization generally increases with increase of furfural content (Table 1), while the current efficiency decreases (Table 2).

Electrolysis in presence of furfural is usually accompanied by the appearance of finely divided metal at the cathode; some of this metal settles on the bottom of the cell. This decreases the weight of metal deposited on the cathode.

The behavior was, in general, similar in electrolytes with a higher palladium content – 5 g/liter (Table 2). Bright metal deposits can be formed at pH 6.0 in presence of furfural, but they are under considerable

TABLE 1

Cathode Polarization (in mv) in Presence of Furfural

Conditions	Current density (ma/cm²)	Furfural concentration (g/liter)		
		0	0.9	3.6
Stationary electrolyte	2	650	760	770
	4	720	770	830
	6	740	800	850
Stirred electrolyte	2	300	260	450
	4	420	440	550
	6	470	520	600

stress and break down soon after the start of electrolysis. At higher pH, under otherwise the same electrolysis conditions, deposits with 68% reflectivity are formed in presence of furfural.

The transition from black or dull to bright palladium deposits under the action of furfural is accompanied by an increase of mechanical stresses, as shown in Fig. 3. This graph shows that the deflection of the free end of the flexible cathode decreases at furfural concentrations higher than 1 g/liter. A possible explanation is that the true thickness of the palladium deposit is less in this case because of the decreased current efficiency.

Calculations show that in absence of furfural the deposits formed have a stress of 5000 kg/cm², whereas in presence of furfural the stress is 10,000 kg/cm². This accounts for the breaks in the palladium layers in presence of furfural. The results therefore indicate that furfural is hardly suitable as an additive to palladium electrolytes. It must also be taken into account that furfural is an unstable substance; this would undoubtedly lead to further difficulties in its use.

Protalbinic acid is a product of the breakdown of proteins. It is often used as a protective colloid in the production of stable sols of metals, especially of the platinum group. It seemed likely that this substance would be absorbed on the surface of the growing palladium layer and decrease the size of the metal crystallites, i.e., increase the brightness of the deposit. Protalbinic acid can be prepared from egg albumin [5] or from casein [6]. Protalbinic acid prepared from egg albumin was used in our experiments.

TABLE 2

Current Efficiency for Palladium (%)

Current density (ma/cm²)	Without furfural		3.6 g furfural per liter	
	without stirring	with stirring	without stirring	with stirring
1	43	83	28	58
2	54	90	20	47
4	40	76	16	30

After being dried at 40° the substance can be easily ground to a yellow-gray powder and can be kept in that form for a long time without decomposition. Samples were dissolved in dilute aqueous ammonia before being added to the electrolyte.

In presence of 0.1 g of protalbinic acid per liter in the electrolyte, bright layers of palladium 1 μ thick, of 67% reflectivity, can be deposited at current density 2 ma/cm² (Fig. 4). The deposits formed under the same conditions but without the additive have only about 40% reflectivity. The favorable effect of protalbinic acid is therefore obvious.

This additive has the same effect in an electrolyte containing 20 g of palladium per liter. The region of current densities in which bright deposits 1 μ thick can be obtained is shown in Fig. 5. Bright palladium deposits 5 μ thick and over can be obtained from this electrolyte.

The current efficiency is not changed by the addition of protalbinic acid to the electrolytes.

The effects of protalbinic acid additions were also studied with amminochloride electrolytes. The effects were found to be the same as the phosphate electrolytes, but the region of favorable current densities was wider. Cathode polarization in electrolytes with low palladium contents increases slightly on addition of protalbinic acid. In just the same way, addition of protalbinic acid to phosphate solutions in absence of palladium salts had almost no effect on the polarization.

Polarization in electrolytes containing 20 g of palladium per liter increases by 50-100 mv in presence of protalbinic acid. The polarization is almost independent of stirring of the electrolyte. This is illustrated by the current density–polarization curves in Fig. 6. The cathode potentials are given on the standard hydrogen scale.

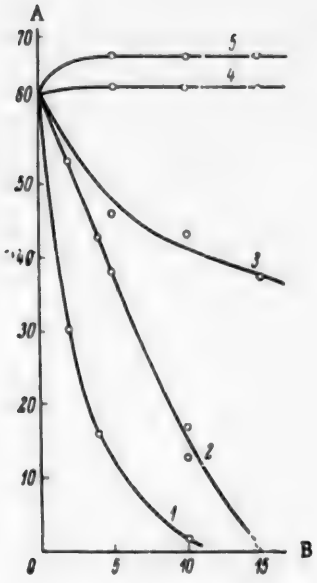

Fig. 1. Effect of additions of furfural on the reflectivity of palladium deposits. Phosphate electrolyte with 1.2 g palladium per liter, pH = 5.6, current density 1 ma/cm^2. A) Reflectivity (%), B) electrolysis time (minutes). Furfural content in solution (in g/liter): 1) 0, 2) 0.5, 3) 2.5, 4) 5.0, 5) 7.5.

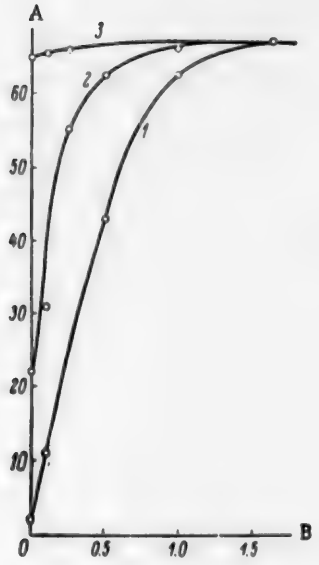

Fig. 2. Effect of additions of furfural on the reflectivity of palladium deposits. Phosphate electrolyte with 1.2 g palladium per liter, electrolysis time 10 minutes, current density 1 ma/cm^2. A) Reflectivity (%), B) furfural concentration (g/liter). Electrolyte pH: 1) 5.6, 2) 6.3, 3) 7.2-9.0.

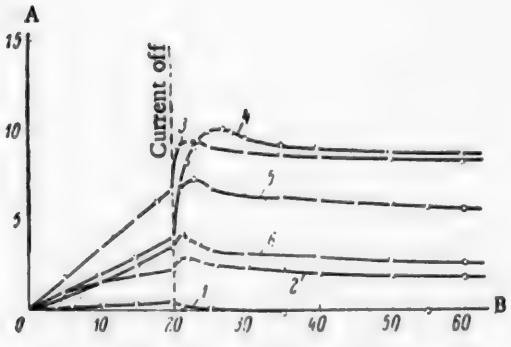

Fig. 3. Deflection of flexible cathode. Phosphate electrolyte with 5 g palladium per liter, pH = 6, current density 1 ma/cm^2. A) Divisions of contractometer scale, B) observation time (minutes). Furfural concentration (g/liter): 1) 0, 2) 0.1, 3) 0.5, 4) 1, 5) 4, 6) 10.

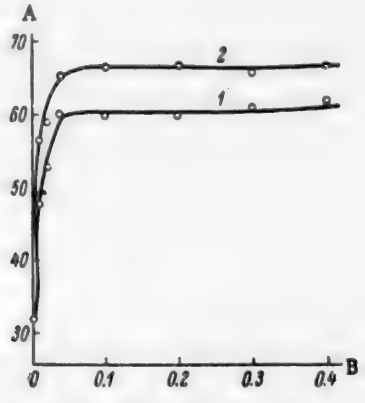

Fig. 4. Effect of additions of protalbinic acid on the reflectivity of palladium deposits. Phosphate electrolyte with 5 g palladium per liter, pH = 9. A) Reflectivity (%), B) protalbinic acid content (g/liter). Current density (in ma/cm^2): 1) 1, 2) 2.

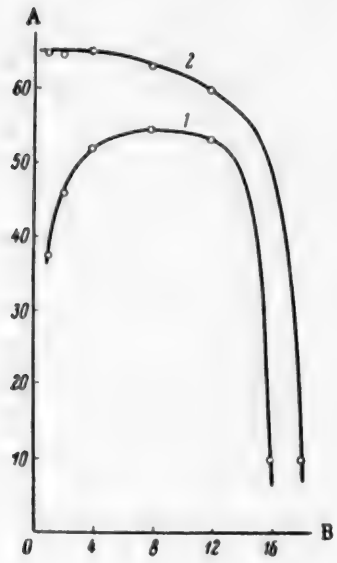

Fig. 5. Region of formation of bright palladium deposits 1 μ thick. Phosphate electrolyte with 20 g palladium per liter, pH = 9.0. A) Reflectivity (%), B) current density (ma/cm^2). Amount of protalbinic acid added (in g/liter): 1) no addition, 2) from 0.1 to 0.4.

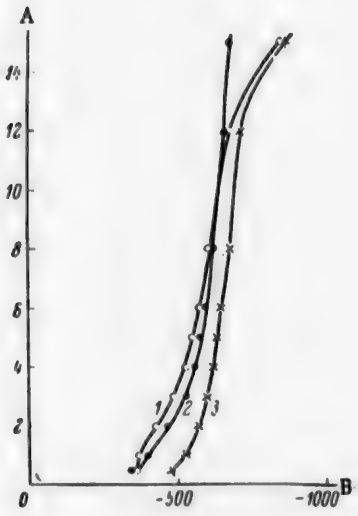

Fig. 6. Cathode polarization. Phosphate electrolyte with 20 g palladium per liter, pH = 9.0. A) Current density (ma/cm^2), B) cathode potential (mv). Curves: 1) Without addition, without stirring; 2) without addition, with stirring; 3) with 0.2 g protalbinic acid per liter (with and without stirring).

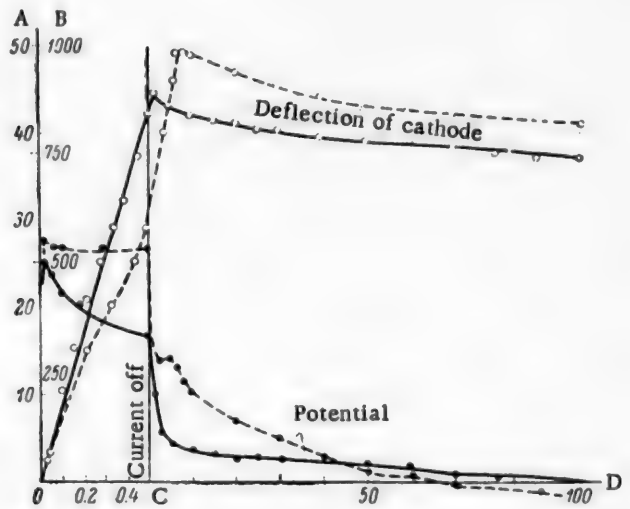

Fig. 7. Deflection and potential of flexible cathode. Phosphate electrolyte with 1.2 g palladium per liter, pH = 9.0, current density 0.5 ma/cm^2. A) Contractometer scale divisions, B) potential (mv), C) thickness of palladium layer (μ), D) observation time (minutes). Continuous line – without additive; dash line – with 0.1 g of protalbinic acid per liter.

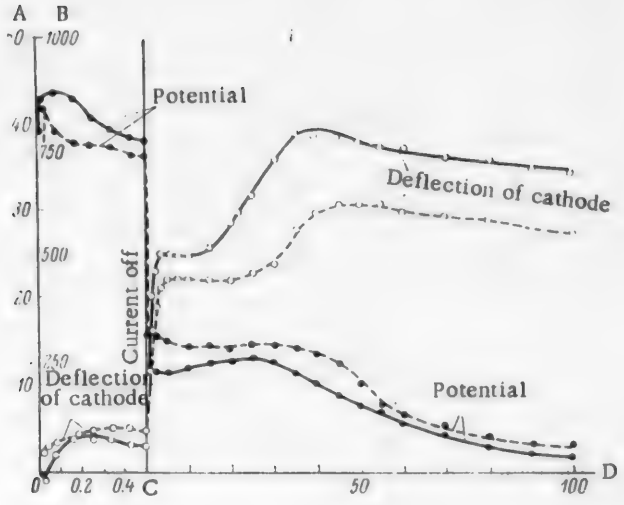

Fig. 8. Deflection and potential of flexible cathode. Phosphate electrolyte with 1.2 g palladium per liter, pH = 9.0, current density 2.0 ma/cm^2. A) Contractometer scale divisions, B) potential (mv), C) thickness of palladium layer, D) observation time (minutes). Continuous line – without additive; dash line – with 0.1 g of protalbinic acid per liter.

Tests showed that the most suitable concentration of this additive is 0.2 g/liter. It was found that protalbinic acid is lost in the course of prolonged electrolysis, and the palladium deposits eventually become dull. A further addition of 0.2 g of this substance per liter makes it possible to obtain bright deposits again. The substance is evidently adsorbed on the surface of the growing deposit and is removed from the electrolyte with the latter.

The presence of protalbinic acid in the electrolyte has almost no effect on the final magnitude of the mechanical stresses in the palladium layers, but it influences the course of their variations.

A phosphate electrolyte containing 1.2 g palladium per liter, with pH = 9, was used for investigation of these variations. One division of the micrometer eyepiece scale (used for observations of the position of the end of the flexibile cathode) corresponded to $9.5 \cdot 10^{-4}$ cm. The cathode potentials were determined at the same time as the deflections.

Figure 7 shows the results obtained in electrolysis at current density 0.5 ma/cm^2, in Fig. 8, at current density 2.0 ma/cm^2. The electrolysis time was so chosen that the final thickness of the palladium layer was 0.5 μ in both cases.

The current efficiencies were taken into account: 77% at current density 0.5 ma/cm^2, and 30% at 2.0 ma/cm^2.

After experiments with an electrolyte without additive, 0.1 g of protalbinic acid per liter was added, and the measurements were repeated.

Figure 7 leads to the conclusion that the presence of protalbinic acid in the electrolyte retards the release of hydrogen from the deposit during electrolysis, but produces a large increase of mechanical stress after the current is switched off. The decrease of potential shows a small halt (at −270 mv) after the end of electrolysis.

The deposit evidently consists of the unstable system Pd + H, the breakdown of which is retarded by the presence of adsorbed layers of protalbinic acid at the intercrystallite boundaries and at the deposit–electrolyte interface.

The foregoing is confirmed by the results of measurements at current density 2 ma/cm^2 (Fig. 8). In presence of protalbinic acid the halt in the increase of mechanical stresses after the current is switched off becomes longer. There is also a longer halt in the decrease of the potential in presence of the additive. In this case the halt is in the range of −250 to −290 mv, as at 0.5 ma/cm^2.

SUMMARY

1. The effects of additions of furfural and protalbinic acid to palladium-plating electrolytes were studied; it was shown that furfural cannot be used as a brightening additive, whereas protalbinic acid at concentrations of 0.1-0.2 g/liter has a favorable effect on the properties of palladium deposits.

2. The presence of protalbinic acid results in some decrease of the breakdown rate of the unstable system Pd + H formed during electrolysis, as it forms interlayers at the intercrystalline boundaries, which hinder the release of hydrogen into the surroundings.

LITERATURE CITED

[1] W. Pfanhauser, Galvanotechnik, 1 (1941).

[2] V. Kohlschutter and F. Jakober, Z. Elektroch. 33, 290 (1927).

[3] O. E. Zvlagintsev and L. K. Amosova, J. Appl. Chem. 10, 1959 (1937).

[4] V. V. Ostroumov, J. Phys. Chem. 31, 8, 1812 (1957).

[5] C. Paal, Ber. 35, II, 2195 (1902); C. Paal and C. Amberger, Ber. 36, I, 124 (1904); 38, II, 1388, 1398, 1406 (1905).

[6] N. A. Gruzdeva, Factory Labs. 15, 10, 1947 (1949).

Received June 28, 1956

INVESTIGATION OF CATHODE PROCESSES IN THE SIMULTANEOUS DEPOSITION OF LEAD AND COPPER

B. I. Skirstymonskaia

The V. I. Ul'ianov (Lenin) Electrotechnical Institute, Leningrad

The electrolytic production of alloys with definite properties is becoming of wide importance. Numerous investigations have been devoted to this question. In most of the published papers [1], however, mainly the purely practical problem of electrolyte composition and conditions for alloy deposition has been considered. Not enough is known about the laws governing the simultaneous discharge of metal ions giving rise to alloys with different phase diagrams, or about the influence of electrolyte composition and of its individual components on the cathode process.

The object of the present work was a study of cathode processes in the simultaneous deposition of metals which are mutually insoluble at low temperatures. The example chosen was lead–copper alloy [2], which is of great practical importance.

The composition of the electrolytes used for production of copper–lead alloys is largely determined by the possibility of deposition of lead from them.

Beliaev et al. [3] showed that copper–lead alloys can be deposited from metabenzenedisulfonate solutions in presence of gelatin. Brittle deposits containing up to 55% lead were obtained from alkaline copper cyanide solutions containing sodium plumbite [4, 5].

There have also been attempts to obtain copper–lead alloys from acetate [6], fluoborate [7, 8] and perchlorate [9] electrolytes. However, none of these methods has been adopted in practice.

Gordienko [10] carried out a search for electrolytes suitable for the production of copper–lead alloys with good antifriction properties over a wide temperature range. Of the electrolytes tested, a nitrate electrolyte of the following composition (in g/liter) was considered to be the most suitable: $Pb(NO_3)_2$ 300, $Cu(NO_3)_2 \cdot 3H_2O$ 12, KNO_3 50, NH_4Cl 10, tartaric acid 20, HNO_3 5 ml/liter.

He did not determine the potentials in the separate and joint deposition of lead and copper, and did not study the influence of the individual electrolyte components on the deposition of metals.

A nitrate electrolyte was used in the present investigation.

EXPERIMENTAL

The vessel used for investigations of the cathode process was divided into 3 compartments by glass diaphragms; there were two outer anode compartments with a cathode compartment between them. The cathode used for determination of the polarization curves had an area of 3 cm^2; current efficiencies were determined with a cathode 24 cm^2 in area.

The usual compensation circuit with a calomel reference electrode was used for measurement of cathode potentials; these could be determined to an accuracy of 10^{-4} v. The potentials are given on the standard hydrogen scale.

The electrolyte was circulated in order to maintain constant concentration in the cathode compartment. Fresh solution was fed into the lower part of the vessel, and excess overflowed through a side tube over the

cathode. The circulation rate was adjusted so that the concentrations of the copper ions in solution before and after electrolysis did not differ by more than 5%.

The solution temperature was maintained at about 18°.

For elucidation of the processes taking place at the cathode in the simultaneous deposition of lead and copper it was first necessary to determine the conditions for the deposition of each metal separately, and also to find the influence of the individual components of the electrolyte.

For investigations of the cathode process, polarization curves were plotted for solutions of copper and lead salts, both in presence and in absence of the other electrolyte components used; the current efficiencies for each metal were determined in each case, and the results were used to calculate the partial currents i_{Cu} and i_{Pb}.

The polarization curves are plotted in "potential–cathode current density" ($\varphi - i$) coordinates, and also in $\varphi - i_{Cu}$ and $\varphi - i_{Pb}$ coordinates.

The current efficiency in the deposition of single metals was determined by the usual method with the aid of the copper coulometer. For determination of the current efficiencies for the metals in the copper–lead alloy, the weighed deposit was dissolved in nitric acid lead was precipitated as $PbSO_4$, while copper was determined by the photocolorimetric method [11]. In some instances the lead contents of the alloys were checked gravimetrically.

The results given are average values for several determinations.

Deposition of Copper

Effects of KNO_3 and HNO_3. The polarization curves for copper in presence of different electrolyte components are given in Figs. 1 and 2.

Figure 1 shows that addition of KNO_3 at constant pH merely lowers the limiting current for copper.

The course of the polarization curve changes sharply with change of solution pH (Fig. 2, Curve 1) produced by addition of HNO_3; at $\varphi \approx 0$ a region of rapid increase of current density with a slight change of potential appears on the curve.

On addition of KNO_3 at low pH values, the polarization curve takes the form of Curve 2 in Fig. 2. The curve has three distinct regions: the first up to a potential of approximately + 0.05 v, a second, almost vertical region, which passes into the horizontal third region at ~ -0.05 v.

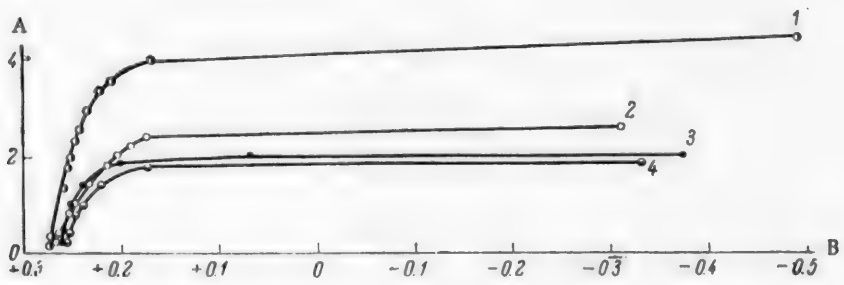

Fig. 1. Effect of KNO_3 on cathode polarization in the deposition of copper from 0.05 M $Cu(NO_3)_2$ solution. A) Current density (ma/cm^2), B) potential (v). Amount of KNO_3 (in moles/liter): 1) 0, 2) 0.5, 3) 1.0, 4) 2.0.

The copper deposited in the first two regions is rose-colored, while in the last region a loose, dark deposit is formed, with simultaneous liberation of large amounts of gas.

If this curve is compared with the partial polarization curve in Fig. 3 (Curve 1), it is seen that i_{Cu} reaches its maximum value at potentials corresponding to the transition from the first to the second region. The rapid increase of current in this region at constant i_{Cu} indicates the occurrence of another reduction process, in addition to the reduction of copper ions.

Further increase of the HNO_3 concentration shifts the polarization curve (Curve 3, Fig. 2) toward more negative potentials; this suggests that hydrogen ions are involved in the reduction process in the second region of the curve. It must be taken into account that the zero-charge potential of copper is −0.034 v [12]. Therefore NO_3 ions may be adsorbed on the copper cathode at the existing more positive potentials, and may then be reduced at the appropriate potential.

The reduction of NO_3^- at the dropping mercury electrode was studied by Frumkin and Zhdanov [13]. They showed that among the possible reactions of the reduction of NO_3^- ions may be the following:

$$NO_3^- + 6e + 7H^+ \longrightarrow NH_3O + 2H_2O$$

or

$$NO_3^- + 6e + 5H_2O \longrightarrow HN_3O + 7OH^-.$$

Increase of the H^+ ion concentration in this process displaced the cathode potentials in the negative direction. In our experiments a similar effect was produced by increase of the nitric acid concentration at constant KNO_3 concentration.

The occurrence of an additional process of the reduction of NO_3^- ions in the second region of the curve may be postulated on the foregoing considerations.

Effect of tartaric acid. The effect of additions of tartaric acid on the cathode process was studied in presence of the other two components, KNO_3 and HNO_3 (Curve 4 in Fig. 2, and Curve 2 in Fig. 3).

The appearance of a horizontal plateau on these curves, and the rapid shift of potentials in the negative direction, indicate that the deposition of copper is retarded in presence of tartaric acid. The copper deposits formed, even at high current densities, are dense, pale rose in color, and microcrystalline.

The current used for deposition of copper from these solutions reaches its limiting value at potentials close to the zero-charge potential of copper.

Fedot'ev and Kruglova [14] obtained similar polarization curves for the deposition of copper from sulfate solutions with additions of Rochelle salt (from 0.2 to 10 g/liter). They explain the presence of the horizontal plateau on the polarization curve in the light of the theory of adsorptional chemical polarization.

The following mechanism may be postulated for the processes taking place at the cathode in presence of tartaric acid. At cathode potentials somewhat on the positive side of the zero-charge point for copper, $C_4H_4O_6^{--}$ anions are adsorbed at the cathode, and a dense adsorbed film is formed through which Cu^{++} and NO_3^- ions cannot penetrate easily. The retardation of the cathode process caused by formation of the adsorbed film displaces the cathode potential to values at which the anions are gradually desorbed. The current for copper deposition again increases at these potentials.

Effect of NH_4Cl. The effects of ammonium chloride were studied in presence of all the additives considered above. The course of the polarization curves alters sharply in presence of NH_4Cl (Curves 5 and 6 in Fig. 2). Each of these curves can be divided into four regions. The first region corresponds to low current densities, and is shifted in the direction of more positive potentials as compared with the other curves; the current efficiencies for copper are lower in this region than at higher current densities. This may be caused by a reduction process: $Cu^{++} + e \longrightarrow Cu^+$ in addition to the main process of copper deposition. Cu^+ ions are unstable under normal conditions of electrolysis, but their stability is increased by the introduction of ammonia or of chloride ions into the solution, so that they can accumulate up to measurable concentrations [15]. It is known that this results in two polarographic waves for copper. When the potential ~ + 0.17 v is reached, the relative proportion of the reaction $Cu^{++} + 2e \longrightarrow Cu$ increases; the limiting current for this reaction forms a third region – a horizontal plateau – on the polarization curve.

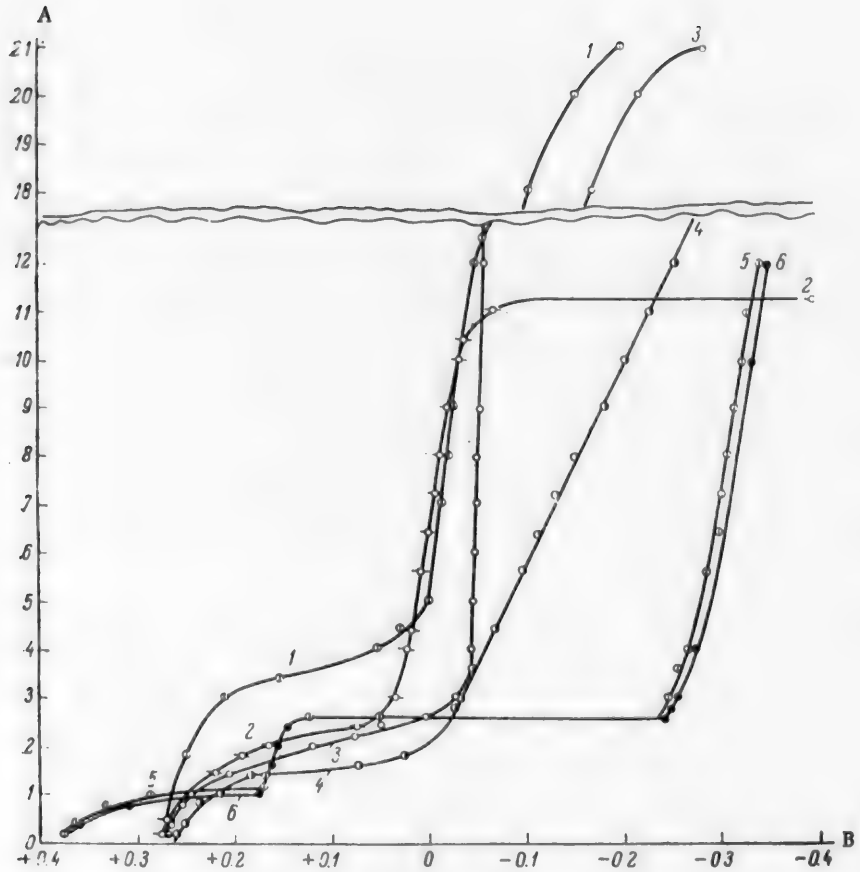

Fig. 2. Effect of additions of HNO_3, $H_6C_4O_6$ and NH_4Cl on cathode polarization in the deposition of copper from 0.05 M $Cu(NO_3)_2$ solution. A) Current density (ma/cm^2), B) potential (v). Additions (in moles/liter): 1) 0.075 HNO_3, pH = 1.35; 2) 0.075 HNO_3, 0.5 KNO_3, pH = 1.40; 3) 0.15 HNO_3, 0.5 KNO_3, pH = 1.10; 4) 0.075 HNO_3, 0.5 KNO_3, 0.135 $H_6C_4O_6$, pH = 1.35; 5) 0.075 HNO_3, 0.5 KNO_3, 0.187 NH_4Cl, pH = 1.35; 6) 0.075 HNO_3, 0.5 KNO_3, 0.135 $H_6C_4O_6$, 0.187 NH_4Cl, pH = 1.35.

In the fourth region, rapid increase of current is accompanied by evolution of large amounts of gas and the formation of a dark, loose deposit of copper.* The limiting value of i_{Cu} is retained at this stage.

It may be noted that Curves 5 and 6 in Fig. 2 coincide with Curves 3 and 4 in Fig. 3 over almost their entire course. Evidently the addition of NH_4Cl counteracts the retardation of copper deposition caused by adsorption of nitrate and tartrate ions. Small amounts of chloride ions had a similar effect in counteracting the retardation of the cathode process in the electrolysis of copper sulfate [14].

It must be pointed out that, as is clear from Fig. 3, the current required for the deposition of copper reaches its limiting value at different potentials in presence of different additives; the potentials are probably determined by the desorption potentials of their anions. The magnitude of the limiting current, however, is almost the same in all cases, and does not depend on the nature of the additive.

* Additional investigations showed that hydrogen is liberated in this region.

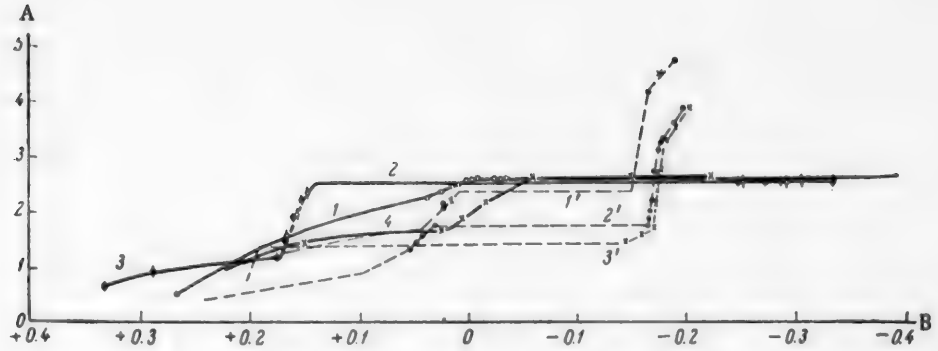

Fig. 3. Current used in the deposition of copper from various electrolytes. A) Current used for deposition of copper (ma/cm^2), B) potential (v). Electrolyte composition (in moles/liter): 1) 0.05 $Cu(NO_3)_2$, 0.5 KNO_3, 0.075 HNO_3; 2) 0.05 $Cu(NO_3)_2$, 0.5 KNO_3, 0.075 HNO_3, 0.135 $H_6C_4O_6$; 3) 0.05 $Cu(NO_3)_2$, 0.5 KNO_3, 0.075 HNO_3, 0.187 NH_4Cl; 4) 0.05 $Cu(NO_3)_2$, 0.05 KNO_3, 0.075 HNO_3, 0.135 $H_6C_4O_6$, 1') 0.05 $Cu(NO_3)_2$, 0.906 $Pb(NO_3)_2$; 2') 0.05 $Cu(NO_3)_2$, 0.5 KNO_3, 0.075 HNO_3, 0.906 $Pb(NO_3)_2$; 3') 0.05 $Cu(NO_3)_2$, 0.5 KNO_3, 0.075 HNO_3, 0.135 $H_6C_4O_6$, 0.187 NH_4Cl, 0.906 $Pb(NO_3)_2$.

Deposition of Lead

Polarization curves determined for $Pb(NO_3)_2$ solutions with and without additives are given in Fig. 4. In presence of additions of KNO_3 and HNO_3 the potential of lead deposition is displaced somewhat in the negative direction (Curve 2, Fig. 4), which may be the result of changes in the activity of the Pb^{++} ions with increase of NO_3^- concentration. In fact, Curve 5 in Fig. 4 shows that the displacement of the potentials is considerable in presence of large amounts of KNO_3.

The presence of $H_6C_4O_6$ and NH_4Cl has almost no effect on the deposition of lead.

It is known [15] that adsorption of surface-active substances on an electrode occurs only in a definite range of potentials, on each side of the zero-charge potential of the electrode. The zero-charge potential of lead is −0.69 v [12]; in the present instance the deposition of lead occurs at considerably more positive potentials, at which adsorption of surface-active substances cannot occur. Lead is liberated without additional retardation; the current efficiencies on all the solutions tested are close to 100%.

Simultaneous Deposition of Lead and Copper

It may be concluded from the foregoing data on the separate deposition of lead and copper that the simultaneous deposition of the two metals is possible at potentials close to the deposition potential of lead, at the limiting current for copper.

We studied the effects of various amounts of $Pb(HO_3)_2$ and of additions of NH_4Cl and $H_6C_4O_6$ on the simultaneous deposition of the metals from solutions containing $Cu(NO_3)_2$, KNO_3 and HNO_3 (Figs. 5, 6, and Table).

Addition of 0.906 M $Pb(NO_3)_2$ to the solution displaces all the regions of the polarization curve into the region of lower current densities, and results in the formation of another region, in the form of an almost vertical straight line (Curve 6, Fig. 5). Analysis of the deposits formed at different current densities showed that simultaneous deposition of lead and copper occurs only over this last region of the curve; only copper is deposited at the cathode over the first three regions.

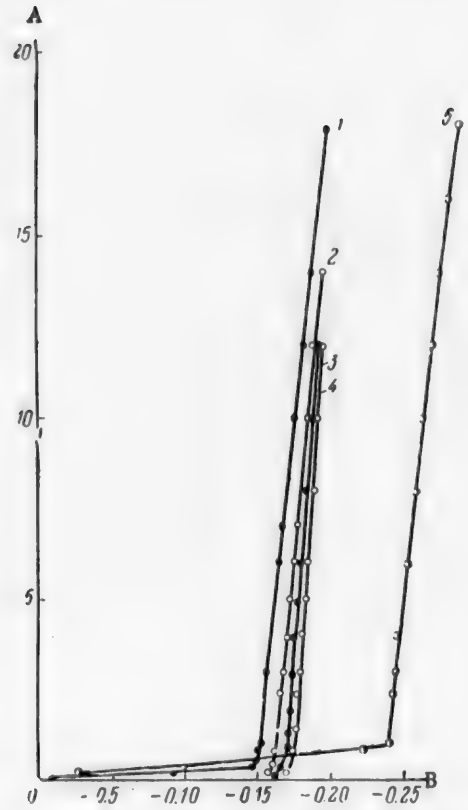

Fig. 4. Effect of additions of HNO_3, KNO_3, $H_6C_4O_6$, NH_4Cl on cathode polarization in the deposition of lead from 0.906 M $Pb(NO_3)_2$ solution. A) Current density (ma/cm^2), B) potential (v). Additions (in moles/liter): 1) Without additions; 2) 0.075 HNO_3, 0.5 KNO_3; 3) 0.075 HNO_3, 0.5 KNO_3, 0.135 $H_6C_4O_6$; 4) 0.075 HNO_3, 0.5 KNO_3, 0.135 $H_6C_4O_6$, 0.187 NH_4Cl; 5) 2.0 KNO_3.

The effects of different amounts of lead salts on the cathode processes in the simultaneous deposition of lead and copper are represented by Curves 2-6 in Fig. 5. The results of parallel determinations of the potentials for deposition of lead from solutions of corresponding concentrations of $Pb(NO_3)_2$ are given in Curves 3'-6' of Fig. 5. It is seen that no appreciable change in the potential of lead deposition takes place in the simultaneous deposition of lead and copper.

Additions of $H_6C_4O_6$ and NH_4Cl have no appreciable influence on the deposition potentials of the alloys, but merely alter the course of the first three regions of Curves 2-4 in Fig. 6.

The decrease in the values of i_{Cu} in the first three regions of Curves 1', 2', and 3' of Fig. 3 is due to the presence of $Pb(NO_3)_2$ in the solution. This effect may be caused by a decrease in the activity of Cu^{++} ions in presence of a large amount of a salt with a common ion, and also by a decrease in the relative amount of these ions in the ions migrating toward the cathode.

The value of i_{Cu} increases in the simultaneous deposition of the two metals, and reaches values considerably in excess of the limiting current for the deposition of copper in absence of lead. This increase is accounted for by the intensified convection of the solution at the cathode as the result of discharge of heavy

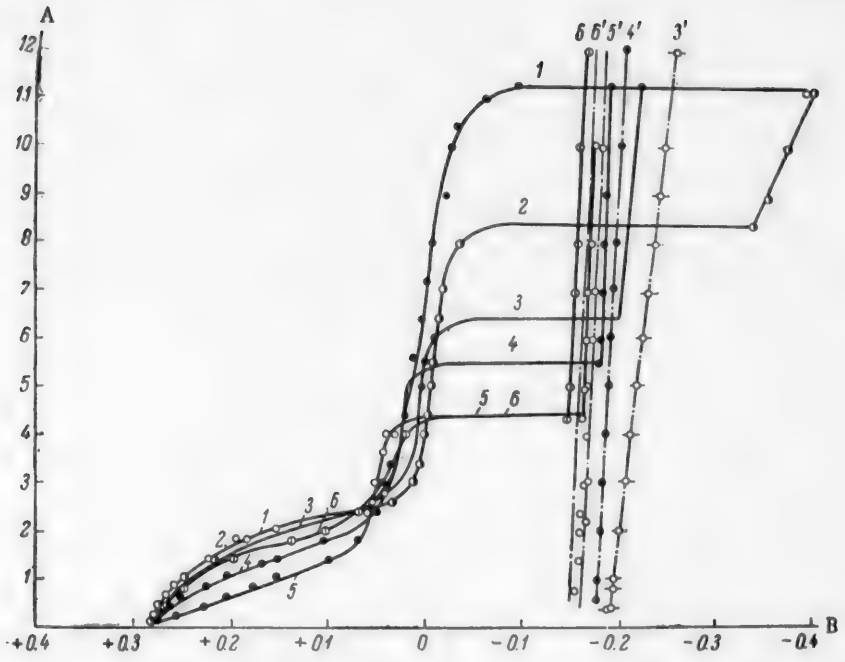

Fig. 5. Cathode polarization curves for solutions containing (in moles/liter): $Cu(NO_3)_2$ 0.05, KNO_3 0.5, HNO_3 0.075 and different amounts of $Pb(NO_3)_2$. A) Current density (ma/cm^2), B) potential (v). Amounts of $Pb(NO_3)_2$ (in moles/liter): 1) 0; 2) 0.02; 3) 0.1; 4) 0.3; 5) 0.906; 6) solution of $Cu(NO_3)_2$ 0.05 + $Pb(NO_3)_2$ 0.906; 3', 4', 5', 6') the corresponding solutions without $Cu(NO_3)_2$.

lead ions, so that the migration of copper ions from solution to the cathode surface is increased. However, the rate of discharge of copper ions becomes higher than the rate of their migration toward the cathode with further increase of the current; the deposition of copper is then retarded, as shown by a break in the curves in Fig. 3.

At a given concentration of copper ions in solution, the copper content of the deposit should be determined by the conditions for the diffusion of ions toward the cathode surface, and by the rate of deposition of lead. In accordance with the equation derived by Kheifets and Rotinian [16] it may be assumed that

$$C_{Cu} = \frac{D\,[Cu^{++}]}{i_{Pb}},$$

where C_{Cu} is the percentage of copper in the deposit, and D is the coefficient of diffusion.

The validity of this expression is confirmed by the linear plots in Fig. 7, based on the experimental data.

The different slopes of the lines may be due to changes of the diffusion coefficient on introduction of salts which transport electricity but do not take part in the cathode process.

Since deposition of the lead–copper alloy takes place at the limiting current for copper, deposits of satisfactory quality can be formed only by the discharge of copper ions into a dense mass of lead crystals.

Influence of Composition of Electrolyte and Current Density on the Quality of Deposition

Current density (ma/cm^2)	Cathode potential (v)	Current efficiency for copper, A_{Cu}	Current efficiency for lead, A_{Pb}	Total current efficiency A_{Me} (%)	Current density for copper, i_{Cu}	Current density for lead, i_{Pb}	Composition of deposit (%) Cu	Composition of deposit (%) Pb	Appearance of deposit
Electrolyte composition (moles/liter): $Cu(NO_3)_2$ 0.05, KNO_3 0.5, HNO_3 0.075, $Pb(NO_3)_2$ 0.02									
8.5	—0.370	35.7	17.9	53.6	3.03	1.56	33.4	61.6	Spongy, gray-brown
10	—0.376	50.8	15.6	66.4	5.08	1.56	50.0	50.0	Spongy, gray-brown
20	—0.410	30.0	7.8	37.8	6.00	1.56	48.5	51.5	Spongy, gray-brown
Electrolyte composition (moles/liter): $Cu(NO_3)_2$ 0.05, KNO_3 0.5, HNO_3 0.075, $Pb(NO_3)_2$ 0.1									
7	—0.207	61.0	38.9	99.9	4.26	2.79	33.0	67.0	Loose, rose-gray
10	—0.225	50.6	48.2	98.8	5.06	4.92	22.5	77.5	
12	—0.237	42.3	56.3	98.6	5.07	6.76	18.5	81.5	Dense, microcrystalline, rose-gray
15	—0.255	20.3	48.0	68.3	3.05	7.2	13.0	86.0	Spongy, gray
20	—0.300	13.7	43.7	57.4	2.74	8.73	8.7	91.3	Spongy, dark gray
Electrolyte composition (moles/liter): $Cu(NO_3)_2$ 0.05, KNO_3 0.5, HNO_3 0.075, $Pb(NO_3)_2$ 0.3									
6	—0.183	61.1	37.9	99.0	3.67	2.25	33.0	67.0	Spongy, rose-gray
8	—0.189	45.4	51.3	96.7	3.63	4.10	22.8	77.2	Dense, microcrystalline, rose-gray
10	—0.1925	34.3	63.4	97.7	3.43	6.34	17.3	82.7	Dense, microcrystalline, rose-gray
15	—0.2160	23.7	71.8	95.5	3.56	10.78	11.2	88.8	Dense, microcrystalline, rose-gray
20	—	20.25	73.3	93.55	4.05	14.65	9.0	91.0	Dense, microcrystalline, rose-gray
Electrolyte composition (moles/liter): $Cu(NO_3)_2$ 0.05, KNO_3 0.5, HNO_3 0.075, $Pb(NO_3)_2$ 0.906									
0.44	+0.2440	97.6	—	97.6	0.433	—	100	—	Dense, rose color

(continued)

Current density (ma/cm^2)	Cathode potential (v)	Current efficiency		Total current efficiency A_{Me} (%)	Current density		Composition of deposit (%)		Appearance of deposit
		for copper, A_{Cu}	for lead, A_{Pb}		for copper i_{Cu}	for lead, i_{Pb}	Cu	Pb	
1.4	+0.0956	66.7	—	66.7	0.935	—	100	—	Dense, dark rose color
3.0	+0.0476	48.7	—	48.7	1.46	—	100	—	Spongy, dark rose color
4.25	+0.0278	41.5	—	41.5	1.76	—	100	—	
4.4	—0.1670	42.5	18.3	60.8	1.78	0.805	27.2	62.8	Spongy, grayish red color
5.0	—0.1700	41.2	49.0	90.2	2.06	2.45	25.0	75.0	
5.6	—0.1714	42.0	50.8	92.8	2.35	2.85	22.0	78.0	Dense, microcrystalline, pale gray with rose tinge
6.0	—0.1726	41.8	52.5	94.3	2.52	3.15	20.3	79.7	
10.0	—0.1781	32.8	65.1	97.9	3.28	6.51	13.1	86.9	
18.0	—0.1920	20.2	79.0	99.2	3.64	14.40	7.4	92.6	
Electrolyte composition (mole/liter): $Cu(NO_3)_2$ 0.05, KNO_3 0.5, HNO_3 0.075, $Pb(NO_3)_2$ 0.906, $H_6C_4O_6$ 0.135, NH_4Cl 0.187									
0.8	+0.2026	100	—	100	0.8	—	100	—	Dense, rose color
2.0	—0.1446	74.1	6.3	80.4	1.48	0.126	78.3	21.7	Spongy, grayish brown
3.0	—0.1724	58.6	11.8	70.4	1.76	0.355	59.1	40.9	
5.0	—0.1748	46.45	36.1	82.55	2.32	1.81	27.9	72.1	
5.6	—0.1752	43.3	60.6	93.9	2.42	2.83	21.0	79.0	Dense, microcrystalline, pale gray with rose tinge
7.2	—0.1780	39.0	63.1	99.1	2.83	4.54	15.8	84.2	
15.0	—0.1950	24.4	75.2	99.6	3.66	11.3	9.5	90.5	
20.0	—0.2050	19.6	80.3	99.9	3.93	16.6	8.3	91.7	

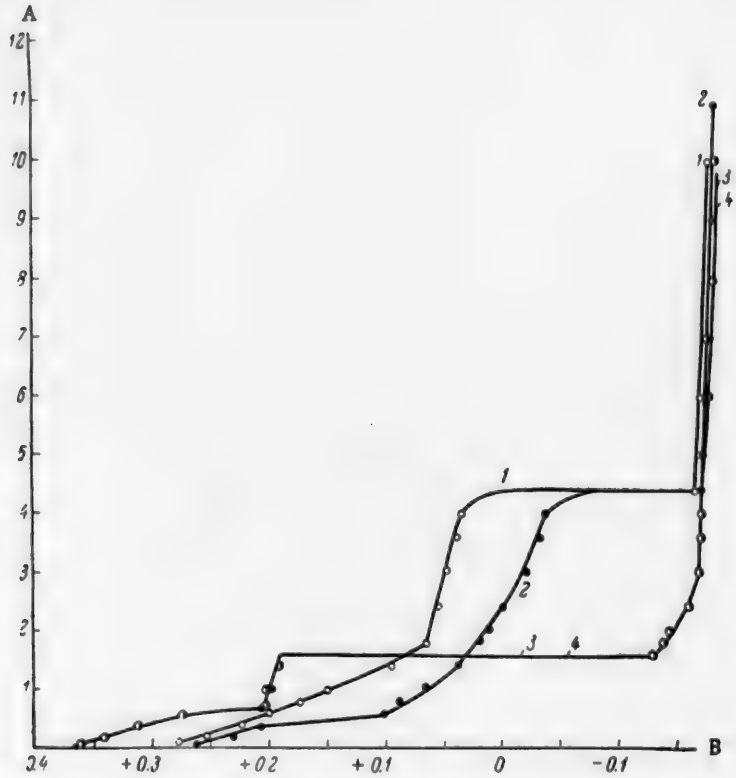

Fig. 6. Effect of additions of NH_4Cl and $H_6C_4O_6$ on cathode polarization in solutions containing (in moles/liter): $Cu(NO_3)_2$ 0.05, KNO_3 0.5, HNO_3 0.075, $Pb(NO_3)_2$ 0.906. A) Current density (ma/cm^2), B) potential (v). Additions (in moles/liter): 1) Without additions; 2) $H_6C_4O_6$ 0.135, 3) NH_4Cl 0.187, 4) NH_4Cl 0.187 + $H_6C_4O_6$ 0.135.

It follows from the data in the Table that the lead content of the deposit generally increases with increase of the cathode current, and at high currents it is almost independent of the lead-ion concentration in solution.

However, the properties of the alloys formed are not determined by their composition. The ratio of the partial currents for lead (i_{Pb}) and copper (i_{Cu}) likewise does not determine the quality of the deposits formed.

It is seen that the quality of the deposits depends on the current efficiency for lead.

It follows from the experiments data (see Table) for solutions with different concentrations of $Pb(NO_3)_2$ that deposits of satisfactory quality are obtained if the current efficiency for lead is not less than 50%.

Lower current efficiencies for lead may be due either to high current efficiencies for copper, as is the case at low current densities in solutions containing NH_4Cl and $H_6C_4O_6$, or to liberation of hydrogen simultaneously with both metals, which may occur in solutions with low Pb^{++} ion concentrations.

Finally, it must be noted that whereas pure lead is deposited from nitrate solutions, even at low current densities, in the form of separate large dendrites which crumble away readily from the cathode, the lead–copper alloy forms dense, smooth deposits which adhere firmly to the cathode, even at high current densities.

I offer my deep gratitude to V. L. Kheifets for his interest and help in discussion of the results.

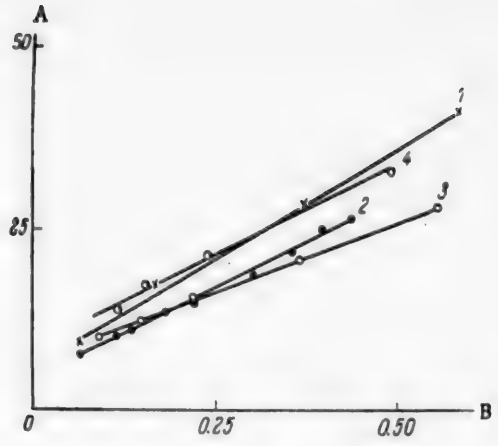

Fig. 7. Variation of C_{Cu} with i_{Pb}. A) Copper content of deposit (%), B) value of $\frac{1}{i_{Pb}}$.

Electrolyte composition (in moles/liter): 1) 0.05 $Cu(NO_3)_2$ 0.906 $Pb(NO_3)_2$; 2) 0.5 $Cu(NO_3)_2$, 0.906 $Pb(NO_3)_2$, 0.5 KNO_3, 0.075 HNO_3; 3) 0.05 $Cu(NO_3)_2$, 0.906 $Pb(NO_3)_2$, 0.5 KNO_3, 0.075 HNO_3, 0.135 $H_6C_4O_6$ 0.187 NH_4Cl; 4) 0.05 $Cu(NO_3)_2$, 0.5 KNO_3, 0.075 HNO_3, 0.3 $Pb(NO_3)_2$.

SUMMARY

1. Investigation of the cathode processes in the deposition of copper and lead from their nitrates in presence and in absence of KNO_3, HNO_3, NH_4Cl and $H_6C_4O_6$ showed that the proportion of the current used in the deposition of copper in presence of these additives reaches almost the same limiting value at different values of the potential. Additions of HNO_3, $H_6C_4O_6$ and NH_4Cl have no effect on the deposition of lead.

2. Simultaneous deposition of lead and copper takes place under the conditions of the limiting current for copper. No appreciable change in the potential of lead deposition takes place in the process. Introduction of the additives studied has no significant effect on the deposition potential of the alloy.

3. It is shown that the magnitude of the $i_{Pb}:i_{Cu}$ ratio and the lead content of the deposit do not determine the quality of the deposits. Electrodeposition of copper–lead alloys of satisfactory quality is possible only if the current efficiency for lead is not less than 50%.

LITERATURE CITED

[1] C. Faust, Trans. Electroch. Soc. 78, 383 (1940).

[2] M. Hansen, Structure of Binary Alloys (Russian translation) (1941).

[3] P. P. Beliaev, A. G. Valezheva and S. P. Gel'man, Metal Industry Herald 6, 117 (1935); 4, 90 (1936).

[4] W. R. Meyer and A. Phillips, Trans. Electroch. Soc. 73, 377 (1938).

[5] A. Ferguson, Nelson and W. Howey, J. Electroch. Soc. 98, 146 (1951).

[6] A. Beerwald and L. Dohler, Archiv Metallkunde, 1, 9, 419 (1947).

[7] U. S. Patent 2,086,841 (1937).

[8] C. Young and C. Struyk, Metal Finishing 47, 49 (1949).

[9] E. Raub, Metalloberfläche 7, 17 (1953).

[10] I. L. Gordienko, Candidate's Dissertation (Leningrad Tech. Inst., 1946).

[11] A. K. Babko and A. T. Pilipenko, Colorimetric Analysis (Goskhimizdat, 1951).*

[12] Chemist's Reference Book, 1 (State Tech. Press, 1952).*

[13] A. N. Frumkin and S. I. Zhdanov, Proc. Acad. Sci. USSR 92, 629 (1952); 93, 793 (1954).

[14] N. P. Fedot'ev and E. G. Kruglova, J. Appl. Chem. 28, 275 (1955).**

[15] A. N. Frumkin, V. S. Bagotskii, Z. A. Iofa and B. N. Kabanov, Kinetics of Electrode Processes (Izd. MGU, 1952).*

[16] V. L. Kheifets and A. L. Rotinian, Proc. Acad. Sci. USSR, 82, 3, 423 (1953).

Received March 16, 1957

*In Russian.

**Original Russian pagination. See C. B. Translation.

EFFECT OF SURFACE-ACTIVE SUBSTANCES ON THE MECHANICAL PROPERTIES OF ELECTROLYTIC DEPOSITS

N. P. Fedot'ev and Iu. M. Pozin

Strength tests of electrolytic metals have been studied little. The tensile strength of electrolytic copper, the influence of surface-active additives on it, and the relationship between the strength and other mechanical properties of copper such as internal stresses and microhardness, were studied in this investigation.

EXPERIMENTAL

The RMP-50 machine of the Moscow Experimental Factory of Testing Machines and Balances, for tensile testing of wire and thin ribbon, provided with special jaws ensuring uniform tension of the specimen across its width, was used for the tensile-strength tests on copper. The test specimens were cut out by means of the punch of the Schopper machine.

Specimens of rolled copper 50 and 75 μ thick were tested first, in order to determine the magnitude of of the experimental error inherent in the test method itself (see Table).

Results of Tensile Strength Tests on Copper

	Tensile strength (kg/mm^2)				
	rolled		electrolytic		
	50 μ	75 μ	25 μ	50 μ	75 μ
	35.9	33.6	22.4	21.7	21.6
	36.5	33.6	23.3	23.0	22.2
	35.8	33.5	22.6	22.4	22.5
	35.8	33.6	22.2	21.0	22.3
	37.3	33.5	20.0	23.4	22.1
	36.9	33.6	21.6	22.6	22.0
	—	—	20.4	21.9	22.7
	—	—	21.8	21.6	21.75
Average hardness	36.37	33.55	22.04	22.2	22.14
Deviation (%)	2.55	0.15	10.9	5.4	2.5

It follows from the table that the experimental error decreases with increase of specimen thickness. The explanation is that the relative irregularity of the specimen along its length decreases, and the influence of mechanical damage caused by stamping diminishes, with increasing thickness. The higher strength of the thinner specimens may be attributed to a greater compression effect in rolling.

The electrolytic copper was deposited from electrolytes of the following composition (in g/liter): $CuSO_4 \cdot 5H_2O$ 250, H_2SO_4 50, at current density 1 amp/dm^2, and 18°. The cathode was a stainless steel plate (115 × 50 mm). The copper was easily detached from the plate after electrolysis; specimens were cut from it for the tensile tests. The thickness was determined to the nearest 3 μ at several points along each specimen, by means of a micrometer, or the average thickness as found by weighing was taken.

The results of the tests are given in the Table.

It follows from these results that the experimental error decreases with increase of specimen thickness in the case of electrolytic copper also. The error is somewhat greater than in the case of rolled copper, as there are some irregularities in the thickness of the electrolytic deposit (up to 3 μ in specimens 75 μ thick).

The absolute values of the tensile strength of electrolytic copper are in good agreement with literature data [1].

Internal stresses in the copper deposits were measured by means of an optimeter by the method described by Glikman, Fedot'ev and Chernova [2]. The copper was deposited on brass specimens 80 × 18 × 1.4 mm in size; the deposits were 35μ thick. The following formula was used for calculation of the internal stresses:

$$\sigma = {}^4/_3 \frac{E \cdot (h+t)^3 \cdot f}{l^2 \cdot h \cdot t} .$$

The elasticity modulus was taken to be $1.1 \cdot 10^4$ kg/mm². The microhardness was measured by means of the PMT-3 microhardness tester at 50 g load.

Results of the Investigations

All the experiments were performed with an electrolyte of the following composition (in g/liter): $CuSO_4 \cdot 5H_2O$ 250, H_2SO_4 5, at current density 1 amp/dm², 18°, with deposits 75 μ thick. The surface-active substance chosen was Rochelle salt, as it produces a gradation from internal forces of extension to internal forces of compression in electrolytic copper deposits [3].

The results are presented in graphical form in Figs. 1-3.

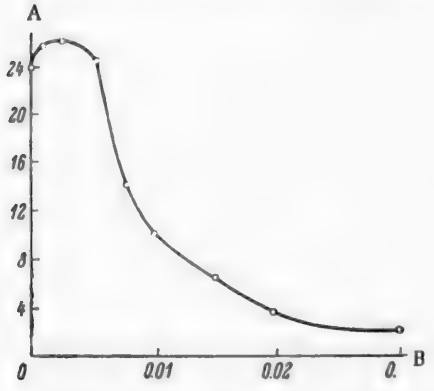

Fig. 1. Tensile strength of electrolytic copper as a function of the Rochelle salt concentration in an electrolyte containing 5 g H_2SO_4 per liter, at D_c = 1 amp/dm². A) Tensile strength (kg/mm²), B) concentration of Rochelle salt (g/liter).

The tensile strength of copper first increases with increase of the concentration of Rochelle salt, to 25.8 kg/mm² with 0.0025 g of Rochelle salt per liter, then begins to decrease, and drops sharply to 3.5 kg/mm² at 0.02 g of Rochelle salt per liter (Fig. 1). On further increase of the Rochelle salt concentration the deposits formed are so brittle that it is impossible to remove the copper from the basis metal and cut test specimens from it. For determination of the variations of tensile strength at high concentrations of Rochelle salt, the steel cathodes were replaced by cathodes of thin sheet copper (115×50×0.05 mm) the tensile strength of which was determined previously. Specimens for tensile testing were cut from the cathode after electrolysis, with the layer of deposited copper 60 μ thick on it. The results of these tests are given below.

Concentration of Rochelle salt (g/liter)	0	0.025	0.1	0.2	1.0	3.0	5.0
Tensile strength (kg/mm²)	23.60	8.56	8.57	8.37	5.66	1.19	0.87

It follows from these results that the tensile-strength curve has a slight slope toward the abscissa axis, approaching a zero value. The discrepancies between the absolute values of the tensile strength of copper formed from electrolytes with high concentrations of Rochelle salt, as determined by the first and second methods, were probably the consequence of partial cracking of the copper deposits during removal from the steel basis metal.

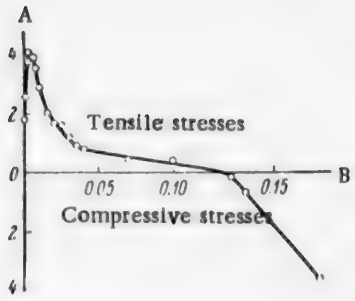

Fig. 2. Internal stresses in electrolytic copper deposits formed from electrolytes containing 5 g H_2SO_4 per liter at D_c = 1 amp/dm^2, with different concentrations of Rochelle salt. A) Internal stresses (g/mm^2), B) concentration of Rochelle salt (g/liter).

The internal tensile stresses, like the tensile strength, increase on addition of small amounts of Rochelle salt. On further increase of concentration they decrease, rapidly at first, then more slowly; with 0.134 g of Rochelle salt per liter they become zero, and pass into internal compressive stresses (Fig. 2).

The microhardness of the copper rises sharply from 152 to 263 kg/mm^2 with increase of the Rochelle salt concentration to 0.02 g/liter. Further increase of the concentration increases the microhardness only slightly (Fig. 3).

Polarization curves were plotted for elucidation of the mechanism of the action of Rochelle salt (Fig. 4). The polarization curves have horizontal plateaus, which are obtained at lower current densities with increase of the Rochelle salt concentration. The presence of these plateaus can be attributed to adsorptional chemical polarization, in the light of Loshkarev's theory [4, 5]. It is clear from the polarization curves that in the current density region of 1 amp/dm^2 low concentrations of Rochelle salt displace the cathode potential somewhat in the negative direction. At Rochelle salt concentrations of the order of 0.02 g/liter the cathode potential is displaced sharply in the negative direction owing to the existence of a horizontal plateau at current densities below the current density used for electrolysis. Further increases of the Rochelle salt concentration displace the potential still further in the negative direction, but to a smaller extent.

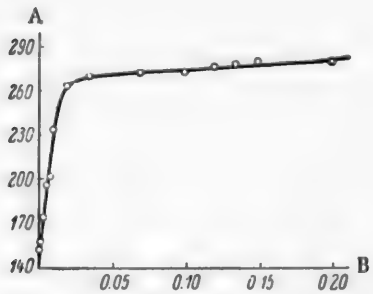

Fig. 3. Microhardness of electrolytic copper as a function of the Rochelle salt concentration in an electrolyte containing 5 g H_2SO_4 per liter, at D_c = 1 amp/dm^2. A) Microhardness (kg/mm^2). B) concentration of Rochelle salt (g/liter).

DISCUSSION OF RESULTS

There is seen to be a close relationship between the tensile strength, internal stresses, and microhardness. Low concentrations of Rochelle salt, of the order of 0.005 g/liter, result in increases of strength, internal tensile stresses, and microhardness. This is caused by the shift of cathode potential in the negative direction, which results in a decrease of the metal grain size. Several workers have reported this effect in the case of microhardness and internal stresses [6, 7].

However, the influence of Rochelle salt is not confined to the change of potential. The salt is adsorbed on the cathode surface and enters the intercrystalline spaces of the depositing metal. This has the effect of separating the individual crystals, with a consequent decrease of the tensile strength and internal tensile stresses in the metal. Moreover, in consequence of changes in its own volume in the intercrystalline layer, the surface-active substance has a kind of "disjoining" action on the crystals, and tends to push them apart. According to Vagramian and Tsareva, this effect is associated with deformation of the molecules of the surface-active substance in the double layer under the action of the electric field. As the crystals grow and cover the molecules included in the intercrystalline spaces, the action of the field on them ceases, and they tend to resume their normal form, thereby pushing the crystals apart [8].

Both the factors – the shift of potential and the disjoining action – operate at any concentration of Rochelle salt. However, the second factor becomes predominant with increase of the Rochelle salt concentration, the tensile strength decreases, and the internal tensile stresses diminish continuously, reach zero, and pass into internal compressive stresses.

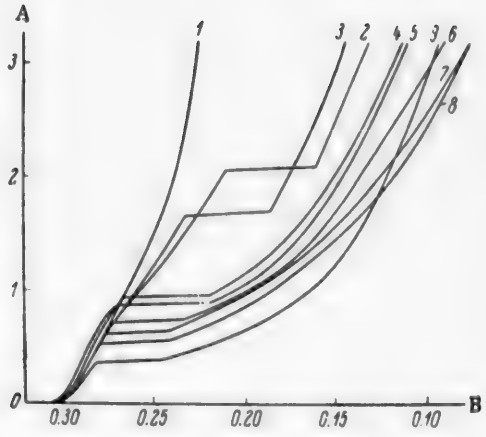

Fig. 4. Cathodic-polarization curves for different concentrations of Rochelle salt in an electrolyte containing 5 g H_2SO_4 per liter. A) Cathode current density (amps/dm^2), B) potential (v). Concentration of Rochelle salt (in g/liter): 1) 0.0, 2) 0.005, 3) 0.007, 4) 0.01, 5) 0.02, 6) 0.05, 7) 0.1, 8) 0.2, 9) 1.0.

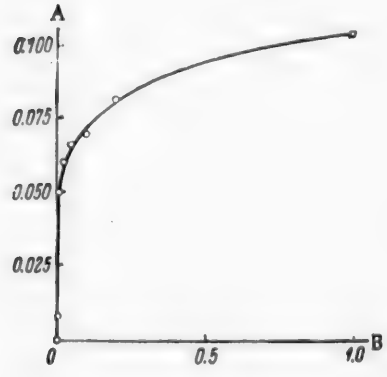

Fig. 5. Variation of the cathode potential with the Rochelle salt concentration at constant current density 1 amp/dm^2. A) Change of cathode potential (v), B) concentration of Rochelle salt (g/liter).

We are therefore inclined to attribute the internal compressive stresses, not to the appearance of some new property in the metal at a definite concentration of the surface-active substance, but to a quantitative change of the disjoining action, which increases continuously with increasing content of the surface-active substance in the intercrystalline layers, and at a definite content begins to prevail over the tendency of the deposit to compression, i.e., over the internal tensile stresses.

This explanation of the appearance of internal compressive stresses satisfactorily accounts for the absence of any changes on the microhardness and tensile-strength curves at concentrations of Rochelle salt which correspond to the change of sign in the internal stresses.

Figure 5 shows how the tensile strength, internal stresses, and microhardness alter rapidly at Rochelle salt concentrations up to 0.02 g/liter, and only slightly with further increase of the concentration. This graph represents the variation of cathode potential with the Rochelle salt concentration in the electrolyte, at constant current density 1 amp/dm^2. It is also seen that the variation of cathode polarization can be represented by a curve analogous to the adsorption isotherm, which may be described by the equation $\Delta\varphi = 0.103 \cdot C^{0.1455}$, where C is the concentration of Rochelle salt in the electrolyte.

If we write this equation in the general form, we obtain the Freundlich empirical equation for the adsorption isotherm:

$$\Delta\varphi = K \cdot C^{\frac{1}{n}}$$

An analogous result was obtained by Matulis and Bodnevas in the electrodeposition of copper in presence of acetic, propionic, malonic, and succinic acids [9]. It seems likely that when a definite concentration of Rochelle salt in the electrolyte is reached, the electrode surface becomes saturated with the surface-active substance, and further increase of its concentration has only a very slight effect.

SUMMARY

It follows from the experimental results that Rochelle salt has a strong influence on the properties of electrolytic copper. Low concentrations of Rochelle salt in the electrolyte increase cathodic polarization, and the strength, microhardness, and internal tensile stresses of the copper deposits increase in consequence. At higher concentrations of Rochelle salt the disjoining action of its molecules, incorporated in the intercrystalline spaces of the metal, increases so that the strength of the metal decreases and internal compressive stresses arise.

It was found that the curve for the variation of cathode polarization at constant current density with increase of the Rochelle salt concentration in the electrolyte is analogous to the adsorption isotherm.

LITERATURE CITED

[1] Iu. V. Baimakov, Electrolytic Deposition of Metals (in Russian) (1925).

[2] P. A. Glikman, N. P. Fedot'ev, and P. A. Chernova, Zavodskaia Lab. 9 (1951).

[3] N. P. Fedot'ev and E. G. Kruglova, J. Appl. Chem. 28, 3 (1955).•

[4] M. A. Loshkarev and A. A. Kriukova, Zhur. Fiz. Khim. 23, 7 (1949).

[5] M. A. Loshkarev and A. A. Kriukova, Zhur. Fiz. Khim. 23, 2 (1949).

[6] V. S. Ioffe, Uspekhi Khim. 13, 1 (1944).

[7] P. M. Viacheslavov, Candidate's Dissertation (in Russian) (Lensoviet Tech. Inst. Leningrad, 1953).

[8] A. I. Vagramian and Iu. S. Tsareva, Zhur. Fiz. Khim. 29, 1 (1955).

[9] Iu. Iu. Matulis and A. I. Bodnevas, Bull. Acad. Sci. USSR, Div. Chem. Sci. 4 (1954).•

Received March 20, 1957

•Original Russian pagination. See C. B. Translation.

INTERNAL STRESSES IN CATHODIC NICKEL DEPOSITS

A. L. Rotinian and E. S. Kosich

The question of internal stresses in cathodic deposits has been studied from various aspects in recent years. Considerable amounts of experimental data have been collected and various views have been put forward concerning the mechanism by which the internal stresses arise [1-7].

However, the available experimental data, and in particular in relation to nickel deposits, are not yet adequate. We therefore present in this paper the results of some of our experiments; these results, together with earlier data [6], give a more detailed picture of the influence of various factors on the formation of internal stresses in electrolytic nickel coatings.

The so-called contractometer method was used for determination of internal stresses. The principle of the method is as follows. Metal is electrolytically deposited under fixed conditions on one side of a thin plate rigidly clamped at one end. As the result of internal stresses and of the deposition of metal on one side only, the plate begins to bend. The degree of bending is usually very small, and can be observed only under the microscope (48-fold magnification was used in our experiments; 40 scale divisions of the micrometer eyepiece were equivalent to 1 mm). The relationship between the deflection of the plate and the internal stresses in the deposit is given by the equation [8]

$$p = \frac{1}{3} \cdot \frac{E \cdot d^2 \cdot \Delta}{\delta \cdot l^2}, \qquad (1)$$

where E is Young's modulus, d is the thickness of the plate, Δ is the deflection of the lower end of the cathode in a given time, l is the free length of the plate, and δ is the thickness of the nickel deposit.

For practical purposes, it is convenient to transform Equation (1) somewhat. The thickness of the nickel deposit is easily found from the Equation

$$I \cdot b \cdot \delta \cdot \sigma = c \cdot \eta \cdot I \cdot \tau, \qquad (2)$$

where I is the current strength, σ is the density of the electrolytic nickel, c is its electrochemical equivalent, τ is the deposition time, b is the width of the cathode, I is the length of its free portion, and η is the cathode current efficiency.

The value of δ is found from Equation (2) and substituted into Equation (1); this gives the formula used for calculation of the internal stresses:

$$p = \frac{1}{3} \cdot \frac{E \cdot d^2 \cdot b \cdot \tau \cdot \Delta}{c \cdot \tau \cdot \eta \cdot I \cdot l}. \qquad (3)$$

In this formula the cathode thickness (d = 0.24 cm), width (b = 1.2 cm), density of nickel, the electrochemical equivalent, deposition time (τ = 300 seconds), and Young's modulus ($2.1 \cdot 10^6$ kg/cm^2) are all constant. The cathode length l was measured separately in each experiment, although it was about 4 cm in each case.

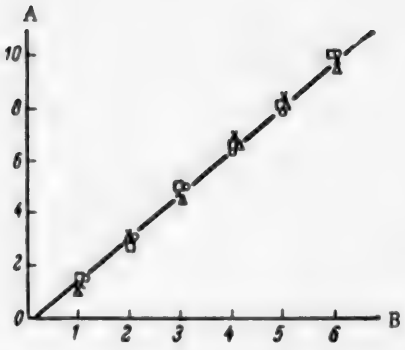

Fig. 1. Reproducibility of parallel experiments at I_a = 0.096 amp, t = 54°, D_c = 200 amps/m². A) Cathode deflection Δ, B) time (minutes).

The results of 4 parallel experiments are plotted in Fig. 1, which shows that the reproducibility is quite satisfactory. The cathode deflection is directly proportional to the time of electrolysis; this shows that the internal stresses are independent of the thickness of the metal deposited under the conditions used.

The values of the internal stresses given below are average results from 3-5 parallel experiments. It must be emphasized that the contractometer method is only applicable to the determination of stresses in continuous deposits.

In the first series of experiments the effect of sodium chloride concentration on internal stresses in the cathode deposits was studied. The results are given in Fig. 2. It is seen that the internal stresses in the deposits increase steadily with increasing sodium chloride concentration in the electrolyte. Up to about 60 g of sodium chloride per liter, the nature of the linear increase of internal stresses is the same as that found by Ioffe [1]. The absolute values found by Ioffe are roughly double ours; this indicates that the electrolyte in Ioffe's experiments was contaminated. From a concentration of 60 g of sodium chloride per liter, however, the two curves begin to differ in character. In Ioffe's experiments the internal stresses rose sharply with increase of NaCl concentration, reaching a maximum at C_{NaCl} = 120 g/liter, whereas our values fit on a straight line over the entire concentration range from 5 to 150 g of NaCl per liter.

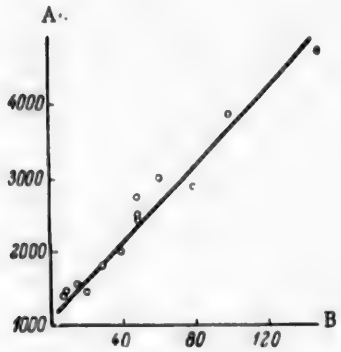

Fig. 2. Effect of sodium chloride concentration on internal stresses in cathode deposits at D_c = 200 amps/m², t = 54°. A) Internal stresses p (kg/cm²), B) NaCl concentration (g/liter). Electrolyte composition (g/liter): Ni 49, Na_2SO_4 18, H_3BO_3 20, NaCl of different concentrations, pH = 4.7.

At the same time, it follows from the literature [9] and from our observations that the grain size of the deposit decreases and cathode polarization diminishes [10] with increase of sodium chloride concentration in the electrolyte. Thus, we have here a somewhat unusual case of a symbatic variation of crystal size and cathode polarization.

In all probability this can be explained if the dual effect of the specific adsorption of chloride anions on the growing cathode is taken into consideration. On the one hand, adsorption of chloride ions leads to a change in the structure of the double layer, facilitating cation discharge, and on the other, it shields the most active centers of the cathode surface.

The first of these factors results in a decrease of polarization with increasing concentration of chloride ions in solution, and the second makes the deposit more finely crystalline.

The purpose of the next 3 series of experiments was to determine the effects of sodium sulfate, boric acid, and nickel sulfate concentrations on the magnitude of the internal stresses.

It was found that up to 100 g of sodium sulfate per liter has no effect on the internal stresses in the cathode deposits.

Boric acid in the concentration range from 3 to 30 g/liter likewise has no significant effect on internal stresses.

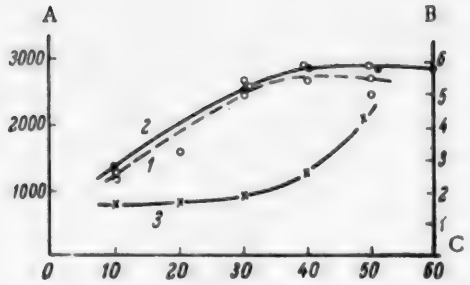

Fig. 3. Effect of nickel concentration in the electrolyte on internal stresses in cathode deposits at D_C = 200 amps/m², t = 54°. A) Internal stresses p (kg/cm²), B) concentration of organic substances in electrolyte (mg/liter), C) Ni concentration (g/liter). Electrolyte composition (g/liter): variable concentration of Ni, Na_2SO_4 18, H_3BO_3 20, NaCl 50; pH = 4.7.

With increase of the nickel concentration in the electrolyte from 10 to 30 g/liter, the internal stresses in the deposits first increase, and then become independent of the concentration (Fig. 3). This is not the result of increased contamination of the electrolyte with organic impurities with increasing concentration of nickel sulfate in the electrolyte, nor is it the consequence of a decrease in current efficiency at low concentrations of $NiSO_4$. The current efficiency did not fall below 96% in any of the experiments. The only noticeable difference was that the deposits formed from electrolytes containing 10 and 20 g nickel per liter had numerous small holes, whereas the deposits formed at nickel concentrations of 30 g per liter and over appeared to be of good quality. Therefore the decrease of internal stresses at low nickel concentrations is illusory, and is caused by extraneous factors, which make the contractometer method inapplicable.

Some of our data on the influence of pH on internal stresses in the deposits were published earlier [6]; our results agree with the findings of McNaughtan [11], Rambridge [12], and Samartsev and Lyzlov [5]. Here we need only add that a change of the sodium chloride concentration in the electrolyte displaces the critical pH value to just the same extent as the same change of NaCl concentration displaces the pH of the start of hydroxide formation. Therefore this fact provides further evidence that the sharp increase in the internal stresses when the critical pH is exceeded is due to the appearance of colloidal formations in the electrolyte.

Next we consider the effects of electrolysis conditions (D_C, t°), on internal stresses in cathode deposits.

It has been reported [5] that internal stresses increase with increasing current density. We obtained similar results in preliminary experiments.

However, it was found later that this occurs because the catholyte layer becomes strongly alkaline at high current densities. If the experiments are performed so that the solution pH does not vary, the internal stresses even decrease somewhat with increasing current density.

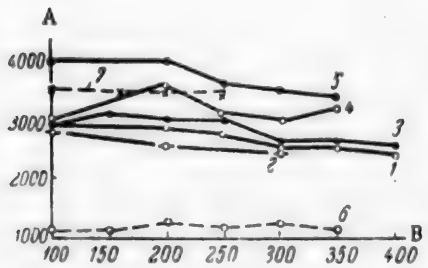

Fig. 4. Effect of current density on internal stresses in cathode deposits, variable D_C, at t = 54°. A) Internal stresses p (kg/cm²), B) current density D_C (amps/m²). Electrolyte composition (g/liter): Ni 50, Na_2SO_4 18, H_3BO_3 20; NaCl 50 – continuous lines, and NaCl 5 – dash lines. pH values: 1) 3.5, 2) 3.8, 3) 4.2, 4) 5.5, 5) 5.7, 6) 4.5, 7) 6.1.

The results are plotted in Fig. 4; it is seen that pH above the critical value the internal stresses are large, while below the critical pH they are of normal values over the entire range of current densities studied. Near the critical pH (Curve 4) unstable values are obtained, owing to the transitional conditions of electrolysis.

The results of experiments on the influence of temperature on internal stresses in deposits are plotted in Fig. 5. The pH values of the solutions were determined at room temperature in these experiments. A fairly complicated picture was obtained. At pH = 5.7 the internal stresses first increase with increasing temperature, reach a maximum, and then decrease. The curve at pH = 4.5 follows a similar course, but much less pronounced. These results can be explained if the effect of temperature on the pH at which colloidal hydroxides

begin to form is taken into consideration. In fact, at low temperatures there is a region of the curve (for pH = 5.7) corresponding to internal stresses of the order of 2800-2900 kg/cm^2; this shows that the critical pH at these temperatures is above 5.7.

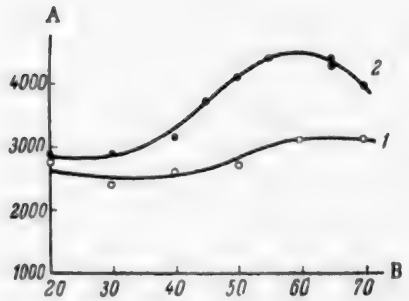

Fig. 5. Effect of temperature on internal stresses in cathode deposits at D_c = 200 amps/m^2. A) Internal stresses p (kg/cm^2), B) temperature (°C). pH values: 1). 4.5, 2) 5.7. Electrolyte composition (g/liter): Ni 49, Na_2SO_4 18, H_3BO_3 20, NaCl 50.

As the electrolyte temperature increases, the pH of the start of hydroxide formation decreases to the critical value; this leads to an increase of the internal stresses. Finally, at high temperatures electrolysis takes place with colloidal hydroxides already present in solution, and further increase of temperature, having a favorable effect on the electrocrystallization of the metal, decreases its internal stresses. This does not mean, of course, that temperature does not have a favorable effect on electrocrystallization at lower temperatures. However, the formation of colloidal hydroxides in the electrolyte is the more powerful factor, and the influence of the first factor is therefore suppressed.

SUMMARY

1. The effects of the composition of the nickel electrolyte, current density, and temperature on the internal stresses in cathode deposits were studied by the contractometer method, and it was found that internal stresses in the deposits increase linearly with the sodium chloride concentration of the electrolyte.

2. The internal stresses are not influenced by changes in the concentrations of sodium sulfate or boric acid in the ranges studied.

3. It is confirmed once again that the critical pH value corresponds to the start of formation of colloidal particles in the electrolyte.

4. Internal stresses are almost independent of current density if the electrolyte pH is kept constant.

5. If the degree of hydrolysis increases so much with temperature that colloidal formations appear in the electrolyte, increase of temperature results in an increase of internal stresses in the deposits. Otherwise the internal stresses decrease somewhat with increase of temperature.

LITERATURE CITED

[1] V. S. Ioffe, Uspekhi Khim. 13, 48 (1944).

[2] N. P. Fedot'ev and E. G. Kruglova, J. Appl. Chem. 28, 275 (1955).*

[3] A. T. Vagramian and Iu. S. Tsareva, Zhur. Fiz. Khim. 29, 184 (1955).

[4] Iu. S. Tsareva, V. G. Solokhina, N. T. Kudriavtsev and A. T. Vagramian, Zhur. Fiz. Khim. 29, 166 (1955).

[5] A. G. Samartsev and Iu. V. Lyzlov, Zhur. Fiz. Khim. 29, 374 (1955).

[6] A. L. Rotinian, E. Sh. Ioffe, E. S. Kozich and Iu. S. Iusova, Doklady Akad. Nauk SSSR, 104, 753 (1955).

[7] K. M. Gorbunova and O. S. Popova, Zhur. Fiz. Khim. 30, 269 (1956).

[8] R. H. Barklie and H. T. Davis, Engineer, 150, 670 (1930).

*Original Russian pagination. See C. B. Translation.

[9] V. I. Lainer and N. T. Kudriavtsev, Principles of Electroplating (in Russian) (Moscow, 1953), 1.

[10] A. L. Rotinian, V. Ia. Zel'des, E. Sh. Ioffe and E. S. Kozich, Zhur. Fiz. Khim. 28, 73 (1954).

[11] D. T. McNaughtan and R. A. F. Hammond, Trans. Faraday Soc. 27, 633 (1931).

[12] F. B. P. Rambridge, Ind. Finishing (L), 56, 512 (1953).

Received July 8, 1956

USE OF SOLUBLE NICKEL– MOLYBDENUM AND NICKEL ANODES FOR THE PRODUCTION OF NICKEL–MOLYBDENUM ALLOYS FROM ALKALINE ELECTROLYTES

D. P. Zosimovich and N. F. Bogatova

Institute of General and Inorganic Chemistry, Academy of Sciences, Ukrainian SSR

It is known that the electrolyte composition is one of the principal factors determining the composition of an electrolytically formed alloy. If insoluble anodes are used, the electrolyte composition is adjusted by addition of concentrated solutions of salts of the metals constituting the alloy. However, it is not always possible to use insoluble anodes. In particular, they cannot be used with electrolytes containing hydroxy acids, which are oxidized at the anodes, so that the electrolyte is spoiled and the current efficiency drops sharply. A necessary condition in the use of soluble anodes is that the cathode and anode current efficiencies should be equal for every component of the alloy.

It is known that anode solubility depends on the electrolyte pH, anode current density, presence of impurities in the anode material, and other factors. Tungsten and molybdenum dissolve easily in alkalies and with difficulty in acids [1-4]; iron and nickel, on the contrary, retain their activity in acids and become passive in alkalies [2]. Nickel anodes are used with acid electrolytes in nickel plating and in the refining of nickel [5]. The purer the nickel, the more easily it becomes passive. Chloride ions are used as activating agents in acid baths. There have been several investigations of the solution mechanism of nickel anodes in acid electrolytes [5-9]. However, alkaline electrolytes which may be used for the production of nickel–molybdenum alloys have not been studied at all in this respect. In some investigations [10-13] alloy or nickel anodes were used for the production of alloys from alkaline electrolytes. However, the anode process was not specially studied in these investigations. It is to be expected that the behavior of nickel or nickel-based alloys when used as anodes in alkaline electrolytes should differ from their behavior in acid electrolytes.

The object of this investigation was to study the behavior of sintered nickel-molybdenum and nickel anodes in the electrolytic production of nickel-molybdenum alloys from alkaline ammoniacal tartrate and ammoniacal electrolytes over a wide range of current densities. The practical task was to find the optimum concentrations of chloride ions at which the anodes would dissolve normally at the given current densities, so that a constant electrolyte composition is maintained and an alloy of definite composition (~ 20% Mo) is formed. Since the cathode current efficiency in this case is 30-40%, the anode current efficiency likewise should not exceed this value.

EXPERIMENTAL

The usual method, described in the literature [11], was used for investigation of the anode process. A constant current density of 100 ma/cm^2, which is the optimum value for production of alloys of nickel with molybdenum or tungsten [11, 12], was maintained at the cathodes. Most of the experiments were performed without circulation of the electrolyte, but in a few experiments the electrolyte was circulated. The electrolysis temperature was 30° for the ammoniacal tartrate electrolytes, and 40° for the ammoniacal electrolytes. The anode was placed in the center of the cell. The anode current densities were 30, 50 and 100 ma/cm^2. The volume of electrolyte in the cell was 500 ml. The electrolysis time was varied according to the anode current density, but was always such that about 1 g of alloy was deposited on the cathode.

The loss in weight of the anode, the weight of the cathode deposit, and the concentrations of nickel and molybdenum (or of nickel only) before and after electrolysis were determined in each experiment. In some cases the composition of the alloy formed on the cathode was determined, in order to compile the material balance.

The ammoniacal tartrate electrolyte had the following composition (in g/liter): Ni 12-14, Mo 5-6, $Na_2C_4H_4O_6 \cdot 2H_2O$ 70 and 150-175 ml of NH_4OH per liter (pH = 10.6-10.8).

The composition of the ammoniacal electrolyte was: Ni 12-14, Mo 7-8, and 200 ml of NH_4OH per liter (pH ≈ 11).

Chloride ions were introduced in the form of NaCl, while at high concentration (above 1 M) part of the $NiSO_4$ in the electrolyte was replaced by $NiCl_2$, because of the limited solubility of NaCl.

In experiments with the ammoniacal tartrate electrolyte the anodes used were made from sintered nickel–molybdenum alloy containing about 20% Mo, and also from rolled and electrolytic nickel.

The results of experiments on the anodic dissolution of sintered nickel–molybdenum alloys in ammoniacal tartrate electrolytes are given in Table 1; the serial numbers of the experiments represent the sequence in which the experiments were performed with the same anode. It follows from these results that the amount of chloride necessary for dissolution of the anodes increases with increasing current density. Thus, to maintain the electrolyte composition constant in the production of nickel–molybdenum alloy at anode current density 30 ma/cm^2 0.1 mole of chloride ions per liter of solution must be added. The amounts required at D_a = 50 ma/cm^2 and 100 ma/cm^2 are 0.15 mole and about 0.3 mole respectively. It also follows from Table 1 that the anodes dissolve better after removal of the top passive layer. Thus, at first (Experiment 1), at D_a = 30 ma/cm^2, 0.1 mole of chloride per liter was not enough for normal dissolution of the anodes (the electrolyte became poorer in nickel). After the same anode had been used at a higher chloride concentration in the electrolyte (0.3 M), 0.1 M chloride (Experiment 4) proved enough for normal dissolution of the anode. By variations of the chloride concentration it is possible to operate over a wide range of current densities, from 30 to 100 ma/cm^2 (Table 2).

TABLE 1

Ammoniacal Tartrate Electrolyte. Anode – Ni–Mo alloy (0.2% Fe)

Expt. No.	D_a (ma/cm^2)	[Cl'] (M)	Electrolyte composition (g/liter) before electrolysis		after electrolysis	
			Ni	Mo	Ni	Mo
1	30	0.1	13.41	6.39	12.20	6.39
2		0.3	11.71	5.51	13.66	5.80
3		0.15	12.93	5.86	13.90	6.10
4		0.1	13.29	5.92	13.29	5.92
5	50	0.1	13.41	6.39	12.68	6.16
6		0.3	11.71	5.51	13.66	5.80
7		0.15	12.93	5.86	12.33	5.86
8	100	0.1	13.41	6.39	10.49	5.80
9		0.3	11.71	5.51	12.07	5.39

The sintered anodes became coated with a pale brown amorphous film, insoluble in the electrolyte, in the course of electrolysis; this film apparently consisted of insoluble molybdenum compounds. In addition, a sludge consisting of metallic nickel and molybdenum formed at the bottom of the cell.

The anode material should have the minimum content of impurities for the production of very pure alloys. The impurities present in the anode material are useful in the dissolution of the anodes, but are harmful in that they enter the electrolyte when the anode dissolves, contaminate the electrolyte, and are liberated at the cathode together with the main alloy components.

TABLE 2

Relationship Between the Amount of Chloride Ions Added to the Ammoniacal Tartrate Solution and the Anode Current Density Used with Anodes of Different Materials

D_a (ma/cm^2)	Cl ion content (M) with anodes of		
	sintered alloy of composition 20% Mo, 80% Ni (0.2% Fe)	rolled Ni (Fe = 0.018%)	electrolytic Ni (Fe = 0.0058%)
30	0.1	0.4	0.75
50	0.15	—	0.90
100	0.8	1.0	1.80

In view of the harmful effects of the impurities which enter sintered and cast anodes during their manufacture, and also of the difficulties and the cost of production of such alloyed anodes, it was decided to investigate the possibility of using nickel anodes.

Rolled nickel was used as the anode material. The results of the experiments are given in Table 3. In contrast to sintered alloy anodes, nickel anodes did not give rise to insoluble products in the sludge and on the anode surfaces. The sludge consisted of metallic nickel.

TABLE 3

Ammoniacal Tartrate Electrolyte. Anode – Rolled Nickel (0.018% Fe)

Expt. No.	D_a (ma/cm^2)	[Cl$'$] (M)	Ni content of electrolyte (g/liter)		Notes
			before electrolysis	after electrolysis	
1*	30	0	12.93	11.46	Anode No. 1
2	50	0.1	13.29	11.95	
3	30	0.1	13.29	11.29	
4	100	0.1	13.29	11.22	
5	50	0.2	13.29	12.07	
6	50	0.3	12.32	11.22	
7	100	0.3	12.32	11.95	Anode No. 2
8	50	0.2	13.29	12.99	Anode treated with abrasive after Experiments 1-6
9	30	0.2	13.57	12.41	Anode No. 3
10	30	0.4	14.01	14.30	Circulation of electrolyte
11	50	0.5	14.89	14.16	
12	100	1.0	14.89	14.16	

*The weight of the anode was unchanged after electrolysis.

Experiments 1-6 were performed with the same anode, in the sequence indicated in Table 3. It follows from the data (Experiment 1) that in absence of chloride ions nickel anodes do not dissolve at all at current density 30 ma/cm^2. Addition of up to 0.3 M chloride ions at D_a = 50 ma/cm^2 did not produce positive results. However, when an unused nickel anode made from the same rolled metal was taken, the nickel dissolved satisfactorily in an electrolyte also containing 0.3 M chloride, even at 100 ma/cm^2 (Experiment 7). Therefore the nickel anode used in the electrolyte without chloride (Experiment 1) became so passive that decrease of current density and increase of the chloride ion concentration to 0.3 M were not enough to ensure removal of

the passive film. After the surface layer had been removed from the anode passivated in Experiments 1-6, by means of an abrasive, the anode was dissolved more easily (compare Experiments 5 and 8). An unused anode (Experiment 9) does not dissolve quite as well as a passivated anode after abrasive treatment. Consequently it follows that nickel anodes which have not yet been used are also coated with passive film, which should be removed to ensure better dissolution.

In addition to the rolled anodes, electrolytic N 0000 nickel was also tested. The results of the experiments are presented in Table 4. It was also found in this case that if the chloride ion content is insufficient for normal dissolution of the anode at a given current density, the anode becomes passive, and a large excess of chloride must be added in order to dissolve the passive film (Experiments 1-8).

TABLE 4

Ammoniacal Tartrate Electrolyte. Anode – Electrolytic Nickel (0.0058% Fe)

Expt. No.	D_k (ma/cm^2)	[Cl'] (M)	Ni content of electrolyte (g/liter)		Notes
			before electrolysis	after electrolysis	
1	30	0.4	14.30	13.72	
2		0.7	13.72	12.04	
3		1.0	14.01	13.87	
4		1.5	12.11	14.01	
5		1.0	13.43	14.31	Circulation of electrolyte
6		0.5	13.57	12.55	
7		0.7	13.57	12.34	
8		0.75	13.57	13.60	Circulation of electrolyte
9		0.75	12.50	13.64	New anode, previously etched in ammoniacal tartrate electrolyte containing 1.0 M Cl'
10		0.65	12.68	12.31	Anode after Experiment 9
11		0.75	12.50	13.89	New anode, previously etched in nickel sulfate bath
12	50	1.0	13.14	13.51	
13		0.9	13.14	13.14	
14		0.9	14.02	14.02	Circulation of electrolyte
15	100	1.5	12.50	13.39	$NiCl_2$ electrolyte, anode after Experiment 15
16		1.4	13.39	13.39	$NiSO_4$ and $NiCl_2$ electrolyte, anode after Experiment 11
17		1.3	13.39	13.14	$NiSO_4$ and $NiCl_2$ electrolyte
18		1.4	13.26	13.38	Circulation of electrolyte
19		1.3	13.26	13.26	Anode after Experiment 17, circulation of electrolyte

If the anodes are used for long periods, the electrolyte becomes gradually richer in nickel owing to decrease of the true current density. In such cases the anode current density can be raised by removal of some of the anodes from the circuit, without any change in the chloride content of the electrolyte.

It was further found (Experiments 9 and 11) that an ammoniacal electrolyte containing excess chloride ions, or the ordinary electrolyte used for refining, can be used for removal of the passive film.

The experiments showed that 86.8% of the nickel dissolved from the anode is utilized in augmenting the nickel content of the electrolyte, while the rest of the nickel goes into the anode sludge. The anode current efficiency is 39.8%.

It had been shown in our laboratory [13] that alloys of nickel with molybdenum or tungsten can be obtained from ammoniacal electrolytes, which have a number of advantages over the ammoniacal tartrate electrolytes. The possibility of using nickel anodes for the production of these alloys was therefore investigated. The results of the experiments are presented in Table 5. It is seen that if electrolytic-nickel anodes are used at current densities of 30, 50, and 100 ma/cm^2, 0.4, 0.5 and 0.8 moles of chloride ions per liter respectively must be added to keep the nickel contents constant.

TABLE 5

Ammoniacal Electrolyte. Anode – Electrolytic Nickel (0.0058% Fe)

Expt. No.	D_a (ma/cm^2)	[Cl'] (M)	Ni content of electrolyte (g/liter) before electrolysis	Ni content of electrolyte (g/liter) after electrolysis
1	30	1.0	12.13	14.40
2		0.8	12.12	14.90
3		0.6	12.12	14.27
4		0.5	12.00	12.68
5		0.4	12.00	12.00
6	50	0.7	11.55	12.07
7		0.8	11.55	12.45
8		0.65	11.55	12.23
9		0.6	11.55	12.07
10		0.5	11.70	11.70
11	100	0.8	12.45	12.07
12		2.0	11.55	12.75
13		0.85	11.55	12.30

Therefore the same relationship holds between the chloride ion content of the electrolyte, and the anode current density necessary for normal dissolution, both for ammoniacal electrolytes and for ammoniacal tartrate electrolytes.

It was shown in analogous experiments that all the relationships found in the studies of anode processes in the production of nickel–molybdenum alloys are applicable to nickel–tungsten alloys.

It must be pointed out that for the cathode process to occur correctly the chloride ion concentration of alkaline electrolytes must be considerably higher than the chloride concentration of the ordinary acid solutions used in nickel refining [5].

SUMMARY

1. The behavior of sintered nickel–molybdenum and of nickel anodes in the electrodeposition of nickel–molybdenum alloys from alkaline ammoniacal tartrate and ammoniacal electrolytes was studied; it was shown that the nickel content of the electrolyte can be kept constant over a wide range of anode current densities (30-100 ma/cm^2) by dissolution of these anodes, the rate of dissolution being regulated by appropriate changes of the chloride ion concentration of the electrolyte.

2. It was found that the amount of chloride ions which must be added to the electrolyte for normal dissolution of the anodes increases with the current density.

LITERATURE CITED

[1] M. Le Blanc and H. G. Byers, Z. phys. Ch. 69, 19 (1909).

[2] W. E. Koerner, Trans. Am. Electrochem. Soc. 31, 221 (1917).

[3] A. Ia. Shatalov and I. A. Marshakov, Zhur. Fiz. Khim. 28, 1, 42 (1954).

[4] R. Kremann and R. Müller, Elektrolyse and Polarization (Leipzig, 1931) 2, 453.

[5] A. I. Lainer and N. T. Kudriavtsev, Fundamentals of Electroplating (Moscow, 1953)** I, p. 425.

[6] F. Foerster and F. Krüger, Z. Elektroch. 33, 406 (1927).

[7] R. L. Dorrance and W. C. Gardiner, Trans. Am. Electrochem. Soc. 54, 303 (1928).

[8] W. Machu, A. Ragheb, Werkstoffe und Korrosion, 5, 217 (1954); Referat. Zhur. Khim. 3 (1955).

[9] G. Trümpler and W. Sazer, Helv. Chim. Acta 36, 1630 (1953); Referat. Zhur. Khim. 15 (1954).

[10] D. W. Ernst, R. F. Amlie and M. L. Holt, J. Electrochem. Soc. 102, 461 (1955).

[11] I. N. Frantsevich, T. F. Frantsevich-Zabludovskaia and E. F. Zhel'vis, J. Appl. Chem. 25, 4, 350 (1952).*

[12] T. F. Frantsevich-Zabludovskaia, A. I. Zaiats and K. D. Modylevskaia, J. Appl. Chem. 29, 11, 1684 (1956).*

[13] T. F. Frantsevich-Zabludovskaia and A. I. Zaiats, J. Appl. Chem. 30, 5, 723 (1957).*

Received June 12, 1956

*Original Russian pagination. See C. B. Translation.
**In Russian.

BEHAVIOR OF THE NITRATE ION AT A Pt ANODE

N. P. Fedot'ev and V. N. Varypaev

It was proposed to study certain anode processes in electrolysis of nitric acid solutions; it was considered necessary first to study the electrolysis of pure nitric acid.

Anode polarization curves were plotted for solutions of nitric acid between 0.05 N and 7 N concentration, with smooth Pt anodes in the current density range from 10^{-5} to 1 amp/cm^2 at room temperature. Certain nitrates were also used.

EXPERIMENTAL

The cell was an H-shaped vessel with the anode and cathode compartments separated by a compact plug of glass wool; in addition, the cathode (a platinum spiral) was enclosed in a cylindrical ceramic diaphragm; the anode consisted of platinum foil, 0.6 cm^2 in area. The anolyte volume was about 100 ml.

The nitric acid was used in the form of 0.05, 0.1, 0.2, 0.3, 0.5, 1, 2, 4, 7 N solutions of pure nitric acid, obtained by distillation of the chemically pure acid, the extreme fractions being rejected. The electrolyte temperature was 25 ± 0.1°.

Anode polarization curves were plotted in these conditions. The potentials were measured by the compensation method, with a potentiometer of the usual type (P-4) and a saturated calomel electrode.

Twenty-two points were recorded in the current density range from 10^{-5} to 1 amp/cm^2, at roughly equal intervals on a logarithmic scale.

The following procedure was adopted in the determination of the polarization curves: 1) the anode was first polarized in the electrolyte at D_a = 0.17 amp/cm^2 (i.e., at 100 ma) until the stationary potential (φ_{st}) was reached, which took up to 30 minutes; the potential was assumed stationary if it did not change by more than 1 mv in 5 minutes; 2) the reverse φ–D curves (i.e., from higher to lower current densities) were determined, φ_{st} being reached at each point; as a rule, this took place in the first few minutes, except in the D_{lim} regions.

The electrode was degreased before electrolysis, kept for a few seconds in 1 N HNO_3 + H_2O_2 solution, and then boiled in distilled water.

If the conditions for preparation of the electrode were strictly maintained, the φ – log D curves were reproducible to within 10-15 mv. The sections of the curves in the transitional region (i.e., corresponding to 0.05-0.2 N HNO_3 at $D_a > 1 \cdot 10^{-4}$ amp/cm^2) were exceptional; here the reproducibility was poor both in regard to the slopes of the curves and to the absolute values of the anode potential.

Results and Discussion

The anode polarization curves for smooth platinum in nitric acid at several different concentrations are given in Fig. 1.

It is seen that the form of the curve depends on the nitric acid concentration. Curves 1 and 2 (7 N and 4 N nitric acid) consist of two linear regions, with the coefficient "b" of the Tafel equation changing from 0.14 to 0.10. Curve 3 (2 N nitric acid) has an intermediate plateau with a slope which differs sharply from the slopes of both the lower and the upper portions. This plateau increases with dilution, reaching 0.35 v for

0.2 N nitric acid (Curve 6), and the stationary potential is established slowly in it, irrespective of the preliminary polarization conditions.

It must be assumed that in the lower region of each curve the formation of O_2 proceeds by discharge of water molecules, as is presumed to be the case, for example, in sulfuric acid [1, 2]. According to the theory developed by Ershler et al., Veselovskii et al., and others, the elementary discharge with formation of atomic oxygen takes place at the surface of oxidized, passive platinum.

In the conditions of our experiments, where the anode potential is in the region of 1.8 v and higher, the principal role in the formation of the electrode surface should be played by the higher oxide PtO[O] which, as Rozental' and Veselovskii [3] showed, is involved in the formation of O_2:

$$Pt \cdot PtO[O] + H_2O \longrightarrow Pt \cdot PtO + O_2 + 2H^+ + 2e.$$

The direct discharge of water molecules, without the agency of Pt oxides, is also possible.

Up to about $D_a = 1 \cdot 10^{-4}$ amp/cm^2 the slope of the Tafel lines increases smoothly from 0.11 for 0.05 N to 0.14 for 7 N nitric acid. In the region $D_a = 0.6\text{-}1.6 \cdot 10^{-4}$ amp/cm^2 and $\varphi_a = 1.9$ v the lines for 2 N nitric acid and acids of lower concentration (Curves 3-7) have slight inflections; this becomes considerable for 0.05 N nitric acid ($\Delta b = 0.04$). At the inflection point the ammeter reading increases suddenly with a 2 to 3-fold increase of current strength, indicating a sharp decrease in the resistance of the circuit. A similar inflection was observed by Izgaryshev and Efimov [1] for 0.001-0.74 N sulfuric acid at the same $D_a \approx 1 \cdot 10^{-4}$ amp/cm^2, but in the region $\varphi_a = 1.7\text{-}1.8$ v; they determined the polarization curves in the reverse direction from that used in our experiments.

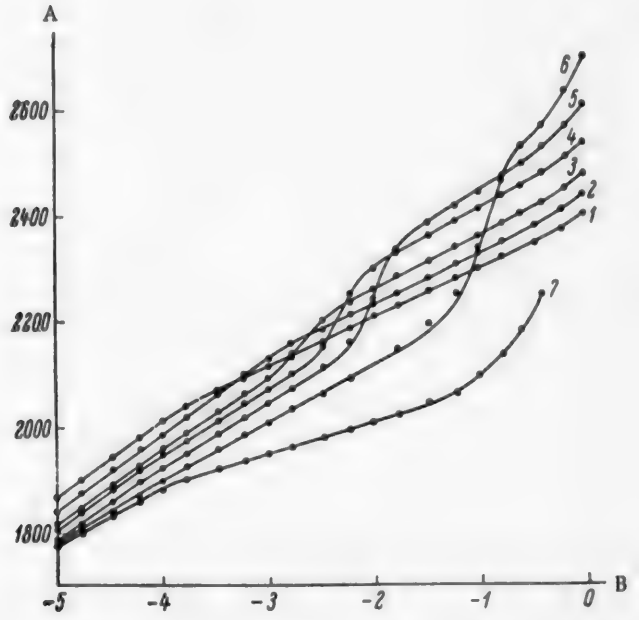

Fig. 1. Anode polarization curves in nitric acid of different concentrations (at 25°). A) Potential φ_a (mv), B) log D_a (amp/cm^2). HNO_3 concentration (normality): 1) 7, 2) 4, 3) 2, 4) 1, 5) 0.5, 6) 0.2, 7) 0.05.

This analogy suggests that the inflection in the region of $D_a \approx 1 \cdot 10^{-4}$ amp/cm^2 is the consequence of an abrupt change in the state of the platinum surface, as the result of which oxygen is formed at a lower overvoltage.

A possible consequence of this effect may be a redistribution of the relative roles played by direct discharge of H_2O and by discharge through PtO[O] in the formation of oxygen.

Analysis of the φ – log D curves (Fig. 1) reveals the following interesting relationships.

1) The lower linear portions of all the curves with plateaus terminate at φ_a = 2.10-2.15 v.

2) The current densities corresponding to the plateaus are in a linear relationship to the nitrate ion activities in the solution, as is clear from Fig. 2. In this graph the logarithms of the current densities at which the plateaus intersect with the upper linear regions of the curves are taken along the abscissa axis, and the logarithms of the average activities of nitric acid [4] are taken along the ordinate axis. There is no analogous relationship for the activity of water in the same solutions [5].

3) The upper linear regions of the curves conform to the Tafel equation at least up to 0.25–0.4 amp/cm^2, spreading out fanwise.* The coefficient "b" increases with dilution, from 0.09 for 7 N to 0.13 for 0.3 N nitric acid.

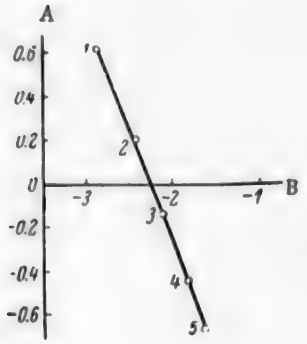

Fig. 2. D_{lim} as a function of the nitric acid activity. A) log $a_{NO_3^-}$, B) log D_a. Concentration of HNO_3 (normality): 1) 4, 2) 2, 3) 1, 4) 0.5, 5) 0.3.

All the foregoing facts suggest that the appearance of the intermediate plateaus, which correspond to peculiar limiting current densities (D_{lim}), is indicative of a new electrode process at the anode. In a solution of pure nitric acid this process can only be discharge of nitrate ions.

The adsorption of NO_3^- on the anode surface probably plays an important role in this process.

It must be pointed out that the laws governing anion adsorption at the high anode potentials in question are unkown. Thus, the latest data on the adsorption of SO_4^{2-} on Pt cover the region up to 1.5 v [6], and apply to the so-called "rapid" adsorption. The curve for "slow" adsorption of SO_4^{2-} on lead dioxide has been determined up to 2 v, but this is related to the high zero-charge potential of PbO_2 – of the order of 1.8-1.9 v [7, 8].

To the best of our knowledge, there are no data in the literature on the adsorption of nitrate ions on platinum. However, there is reason to believe that at φ_a > 1.8 v (the zero-charge potential of oxidized platinum in nitric acid is apparently not higher than 1 v) the adsorption of NO_3^- on the surface of the Pt anode becomes considerable, hindering the discharge of water molecules and thereby bringing nearer the discharge on nitrate ions.

Thus, whereas at the lower linear regions, which correspond to the 1st stage of the process, O_2 is formed only by discharge of H_2O, at the 2nd stage, corresponding to the upper linear regions, O_2 is also formed by discharge of NO_3^- anions according to the following scheme:

$$4NO_3^- \longrightarrow 4NO_3 + 4e, \quad (1)$$

$$4NO_3 \longrightarrow 4NO_2 + 4O, \quad (2)$$

$$O + O \longrightarrow O_2, \quad (3)$$

$$4NO_2 + 2H_2O \longrightarrow 2HNO_2 + 2H^+ + 2NO_3^-, \quad (4)$$

$$2HNO_2 + 2O \longrightarrow 2H + 2NO_3^-. \quad (5)$$

The higher the NO_3^- activity in solution, i.e., the sooner the equilibrium $NO_{3\,sol}^- \rightleftarrows NO_{3\,ads}^-$ at which the concentration of adsorbed anions is high enough for their discharge to begin is reached, the lower is the current density at which Reaction (1) begins.

*The subsequent bending of the curves is due to errors in determination of φ_a, since the IR component becomes appreciable and increases rapidly.

Reactions (4) and (5) incorporate a number of different possible routes for the oxidation of NO_2. The important thing is that the reduction products of the radicals, formed in their discharge, cannot exist for any length of time at the anode surface and are inevitably oxidized to NO_3^-.

Nevertheless, we attempted to detect the reduction products of the nitrate ions.

The anode gas, consisting of O_2 and O_3, as was to be expected, did not contain NO_2. Nitrogen dioxide is readily absorbed by nitric acid of the concentrations used, and is hydrolyzed according to Equation (4) with formation of the weakly dissociated nitrous acid. However, HNO_2 is too unstable in aqueous solutions, and could not be detected even though the temperature of the electrolyte was lowered to 1°* and the highly sensitive (1:1,000,000) Griess–Ilosva reagent was used [9].

Nitrites are very much more stable, and the subsequent experiments on determination of NO_2^- in the anolyte were performed with aqueous solutions of $NaNO_3$ and KNO_3.

The φ – log D curves were first plotted for these salts at 0.5-4.0 N concentrations, at 25 and 1°.

The reproducibility of the curves was less good than in the case of the acid, but in general they were approximately parallel to the corresponding acid curves, while the values of D_{lim} were always in the region of D_{lim} for the acids; therefore the use of nitrates instead of nitric acid was fully justified.

The same cell was used in the experiments on determination of NO_2^-, but the Pt foil ($S = 0.6\ cm^2$) was replaced by a Pt plate ($S = 9\ cm^2$), so that greater currents could be passed. A flowing instead of a stationary electrolyte was used, and the catholyte level was 5 cm below the general level of the electrolyte. Samples for the NO_2^- tests were taken both from the anode and from the middle compartments. Not less than 0.03 amp-hr was passed at each test point.

The presence of NO_2^- in the anolyte, but only at the start of the upper linear region, was repeatedly detected by means of the Griess–Ilosva reagent.

For example, in one of the experiments (electrolysis of 1 N $NaNO_3$ at 10°), when D_a was increased to $1.1 \cdot 10^{-2}$ amp/cm² sample gave a pink color after 10 minutes; after 20 minutes the color became a bright lilac, corresponding to roughly a 5-fold increase of the NO_2^- concentration. After 30 minutes the color disappeared and did not reappear either at the same D_a or when the latter was increased.

In some experiments the color disappeared earlier or was not detected at all.

The appearance of nitrite ions in the anolyte confirms that NO_3^- ions are discharged at the anode, while their rapid disappearance suggests that the oxidation of NO_2^- to NO_3^- is an autocatalytic reaction.

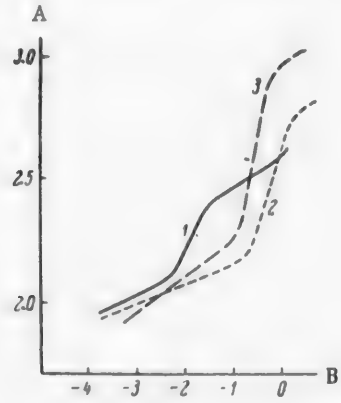

Fig. 3. Comparison of anode polarization curves for nitric, perchloric, and sulfuric acids. A) Potential φ_a (v), B) log D_a (amp/cm²). Acids: 1) 0.5 N HNO_3 (25°), 2) 0.5 M $HClO_4$ (0°) [11], 3) 7 N H_2SO_4 (20°) [10].

In conclusion, it is of interest to compare our data with the results of analogous experiments with sulfuric and perchloric acids [10, 11], published in 1956.

All three acids give rise to groups of curves similar both in shape and in their relative positions for different concentrations.

In all three cases the lower linear regions terminate by transition to limiting-current plateaus in the region $\varphi_a = 2.2 \pm 0.15$ v; this suggests that the acid anion has little influence on the mechanism of O_2 formation at the 1st stage of the process. In the 2nd stage (regions beyond D_{lim}) the situation depends entirely on the nature of the anion.

The size of the plateaus before D_{lim}, and the value of D_{lim} itself, is least for nitric acid, for equal activities of all three anions; D_{lim} disappears in 4 N nitric acid.

*It was first confirmed that the nature of the φ – log D curves remains unchanged with decrease of temperature. The curve is merely displaced parallel to itself into the region of higher φ_a, while $D_{lim}^{1°} < D_{lim}^{25°}$.

In the case of sulfuric acid in the range up to 1 amp/cm^2 D_{lim}* is reached only in the region of high concentrations (according to the results of Kaganovich et al. [10] it is found in 7, 10, and 15 N sulfuric acid, but not in 1 N) and the D_{lim} plateaus are greatest in this case.

$HClO_4$ occupies an intermediate position in this respect; D_{lim} disappears in 9 N solution.

The activation energy of anion discharge increases along the series HNO_3–$HClO_4$–H_2SO_4; this is shown by the potentials of the upper linear regions for solutions of equal anion activity.

It is not possible to show all the three groups of φ – log D curves together; we therefore confine ourselves to Fig. 3, which gives the curves for 0.5 N nitric acid (at 25°) and 0.5 M perchloric acid (at 0°) [11], these acids having similar anion activities; and also for 7 N sulfuric acid (at 20°) [10], which is the first of the curves given by the authors to have a D_{lim} plateau, the activity of this acid being much higher (approximately 8 times as high).

Despite the different conditions in which these curves were determined, the diagram gives an idea of the interrelationship between the three cases under consideration.

SUMMARY

1. The anodic φ – log D curves for electrolysis of 0.05-7 N solutions of nitric acid at 25°, with smooth platinum anodes, were studied; it is shown that the shape and relative configuration of the curves depend distinctly on the nitric acid concentration.

2. The results suggest the possibility of discharge of NO_3^- ions, which corresponds to the upper linear regions of the φ – log D curves.

3. Aqueous solutions of KNO_3 and $NaNO_3$ give φ – log D curves of similar shape.

When these solutions are electrolyzed, nitrite ions are detected in the anode compartment; this confirms that NO_3^- is discharged with formation of O_2 and NO_2.

LITERATURE CITED

[1] N. A. Izgaryshev and E. A. Efimov, Zhur. Fiz. Khim. 30, 1807 (1956).

[2] V. L. Kheifets and I. Ia. Rivlin, J. Appl. Chem. 28, 1291 (1955).**

[3] K. I. Rozental' and V. I. Veselovskii, Proc. Acad. Sci. USSR Phys. Chem. Div. 111, 637 (1956).**

[4] R. A. Robinson and R. H. Stokes, Trans. Far. Soc. 45, 612 (1949).

[5] E. Abel, O. Redlich and B. V. Lengyel, Z. phys. Ch. 132, 189 (1928).

[6] N. A. Balasheva, Doklady Akad. Nauk SSSR, 103, 639 (1955).

[7] B. N. Kabanov, I. G. Kiseleva and D. I. Leikis, Doklady Akad. Nauk SSSR, 99, 805 (1954).

[8] D. I. Leikis and E. K. Venstrem, Doklady Akad. Nauk SSSR, 112, 97 (1957).**

[9] H. W. Webb, Absorption of Nitrous Gases (Russian translation) (Khar'kov, 1931).

[10] R. I. Kaganovich, M. A. Gerovich and E. Kh. Enikeev, Proc. Acad. Sci. USSR, Phys. Chem. Div. 108, 107 (1956).**

[11] T. R. Beck and R. W. Moulton, J. Electroch. Soc. 103, 247 (1956).

Received April 8, 1957

*Kaganovich et al., [10] did not reach any conclusions concerning the anion discharge, and the concept D_{lim} is not used in their paper. (sic).

**Original Russian pagination. See C. B. Translation.

FUNDAMENTALS OF THE THEORY AND PRACTICE OF THE CONTINUOUS OXIDATION OF SHORT-CHAIN NORMAL PARAFFINS IN THE LIQUID PHASE

V. K. Tsyskovskii

For many years the synthesis of higher saturated fatty acids was effected by oxidation of paraffins of high molecular weight, containing 19-36 carbon atoms in the molecule. No other methods for the production of fatty acids have been proposed up to now [1].

Early in 1956 Tsyskovskii and his associates demonstrated that it is possible in principle to synthesize higher fatty acids by the liquid-phase oxidation of mixtures of paraffinic hydrocarbons with shorter chains [2, 3]. In contrast to solid paraffins melting at 52°, these paraffins are liquid at ordinary temperatures. This process was made possible by the continuous removal of the fatty acids from the reaction zone in the course of oxidation [4].

While under the ordinary conditions of prolonged oxidation of high-molecular paraffins in the liquid phase the higher fatty acids formed had, on the average, half the number of carbon atoms in the molecule, the molecular weight of the acids formed by the new process differed little from the molecular weight of the paraffins used.

As the result of a deep study of the process, earlier views on the mechanism of formation of intermediate oxidation products of paraffinic hydrocarbons were largely rejected, and it proved possible to work out the principles of a new industrial process for the synthesis of higher fatty acids from new and more abundant raw materials.

The purpose of the present paper is to present, in very concise form, the principles of the processes taking place in the continuous oxidation of paraffinic hydrocarbons with shorter chains.

Duration of the oxidation reaction and the molecular weight of the fatty acids. The kinetics of formation of the various reaction products in the oxidation of paraffinic hydrocarbons has not been studied sufficiently. Therefore many authors drew conclusions concerning the oxidation mechanism merely from the results of studies of the composition of the final reaction products.

It is for this reason that the formation of fatty acids of considerably lower molecular weights (as compared with the original paraffins) was attributed to the equivalence of all the methylene groups in the chain with respect to the action of oxygen.

This view was held by Hinshelwood [5], Man'kovskaia [6], Benton [7], and many others.

However, Prückner [8], Pardun [9], Asinger [1], and Zerner [10] found that the molecular weight of the fatty acids increases with decreasing conversion of the hydrocarbons during oxidation. The results of our investigations (Fig. 1) led to the same conclusion.

The fatty acids had the greatest molecular weight (especially at high reaction temperatures) at very low degrees of conversion of the paraffins. This was an indirect indication that the oxygen attacked some definite point of the hydrocarbon chain, and the decrease in the molecular weight of the fatty acids with increase of the oxidation time was a consequence of subsequent destructive oxidation and decarboxylation.

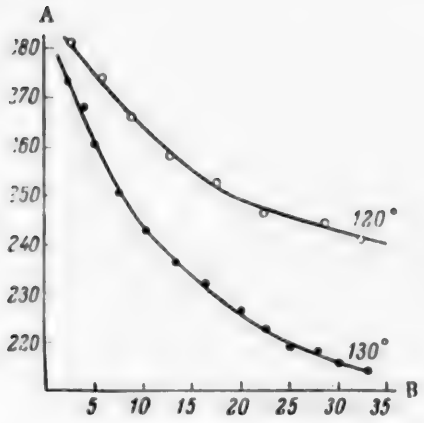

Fig. 1. Variation of the molecular weight of fatty acids with the degree of conversion of normal paraffins of the 240-350° fraction. A) Molecular weight of higher fatty acids, B) amount of paraffins converted in the oxidation (wt. %).

Ivanov [11] showed that in the case of the low-temperature oxidation of n-hexane oxygen attacks the C–H bond at the second carbon atom in the chain, with formation of hexane hydroperoxide. During the subsequent conversion this hydroperoxide should decompose into formic and valeric acids, with cleavage of the C–C bond.

Comparison of Ivanov's results with available data on the variation of the molecular weight of the fatty acids with time led to the conclusion that formation of acids with the maximum molecular weight can take place only if the O_2H group of the alkyl hydroperoxide is as close as possible to one of the methyl groups of the chain.

As was convincingly shown by Paquot [12], the variation of the molecular weight of the fatty acids with increasing oxidation time is caused by subsequent destructive oxidation of the acids (which occurs even at low temperatures).

Acids with the greatest radical length proved to be the least resistant to oxidation. Oxidation of such acids yielded homologs of lower molecular weight, and even dicarboxylic acids (mainly oxalic).

Leibnitz [13] and Marzin [14] obtained results similar to those of Paquot.

It follows that the sharp decrease in the molecular weight of the acids, relative to the original hydrocarbons, with increase of the reaction time is in no way consistent with the views of the authors cited above.

If it is assumed that an alkyl hydroperoxide is formed, of the type

$$CH_3—\underset{\displaystyle OOH}{\underset{|}{CH}}—CH_2—(CH_2)_n—CH_3,$$

then the formation of acids from such hydroperoxides (in the course of subsequent conversion) should proceed as follows:

$$CH_3—\underset{\displaystyle OOH}{\underset{|}{CH}}—CH_2—(CH_2)_n—CH_3$$

$$\downarrow$$

$$HCOOH + HOOC—CH_2—(CH_2)_n—CH_3.$$

According to this mechanism, the final decomposition products of the hydroperoxide are two acids, one of which is formic and the other is a fatty acid with one C atom less than the original hydrocarbon. The presence of formic acid is a direct indication that such hydroperoxides may be formed.

It is highly significant that the formic acid concentration is highest only at the initial stage of the reaction (Table 1). The concentration of formic acid subsequently decreases with increasing yields of C_2, C_3, and C_4 acids formed by destructive oxidation of the higher acids. The decrease of the formic acid concentration shows good correlation with the continuous decrease in the molecular weight of the higher fatty acids with increase of the reaction time.

Of course, it is possible that the formation of C_2, C_3, and C_4 acids may be attributed not only to the destructive oxidation of the higher acids, but also to formation of alkyl hydroperoxides of other types, and reactions between them.

Nevertheless, continuous removal of acids of the highest molecular weight from the reaction zone excludes the possibility of their further conversion, and makes it possible to obtain these acids from paraffins of considerably shorter chain length.

Kinetics of the formation of intermediate reaction products. Our study of the variations in the composition of the intermediate products with increasing degree of conversion in the oxidation of paraffins revealed certain discrepancies between our results and the views of a number of authors.

For example, Langenbeck and Pritzkow [15], who studied the final products of the deep oxidation of hydrocarbons, put forward the hypothesis that ketones are the principal decomposition products of secondary alkyl hydroperoxides.

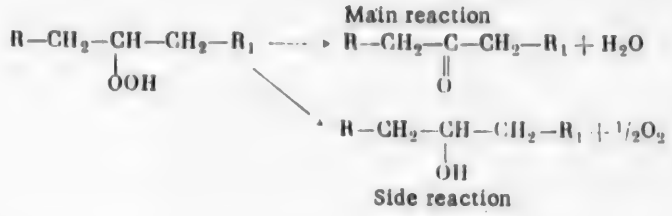

According to Langenbeck, the secondary alcohols subsequently remain unchanged, while the ketones are transformed further:

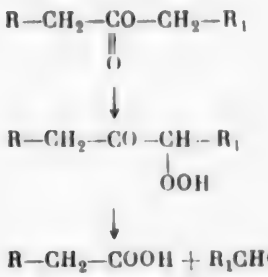

i.e., acids must be formed from ketones by way of keto hydroperoxides.

It is noteworthy that the Langenbeck–Pritzkow mechanism entirely excludes the possibility of decomposition of alkyl hydroperoxides to primary alcohols.

These authors criticize Rieche's views [16] and reject this route for the decomposition of alkyl hydroperoxides.

In our experiments, as in those of Chertkov [17], the principal decomposition products of alkyl hydroperoxides in the initial stages of paraffin oxidation were aliphatic alcohols and not carbonyl compounds (Fig. 2).

The yield of alcohols gradually decreases and the amount of carbonyl compounds begins to increase with increasing conversion of the hydrocarbons. At higher temperatures (and therefore at higher conversions) the yield of carbonyl compounds and acids gradually becomes greater than the yield of alcohols in the oxidation of n-decane; this was also observed by Emanuel' et al., [18].

Therefore it must be assumed that the carbonyl compounds (both ketones and aldehydes) in the reaction mass are intermediate products formed in the oxidation of alcohols. Investigation of the composition of the

alcohols isolated at the initial stage of the oxidation reaction, by the method developed by Bashkirov and Kamzolkin [19], revealed the presence of both primary and secondary (Table 2) alcohols.

Because of the predominant formation of alcohols in the early stages of oxidation of paraffins (including those of normal structure), which was also reported by Emanuel' et al., [20], we cannot accept the mechanism proposed by Langenbeck and Pritzkow for the formation of the intermediate products in the oxidation of these hydrocarbons.

In the light of recent data the following working hypothesis, which accounts for the formation of the intermediate products in the decomposition of alkyl hydroperoxides, seems to us more probable.

The decomposition of alkyl hydroperoxides with formation of fatty acids is represented schematically below.

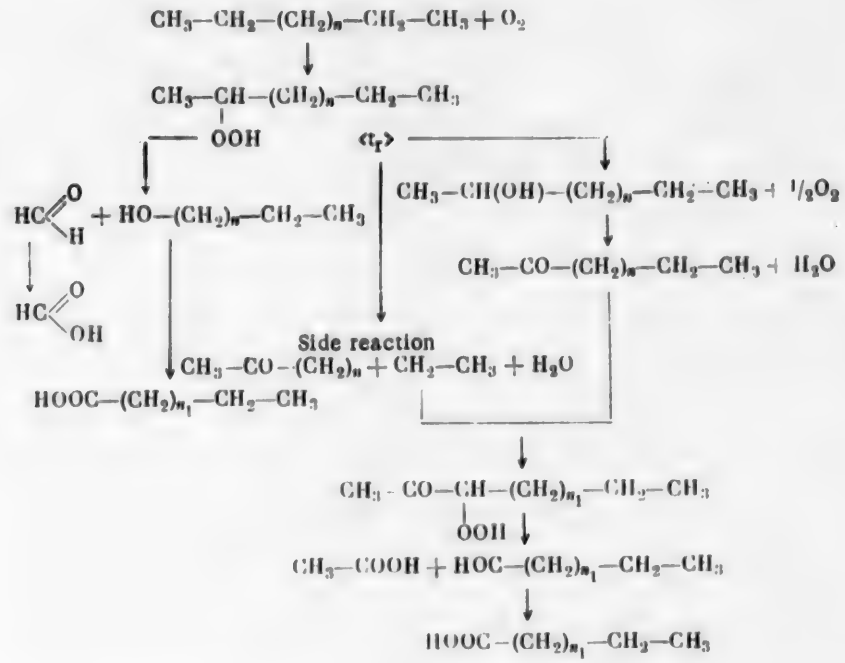

According to this hypothesis, paraffins are oxidized with formation of alkyl hydroperoxides with O_2H groups as near as possible to one of the methyl groups in the chain.

The first and principal decomposition product of such an alkyl hydroperoxide consists of primary and secondary alcohols. A certain proportion of carbonyl compounds (Fig. 2) may also be formed directly from the alkyl hydroperoxide. However, this is a side reaction.

The main quantity of the carbonyl compounds is formed in the subsequent oxidation of primary and secondary alcohols [20]. The fatty acids are formed by oxidation of ketones and aldehydes, possibly by the mechanisms postulated by Langenbeck, Pritzkow, and Rieche.

The above hypothesis is in very good agreement with our experimental data and with the practical results obtained in continuous oxidation of normal paraffins with shorter chains.

The role of catalysts. In 1949 Tsyskovskii and Kiseleva [21] showed that catalysts merely initiate the chain reaction of oxidation, which subsequently develops without their participation. This was tested and confirmed somewhat later by Emanuel' et al., [22].

TABLE 1*

Relationship Between Formic Acid Concentration in the Acid Mixture, Molecular Weights of Higher Fatty Acids, and Duration of the Oxidation Reaction

Oxidation time (min)	HCOOH concentration in mixture of C_1–C_4 acids (wt. %)	Molecular weight of fatty acids
10	57	280
20	43	262
40	41	241
60	35	228
120	31	218
180	27	204

*This table is based on data obtained for the 240-350° fraction of normal paraffins.

It was recently shown by us that the catalyst influences the first macroscopic stage of the reaction (the induction period).

During this stage the catalyst determines both the rate and the direction of the oxidation reaction, which subsequently develops in its absence.

All the primary chemical actions taking place under influence of the catalyst in the initial macroscopic stage of the oxidation reaction are reflected in the subsequent course of the reaction. This is demonstrated very convincingly by the curves for the effects of the catalyst concentration on the rate of the temperature rise at the initial macroscopic stage and when the reaction has fully developed (Fig. 3). The two curves are identical in character.

Once the direction and rate of the reaction have been determined by the catalyst at the first macroscopic stage of oxidation, they remain unchanged for a long time.

This is illustrated very clearly in Table 3 for conditions of continuous oxidation, when the catalyzing metal can be present only in the initial macroscopic stage (it is subsequently automatically removed by reaction with caustic soda solution).

The data in Table 3 (reproduced repeatedly), obtained in a large pilot unit, prove incontrovertibly that, contrary to the views of several authors [15, 23], the presence of catalyzing metal is by no means essential throughout the entire oxidation reaction. The decomposition of alkyl hydroperoxides and the formation of free radicals which initiate the chains take place without participation of the catalyst. A very significant fact is that this process is precisely reproducible in time, both qualitatively and quantitatively, as shown by the fact that the composition of the intermediate reaction products remains constant.

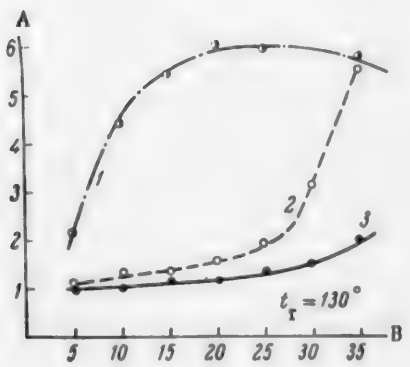

Fig. 2. Effect of reaction time on the concentration of the intermediate products in the oxidation of pentadecane. A) Concentration (wt. %), B) oxidation time (min), 1) Alcohols, 2) carbonyl compounds, 3) acids.

This discovery makes it possible to put into practice a directed continuous process for the oxidation of paraffins at a constant rate of reaction, predetermined for the given conditions by the action of the catalyst in the initial macroscopic stage.

Influence of temperature. In the batch oxidation of paraffins, owing to the fact that the oxidation products are not removed from the reaction zone and are subject to continuous peroxidation, increase of temperature strongly influences the quality and yields of the acids. In conditions of continuous oxidation, temperature does not have this effect, as the fatty acids formed are immediately removed from the reaction mass almost at the instant of their formation.

We have shown [24] that the qualitative and quantitative results of the oxidation reaction can be deliberately controlled by regulation of the temperature in conjunction with the contact time between the oxidation mass and atmospheric oxygen.

TABLE 2

Qualitative Characteristics of Alcohols Isolated from the Early Oxidation Products of Normal Paraffins of the 240-350° Fraction

Source	Characteristics		
	hydroxyl number	composition (wt. %)	
		primary	secondary
From fractions up to 100° (5 mm Hg)	327.7	76	24
From 100-150° fractions (5 mm Hg)	267.3	52	48
From 150-200° fractions (5 mm Hg)	233.2	47	53

Figure 4 shows the variations in the yield of higher C_{10}–C_{20} fatty acids, calculated on the raw material consumed, in the continuous oxidation of liquid paraffins of the 240-350° fraction (synthine).

It is easy to see that equivalent yields of this acid fraction can be obtained either at high temperatures with short contact times, or vice versa (with different degrees of conversion).

A very interesting fact is the relatively small change in the yield of higher acids with increase of oxidation time at low reaction temperatures. This shows, in particular, that the destructive oxidation of higher acids to their homologs is less intensive under these conditions.

The possibility of increasing the temperature allows of higher rates of oxidation, considerably higher than the rates of oxidation of paraffins in the batch process, with almost no change in the qualitative characteristics of the synthetic acids formed (Table 4).

One of the most characteristic features of the continuous process is the possibility of carrying out the oxidation of liquid paraffins at high temperatures.

TABLE 3

Characteristics of the Continuous Oxidation of Liquid Paraffins of the 240-350° Fraction after Different Times

Oxidation time (hours)	Characteristics of oxidation product circulating in system (without catalyst)				
	concentration (wt. %)			yield of acids > C_5* (kg/day/1 m^3 reactor)	C_5–C_9 acids in mixture of acids (%)
	oxygen compounds	C_5–C_{20} acids	higher alcohols		
5	19.5	1.65	13.7	342	23.4
15	20.5	1.75	14.1	360	22.2
25	21.2	1.84	14.6	365	21.6
45	21.4	1.91	14.8	372	25.3
55	20.4	1.76	13.9	362	22.1
85	24.1	2.04	15.1	376	23.1
100	21.2	1.89	14.65	369	22.6

*Before thermal treatment.

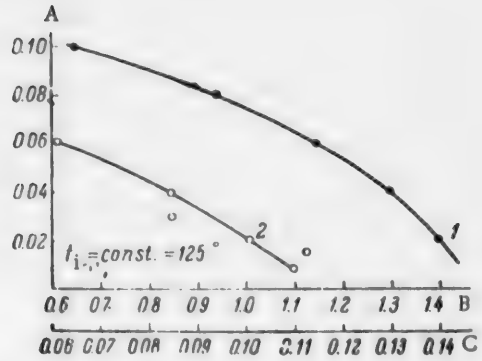

Fig. 3. Rate of temperature increase at the first and second macroscopic stages of the oxidation reaction. A) Mn concentration in the pentadecane (wt. %), B) average rate of temperature increase $\frac{(t_{max} - t_c)}{\tau_2}$, C) average rate of temperature increase $\frac{(t_{max} - t_1)}{\tau_1}$. 1) Developed chain process (τ_2) in absence of catalyst, 2) during the transition of the catalyst metal from the lowest to the highest valence state (τ_1).

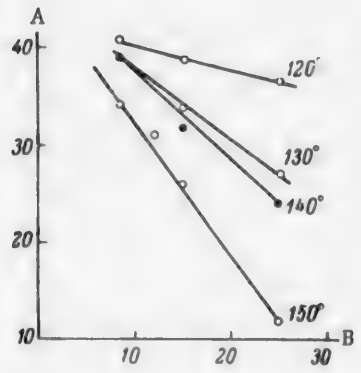

Fig. 4. Variation of the yield of the required acid fraction with the temperature and the time in the oxidation zone. A) Yield of > C_{10} acid fraction, on the raw material consumed (in wt. %), B) time in the oxidation zone (minutes).

TABLE 4

Comparative Results of the Oxidation of Solid and Liquid Paraffins Under Different Conditions

Characteristics	Oxidation	
	batch process, solid, 110°	continuous, liquid, 130°
Yield of C_{10}–C_{20} acid fraction (kg/day per 1 m^3 of reactor)	85.0	205
Characteristics of crude acids after heat treatment: acid number in mg KOH per g	231.7	280.6
Ester number	9.3	10.5
Carbonyl number	8.56	11.4

TABLE 5

Properties of Liquid Paraffins Isolated by Means of Urea from Diesel Fractions of Romashkin Oil

Characteristics	Values
Hydrocarbon composition (in wt. %)	
C_{13}	3.3
C_{14}	6.7
C_{15}	10.2
C_{16}	13.9
C_{17}	14.0
C_{18}	9.9
C_{19}	9.8
C_{20}	7.7
C_{21}	5.5
$>C_{21}$	5.0
Density d_{20}^4	0.8
Melting point (°C)	+18.0
Chemical composition (in wt.%)	91.94
n-paraffins	7.56
iso-paraffins	
aromatic hydrocarbons	0.5

Raw materials and the technological process. The discovery that it is possible to obtain higher fatty acids by the continuous oxidation of paraffins of shorter chain length has opened up wide possibilities of the use of more abundant and cheaper raw materials than the solid paraffins used at present.

The investigations showed that the liquid paraffins obtained in the deparaffinization of Diesel fuel by means of urea should serve as such raw materials in the near future. The characteristics of these paraffins are given in Table 5.

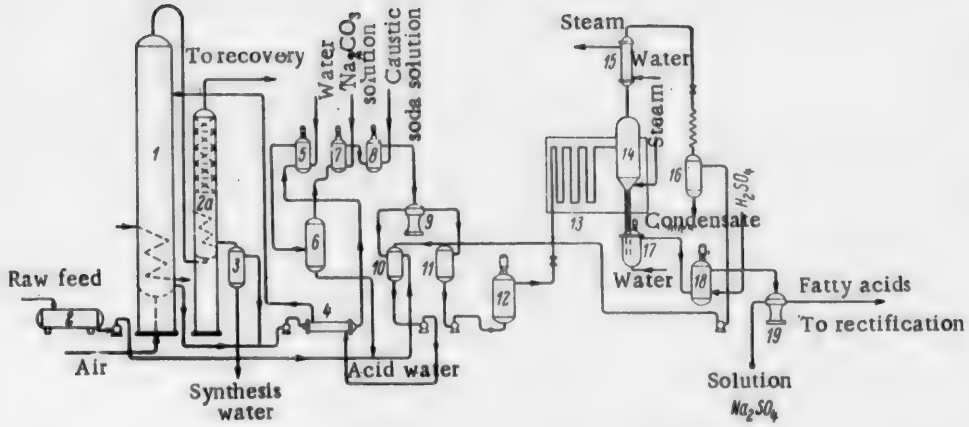

Fig. 5. Process scheme for the production of synthetic fatty acids by the continuous oxidation of liquid paraffins. 1) Oxidation column; 2) container for raw material; 2a) dephlegmator; 3, 16) water traps; 4) heat exchanger; 5,7,8) mixers; 6) vessel for separation of wash water from the oxidation product; 9, 19) centrifuges; 10, 11) intermediate vessels; 12) autoclave; 13) thermal furnace; 14) separator; 15) waste-heat boiler; 17) mixer for preparation of soap paste; 18) mixer for decomposition of soap paste.

TABLE 6

Material Balance for the Continuous Oxidation of Liquid Paraffins

Substances	Yield (wt. % on raw material consumed)
Fresh raw material taken for oxidation	100
Obtained by oxidation:	
$C_1 - C_4$ acids	30
Including formic	15.1
Distillation acids:	
$C_5 - C_6$ }	7.8
$C_7 - C_9$ }	
$C_{10} - C_{16}$	33.1
$C_{17} - C_{20}$	16.0
Pitch	12
Total	98.9
Total losses in heat treatment and distillation	17.3

The chemical composition of the liquid paraffins isolated by means of urea differs advantageously from that of solid paraffins in the content of paraffin hydrocarbons of isomeric structure.

Experimental studies showed that the fractional and chemical composition of the liquid paraffins is very close to the optimum.

The yields of commercial fractions of fatty acids obtained by the continuous oxidation of these paraffins differ very little from the yields of the same acids usually obtained by batch oxidation of solid higher paraffins.

As the result of lengthy experimental work, the following conditions were adopted for the conversion of liquid paraffins into higher $C_5 - C_{20}$ fatty acids (conversion coefficient 0.7-0.85): reaction temperature 130°, contact time of oxidation product with atmospheric oxygen 20 minutes, recycle coefficient 33, concentration of higher fatty acids in the oxidation product not greater than 2.0%; air velocity in the open section of the oxidizing column 0.2 m/second; catalyst concentration (%): manganese 0.035, potassium 0.025 (in the form of manganese and potassium naphthenates).

The technological process for continuous oxidation of liquid paraffins differs radically from the methods for the oxidation of solid paraffins now in use (Fig. 5).

The raw feed containing the catalyst (of the composition indicated above) enters the oxidation column 1, where air is bubbled through it at 130°. At the end of the initial macroscopic stage, i.e., at the instant when the chain oxidation reaction begins, the oxidation product (containing up to 25% of oxygen compounds, including 2.0% of higher fatty acids) begins to circulate through the system.

The spent air containing the volatile oxidation products and low-boiling paraffins passes from the oxidation column 1 to the dephlegmator 2a. The air is separated completely in this apparatus, at 40°, from the low-boiling paraffins and about 90% of the lowet reaction products (C_1–C_4 acids and aldehydes). The mixture of hydrocarbons and oxidation products from the dephlegmator passes through the water trap 3, where the reaction water is separated from the hydrocarbons, containing higher fatty acids and neutral oxygen compounds (residues). The latter are mixed with the oxidation products from the oxidation column and pass to the circulation pump.

The mixture is then pumped through the heat exchanger 4 (where it is cooled to 120° by the stream of return oxidation product), and then enters the mixer 5. It is washed with softened water (at 120° under pressure) in 10:1 ratio.

A part of the lower fatty acids enters the wash water. The concentration of C_1–C_4 acids in the wash water does not exceed 3%.

The washed oxidation product and the acid water are quantitatively separated in the settling tank 6 at 90°. The water is collected for further treatment, while the oxidation product passes consecutively through the mixers 7 and 8, where it is treated first with 10% sodium carbonate solution and then with 4% caustic soda solution for complete extraction of the higher fatty acids. Esters are also partially hydrolyzed by the action of caustic soda. The neutral oxidation product and the soap (in emulsion form) then pass from the mixer 8 to the centrifuge 9 for separation.

The neutral oxidation product flows by gravity from the centrifuge 9 into the intermediate vessel 10, into which fresh raw material and the unsaponifiable materials from the thermal section are also fed. The raw material is fed automatically by means of a level regulator installed in the oxidation column. The mixture of neutral oxidation product, fresh raw material, and unsaponifiables is returned from the intermediate vessel to the oxidation column through the heat exchanger 4, by means of a second circulation pump. The soap solution, containing 20-25% dry solids, is pumped by means of a high-pressure pump from the intermediate vessel 11 through the autoclave into the thermal section.

In this autoclave the ether acids and estolides are broken down at 20 atm pressure by the action of the residual NaOH present in the soap solution. The soap solution remains in the autoclave for about 3 hours.

The operating principle of the thermal section used in this process differs considerably from the existing one [25].

The soap solution is separated into two phases in the furnace 13 at 330° and 5 atm: a vapor phase, consisting of a mixture of steam and unsaponifiable substances, and a liquid phase, consisting of soap in the aerosol state. The mixture is separated in the settling vessel 14 at the same pressure and temperature.

The steam and vapors of the unsaponifiable substances pass through the waste-heat boiler 15. The waste-heat boiler 15 uses the heat of condensation of the vapor and steam to produce saturated steam at 3 atm, which is then used for heating the equipment. After condensation in the end condenser, the water and unsaponifiables enter the water trap 16 for separation. The condensate (containing traces of sodium soaps of the acids) passes from the trap and is used in the preparation of the sodium carbonate and caustic soda solutions, while the unsaponifiables are pumped back to the intermediate vessel 10.

The melted soap in the lower part of the settling vessel 14 is treated for 30-45 minutes with superheated steam in order to remove the unsaponifiable matter formed during the heat treatment. Not more than 0.8-1.0% of unsaponifiable matter remains in the dry soap. The soap continuously passes, by means of an automatic level regulator at the bottom of the vessel 16, into the mixer 17 for preparation of the soap paste; here it is mixed with water, forming a 30-40% solution. The soap paste is decomposed in the propeller stirrer 18, by means of 96% sulfuric acid at 80°. The mixture of separated fatty acids ("crude" acids) passes to the centrifuge 19 for separation.

The solution of sodium sulfate is sent to recovery, while the dried fatty acids, C_4 and higher, then pass to the rectification unit (not shown in the diagram).

The entire process is continuous and automatic, the equipment being provided with the appropriate control and measurement instruments.

TABLE 7

Comparative Data on the Yields of Principal Fractions of Fatty Acids Obtained by Rectification

Product	Yield fatty acids on raw material consumed (wt. %)			
	240-350° fraction	300-400° IZhT	Drogobych paraffin	Kuibyshev paraffin
Crude acids	71.5	50.0	55.0	59.9
Fraction of C_{10}–C_{20} acids obtained by rectification of crude acids	86.7	81.7	81.1	19.3

The above description applies to a pilot plant in operation, which forms the basis of a large unit to be installed.

The results of oxidation of liquid paraffins of normal structure. The results obtained by the oxidation of normal paraffins containing individual hydrocarbons from C_{13} to C_{12}* under the conditions described above are given in Table 6.

It is clear from the data in Table 6 that the material balance is more favorable (with regard to the yield of distilled C_{10}–C_{20} acids) for the continuous oxidation of liquid paraffins than for the low-temperature extended oxidation of paraffins containing from 18 to 90 carbon atoms [26].

The yield of the main fatty-acid fractions obtained by rectification is also considerably higher in our experiments than in the data published by Man'kovskaia et al., [27] (Table 7).

Composition and properties of the fatty acids formed. Investigation of the properties of "crude" fatty acids (after thermal treatment), and of the separate fractions obtained from them by distillation showed that they are almost equivalent to the higher fatty acids usually obtained by the batch oxidation of solid paraffins (Table 8).

TABLE 8

Characteristics of Fatty Acids Obtained by Oxidation of Liquid Paraffins of Normal Structure in the Pilot Plant

Products	Acid number	Ester number	Carbonyl number	M. p. (°C)	Unsaponifiable content (%)
Acids isolated from oxidation mixture	232.9	39.63	37.63	Liquid	—
Crude fatty acids	280.6	10.5	11.4	Ditto	0.8
Acid fractions:					Traces 0.3
C_5 — C_6	446.6	1.4	0.1	"	
C_7 — C_9	387.9	1.8	0.08	"	0.7
C_{10} — C_{16}	282.45	9.65	4.5	18.3	2.6
C_{17} — C_{21}	223.05	17.35	10.45	38.4	5.3

*As in original — Publisher's note.

The somewhat higher ester and carbonyl numbers of the "crude" acids and their individual fractions can be attributed to iron entering the reaction zone from the system, with disturbance of the fixed catalytic conditions.

However, the composition of the fatty acids (Table 9) obtained by us differs considerably from that of the fatty acids isolated from oxidized solid paraffins [28].

The data show that the $C_{10}-C_{20}$ fatty-acid fraction obtained by the oxidation of solid paraffins contains over 40% of acids with C_{16} and over. In our case the $C_{10}-C_{20}$ fraction had a considerably lower content of these acids.

Nevertheless, investigations of the All-Union Scientific Research Institute of Fats showed that the quality of the synthetic soap obtained with this fraction as the fatty component is quite satisfactory (Table 10).

TABLE 9

Composition of the $C_{10}-C_{20}$ Fatty-Acid Fractions Obtained by Different Methods

Individual acids	Composition of $C_{10}-C_{20}$ acid fractions (wt. %) — oxidation of	
	solid paraffins	liquid paraffins
C_{10}	5.9	11.8
C_{11}	9.0	16.3
C_{12}	10.3	16.3
C_{13}	4.3	10.9
C_{14}	9.6	11.8
C_{15}	13.0	10.0
C_{16}	7.4	6.4
C_{16}	40.5	16.5

TABLE 10

Properties of Synthetic Soap Made from Different Fatty-Acid Fractions

Acid fractions	Foaming power in distilled water at 40°, with 0.5% of active substance		Washing effect (%)
	V_0	V_5	
$C_{10}-C_{16}$	545	380	380
$C_{17}-C_{20}$	535	450	380

TABLE 11

Technical and Economic Data for the Production of 1 Ton of Mixed Fatty Acids in the Proposed Synthetic Fatty Acid Plants Designed to Produce 15,000 Tons of Acid Annually

Quantities	Liquid paraffins	Solid paraffins
Raw material (tons)	1.205	1.41
Sulfuric acid (tons)	0.867	0.508
Caustic soda (tons)	0.049	0.154
Soda ash (tons)	0.33	0.091
Catalyst (kg)	0.047	8.4
Water (m^3)	241.4	331.3
Steam (mgc)	1.1	4.8
Electric power (kw-hrs)	606	467
Fuel—gas (tons)	0.434	0.464
Capital investment (rubles)	1974	2868.2
Processing costs (rubles)		
Cost of 1 ton of synthetic fatty acids (rubles)	729.51	1114.7
	1091.01	3027.5
Labor productivity (rubles)	2295.4	1432.3

Despite the low concentration of C_{16} acids in $C_{10}-C_{20}$ fraction, it yielded a solid 72% household soap, conforming to all GOST specifications, without any additives.

Because of the low concentration of high-molecular acids in this soap, it has a good detergent action even in cold water.

Therefore the fatty acids obtained by oxidation of liquid paraffins of normal structure are not inferior in properties to acids obtained from solid paraffins, and should eventually occupy a worthy position in our national industry.

According to the available project data (Table 11) the production cost of fatty acids made by continuous oxidation of liquid paraffins of normal structure should be about 1/3 of the cost of the present production. The decrease in the production costs is due both to the greater efficiency of the process as a whole, and to the low cost of the raw material.

SUMMARY

A process for the synthesis of higher fatty acids by continuous oxidation of liquid paraffins, based on recent kinetic data on the intermediate products in the oxidation of normal paraffins and on the mechanism of homogeneous catalysis, has been developed and tested.

The range of raw materials for the synthetic fatty-acid industry can be extended considerably by the introduction of the continuous-oxidation process, and a solution to the problem of substitutes for edible fats in industry is thereby brought nearer.

LITERATURE CITED

[1] F. Asinger, Chemie and Technologie der Paraffin-Kohlenwasserstoffe (Berlin, 1956).

[2] V. K. Tsyskovskii, S. G. Soltan, Ts. N. Shcheglova and B. G. Freidin, Masloboino-Zhurovaia Prom. 3 (1955); Authors' Certif. 109712, October 11 (1957).

[3] V. K. Tsyskovskii, Ts. N. Shcheglova and E. M. Nebylova, Khim. i. Tekhnol. Topliva, 6 (1956).

[4] V. K. Tsyskovskii, Questions of Chemical Kinetics, Catalysis, and Reactivity (in Russian) (Izd. AN SSSR, Moscow, Leningrad, 1955).

[5] C. N. Hinshelwood, Disc. Faraday Soc. 10, 226 (1951).

[6] N. K. Man'kovskaia, N. V. Barsegian and E. I. Moskvina, Masloboino-Zhurovaia Prom. 6 (1956).

[7] S. Benton and M. Wirth, Nature 171,269 (1953).

[8] H. Prückner, Chem. Techik 5, (1952).

[9] G. Pardun and R. Kuchinka, Erdöl and Kohle 3, 109 (1950).

[10] E. Zerner, Chem. Z. 54, 257 (1930).

[11] K. I. Ivanov, Problems of Hydrocarbon Oxidation (in Russian) (Izd. AN SSSR, 1954).

[12] C. Paquot, Bull. Soc. Chim. France 172 (1950).

[13] E. Leibnitz, J. Pract. Chem. 1, 337 (1955).

[14] A. Marzin, German Patent 9543, April 7 (1955).

[15] W. Langenbeck and W. Pritzkow, Fette und Seifen 67, 399 (1955).

[16] A. Rieche, Angew. Chem. 50, 123 (1937); 51, 707 (1938).

[17] Ia. B. Chertkov, J. Appl. Chem. 29, 9 (1956).*

[18] D. G. Knorre, Z. K. Maizus and N. M. Emanuel', Zhur. Fiz. Khim. 29, 4 (1955).

[19] A. N. Bashkirov and V. N. Kamzolkin, Khim. i Tekhnol Topliva, 4 (1957).

[20] V. G. Knorre, Z. K. Maizus, L. K. Obukhova and N. M. Emanuel', Uspekhi Khim. 26, 4 (1957).

[21] V. K. Tsyskovskii, Production of Synthetic Acids by Oxidation of Kerosene Fractions (in Russian) (Gostoptekhizdat, 1954).

[22] N. M. Emanuel', Doklady Akad. Nauk SSSR, 45, 603 (1954).

[23] S. Vibaut and A. Strong, Proc. Acad. Sci. Amsterdam, 54, 102 (1951); 55, 207 (1952).

[24] V. K. Tsyskovskii, Ts. N. Shcheglova and E. M. Nebylova, J. Appl. Chem. 30, 3 (1957).*

[25] B. S. Alaev, Production of Synthetic Fatty Acids (in Russian) (Pishchepromizdat, 1952).

[26] Iu. A. Rabinovich, Problems of the Oxidation of Petroleum Hydrocarbons (in Russian) (Izd. AN SSSR, 1954).

[27] N. K. Man'kovskaia, P. V. Barsegian and G. I. Moskvina, Masloboino-Zhurovaia Prom. 6 (1956).

[28] E. Leibnitz, Eröffnungs and Vortragstagung (Leipzig, 1953), 21.

Received June 17, 1957

*Original Russian pagination. See C. B. Translation.

MECHANISM OF THE REACTIONS OCCURRING DURING THE HEAT TREATMENT OF UREA UNDER THE PRESSURE OF THE GASES FORMED

S. N. Kazarnovskii and N. I. Malkina

The A. A. Zhdanov Polytechnic Institute, Gor'kii

Several methods for the preparation of melamine are described in the literature, but on the industrial scale it is synthesized only from dicyandiamide. A more rational method from the economic standpoint is the production of melamine from urea, which is a more readily available substance, made from ammonia and carbon dioxide.

In relation to the development of an industrial process for the production of melamine and other triazine derivatives, it is of interest to study the processes which take place during the heat treatment of urea under the pressure of the reaction gases. Little attention is devoted to this question in the literature.

It was reported in a 1945 Soviet patent [1] that urea, ammonium cyanate, ammelide, ammeline, and guanylurea are converted into melamine, carbon dioxide, and ammonia at temperatures not below 300° under 100 atm pressure. The mechanism of the reactions was not investigated, and the following scheme was postulated for the formation of melamine from urea:

$$6CO(NH_2)_2 \rightarrow C_3H_6N_6 + 3CO_2 + 6NH_3.$$

In 1953 the Japanese scientist Kinoshita published a paper on the synthesis of melamine from urea [2].

He represented the mechanism of the synthesis as follows: two molecules of urea give rise to a molecule each of ammonia and biuret on heating. On heating, the biuret liberates another ammonia molecule, with formation of cyanuric acid; amination of the latter yields ammelide and ammeline, and then melamine.

In the second part of the investigation [3] the reactions of ammonia with urea, cyanuric acid, and hydroxyamino derivatives of triazine were studied. In his studies of the reaction between urea and ammonia, Kinoshita concluded that excess of ammonia does not influence the yield of melamine. In studies of the reactions of cyanuric acid and hydroxyamino derivatives of triazine with ammonia it was established that the first stage is the formation of urea, the amount of which decreases with time; the amount of cyanuric acid decreases and that of melamine increases at the same time. It is noted that the nitrogen content of the hydroxyamino derivatives increases with temperature, i.e., the formation of melamine can be represented by the following mechanism: cyanuric acid → substances insoluble in water → melamine.

The synthesis of melamine from urea was also studied by Ivliev [4]. He found that the synthesis consists of a number of consecutive and parallel reactions, and is accompanied by the formation of "substances soluble in water" (not based on the triazine ring) and "readily volatile" substances, the nature of which was not investigated. The yield of the latter increases with temperature, but at 400° does not exceed 65% on the weight of the urea taken. It is stated that the formation of melamine can be regarded as taking place in two stages: 1) formation of cyanuric acid, and 2) amination of cyanuric acid by ammonia to give melamine by way of hydroxyamino derivatives of triazine. The relatively low yield of melamine from urea (35%) is attributed by Ivliev to side reactions accompanying the amination process, leading to breakdown of the triazine ring to yield "readily volatile" substances.

A defect common to the above investigations is that the product was dried at 65° to constant weight and then analyzed. Therefore such intermediate products as ammonium cyanate and carbonate were volatilized, and were not ascribed any role in the reaction mechanism. Moreover, the synthesis of melamine was studied at temperatures of 200° and over. The mechanism of reactions taking place below 200° was not studied. The hydroxyamino derivatives of triazine (ammelide and ammeline), formed as intermediate products in this process, were not determined quantitatively because of the lack of a method for their separate determination.

It is clear from the above survey of the literature that the mechanism of formation of melamine from urea has not been studied sufficiently.

The purpose of the present work was to study the mechanism of the reactions taking place in the heat treatment of urea.

EXPERIMENTAL

The investigations of the heat treatment of urea under pressure of the gases formed were performed in a specially designed unit, calculated to operate at 800 atm and 500°. The autoclaves were cylindrical vessels 13 ml in capacity, made from special steel. A salt bath was used to maintain the required temperature.

The experimental procedure was as follows: the urea was put into the autoclave ampoules, which were then closed by means of air-tight lids and weighed. They were then placed in the salt thermostat at a fixed temperature, removed after a definite time, and again weighed to check for air-tightness during the experiment. After release of the pressure the ampoules were opened and again weighed to determine the weight of the gas phase. The product was rapidly transferred from the ampoules into closed weighing bottles, and analyzed. The yield of the product was found from the difference between the weight of the full and the empty ampoule.

The analysis was performed as follows: 0.5-1 g of the product was dissolved in 400 ml of water on warming to 80-90°. After 10-12 hours the solution was filtered. The residue, consisting of corrosion products from the apparatus, was rejected. Urea, biuret, melamine, and cyanuric acid were determined in the filtrate. Urea was determined by the urease method [5], biuret was determined colorimetrically [6], and melamine and cyanuric acid, gravimetrically [7]. Ammonium carbonate and cyanate, ammelide, ammeline, and melamine cyanurate were determined in a sample of the dry product. Ammonium cyanate was determined by potentiometric titration [8], and ammonium carbonate, by a volumetric gas method [9].

The nature of the carbonates was not established; they were determined as carbon dioxide and calculated as nominal ammonium carbonate. The method for the separate determination of ammelide, ammeline, and melamine cyanurate was based on the extraction of these compounds from the product by means of alkali. The subsequent determination of ammelide and ammeline was performed colorimetrically, and of melamine cyanurate, gravimetrically [10].

The mechanism of the reactions taking place when urea is heated was studied in the 132-400° temperature range, in experiments lasting 15, 30, 60, 120, and 180 minutes. Three g of urea was used in each experiment. For a more detailed investigation of the mechanism by which triazine derivatives are formed from urea, series of experiments were performed with addition of cyanuric acid to urea, and experiments on the amination of ammeline. If ammelide, ammeline, and melamine are formed by amination of cyanuric acid, the contents of triazine derivatives should increase when cyanuric acid is added to urea. It must be noted that when cyanuric acid was heated alone, these substances were not formed.

The first series of experiments was performed as follows: one autoclave contained 2 g of urea, and another, 2 g of urea and 1 g of cyanuric acid (the optimum conditions). The experiments were performed at 230, 250, 270, 300, 350 and 400°, the time being 180 minutes.

The second series of experiments was performed at 400°, and ammonia was added to ammeline in 2:1 ratio (optimum conditions). The starting material had the following composition (%): ammeline 84, ammelide 6, melamine cyanurate 7, melamine 2.5. The times of the experiments were 15, 60, and 180 minutes. The apparatus described above was used.

The results of the experiments are presented in the Table and plotted graphically in Figs. 1-5.

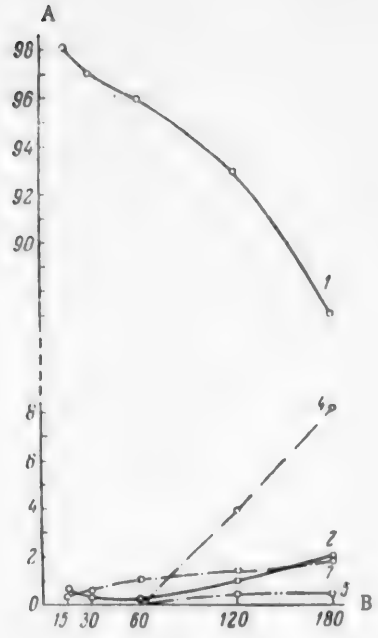

Fig. 1. Variations of the contents of urea (1), ammonium cyanate (2), biuret (4), cyanuric acid (5), and ammonium carbonate (7) in the product, with the time of heating of urea at 132°. A) Composition (% of urea taken), B) heating time (minutes).

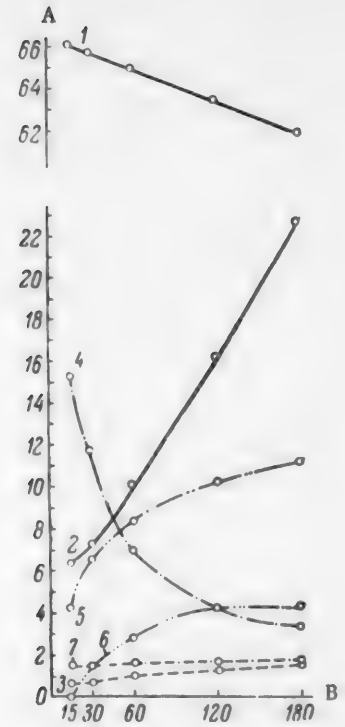

Fig. 2. Variations of the contents of urea (1), ammonium cyanate (2), cyanuric acid (5), ammonium carbonate (7), biuret (4), oxyamino derivatives of triazine (6), and gas phase (3) in the product, with the heating time of urea at 200°. A) Composition (% of urea taken), B) heating time (minutes).

DISCUSSION OF RESULTS

As Fig. 1 shows, when urea is heated under pressure of the reaction gases it begins to decompose at 132°, and its content decreases from 98 to 87%. Ammonium carbonate and cyanate are simultaneously formed, and their contents increase only slightly with time. Somewhat later cyanuric acid and biuret are formed, the latter being formed at the higher rate; thus, the products after 3 hours reaction time contain 8 and 0.5% of these compounds respectively. When the temperature is raised to 200° (Fig. 2), the amount of biuret drops sharply from 15 to 3%. The amounts of ammonium cyanate and cyanuric acid increase under these conditions, reaching 23 and 11% respectively in the product after 3 hours. The urea content of the product changes only slightly. Hydroxyamino derivatives of triazine appear for the first time in the experiments performed at 200°.

At 250° (Fig. 3) the amounts of urea, ammonium cyanate, and cyanuric acid decrease rapidly with time to 10, 4, and 5% respectively. The contents of ammonium carbonate, gas phase, and triazine derivatives increase in this series of experiments. The triazine derivatives consist of ammelide, ammeline, and melamine cyanurate, with rather more ammeline than ammelide. When the temperature is raised to 400° (Fig. 4), the product does not contain ammelide or ammeline, but considerable amounts of melamine appear; the melamine content reaches its maximum (63%) in 15 minutes and then decreases to 18% at the end of 3 hours. The contents of ammonium carbonate and gas phase continue to increase. It follows from Fig. 5 that when cyanuric acid is added to urea the contents of ammelide, ammeline, and melamine in the product are greater than in experiments with urea alone. Thus, at 300°, the amount of hydroxyamino derivatives of triazine in the experiment with urea alone is 0.29 g, and in the experiment with the addition of cyanuric acid it is 1.7 g; the amount of melamine is 0.37 g in the first case, and 0.7 g in the second.

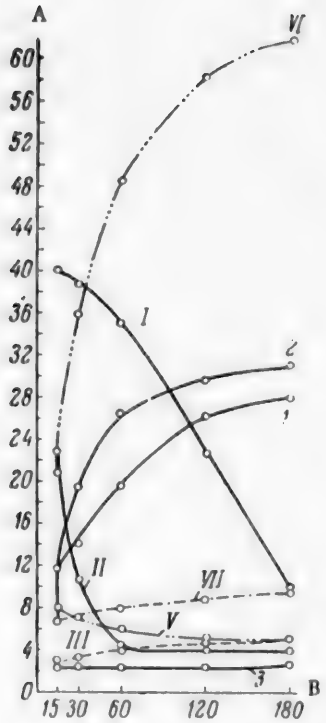

Fig. 3. Variations of the contents of urea (I), ammonium cyanate (II), cyanuric acid (V), ammonium carbonate (VII), hydroxyamino derivatives of triazine (VI), gas phase (III), ammelide (1), ammeline (2), and melamine cyanurate (3) in the product, with the heating time of urea at 250°. A) Composition of product (% of urea taken), B) heating time (minutes).

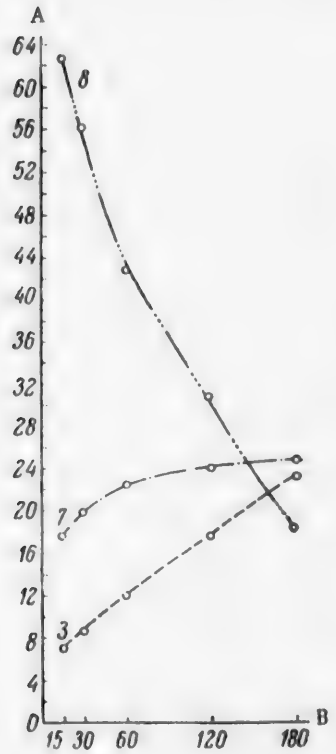

Fig. 4. Variations of the contents of ammonium carbonate (7), melamine (8), and gas phase (3) in the product, with the heating time of urea at 400°. A) Composition (% of urea taken), B) heating time (minutes)

It follows from the data in the Table that when ammeline is aminated by means of ammonia at 400° the reaction product after 15 minutes consists mainly (90%) of melamine, with small amounts of urea (13%) and ammonium carbonate (7%). With increasing time (180 minutes) the amount of melamine decreases somewhat owing to breakdown of the triazine ring, and the ammonium carbonate content increases to 9% as a result.

It is clear from Figs. 1-4 that the heat treatment of urea under pressure of the reaction gases is a complex and diverse process. It is accompanied by conversions of urea with formation of ammonium cyanate and carbonate, biuret, cyanuric acid, ammelide, ammeline, and melamine.

Urea begins to undergo change at 132°, and the main factors which influence its decomposition are the temperature and time of heating. At the start of the process (Fig. 1) urea is converted into ammonium cyanate, which passes into cyanic acid and ammonia under these conditions. This is a reversible reaction. The equilibrium is shifted owing to the formation of biuret by the reaction between cyanic acid and urea. In fact, it is clear from Fig. 1 that under these conditions biuret is formed at a greater rate than ammonium cyanate and cyanuric acid. On further heating (Fig. 2) biuret begins to decompose into the substances from which it was formed, i.e., cyanic acid and urea. The latter is unstable at 200° and also decomposes into ammonia and cyanic acid; this results in a sharp increase of the ammonium cyanate and cyanuric acid contents of the product. Hence it may be said that cyanuric acid is formed by polymerization of cyanic acid. The cyanuric acid is aminated by the ammonia formed in the decomposition of urea, and is converted into ammelide and ammeline, as shown by the sharp decrease in the contents of ammonium cyanate and cyanuric acid (Fig. 3). Ammelide and ammeline

Reaction of Ammeline with Ammonia at 400°

Amounts taken (in g)		Duration of experiment (min)	Amount of product		Yields calculated on ammeline (%)						
									hydroxyamino derivatives of triazine		
ammeline	ammonia		g	%	melamine	cyanuric acid	urea	ammonium carbonate	ammeline	ammelide	melamine cyanurate
3	0.80	15	3.48	116.00	89.70	0	12.70	6.60	0	0	0
3	0.85	60	3.51	117.00	89.70	0	13.20	6.60	0	0	0
3	0.84	180	3.50	116.67	82.70	0	13.20	8.60	0	0	0

are formed simultaneously and at almost equal rates. The products formed in this series of experiments contain melamine cyanurate. Its presence indicates that at this temperatue melamine is formed, and combines with the residual cyanuric acid to form melamine cyanurate. The ammonium carbonate content increases sharply, owing to decomposition of urea or ammonium cyanate by the water formed in the amination of ammelide and ammeline. Melamine is formed by amination of hydroxyamino derivatives of triazine. Its content reaches 63% at 400° (Fig. 4), and then decreases with time; this indicates that the triazine ring is partially decomposed to carbon dioxide and ammonia, with a consequent increase in the amounts of gas phase and ammonium carbonate.

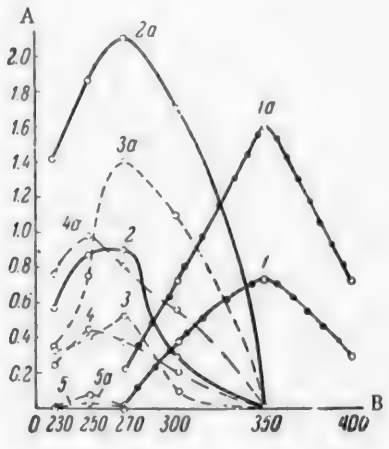

Fig. 5. Variations of the contents of melamine (1), hydroxyamino derivatives of triazine (2), ammelide (3), ammeline (4), and melamine cyanurate (5), with temperature, in experiments with urea alone and in experiments with addition of cyanuric acid. A) Yields (g), B) reaction temperature (°C). Experiments with urea alone: 1, 2, 3, 4, 5; experiments with addition of cyanuric acid: 1a, 2a, 3a, 4a, 5a.

The mechanism suggested for the formation of triazine derivatives from urea is confirmed by the results of experiments with addition of cyanuric acid (Fig. 5). The considerable increase in the contents of ammelide, ammeline, and melamine in the products proves that the ammonia formed in the decomposition of urea aminates the added cyanuric acid so that the amount of triazine derivatives formed is approximately double that obtained in experiments with urea alone. Further confirmation of the reaction mechanism is provided by the experiments of amination of ammeline, which is mainly converted into melamine when heated with ammonia at 400°.

This investigation showed that the conversion products of urea, formerly described [4] as "substances soluble in water" (not containing the triazine ring), consist of biuret and unreacted urea. The reaction products of urea formerly classified [4] as "readily volatile" are ammonium cyanate and carbonate. The latter is formed mainly in the amination of cyanuric acid and hydroxyamino derivatives of triazine.

The amination products of cyanuric acid, previously termed "substances soluble in alkali" [4], are ammelide and ammeline.

SUMMARY

1. A study of the kinetics of formation of the intermediate reaction products and of melamine, obtained by the action of heat on urea under pressure of the reaction gases in the 132-400° range, showed that the heat

treatment of urea results in isomerization of urea to ammonium cyanate and decomposition of the latter into cyanic acid and ammonia (a reversible reaction).

2. Biuret is formed from cyanic acid and unreacted urea. This is a reversible process. Cyanuric acid is formed by polymerization of cyanic acid.

3. The amination products of cyanuric acid are ammelide, ammeline, and melamine; ammelide and ammeline are formed simultaneously and at almost equal rates. The yield of melamine is increased by addition of cyanuric acid to urea in 2:1 ratio.

LITERATURE CITED

[1] D. Paden and D. Mockey, Soviet Patent 492-45, 336867, Peoples Commissariat of the Chemical Industry, January 4, 1945.

[2] H. Kinoshita, Rev. Phys. Chem. Japan, 23, 1, 1-9 (1953).

[3] H. Kinoshita, Rev. Phys. Chem. Japan 24, 1, 19-27 (1954).

[4] N. N. Ivliev, Dissertation "Study of the Synthesis of Triazine Derivatives from Urea" (Gor'kii, 1955).*

[5] G. H. Buchanan, Cyanide Compounds and Their Analysis (Russian translation) (Goskhimizdat, 1933).

[6] Beilst. III, 71 (1921).

[7] S. N. Kazarnovskii and O. L. Lebedev, Trans. Gor'kii Polytech. Inst. Chem. Tech. and Silicate Faculties 11, 3, 52 (1955).*

[8] A. I. Krasil'shchikov and I. D. Nefedova, Zhur. Fiz. Khim. 13, 10, 1429 (1939).

[9] A. P. Groshev, Technical Analysis (Goskhimizdat, 1953).*

[10] S. N. Kazarnovskii and N. I. Malkina, Trans. Gor'kii Polytech. Inst. Chem. Tech. and Silicate Faculties 11, 3, 56 (1955).*

Received October 4, 1956

*In Russian.

A STUDY OF THE XANTHATION OF CELLULOSE PREPARATIONS

A. A. Konkin and Iu. A. Rymashevskaia

The behavior of cellulose in the technological production of viscose fibers is significantly influenced by the properties of cellulose xanthates. Xanthation yields cellulose xanthates with degree of substitution γ of the order of 50. At these relatively low degrees of substitution, cellulose xanthates with equal average values of γ may differ considerably in chemical heterogeneity, and this can undoubtedly have an important influence on the properties of the spinning solutions, which largely determine the extrusion conditions, structure, and the physical and mechanical properties of the fibers. It was therefore considered to be of practical and theoretical interest to study the influence of the structure of different cellulose preparations on the rate of xanthation reaction, as in all probability there is a definite connection between chemical heterogeneity and the xanthation kinetics, which depends on the cellulose structure and the process conditions.

The literature contains contradictory data concerning the influence of the structure of the original cellulose on the rate of the xanthation process [1-3]. This is partially explained by the fact that study of the xanthation of cellulose is a rather complex problem. The xanthation reaction in a heterogeneous medium may be either a kinetic or a diffusional process. In the former case the rate of the process is determined by the reactivity of the hydroxyl groups, and in the latter by the diffusion rate of carbon disulfide, which depends on the structure of the cellulose and on the experimental conditions. Therefore, as has been shown in investigations of cellulose hydrolysis [4], more or less definite conclusions as to the role played by the structure must be based on preliminary studies of the xanthation of cellulose in a homogeneous medium. In this case the influence of structure factor on the results of the reactions is eliminated, and it is therefore possible to study the course of the reaction as a kinetic process. If the xanthation reaction is simultaneously studied in a heterogeneous medium, and the results are compared with the results of homogeneous xanthation, it should be possible to draw definite conclusions concerning the course of the reaction and the role and significance of polysaccharide structure in heterogeneous xanthation. However, such investigations involve additional complications in the case of the reaction in question because there are certain difficulties in establishing conditions for homogeneous and heterogeneous xanthation. Moreover, side reactions lead to certain complications.

EXPERIMENTAL, AND DISCUSSION OF RESULTS

The materials chosen were cotton cellulose, sulfite cellulose, regenerated cellulose (viscose rayon) in which the morphological structure had been destroyed, low-molecular hydrate cellulose formed by hydrolysis of viscose rayon, and xylan isolated from wheat straw by the method described by Konkin and Rogovin [5]. The xanthation reaction was studied in homogeneous and heterogeneous conditions.

The course of the process was followed by the degree of xanthation. For determination of the latter, the cellulose xanthates were converted into dixanthides, which have been studied in detail by Danilov et al., [6-8]. Since these compounds are more stable than xanthates, it is possible to determine the degree of substitution more accurately. The sulfur content of the dixanthides was determined by oxidation of the sulfur by bromine in an alkaline medium, followed by precipitation as $BaSO_4$ [9]. The reproducibility was tested for different cellulose samples; results agreeing within the limits of experimental error were obtained.

The amount of carbon disulfide taken was 100% on the weight of the cellulose in all the experiments. The reaction was performed at 20°.

Xanthation of polysaccharides in solution. The xanthation of polysaccharides in a homogeneous medium been studied by a number of workers.

Lieser and Leckzych [10] xanthated cellulose in tetraethylammonium hydroxide solution. Scherer xanthated soda cellulose in liquid ammonia [11], and Rogovin and Neiman [12] xanthated regenerated cellulose. However, in most cases these workers mainly confined themselves to determinations of the xanthate composition and studies of the xanthate properties. Recently Gherkasskaia, Pakshver, and Kargin [13] studied the rate of xanthation of cellulose in caustic soda solution.

The solvents chosen for our studies of xanthation in homogeneous media were triethylbenzylammonium base and caustic soda. Triethylbenzylammonium base is the most suitable solvent. Cellulose of any molecular weight is soluble in a 33% aqueous solution. Therefore the reaction can be effected in homogeneous conditions with the use of this solvent. However, preliminary experiments showed that the cellulose xanthate formed is immediately precipitated, and the reaction therefore becomes heterogeneous with respect to the precipitated xanthate. The reaction was therefore performed in a mixture of triethylbenzylammonium base and water in 1:1 ratio by volume. The starting materials and the reaction products are all soluble in this mixture. The polysaccharide concentration of the solution was 2%. The results of the xanthation of three types of cellulose and of xylan are presented in Table 1.

These results show that if the polysaccharides and carbon disulfide are present in solution the xanthation reaction is very rapid, and the formation of cellulose xanthates is completed in less than 5 minutes. The degree of substitution of the cellulose xanthates is γ = 50-65, and of xylan xanthates, about 40. The degree of substitution is not changed on further increase of the reaction time to 160 minutes. Therefore the carbon disulfide is immediately used almost completely for the formation of polysaccharide xanthates and by-products. The degree of substitution is increased only if additional carbon disulfide is introduced into the reaction mixture.

Comparison of the data for different types of cellulose shows that the xanthates of cotton and wood cellulose have approximately the same degree of substitution, whereas a somewhat higher value of γ is obtained for hydrate cellulose. Since the hydroxyl groups have the same reactivity in all the cellulose samples, this difference in the degrees of substitution may be due to the fact that the intermolecular interaction is more intense with higher molecular weight, as is the case for cotton and wood cellulose. The hydroxyl groups involved in hydrogen bonding react less rapidly with carbon disulfide, and therefore rather more carbon disulfide is expended in side reactions, with a decrease of γ.

Xylan, in contrast to cellulose, does not contain primary hydroxyl groups, and yet the xanthates of hydrate cellulose and xylan have approximately the same degree of substitution. This may be explained on the assumption that under the experimental conditions used the carbon disulfide reacts mainly with the secondary hydroxyl groups which, according to the literature [14], are more reactive than primary hydroxyl groups in an alkaline medium.

The xanthation of cellulose in 10% caustic soda solution was studied next. For preparation of alkali-soluble samples, cotton and sulfite celluloses were ground, and hydrate cellulose was first depolymerized by hydrolysis in 2 N hydrochloric acid. The polysaccharide concentration in solution was 1%. Since carbon disulfide is only partially soluble in alkali, the reaction in this case takes place in a heterogeneous medium, although the cellulose is in solution. As the reaction rate is determined in this instance by the state of the carbon disulfide and, in particular, by the particle size of the emulsion, the stirring rate was maintained constant in all the experiments in order to ensure more or less comparable results.

The results of these experiments are given in Table 2.

It follows from the data in Table 2 that the reaction rate is much lower in xanthation in alkali solution. The reaction time necessary to obtain cellulose xanthates of the same value of γ is 30-60 minutes in alkali solution, and less than 5 minutes in the quaternary ammonium base.

In this instance the cellulose reacts with the part of the carbon disulfide which is present in the dissolved state, and therefore the reaction rate depends on the solution rate of carbon disulfide, which is in turn determined by the particle size of the carbon disulfide emulsion. When carbon disulfide is introduced into the reaction mixture in the form of gas, it is condensed in the solution with formation of very fine droplets of carbon disulfide, and the reaction rate increases considerably. After 20 minutes the degree of xanthation (γ) of sulfite

TABLE 1

Homogeneous Xanthation in a Medium of Triethylbenzylammonium Base and Dioxane

Starting material	Reaction time (min)	S content (%)	Degree of substitution γ (%)	Amount of substituted hydroxyl groups (%)	
Cotton cellulose	5	16.30	51		17.0
	10	16.85	53		17.6
	20	17.00	54		18.0
	40	16.55	52		17.3
	80	16.70	53		17.6
	160	16.25	51		17.0
				Mean	17.4
Sulfite cellulose	5	16.60	52		17.3
	20	16.35	51		17.0
	40	16.15	50		16.6
	80	16.80	53		17.6
	160	16.95	54		18.0
				Mean	17.3
Hydrate cellulose (viscose rayon)	5	19.25	64		21.3
	20	20.10	67		22.3
	40	20.30	68		22.6
	80	18.55	61		20.3
	160	19.70	65		21.6
				Mean	21.6
Xylan	5	17.55	44		22.0
	20	15.25	38		19.0
	40	16.25	41		20.5
	80	16.10	40		20.0
	160	17.60	44		22.0
				Mean	20.7

TABLE 2

Xanthation in 10% Caustic Soda Solution

Starting material	S content and degree of substitution after xanthation time (min)									
	10		20		30		60		240	
	S	γ	S	γ	S	γ	S	γ	S	γ
Degraded cotton cellulose	6.35	18	9.45	27	16.06	50	19.21	63	22.35	77
Degraded sulfite cellulose	7.53	21	12.84	39	16.58	52	21.10	71	24.42	87
Hydrate cellulose (viscose rayon)	9.87	29	13.96	43	17.22	55	22.55	78	27.00	100

cellulose reaches 52 instead of the 39 (see Table 2) which is obtained when carbon disulfide is added in liquid form. These results show convincingly that if the carbon disulfide is present in the undissolved state, the reaction is determined by diffusion irrespective of the state of the cellulose.

Despite the fact that preparations of low molecular weight were used in these experiments, the rate of xanthate formation varies in the same sequence as in the reaction in a solution of the quaternary ammonium base.

With equal reaction times, the highest degree of substitution is obtained for hydrate cellulose, and the lowest, for cotton cellulose. The difference in the reactivities of these samples is due to their different states in solution. Mechanical grinding of cotton and wood celluloses decreases their average degree of polymerization, and samples soluble in alkali are thereby obtained, but nevertheless elements of the native structure are retained, with dense packing and strong intermolecular interaction.

When the celluloses are dissolved in alkali these elements of the native structure are, in all probability, not destroyed completely and the intensive intermolecular interaction, which retards the reaction rate, is retained.

The degree of xanthation of cellulose is higher in xanthation in alkali solution than in xanthation in the quaternary ammonium base. The probable explanation is that less carbon disulfide is used in the formation of by-products in the former case.

Xanthation of polysaccharides in a heterogeneous medium. The heterogeneous xanthation of cellulose may be effected by different methods, according to the state of the carbon disulfide in the reaction zone. The reaction takes place under heterogeneous conditions when alkali cellulose is xanthated by means of carbon disulfide dissolved in organic solvents which are inert toward cellulose and cellulose xanthate, or by means of liquid, gaseous, or emulsified carbon disulfide. The rate of the process evidently depends on the reaction conditions, but the structure of the cellulose and the form of the material used have a significant influence on the results in all cases. Our experiments on heterogeneous xanthation were performed by the emulsion method and also with liquid carbon disulfide.

The same samples were subjected to emulsion xanthation by the method described by Shuliatikova and Olevskaia [15]. In emulsion xanthation most of the cellulose is in the undissolved state, and therefore the reaction takes place at the interface between the cellulose and the liquid phase in which carbon disulfide is dissolved.

TABLE 3

Emulsion Xanthation

Starting material	S content and degree of substitution after xanthation time (min)									
	10		20		40		80		240	
	S	γ	S	γ	S	γ	S	γ	S	γ
Cotton cellulose	0	0	0	0	8.03	23	13.93	43	16.20	51
Sulfite cellulose	0	0	5.53	16	9.24	26	15.30	47	17.26	55
Hydrate cellulose (viscose rayon)	3.37	9	9.49	20	13.18	40	17.77	57	21.70	74

The results (Table 3) show that emulsion xanthation is considerably slower than xanthation in caustic soda solution. An additional factor in decreasing the reaction rate is the cellulose structure, and therefore differences in the xanthation rates of different cellulose samples should be more pronounced in this case. In fact, in the early stages the xanthation of cotton cellulose is slower than that of sulfite cellulose, but with increase of the xanthation time the absolute difference between the degrees of substitution is not great, although such a difference persists. As was to be expected, the xanthation of hydrate cellulose proceeds at an appreciably greater rate. This is because the macromolecular packing in hydrate cellulose samples is less dense, and also because hydrate cellulose is partially dissolved under conditions of emulsion xanthation, and the reaction therefore proceeds under homogeneous and heterogeneous conditions simultaneously with respect to cellulose.

In xanthation by means of liquid carbon disulfide, the reaction takes place at the boundary of direct contact between the alkali cellulose and liquid carbon disulfide, and under the action of carbon disulfide vapor. The area of contact between liquid carbon disulfide and cellulose is relatively small, and the reaction therefore proceeds mainly by the action of gaseous carbon disulfide; its rate is consequently determined by the rate of evaporation of carbon disulfide, and the rate of its penetration into the cellulose material.

It is clear from Table 4 that the reaction rate is much lower in this case than in emulsion xanthation. The reason is that in emulsion xanthation the cellulose swells, and therefore the structural elements of the cellulose have less influence on the reaction rate, because carbon disulfide has greater access to the inner regions of the cellulose. As in the preceding series of experiments, the xanthation reaction is most rapid with regenerated cellulose (viscose rayon) and slowest with cotton cellulose, and wood cellulose occupies an intermediate position; the differences in the reaction rates are most prominent in the early stages of the process.

TABLE 4

Heterogeneous Xanthation

Starting material	S content and degree of substitution after xanthation time (hours)									
	2		4		8		24		48	
	S	γ	S	γ	S	γ	S	γ	S	γ
Cotton cellulose	5.74	16	11.27	33	13.30	40	15.30	47	16.20	50
Sulfite cellulose	6.05	17	12.01	39	15.00	46	17.56	55	18.41	58
Viscose rayon	9.64	28	13.44	41	15.20	47	18.01	57	20.30	68
Degraded viscose rayon	—	—	—	—	—	—	5.03	14	15.12	40
Xylan	—	—	—	—	—	—	1.23	3	5.77	16

The xanthation of degraded viscose rayon and of xylan is very slow. The explanation of this fact, unexpected at first sight, is that these materials were used in powder form, so that access of carbon disulfide to the inner regions of the polysaccharides was hindered. Consequently the rate of heterogeneous xanthation is greatly influenced by the form of the material; in particular, carbon disulfide diffuses more easily into polysaccharides of fibrous structure.

SUMMARY

1. It is shown that if cellulose and carbon disulfide are present in the dissolved state the xanthation reaction is very rapid, and is completed in a few minutes.

2. The reaction rate is much lower in xanthation in a heterogeneous medium; the factors which decrease the rate of the process, according to the experimental conditions, are the structure of the polysaccharides and the state of the carbon disulfide in the reaction zone.

3. Different celluloses form the following sequence according to their xanthation rates in homogeneous and heterogeneous media: viscose rayon > sulfite cellulose > cotton cellulose.

LITERATURE CITED

[1] K. Jung, Kolloid-Z. 98, 192-199 (1942).

[2] K. Jung, Kolloid-Z. 108, 2/3, 120-125 (1944).

[3] K. Heiss, Kunstseide und Zellwolle 27, 2, 37 (1949).

[4] Z. A. Rogovin and N. N. Shorygina, Chemistry of Cellulose and Associated Substances (State Sci. Tech. Press Chem. Lit., 1953).*

[5] A. A. Konkin and Z. A. Rogovin, J. Appl. Chem. 23, 536 (1950).**

[6] S. N. Danilov and D. S. Brokhina, Zhur. Obschei Khim, 4, 7, 995 (1934).

[7] S. N. Danilov and O. P. Kuz'mina, Zhur. Priklad. Khim. 19, 1056 (1946).

*In Russian.

**Original Russian pagination. See C. B. Translation.

[8] S. N. Danilov and N. M. Grad, Zhur. Obshchei Khim. 17, 2193 (1947).

[9] I. Kolthoff and E. Sandell, Quantitative Analysis (Russian translation) (State Sci. Tech. Press Chem. Lit., 1941).

[10] Th. Lieser and E. Leckzych, Ann. 522, 1, 56 (1936).

[11] P. Scherer, Rayon Text. Monthly, 20, 11, 39 (1939).

[12] Z. A. Rogovin and R. S. Neiman, Zhur. Priklad. Khim. 12, 2 (1939).

[13] P. M. Cherkasskaia, A. B. Pakshver and V. A. Kargin, J. Appl. Chem. 26, 3, 311 (1953).••

[14] Z. A. Rogovin, A. A. Konkin and Iu. A. Rymashevskaia, Proc. 6th Conf. on High-Molecular Compounds, 140 (Izd. AN SSSR, 1952).•

[15] N. V. Shuliatikova and O. M. Olevskaia, Sci. Res. Trans. Sci. Res. Inst. Artificial Fibers, 82 (State Light Industry Press, 1951).•

Received July 11, 1956

•In Russian.

••Original Russian pagination. See C. B. Translation.

CHARACTERISTICS OF THE FUSEL OIL FORMED IN THE FERMENTATION OF COTTON-HULL HYDROLYZATES

Z. N. Nazarova

Cotton hulls and wood differ greatly in their composition and hydrolysis conditions. Therefore the products formed by fermentation of cotton-hull hydrolyzates should differ considerably from the corresponding products of wood hydrolysis.

It was of interest in this connection to investigate the fusel oil formed in the fermentation of cotton-hull hydrolyzates, and also to determine the regions of its highest concentration in the column in the distillation and rectification of the alcohol.

The fusel oil collected from the rectification column of the Fergana hydrolysis plant is a thick tarry liquid with density $d_4^{20} = 1.090$, and with an odor very unlike that or ordinary fusel oils.

Fractionation experiments showed that this fusel oil has a low content (about 20%) of the lower alcohols, including amyl, and is rich in fractions boiling above 140°; most of it distills in the 140-260° range. Nearly all the fractions so obtained decolorize bromine water. The undistilled fusel oil is 50% soluble in alkali and contains 3% of bases. The alkali solubility, low acidity, and the odor of the fusel oil suggested that it contains substances of a phenolic character.

Our investigations of the fusel oil were based mainly on the scheme devised by Shorygin et al. [1] for investigations of still residues, and on the scheme of Tsukervanik and Vladimirova [2] for investigations of fusel oil (from food raw materials), with some modifications due to the fact that the oil has a high content of alkali-soluble substances (see Scheme). Two methods were used for the investigation.

Method A. The undehydrated fusel oil, containing about 5% water, was distilled in the 90-250° range, and the distillate was separated into the basic, acidic, phenolic, and neutral portions (see Scheme). The bases were isolated from the distilled fusel oil by treatment with 15% HCl. Acids were then extracted by means of 10% $NaHCO_3$ solution, and phenols by means of 10% NaOH solution. The neutral residue (alcohols, hydrocarbons, ethers, and esters) was saponified by means of 20% NaOH solution on a boiling salt bath for 14 hours. The alkaline solution was treated with ether, heated to remove volatile substance, and acidified to liberate a mixture of acids and phenols, which was then separated by consecutive treatment with $NaHCO_3$ and NaOH solutions. The unsaponifiable neutral residue was distilled over a column (12 theoretical plates) to yield 8.45% of lower alcohols and 11.2% of amyl alcohols (calculated on the weight of the fusel oil); extraction of the higher-boiling fractions with ethyl alcohol yielded 5% of higher alcohols (hexyl, heptyl, octyl). The residue (hydrocarbons, ethers, and possibly higher alcohols) was not investigated.

Method B. The undistilled fusel oil was extracted with water. The aqueous extract was salted out by addition of solid NaOH, and extracted first with ether and then with benzene. The aqueous extract yielded a total of 2.6% (on the weight of the fusel oil) of a mixture of substances, and this, like the fusel oil washed with water, was subjected to the treatment used in the first method (see Scheme).

Significant differences were found between the phenolic portions of the distilled and undistilled fusel oil.

Scheme

Fusel Oil

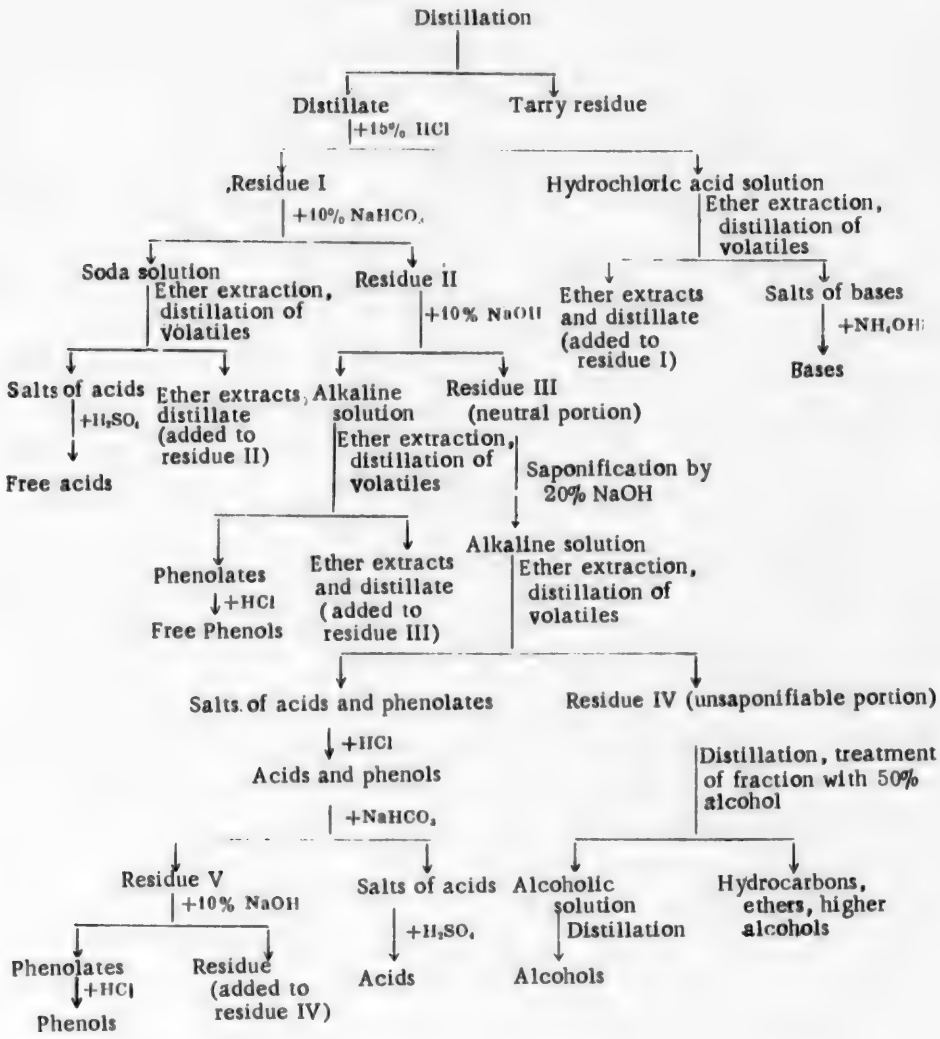

It was found that phenols form the main constituent of undistilled fusel oil, up to 49% (of which 3% is present in the oil in ether or ester form), whereas the distilled oil contains only 19% phenols. Distillation of phenols from undistilled fusel oil leaves 27% residue, whereas the corresponding residue for distilled fusel oil is 7.3% (the main bulk of the residue in the distillation of fusel oil evidently consists of higher phenols).

The results of fractional distillation of the free phenols over a column of 12 theoretical plates, presented in Table 1, show that they contain up to 20% of lower phenols, the remaining 27% being phenols of higher molecular weight. The individual fractions were treated with monochloroacetic acid to give the corresponding

TABLE 1

Composition of Free Phenols

Fraction No.	Boiling range (°C)	Amount (%) on		Phenoxyacetic acids		Name of corresponding phenol	Molecular weight of phenol (calculated)	Literature data [3]	
		total phenols	fusel oil	m. p. (°C)	molecular weight of phenol (found)			b. p. (°C)	m. p. of phenoxy acid (°C)
1	185—190	1.00	0.09	146—147	108.1	o-Cresol	108	190.8	151—152
2	190—195	3.58	0.33	147—148	109.3	1,3-Xylenol-2	122	205	140
				139—140	123.1	Guaiacol	124	205	116
3	195—200	4.58	0.43	114—116	122.2	Guaiacol	124	205	116
4	200—205	24.10	2.25	114—116	122	1,3-Xylenol-5	122	211—212	118; 111
5	205—210	3.09	0.29	117—118	122	1,3-Xylenol-4	122	218	142
				140—142	121	1,3-Xylenol-5	122	211—212	111
6	210—215	6.07	0.62	111—113	121	2,4,6-Mesitol	136	221	132
7	215—225	32.41	3.02	129—130	137	Creosol	138	221	
				60—62	175	—	—	—	—
8	225—230	14.49	1.35	Oil	175	—	—	—	—
9	230—236	1.49	0.14	Oil	176	—	—	—	—
10	Residue	5.54	0.51	63—64	—	—	—	—	—

phenoxyacetic derivatives; the latter were titrated for determination of their equivalents and calculation of the molecular weights of the corresponding phenols. Similar values were obtained, indicative of the presence of isomeric compounds, mainly cresols, xylenols, guaiacol, creosol, mesitol, etc.

The alcohol yield was 25% on the weight of the fusel oil; the composition of the alcohols does not differ significantly from that of alcohols from other fusel oils.

The total content of free and esterified acids was less than 1%. The total acids were not studied in detail.

Bases of the pyridine and pyrazine series were isolated by fractional distillation of the total bases (4.18%), and confirmed by the formation of picrates and analysis of the latter for nitrogen (Table 2). The fractions boiling above 190° were not studied in detail.

The presence of bases of the pyrazine series is characteristic of still residues from fusel oils of different origins [1, 2], but dimethylpyridines had not previously been found in fusel oils.

The principal component of the 3.25% of carbonyl compounds was furfural. The neutral unsaponifiable substances (14.8%) were not studied in detail.

Two samples of fusel oil, collected from the 3rd and 4th plates of the rectification column, were studied.*

The sample from the 3rd plate (d = 0.998) had a low content of isoamyl and lower alcohols (up to 33% on the dehydrated oil), and was rich in alkali-soluble substances phenols acids), whereas the sample from the 4th plate (d = 0.872) consisted mainly of isoamyl alcohol (45.88% on the weight of the fusel oil, or 62% on the weight of the fusel oil after removal of water and ethyl alcohol), and contained only 3% phenols. This sample is similar to ordinary fusel oils in its density and content of isoamyl alcohol, and can be used as a source of isoamyl alcohol.

Table 3 shows the results of group analyses of all the fusel oil samples studied; data for fusel oils obtained in the production of alcohol from food raw materials [5] and wood [6], and analytical data on the still residues [3], are presented for comparison.

It follows from the data in Table 3 that the composition of the fusel oil collected in the rectification of alcohol made from cotton hulls differs considerably from that of other samples of fusel oil, and of the still residues. Not only the quantitative proportions of the individual components, but also the

*With the assistance of S. I. Slepakova.

TABLE 2

Composition of Bases

Fraction No.	Boiling range (°C)	Amount (%) on		Picrates			Literature data		
		total bases	fusel oil	m. p. (°C)	N (%) found	N (%) calc.	name of compound	b. p. (°C)	m. p. of picrate (°C)
1	100—120	5.00	0.15	156—167	18.21 18.29	18.18	Pyridine [4]	115	165—167
2	134—145	5.00	0.15	166—168	16.42 16.32	16.67	2,5-Dimethylpyridine [3]	142—143	168
3	150—158	8.33	0.25	168—169 155—157	16.39 20.24	16.67 20.77	2,5-Dimethylpyridine [3] 2,5-Dimethylpyrazine [1]	154—160 151—153	169 155—157
4	158—166	9.44	0.28	155—157 163—164	20.01 —	20.77 —	2,5-Dimethylpyrazine [1]	151—153	155—157
5	166—172	14.66	0.44	139—140	19.76 19.86	19.94	Trimethylpyrazine [1]	171—172	140—141
6	172—180	7.00	0.21	167—169 139—140	—	—	Trimethylpyrazine [1]	171—172	140—141
7	180—190 (M.p. 84—85)	18.38	0.57	193—195	19.52 19.54	19.17	Tetramethylpyrazine [1]	189—190	194—195
8	190—210	13.33	0.40	—	—	—	Diethylpyrazine [1]	—	97—98
9	Residue	15.00	0.45		—	—	Triethylmethylpyrazine [1]	232	101—102

TABLE 3

Principal groups	Group composition of fusel oils isolated during the conversion of cotton hulls (% on the fusel oil)								Group composition of fusel oils obtained from		
	Sample I d = 1.090	Sample II d = 1.002				Sample III from 3rd plate, d = 0.998	Sample IV from 4th plate, d = 0.872	Shorygin's data [3] (% on the still residues) d = 0.873	potatoes [5] (% on fusel oil free from water and C_2H_5OH) d = 0.835	grain [5] (% on fusel oil free from water and C_2H_5OH) d = 0.840	wood [6] (% on the dewatered fusel oil)
		(90–280°) distilled	not distilled								
			washed with water	aqueous extract	entire						
Water and ethyl alcohol	5.50	4.38	—	—	4.83	25.00	26.00	1.60	—	—	—
Bases	3.00	3.00	3.33	0.85	4.18	1.06	1.10	4.50	0.005	0.02	0.08
Acids											
Total	—	0.63	0.65	—	—	—	—	14.40	0.03	0.47	—
Free	—	0.20	0.20	0.06	0.26	4.21	0.78	1.40	0.01	0.16	5.00
Esterified	—	0.40	0.45	—	—	—	—	13.00	0.02	0.31	—
Phenols:											
Total	—	19.30	48.75	—	—	—	—	—	—	—	—
Free	17.00	17.30	45.70	0.07	45.77	13.00	3.00	—	—	—	0.01
As ethers or esters	—	2.00	3.05	—	—	—	—	—	—	—	—
Carbonyl compounds calculated as furfural	2.50	3.25	—	—	—	—	5.50	—	—	—	2.00
Neutral substances (alcohols, ethers and esters, hydrocarbons)	42.00	42.27	41.40	0.95	42.35	49.00	69.00	50.61	—	—	—
Including:											
Unsaponifiables (alcohols, ethers, hydrocarbons, etc.)	—	39.60	40.25	—	—	—	—	45.60	—	—	—
Composition of unsaponifiables:											
Total alcohols	25.00	24.84	—	—	—	—	—	36.00	99.96	99.43	—
Up to 125°	10.0	8.45	9.60	0.10	9.70	25.36	12.00	27.90	31.20	19.45	17.20
Amyl	13.00	11.20	10.60	0.25	10.85		45.88		68.76	79.85	65.00
Higher	—	5.15	—	—	—	—	—	5.01	—	0.13	—
Hydrocarbons, ethers, higher alcohols	—	18.29	18.80	0.55	19.35	—	—	—	—	—	—
Hydrocarbons	—	—	—	—	—	—	—	9.60	—	—	10.00
Distillation residues (above 280°)	30.00	24.30	—	—	—	—	—	—	—	—	—

group composition differs sharply (there is a high phenol content). The presence of phenols is undoubtedly due to the higher lignin content of the raw material; this lignin undergoes extensive decomposition during hydrolysis,* with the formation of considerable amounts of methyl alcohol (in the first runnings [8]) and substances of a phenolic character (in the last runnings).

For isolation of the phenols it is expedient to distill off the main quantity of the alcohol (up to 150°), and to the extract the phenols from the residue. The yield of phenols can be increased from 20 to 40% if the residue after distillation of the alcohols is saponified, and phenols then extracted. These phenols can be used in the production of chlorophenolacetic acids and their esters, for which there is a great demand in agriculture.

SUMMARY

1. The fusel oil isolated in the rectification of alcohol made from cotton hulls differs in composition from other samples of fusel oil and still residues by a higher content of phenols and bases.

2. The composition of the fusel oil depends on the part of the distillation column from which it is taken. The most valuable is oil from the 4th plate; this contains up to 62% isoamyl alcohol. This oil is closest to the standard oil, and can be used as a source of isoamyl alcohol.

3. The high phenol content of this fusel oil, especially from the 3rd plate, indicates that it may be used as a source of phenols after preliminary distillation of most of the alcohols (up to 150°).

4. The considerable content of bases (from 3 to 4%), as compared with other samples of fusel oil, suggests that it may be possible to use this oil as a source of pyrazine bases, which are difficult to obtain by synthesis.

LITERATURE CITED

[1] P. P. Shorygin, V. I. Isaguliants, V. N. Belov and Z. P. Aleksandrova, Zhur. Obshchei Khim. 4, 372 (1934).

[2] I. P. Tsukervanik and N. G. Vladimirova, Bull. Sr. Az. Gos. Universiteta 23, Iubileinye (1945).

[3] P. P. Shorygin and S. V. Savenkov, Zhur. Priklad. Khim. 9, 1437 (1936).

[4] Beilstein (4), 20.

[5] A. A. Fuks, Technology of Alcohol Production (Food. Ind. Press, 1951).**

[6] V. I. Sharkov, The Hydrolysis Industry 3, 2 (State Wood and Paper Press, 1943).**

[7] V. G. Panasiuk et al., Gidroliz. i. Lesokhim. Prom. SSSR 2, 17 (1953); J. Appl. Chem. 26, 763 (1953).***

Received June 30, 1956

*Panasiuk et al., [7] showed that pyrolysis of cotton-hull lignin yields up to 6% phenols, considerable amounts of neutral substances, and also acids and pyridine.

**In Russian.

***Original Russian pagination. See C. B. Translation.

OXIDATION OF MONOOLEFINIC HYDROCARBONS

Ia. B. Chertkov

Studies of the oxidation of unsaturated hydrocarbons involve certain difficulties owing to the fact that oxidation is accompanied by condensation processes, with formation of considerable amounts of products of very complex transformations, the nature of which has been studied little. The available information in this field is very restricted.

It has been suggested that, in addition to its oxidizing action, oxygen accelerates the polymerization of unsaturated hydrocarbons and their oxidation products [1, 2].

With regard to the mechanism of the addition of oxygen to unsaturated compounds, including olefins, most investigators consider that oxygen is added in the first instance to the carbon atom in the β position relative to the double bond. The unsaturated bond is retained in the process. However, the opposite view has also been advanced; namely, that the oxidation of unsaturated olefins, like the oxidation of normal paraffins boiling in the same range, yields saturated oxygen-containing compounds, such as acids [3]. It is quite evident that the final composition of the oxidation products of hydrocarbons, and especially unsaturated compounds with a high tendency to oxidative polymerization, should be determined to a considerable extent by the rate of the oxidation reaction and of the subsequent conversions as a whole.

The rate of an oxidation reaction taking place within the volume of a liquid depends to a considerable degree on the concentration of one of the components of the reaction mixture – dissolved oxygen. The concentration of the dissolved oxygen, in its turn, is proportional to the partial pressure of oxygen in the gaseous mixture passed through the liquid phase of the hydrocarbons being oxidized. Therefore, by regulation of the oxygen content of the oxidizing agent it is possible to vary the oxidation rate to some extent, and thereby to influence the degree of the oxidation process and the subsequent conversions of the oxygen-containing substances.

Very little is known of this aspect of the problem in relation to oxidation reactions in the liquid phase.

This is confirmed by the fact that nearly all known oxidation processes take place in presence of an enormous excess of oxygen. For example, the exit air after oxidation of normal paraffins to acids differs very little from the air entering the reaction mixture. Over 70% of the oxygen remains unchanged, with very small amounts of CO_2 and traces of CO in the gaseous mixture [4].

No definite conclusions can be drawn from a comparative examination of the few investigations devoted to the influence of the oxygen concentration on the rate of the oxidation reaction [3, 5-8].

In our opinion variations of the oxygen concentration in the reaction zone can be used to restrict appreciably the development of secondary processes, which usually involve further conversions of valuable oxygen-containing substances. Therefore regulation of the oxygen concentration, together with other factors, is a convenient means for directing the oxidation process with the aim of obtaining valuable products. Confirmation for this view was found in the oxidation of normal paraffins of high molecular weight to alcohols. A process, developed with our assistance, for the direct oxidation of normal paraffins (from petroleum, and synthesized from CO and H_2) at 165-175° by means of oxygen in presence of boric acid, the oxygen being present in a strictly limited amount in the gas mixture, yielded up to 60% of monohydric alcohols, calculated on the raw material [9].

The alcohols were of normal structure and the number of carbon atoms in the alcohol molecule was close to that in the hydrocarbon oxidized.

Equal interest attaches to the possibilities which this opens up for the oxidation of olefins, when oxidation is complicated by condensation processes.

A mixture of high-molecular olefins was prepared by dehydration of the above-named aliphatic alcohols over a standard catalyst – aluminum oxide. The alcohols were dehydrated in a tube at 275° under 10 mm Hg residual pressure.

The olefin mixture was separated by vacuum fractionation in a laboratory column of 16 theoretical plates.

The olefin fraction chosen for the oxidation had the following characteristics.

Boiling point at 11 mm Hg (°C)	130-135
Molecular weight	200
Refractive index (n_D^{20})	1.4432
Iodine number (g I_2/100 g)	122
Elementary composition (%):	
C	85.85
H	14.15
Average formula	$C_{14.3}H_{28.3}$

The olefins were oxidized in a reactor with a sealed-in No. 1 glass filter, through which air was passed at 550 liters/kg·hour. The oxidation was performed under the mildest conditions adopted for the oxidation of normal paraffins to acids, namely: temperature 110°, time 8 hours, amount of potassium permanganate catalyst 0.2% on the weight of hydrocarbons [10]. The oxidation was performed at approximately normal pressure in the reactor, and also at 150 mm Hg, when the partial pressure and therefore the weight of oxygen was about 1/5 of that in the process under normal pressure.

The reaction mass was extracted quantitatively from the reactor, and saponified by means of 7-8% KOH solution in methanol. After removal of the methanol, the salts of acid compounds and the neutral portion were separated by treatment with ether. The salts were decomposed by sulfuric acid solution, and the acid compounds were extracted in ether. The unreacted hydrocarbons were separated from the neutral portion by a chromatographic procedure on "ShSM" silica gel of 150-65 mesh, at a volume rate of 0.01 $hour^{-1}$. The hydrocarbons were desorbed by means of isopentane, and the oxygen compounds by means of methanol. The neutral and acid oxygen compounds were distilled in vacuum.

The unreacted hydrocarbons, and the acid and neutral oxygen compounds, both distillable and tarry (undistillable), were characterized by the usual methods. The total losses in oxidation did not exceed 5%, and in the compilation of the balance they were distributed in proportion to the weights of the isolated products.

A comparison of the weight balances for the oxidation of olefins under normal conditions and under 150 mm Hg residual pressure is presented in Table 1.

It follows from Table 1 that when the concentration of oxygen in the reaction zone is higher the total amount of olefins oxidized is much greater. The rate and degree of oxidation are also higher. The amount of neutral oxygen compounds formed under reduced pressure is ½ the amount formed under normal pressure in the same time and at the same oxidation temperature. The decrease is due mainly to the formation of undistillable compounds – products of extensive conversion.

The fact that the amounts of acid compounds formed under normal pressure and under vacuum are similar, and much less than the amount of neutral substances, suggests that these acid products must largely be formed as the result of further oxidation of the oxygen compounds formed.

The qualitative aspects of the question are also of interest.

The general characteristics of the oxidation product, treated with water on heating, are given in Table 2.

It is seen that the iodine number of the oxidation product is appreciably lower than that of the original hydrocarbons, while the ester number is high; these facts suggest that products of more extensive conversion are formed.

The characteristics of the acid and neutral oxygen compounds, isolated from the oxidation products and distilled under vacuum, are given in Tables 3 and 4.

These results show, first, that when olefins are oxidized under the conditions used for oxidation of normal paraffins to acids, not only oxidation but also oxidative condensation of the previously formed oxygen compounds is very rapid.

The reaction products are compounds with considerable contents of oxygen in their molecules.

TABLE 1

Balance of Olefin Oxidation (%)

	Under normal pressure	Under 150 mm Hg residual pressure
Unreacted hydrocarbons		
Unreacted hydrocarbons	18.5	53.7
Neutral oxygen compounds	56.2	25.6
Including:		
a) distillable	23.4	19.0
b) tarry	32.8	6.6
Acid compounds	25.3	20.7
Including:		
a) distillable	12.5	11.2
b) tarry	12.8	9.5
Total	100	100

TABLE 2

Characteristics of the Oxidation Product

Characteristic	Oxidation under normal pressure	Oxidation under 150 mm Hg
Iodine number (g I_2/100 g)	32	57
Acid number (mg KOH/g)	20	15
Hydroxyl number (mg KOH/g)	68	50
Ester number (mg KOH/g)	110	84
Carbonyl number (mg O_2/g)	7	9

Thus the acid distillates contain not only oxygen in carboxyl groups, but also oxygen present in a different form in the molecule. In the acid distillate obtained under normal pressure the total oxygen content in the average molecule is 2.8 atoms, while in the vacuum distillate it is more than 5 atoms. The explanation for this difference is that oxidative condensation processes occur at a high rate during oxidation by oxygen of high concentration under normal pressure, with formation of products of extensive transformation, which cannot be distilled.

TABLE 3

Characteristics of Distilled Acid Compounds

Characteristic	From olefins oxidized under normal pressure	From olefins oxidized under 150 mm Hg
Boiling point at 3 mm Hg (°C)	77—184	76—253
Iodine number (g I_2/100 g)	37	39
Molecular weight	193	375
Acid number (mg KOH/g)	285	145
Refractive index (n_D^{20})	1.4580	1.4600
Elementary composition (%):		
C	66.38	68.86
H	10.45	7.98
O	23.17	23.16
Average formula	$C_{10.7}H_{20.2}O_{2.8}$	$C_{21.5}H_{30.0}O_{5.4}$
Olefin bonds in average molecule	0.28	0.58

The distillate contains condensation products formed at the initial stage of the process. The yield of undistillable compounds formed during oxidation under vacuum, i.e., by means of oxygen of lower concentration, is considerably less. However, even in this case the distillate contained products with a higher oxygen content in the molecule and correspondingly of higher molecular weight. The same is true of distillates of the neutral oxygen compounds.

Despite these very intensive processes of condensation of the oxygen compounds, the products still contain unsaturated bonds, the content of which per average molecule is less after oxidation under normal pressure than after oxidation under reduced pressure. This confirms that the formation of primary oxygen compounds takes place without loss of olefin bonds, the number of which decreases as the result of condensation processes.

Nevertheless, we consider that it is wrong to assume that condensation of the molecules takes place mainly at the double bonds. Evidence against this assumption is provided by the lower hydrogen contents in the average molecule of the distilled oxygen compounds formed under vacuum, and their relatively high iodine numbers, and also the low hydroxyl numbers of the neutral compounds.

It seems that condensation of oxygen compounds takes place not only at the unsaturated bonds, but also at the functional oxygen-containing groups and hydrogen atoms; this should be accompanied by some dehydrogenation and dehydration of the molecules. Indirect confirmation for this view is provided by the characteristics of the undistillable neutral oxygen compounds.

TABLE 4

Characteristics of Neutral Distilled Compounds

Characteristic	From olefins oxidized under	
	normal pressure	150 mm Hg
B. p. at 3 mm Hg (°C)	59—150	80—238
Iodine number (gI_2/100 g)	42.5	79
Molecular weight	131	300
Hydroxyl number (mg KOH/g)	123	43
Refractive index (n_D^{20})	1.4450	1.4620
Elementary composition (%):		
C	73.02	77.27
H	13.02	11.49
O	13.96	11.24
Average formula	$C_{8.0}H_{17.1}O_{1.1}$	$C_{19.3}H_{34.4}O_{2.1}$
Olefin bonds in average molecule	0.22	0.93

The undistillable neutral oxygen compounds formed under normal pressure had a hydroxyl number of about 90 mg KOH/g, molecular weight 796, iodine number 38 g I_2/100 g, and refractive index n_D^{20} 1.6389. It follows that even in this complex mixture more than one unsaturated bond was retained per average molecule.

Processes of oxidative degradation probably accompany the processes of oxidative condensation under the conditions used for the oxidation of olefins. This follows from a comparison of the empirical formulas of the average molecules of the original olefin mixture and of the oxidation products. The number of carbon and hydrogen atoms in the average molecules of the distillates of acid and neutral oxygen compounds formed by oxidation under normal pressure is appreciably less than in the molecule of the original hydrocarbons. It must be remembered that the oxidation of normal paraffins to acids under these conditions is also accompanied by degradation with formation of acids of different molecular weights.

SUMMARY

Oxidation of normal monoolefinic hydrocarbons under "acid" conditions, in which normal paraffins yield mainly monobasic fatty acids of different molecular weights, revealed the following facts.

1) Formation of primary oxygen-containing compounds with retention of the unsaturated bonds and degration of the original hydrocarbon molecules proceeds simultaneously with condensation of the oxygen compounds at the unsaturated bonds, functional groups, and hydrogen atoms, yielding complex molecules with a high oxygen content.

2) The yields of tarry compounds, the degree of condensation of the oxygen compounds, and their oxygen contents all increase with increasing weight concentration of oxygen in the reaction zone.

LITERATURE CITED

[1] N. I. Chernozhukov and S. E. Krein, Oxidizability of Mineral Oils (1955).*

[2] W. Kern and H. Willersin, Angew. Chem. 67, 19/20, 573 (1955).

[3] D. Galle, M. A. and C. C. Hall, Fuel 27, 5, 155 (1948).

[4] F. Wittka, Gewinnung der höheren Fettsäuren durch Oxydation der Kohlenwasserstoffe (1941).

[5] F. Fischer and W. Schneider, Gesammelte Abhandlung Zur Kentnis der Kohle, 4, 26 (1919).

[6] I. Gutt and A. Plotko, Azerbaidzh. Neprian. Khoz. 9, 9 (1930).

[7] V. A. Molodovskii and M. B. Neiman, Zhur. Fiz. Khim. 23, 1, 30 (1949).

[8] P. George and A. Robertson, Pr. Roy. Soc. A. 1000-1003, 185, 309, 1 (1946).

[9] A. N. Bashkirov, Khim. Nauka I. Prom. 1, 3, 273 (1956).

[10] A. N. Bashkirov and Ia. B. Chertkov, Izd. AN SSSR, OTN, 8, 817 (1947).

Received September 21, 1956

*In Russian.

SYNTHESIS OF METHYLPENTADIENE BASED ON PROPYLENE

S. I. Kriukov and M. I. Farberov

The Iaroslavl Technological Institute

Methylpentadiene is of definite interest as a monomer for the production of synthetic rubbers. For example, it is known [1] that methylpentadiene polymers, like natural rubber, have a high degree of tackiness and confer tackiness to mixtures of ordinary synthetic rubbers (butadiene–styrene, etc.). There is no doubt that further studies of methylpentadiene polymers and copolymers should reveal their useful properties. However, methylpentadiene is not readily available at present.

The literature contains only one method which may be of industrial importance; this is based on a three-stage conversion of acetone (through diacetone alcohol) [2]. We recently published the description of a process for the production of methylpentadiene, in good yields, from isobutylene and acetaldehyde (through the corresponding alkyl dioxane) [3]. In the present paper another method for the preparation of methylpentadiene, which we consider may be of definite technical interest, is considered. The starting material for this process is propylene.

Ziegler's investigations of the polymerization of olefins in presence of triethylaluminum showed that it is possible to bring about selective dimerization of propylene into a dimer of individual structure – 2-methylpentene-1 [4].

$$\begin{matrix} CH_3{-}CH{=}CH_2 \\ + \\ CH_3{-}CH{=}CH_2 \end{matrix} \xrightarrow{Al(C_2H_5)_3} \begin{matrix} CH_3{-}CH_2{-}CH_2 \\ | \\ CH_3{-}C{=}CH_2 \end{matrix} \qquad (1)$$

This reaction is effected at 200-230° under 100-120 atm. pressure; triethylaluminum serves as a catalyst and is not expended in the process. The yield of dimer is nearly quantitative. The reaction proceeds smoothly and makes the propylene dimer and accessible material for a number of technical syntheses. The dehydrogenation of 2-methylpentene-1 to methylpentadiene is considered in this paper.

Thermodynamic Calculations

The free energies of formation of methylpentadiene are not given in the literature, and the values were therefore determined by calculation. Two independent calculation methods were used: a) from the structural groups (Franklin's method) [5], and from molecular structure data [6].

The first method consists of summation of the values for the different structural groups ($-CH_3$; $=C=CH_2$; $-CH_2$ etc.) in the molecule of the compound. This sum gives the free energy of formation (ΔZ°_T) of the given compound in the ideal gaseous state.

In the second method the thermodynamic and thermal properties of compounds (ΔH°_{298}, ΔS°_{298}, and the coefficients for the C_p equation) in the ideal gaseous state are found by summation of the numerical values of these properties for methane, with additions to allow for the replacement of its hydrogen atoms by other groups and for the substitution of double for single bonds.

As a check, the free energies of formation of 2-methylpentene-1 were calculated by both these methods.

The results were compared with published values of the free energies of formation for this olefin [7] (Table 1).

TABLE 1

Values of Free Energies of Formation of 2-Methylpentene-1, Calculated by Franklin's Method, the Molecular-Structure Method, and Taken from the Literature

Calculated by	Free energies (in cal/mole) at temperatures				
	327° C (600° K)	427° C (700° K)	527° C (800° K)	627° C (900° K)	727° C (1000° K)
Franklin's method	52300	64000	76090	88120	100200
Molecular-structure method	50870	62900	75200	87700	101500
Literature data	51100	62700	74500	86400	98300

It is seen that the two calculation methods give results in good agreement with each other and with literature data. This justified the use of these methods for calculation of the free energy of formation of methylpentadiene.

Dehydrogenation of 2-methylpentene-1 (I) can lead to the formation of three methylpentadiene isomers – 2-methylpentadiene-1,3 (II) in the cis and trans forms, and 4-methylpentadiene-1,3 (III).

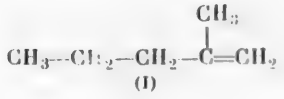

(I)

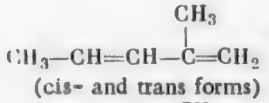

(II)

(cis- and trans forms)

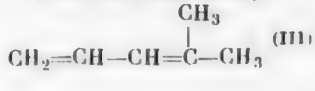

(III)

Table 2 gives the free energies of formation, in the 327-727°C range, of the different isomeric methylpentadienes, calculated by Franklin's method.

Table 3 gives the changes of free energy in the dehydrogenation of 2-methylpentene-1 to methylpentadienes, calculated from the equation: $\Delta Z_{reaction} = \Sigma \Delta Z^{\circ}_{products} - \Sigma \Delta Z^{\circ}_{init.subs.}$ for the 327-727°C range, and the corresponding equilibrium constants (K) calculated from the isotherm $\Delta Z = -RT\ln K$.

The over-all equilibrium constant for the reaction of dehydrogenation of 2-methylpentene-1 is the sum of the individual constants:

$$K = K_1 + K_2 + K_3,$$

where K is the over-all equilibrium constant for the dehydrogenation reaction, and K_1, K_2, and K_3 are the equilibrium constants for the individual isomers.

The equilibrium constants calculated in this way could be used for determination of the degree of conversion of 2-methylpentene-1 at different temperatures in the 327-727°C range, and at different dilutions with an inert diluent (steam), with the aid of the equation

$$\frac{\alpha^2}{1-\alpha} = K_p(1 + \alpha + w),$$

where α is the degree of conversion, K is the over-all equilibrium constant, and w is the number of moles of diluent per mole of the starting substance.

TABLE 2

Free Energies of Formation of Isomeric Methylpentadienes, Calculated by Franklin's Method

Compounds (gaseous)	Free energies (in cal/mole) at temperature				
	327° C (600° K)	427° C (700° K)	527° C (800° K)	627° C (900° K)	727° C (1000° K)
2-Methylpentadiene-1,3 (cis)	62900	71400	80500	89500	98500
2-Methylpentadiene-1,3 (trans)	62200	71000	79800	88800	97800
4-Methylpentadiene-1,3	61300	71100	79900	87900	97900

TABLE 3

Variations of the Change of Free Energy and the Equilibrium Constant for the Reaction of Dehydrogenation of 2-Methylpentene-1 to Isomeric Methylpentadienes

Temperature		$\Delta Z_{reaction}$ (cal/mole)			K (atm)		
°C	°K	2-methyl-pentadi-ene-1,3 (cis)	2-methyl-pentadi-ene-1,3 (trans)	4-methyl-pentadi-ene-1,3	2-methyl-pentadi-ene-1,3 (cis)	2-methyl-pentadi-ene-1,3 (trans)	4-methyl-pentadiene-1,3
327	600	10680	9980	10890	0.00013	0.00023	0.00049
427	700	7570	6910	8700	0.00437	0.00684	0.00646
527	800	4510	3830	5540	0.058	0.09	0.086
627	900	1440	730	1310	0.445	0.665	0.29
727	1000	—1630	—2360	—900	2.282	3.295	3.14

This equation is a transformed version of the chemical equilibrium equation for dehydrogenation in presence of an inert diluent [8]. The calculated data are presented graphically in Fig. 1.

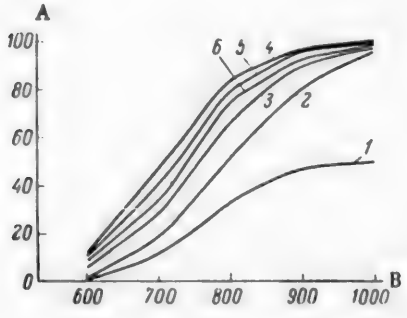

Fig. 1. Conversion of 2-methylpentene-1 into methylpentadienes with and without dilution with steam. A) Conversion (%), B) temperature (°K). Dilution: 1) no diluent, 2) 1:1, 3) 1:4, 4) 1:8, 5) 1:12, 6) 1:16.

EXPERIMENTAL*

Apparatus and method. The dehydrogenation of methylpentene was performed in a laboratory contact apparatus by the method described earlier in one of the papers published by our laboratory [8]. 40 cc of the catalyst (in the form of turnings, 1.5-2 mm in diameter and 4-5 mm long) was placed in a quartz tube 20 mm in diameter and 100 mm long. The duration of each experiment was 1 hour. After every experiment the catalyst was regenerated by means of air-steam mixture.

2-Methylpentene-1, prepared by Ziegler's method, had the following constants: b. p. (760 mm) 60.5-62.5° d_4^{20} 0.6813, n_D^{20} 1.3920. The literature values are [9]: b. p. 61.5-62.0, d_4^{20} 0.6817, n_D^{20} 1.3921.

*M. Iu. Tikhvinskaia took part in the experimental work.

Catalysts. Three types of industrial catalysts used for dehydrogenation of hydrocarbons were tested: K-12, K-16, and K-18.

The space velocity (SV) was expressed as ml of methylpentene passed through 1 liter of catalyst per hour (ml/liter of catalyst·hour).

Dilution of methylpentene by steam was effected in the following molar ratios: 1:4, 1:8, 1:12, 1:16 (mole).

The yield of catalyzate was determined as the ratio of the weight of dewatered catalyzate to the weight of methylpentene passed.

The yields of the desired products in experiments on the influence of individual factors on dehydrogenation were found from the amounts of dienes obtained, calculated on the amount of methylpentene passed and decomposed. The amount of unreacted methylpentene was found from the difference between the amount of catalyzate (distilled up to 85°) and the amount of dienes found in it. In experiments for determination of the balance, these yields were calculated from the amount of methylpentadiene found in the 40-85° catalyzate fraction.

Method of analysis of the reaction products. The contact gas was analyzed in the Orsat-Jäger apparatus for carbon dioxide (in KOH solution), isobutylene together with isoprene (in 68% H_2SO_4 solution), propylene and butylenes (in 84% H_2SO_4 solution), and ethylene (in mercury sulfate solution in 20% H_2SO_4). In some experiments the contents of hydrogen and saturated hydrocarbons were determined by fractional combustion over copper oxide. In addition, the diene content of the gas in each experiment was determined (by absorption in maleic anhydride in Bushmarin's apparatus) [10]; the dienes in the gas were reckoned as isoprene. The catalyzate distilled up to 85° was analyzed for the diene content (reckoned as methylpentadiene) by the reaction with maleic anhydride in sealed tubes.

Influence of Individual Factors on the Dehydrogenation of 2-Methylpentene-1 to Methylpentadiene

In the experimental data summarized in Table 4 each value is the average result of from 3-4 experiments.

TABLE 4

Effects of Temperature, Space Velocity, and Dilution on the Dehydrogenation of Methylpentene to Methylpentadiene over K-16 Catalyst

Temperature (°C)	Dilution with steam (molar)	Space velocity (ml/liter catalyst·hour)	Yield (molar %)		Yield of catalyzate (wt. %)
			methylpentene passed	methylpentene decomposed	
475	1:12	600	25.1	78.1	95.4
500	1:12	600	38.6	70.0	81.5
525	1:12	600	34.6	59.5	72.0
550	1:12	600	33.4	52.4	66.8
575	1:12	600	22.1	40.0	57.8
500	1:8	400	35.5	62.3	73.0
500	1:8	600	36.7	65.0	75.6
500	1:8	800	36.0	66.8	78.4
500	1:8	1000	35.7	68.3	79.3
500	1:4	600	33.2	60.7	69.2
500	1:8	600	36.7	65.0	75.6
500	1:12	600	38.6	70.0	81.5
500	1:16	600	40.7	71.9	83.1

Selection of catalyst. The determining condition in the selection of the catalyst was the yield of diene hydrocarbons as a function of the temperature, under otherwise equal conditions (SV = 400 ml/liter catalyst·hour, dilution 1:8). It was found that K-16 catalyst (which consists of the oxides of zinc, chromium, and iron)

has definite advantages with regard to activity and selectivity. K-16 catalyst was used for the subsequent investigations of the influence of the main process factors (see Table 4).

The temperature is the most important factor influencing the yield of the required product. The optimum temperature appears to be 500°. Increase of temperature results in a sharp decrease of the yield calculated on the methylpentene passed, and especially on the decomposed methylpentene, evidently because of side reactions. A decrease of the temperature to 475° increases the yield calculated on the decomposed material, but results in a considerable decrease of the yield on the methylpentene passed. Variations of the space velocity have relatively little effect on the yield. The influence of dilution with steam is more significant; the yields both on the passed and on the decomposed methylpentene increase appreciably. This is probably the result of the influence of kinetic rather than thermodynamic factors; the rate of polymerization of the diene, and of other side reactions, decreases considerably with decrease of its partial pressure.

An attempt was made to determine the quantitative relationship between the temperature and the reaction rate. To exclude side reactions, the kinetic studies of the dehydrogenation process were performed at low temperatures, when the relative significance of the side reactions is slight. The experiments were carried out at 350, 375, and 400°, at space velocities 200-800 ml/liter catalyst·hour, with 1:12 dilution with steam. The contact time was determined from the formula:

$$\tau = \frac{v_c \cdot 273}{v_g \cdot T},$$

where τ is the contact time (seconds), v_c is the volume of catalyst (ml), T is the absolute temperature of the reaction, and v_g is the volume of gases (methylpentene + water) entering the contact zone (in ml/second).

The results of these experiments are plotted in Fig. 2.

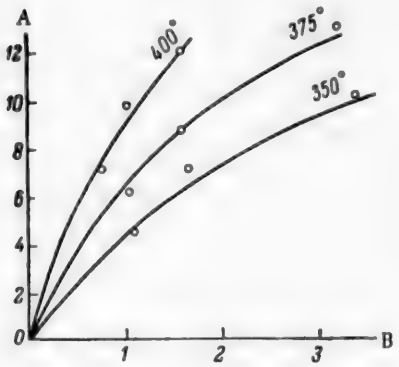

Fig. 2. Effects of temperature and contact time on the yield of methylpentene at 350-375-400°. A) Yield of methylpentene (%), B) contact time (seconds).

The curves in Fig. 2 were used for calculation, for constant degrees of conversion of methylpentene (5, 6, 7 and 8%), of the apparent energy of activation, from the Arrhenius equation, the ratio of the rate constants being replaced by the inverse ratio of the contact times (for the same degree of conversion $\frac{K_2}{K_1} = \frac{\tau_1}{\tau_2}$):

$$E = \frac{4.575 \log \frac{\tau_1}{\tau_2} \cdot T_1 \cdot T_2}{T_2 - T_1}$$

The average value of the activation energy is about 17,800 cal/mole.

On the assumption that the activation energy retains the same value at 500°, the temperature coefficient of the reaction near this temperature can be calculated; it is found to be 1.15.

Material-balance experiment. The results of a typical balance experiment, performed under the optimum conditions for the process, are given in Table 5. It was assumed in compilation of the material balance that all the ethylene and propylene are formed as the result of cracking of methylpentene: into isobutylene and ethylene in the former case, and into two molecules of propylene in the latter. The amount of carbon on the catalyst was found from the total carbon dioxide in the contact gas and in the regeneration gas.

Characterization and Identification of the Reaction Products, and the General Conversion Scheme

For characterization and identification of the reaction products, the dehydrogenation condensate from one

of the typical balance experiments was fractionated through a precision laboratory column of 60 theoretical plates. The distillation curve is given in Fig. 3.

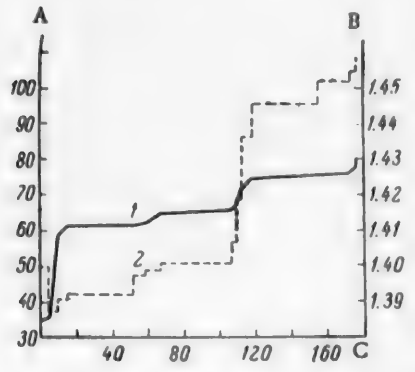

Fig. 3. Fractionation of the condensate after dehydrogenation of 2-methylpentene-1. A) Temperature (°C), B) value of n_D^{20}, C) volume distilled (ml). 1) Temperature, 2) value of n_D^{20}.

The 75-77.2° fraction was characterized as a mixture of methylpentadiene isomers, and had the following constants: d_4^{20} 0.7224, n_D^{20} 1.4467, MR_D 30.307, calc. 30.07. Literature data: for 2-methylpentadiene-1,3 [11] – b. p. (760 mm) 75-76°, d_4^{24} 0.7215, n_D^{20} 1.4418; for 4-methylpentadiene-1,3 [11] – b. p. (760 mm) 76-77°, d_4^{24} 0.7204, n_D^{20} 1.4472. Hydrogen number (found) + 538 ml of hydrogen under normal conditions, per g of substance; calculated for C_6H_{10}, 540 ml.

The quantitative determination of methylpentadiene isomers in the mixture was based on differences in their behavior with maleic anhydride [12]: 2-methylpentadiene-1,3 (II) forms an addition compound, whereas 4-methylpentadiene-1,3 (III) forms a copolymer; in presence of inhibitors the tendency of (III) to polymerization is suppressed, and it can be separated from (II). This determination was performed by the method described earlier [10], with certain modifications: a small sealed ampoule with an exact amount (0.5-0.7 g) of methylpentadiene with an addition of hydroquinone was introduced into a large cooled ampoule containing a weighed quantity of maleic anhydride in 5-7 ml of toluene, and the smaller ampoule was broken. After three days at room temperature the large ampoule was opened, and toluene and unreacted (III) were drawn off (under vacuum) to constant weight. The m. p. of the addition compound of (II) with maleic anhydride was 57.9-58.9°; the literature value [12] is 57°.

The amounts of the (II) and (III) isomers were in the ratio 55 : 45, which is close to the ratio of the methylpentadiene isomers found by us by another method – by means of isobutylene and acetaldehyde [3]. This is evidently the ratio which becomes established between the methylpentene isomers during the dehydrogenation.

TABLE 5

Results of a Material-Balance Experiment on the Dehydrogenation of 2-Methylpentene-1 to Methylpentadiene. (Temperature 500°; space velocity 600 ml/liter catalyst·hour); molar dilution with steam 1 : 12; 65.2 g of 2-methylpentene passed.

Reaction products	Amounts of product		Yield (molar %) calculated	
	by weight (g) on the dimer consumed	dimer (moles)	amount passed	amount decomposed
Methylpentadiene	24.152	0.288	37.0	71.8
Isoprene	1.16	0.0138	1.77	3.4
Isobutylene	2.21	0.0263	3.38	6.4
Propylene	0.88	0.0105	1.34	2.3
Returned methylpentene	31.26	0.373	—	—
Carbon on catalyst	2.1	0.025	3.22	6.00
Higher hydrocarbons	0.93	0.0110	1.42	2.6
Losses	2.508	0.0307	3.95	7.6
Total	65.2	0.778	—	100.0

The 61.0-62.5° fraction with n_D^{20} 1.3935 is unreacted 2-methylpentene-1.

The 65.5-67.5° fraction was characterized as 2-methylpentene-2, $CH_3-CH_2-CH=C(CH_3)-CH_3$. This compound was evidently formed as the result of partial isomerization of 2-methylpentene-1 with migration of the double bond. The two isomers are found in roughly equal quantities in the return methylpentene. The product was redistilled, and had the following constants: b. p. (760 mm) 67.0-67.5°, d_4^{20} 0.6898, n_D^{20} 1.4008. Literature data [9]: b. p. (760 mm): 67.25-67.5°, d_4^{20} 0.6904, n_D^{20} 1.405.

This type of isomerization with migration of the double bond within the molecule is common, and is attributed to the mobility of the hydrogen atom in the β position relative to the double bond. According to Rice and Rice [13] the reason is that the strength of the C−H bond in the β position is at least 6 kcal. less than that of a primary C−H bond in paraffinic hydrocarbons.

Therefore the principal reactions in the contact conversion of 2-methylpentene-1 under dehydrogenation conditions can be represented by the following scheme:

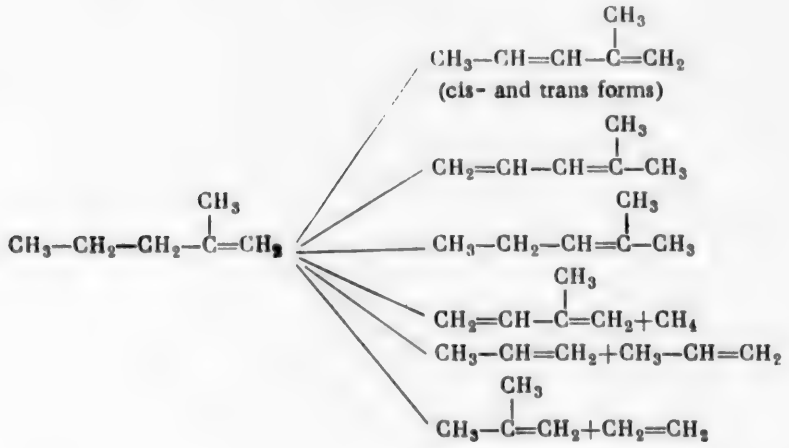

SUMMARY

1. The synthesis of methylpentadiene from propylene was effected in two stages: a) dimerization of propylene to 2-methylpentene-1 in presence of triethylaluminum, and b) dehydration of the resultant dimer to methylpentadiene.

2. The degree of conversion of the starting material under different conditions was determined from thermodynamic calculation data for the dehydrogenation of 2-methylpentene-1 to methylpentadiene over a wide range of temperatures and dilutions with steam.

3. A catalyst was selected, and the influence of individual factors (temperature, space velocity, dilution with steam) on the dehydrogenation process was determined; the optimum process conditions were found from the results.

4. A material-balance experiment was performed under the chosen optimum dehydrogenation conditions; it was found that methylpentadiene can be obtained in yields of over 70%, calculated on the methylpentene decomposed.

5. Two methylpentadiene isomers are formed as the result of dehydrogenation. In addition, the original 2-methylpentene-1 is isomerized into 2-methylpentene-2 with migration of the double bond.

LITERATURE CITED

[1] F. M. McMillan, E. T. Bishop, K. E. Marple and T. W. Evans, India Rub. World, February (1946).

[2] H. G. Staaterman, R. C. Morris, R. M. Stager and G. J. Pierotti, Chem. Eng. Progr. 43, 148 (1947).

[3] M. I. Farberov, K. A. Machtina and S. I. Kriukov, Proc. Acad. Sci. USSR 114, 807 (1957);* M. I. Farberov and K. A. Machtina, Sci. Mem. Iaroslavl Tech. Inst. 2 (1957).

[4] K. Ziegler, Angew. Chem. 64, 323 (1952).

[5] J. L. Franklin, Ind. Eng. Chem. 41, 1070 (1949).

[6] O. A. Hougen, and K. M. Watson, Chemical Process Principles, II (New York, 1948) pp. 758.

[7] M. D. Tilicheev (Editor), Physicochemical Properties of Individual Hydrocarbons, 3 (State Fuel Tech. Press, 1953).**

[8] A. V. Bondarenko, M. I. Bogdanov and M. I. Farberov, J. Appl. Chem. 30, 927 (1957).*

[9] I. M. Heilbron and H. M. Bunbury, Dictionary of Organic Compounds 2, (Russian translation) (1949).

[10] A. I. Guliaeva, V. P. Polikarpova and Z. K. Remiz, Analysis of Intermediates in the Production of Divinyl and Ethyl Alcohol by the Lebedev Process (Goskhimizdat, 1952).**

[11] G. S. Whitby and W. Gallay, Canad. J. Res. 6, 282 (1932).

[12] G. Bachman and G. Hoebel, J. Am. Chem. Soc. 64, 787 (1942).

[13] F. O. Rice and K. K. Rice, Aliphatic Free Radicals (Russian translation) (ONTI, Chem. Theoret. 1937) p. 112.

Received May 13, 1957

*Original Russian pagination. See C. B. Translation.

**In Russian.

DECOMPOSITION OF NITROGLYCERIN AT HIGH TEMPERATURES

K. K. Andreev

The D. I. Mendeleev Institute of Chemical Technology, Moscow

Nitroglycerin, like other nitrate esters of polyhydric alcohols, belongs to the class of explosive substances with relatively high rates of thermal decomposition. Another of its characteristics also common to many nitrate esters, is the very great autoacceleration of the decomposition which takes place under certain conditions. This autoacceleration may lead to explosion, even at relatively moderate temperatures and charge sizes. The decomposition can also be accelerated considerably by water dissolved in the ester, probably as the result of its hydrolytic action.

Certain observations made in a study of the decomposition of nitroglycerin, and brief comments on nitroglycol and nitrocellulose, are presented in this paper.

The thermal decomposition of nitroglycerin is described in two important papers: by Robertson [1], and by Roginskii et al., [2]. Their main results were the following.

When liquid nitroglycerin decomposes in a current of inert gas (CO_2) in the 90-135° range, nitrogen is split off at a constant rate and entirely in the form of NO_2, at least at the start of the decomposition. The rate of this removal increases rapidly with temperature. For the 90-125° range the relationship between the rate constant and the reciprocal temperature can be represented by the Arrhenius equation.

$$K = 10^{18.6} e^{-\frac{43700}{RT}}$$

If liquid nitroglycerin decomposes in a confined space without removal of the gaseous products, the nature of the $p = f(\tau)$ curve depends to a great extent on the ratio of the mass of nitroglycerin m to the volume of the vessel v, and also on the temperature. At low values of m/v and relatively high temperatures the decomposition proceeds at a rate which decreases with time according to a law close to the first-order reaction law. At high values of m/v and relatively low temperatures the decomposition accelerates sharply. The "monomolecular" decomposition of nitroglycerin is characterized by a strong dependence of the reaction rate on the temperature; this leads to high values of the activation energy and of the preexponential term (according to Roginskii, at 150-190° $K = 10^{23.5} e^{-\frac{50000}{RT}}$)

In investigations performed in our laboratory (by Bespalov, Glazkova, Maurina, and Svetlov [3]) the thermal decomposition of nitroglycerin was studied with the aid of a Bourdon-type gage, by the amount of gas formation under different conditions which have a significant influence on the course of the process.

EXPERIMENTAL

Decomposition of nitroglycerin in the vapor phase. With low values of m/v it is possible to decompose nitroglycerin in the vapor phase. Under these conditions, the rate of gas formation decreases with time, according to an approximately monomolecular law over a considerable part of the decomposition process (Fig. 1), but the reaction constant fluctuates considerably from experiment to experiment. The contents of the vessel become

yellow as the decomposition proceeds. The relative rate of gas formation is not altered if the initial vapor pressure is doubled ($m/v = 0.44 \cdot 10^{-4}$ g/cc and $1.05 \cdot 10^{-4}$ g/cc). The "half life" at 150° is about 25 minutes.

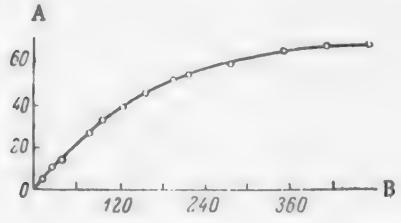

Fig. 1. Decomposition of nitroglycerin in the vapor phase at 140°; $m/v = 0.44 \cdot 10^{-4}$ g/cc. A) Pressure (mm Hg), B) time τ (minutes).

In experiments in vessels packed with glass tubing the rate of gas formation was higher; i.e., a heterogeneous reaction took place at the glass surface, at a rate of the same order as that of the homogeneous reaction in the gas volume. The final gas volume was lower in experiments with packed vessels than in the homogeneous reaction.

Decomposition of liquid nitroglycerin at low pressures of the gaseous decomposition products. These conditions are obtained if the decomposition is performed at low values of m/v, or at high values of m/v but at the initial stages of the decomposition.

Gas is then formed at a slowly increasing rate (not only relatively, but absolutely) (Fig. 2), close to the rate observed in Robertson's experiments, where the decomposition products were removed in a current of inert gas. The effect of temperature on the rate is also similar. These results lead to the conclusion that at the first stage of the reaction the decomposition products do not have an accelerating effect. No such effect was found even if the nitroglycerin was first partially decomposed at a higher temperature (140°, $m/v = 10 \cdot 10^{-4}$ g/cc, τ = 24 minutes) until the pressure of the decomposition products reached 47 mm, and then decomposed at 99° for 100 hours.

The rate of gas formation at the initial stage decreases somewhat with increase of m/v. The maximum rate attained in conditions of slow rate increase does not depend to any significant extent on m/v, but appears to diminish with increase of the latter.

In the case of liquid nitroglycerin the rate of gas formation, even at the maximum, is considerably lower (several-fold at 140-150°) than the rate observed for the vapor-phase decomposition of nitroglycerin.

The combination of all these results suggests that the decomposition of nitroglycerin, even under conditions in which the rate of gas formation does not increase, should be regarded as a complex reaction, consisting of at least two consecutive macroscopic stages [4], each of which may include several elementary reactions.

The first of these stages is characterized by the formation and accumulation of nitrogen dioxide, which is reduced in the second stage.

Another argument against regarding this decomposition as a simple monomolecular reaction is provided by the high temperature coefficient of the reaction rate, which leads to anomalously high values, for nitrate esters, of the activation energy E and the factor B in the rate-constant equation $K = Be^{-E/RT}$. Further evidence is provided by deviations of the gas formation from the equation for a first-order reaction, especially for decomposition in the liquid state. It is also found that the nitrogen content of the liquid decreases during the decomposition, probably as the result of the formation of an intermediate condensed product, which is in harmony with the accumulation of nitrogen dioxide in the gas at the start of the decomposition.

Indirect confirmation of the complex nature of the decomposition of nitroglycerin is found in studies of the decomposition of the nitrates of the simplest monohydric alcohols, which was established to be stepwise in character [5]; the course of the $p = f(\tau)$ curves (Fig. 3) for the decomposition of glycol dinitrate, and especially of glycol dinitrite (as determined by B. N. Kondrikov) also clearly represents a complex reaction with macroscopic stages separated in time. This gives all the more reason to expect a complex reaction in the decomposition of nitroglycerin – the trinitrate of a trihydric alcohol.

The decomposition characteristics considered above relate to comparatively high temperatures (80° and over). If we assume that the relationship established between the decomposition rate and the temperature is applicable at lower temperatures, down to the usual storage temperatures, we can calculate, from Robertson's data for example, the corresponding decomposition rates.

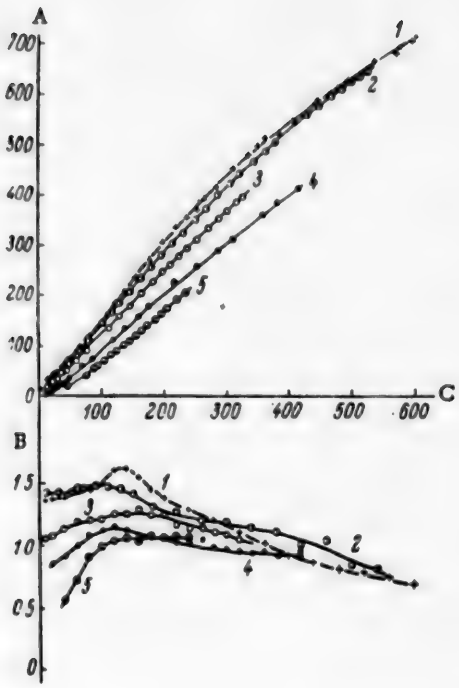

Fig. 2. Decomposition of liquid nitroglycerin at 140° and at different values of m/v. A) Pressure $\frac{pv}{m}$ ($\frac{mm \cdot cc}{g} \cdot 10^{-3}$), B) rate of gas formation $\frac{\Delta p}{\Delta \tau}$ ($\frac{mm \cdot cc}{g \cdot min} \cdot 10^{-3}$), C) time τ (min.). Values of m/v ($\frac{g}{cc} \cdot 10^{-4}$): 1) 5.0, 2) 9.8, 3) 18.9, 4) 18.6 5) 47.0.

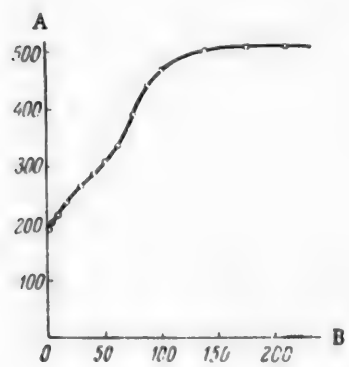

Fig. 3. Variation of pressure during the decomposition of glycol dinitrite in the vapor phase. Temperature 170°, m/v = $30 \cdot 10^{-4}$ g/cc. A) Gas formation V (cc/g), B) time τ (minutes).

These rates are found to be so low (for example, at 20° K = 10^{-14} sec^{-1}, and the time required for the decomposition of 1% of the substance is over 30,000 years) that they cannot in themselves be of any practical importance.

Decomposition of liquid triglycerin under considerable pressures of the gaseous decomposition products. The slow increase of the rate of gas formation, when the increase of the rate is approximately proportional to $p^{1/2}$, is observed only until the pressure of the gaseous products over the nitroglycerin reaches a certain critical value. After this the rate of gas formation begins to increase much more rapidly (approximately in proportion to p^2), and may reach very high values, hundreds and thousands of times the initial value (Figs. 4 and 5). The composition of the gaseous products also changes, as is shown by the sharp intensification of their brown color (NO_2) and by the great increase of gases condensing at room temperature.

It follows from Fig. 5, in which only a part of the experimental data is shown, that over a considerable range of m/v (23-1120 · 10^{-4} g/cc) the rate of gas formation alters sharply at almost the same pressure (180-200 mm) although the times required to reach this pressure differ greatly. It is seen that whereas before the critical pressure is reached the rate of gas formation depends somewhat on the value of m/v, generally decreasing with increase of the latter, at pressures above the critical the rates for a given pressure of the decomposition products are almost equal, irrespective of the value of m/v. Only if the values of m/v are very large, i.e., if the pressure increase rapidly with time, in other words, if the induction period is short, does the critical pressure increase; it is 800-900 mm when m/v is close to the maximum possible value. Therefore the critical pressure depends to some extent on the degree of decomposition; the gases are somewhat more effective at the later stages than at the start of decomposition. This is probably associated with changes in the composition of the gases, and in particular with their enrichment with water. The critical pressure increases with increase of the temperature. The causes of the sharp change in the rate of gas formation when a definite pressure of the gaseous decomposition products is reached, i.e., at a definite concentration of these products in the liquid phase, are not quite clear, but are undoubtedly worthy of attention.

Since the rapid acceleration of decomposition occurs at a definite pressure, the time required to reach it naturally depends on m/v, decreasing with increase of the latter. At the maximum possible value of m/v close to the density, a sharp acceleration of gas

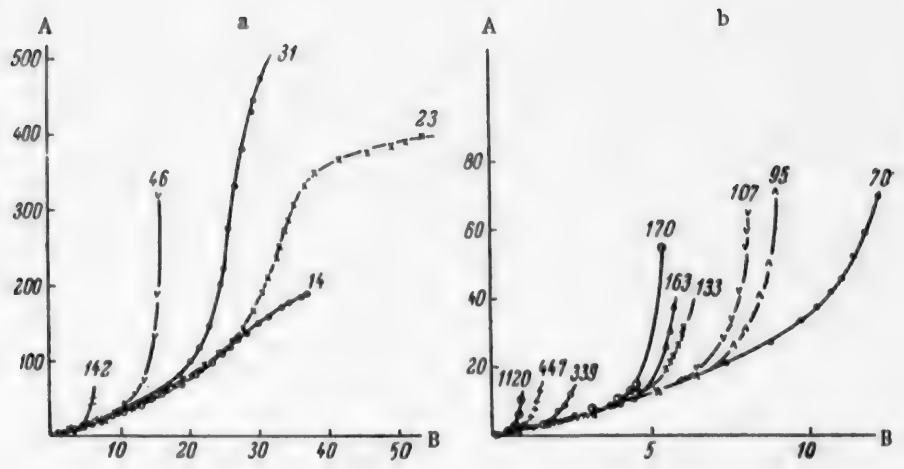

Fig. 4. Decomposition of nitroglycerin at 100°, with different values of m/v. A) Gas formation V (cc/g), B) time τ (min·10^{-3}). Values of m/v: a) small and moderate; b) large; the numbers on the curves represent values of m/v (in $\frac{g}{cc}\cdot 10^{-4}$).

formation begins at 100° after about 6 hours, which corresponds to a low degree of decomposition – the formation of 1 cc of gas* per 1 g of substance.

At 100° and moderate values of m/v, the time before the acceleration begins is approximately in inverse proportion to m/v. When m/v = $107\cdot10^{-4}$ g/cc, the time is 6600 minutes. At very low values of m/v the stage of rapid acceleration is not reached at all.

Thus, if the decomposition conditions are such that the gaseous decomposition products can accumulate in the liquid in considerable concentrations, rapidly self-accelerating decomposition of nitroglycerin begins. Under such conditions the length of the induction period can really serve as a measure of stability, as after the end of that period the maximum rate is reached relatively very quickly.

The induction period increases with fall of temperature. Thus, at 100° and m/v = $500\cdot10^{-4}$ g/cc the induction period is 1500 minutes, and at 80° and the same value of m/v it is 11,000 minutes. The relationship between the length of the induction period and the temperature is in general complex, as it involves the effects of temperature not only on the reaction rates but also on the solubility of the gaseous reaction products in nitroglycerin.

Decomposition of liquid nitroglycerin in presence of water and acids. The results presented above refer to nitroglycerin which had been thoroughly purified by evacuation to remove volatile impurities, including water. When this nitroglycerin was heated to 100° at moderate values of m/v, the initial pressure of the volatile impurities did not exceed 1 mm.

Nitroglycerin prepared by the usual method contains some dissolved water. The manometric curve obtained in the decomposition of such nitroglycerin is different in character (Fig. 6). It is particularly significant that the length of the region before rapid acceleration begins is much less.

Thus, whereas at 100° and m/v = $500\cdot10^{-4}$ g/cc the time required to reach a high rate of gas formation is 40 hours for dry nitroglycerin, if the water-vapor pressure over the nitroglycerin is about 300 mm the time decreases to 3-4 hours.

*Based on the results of experiments at low values of m/v, on the assumption that the initial rate of decomposition of the liquid is independent of m/v.

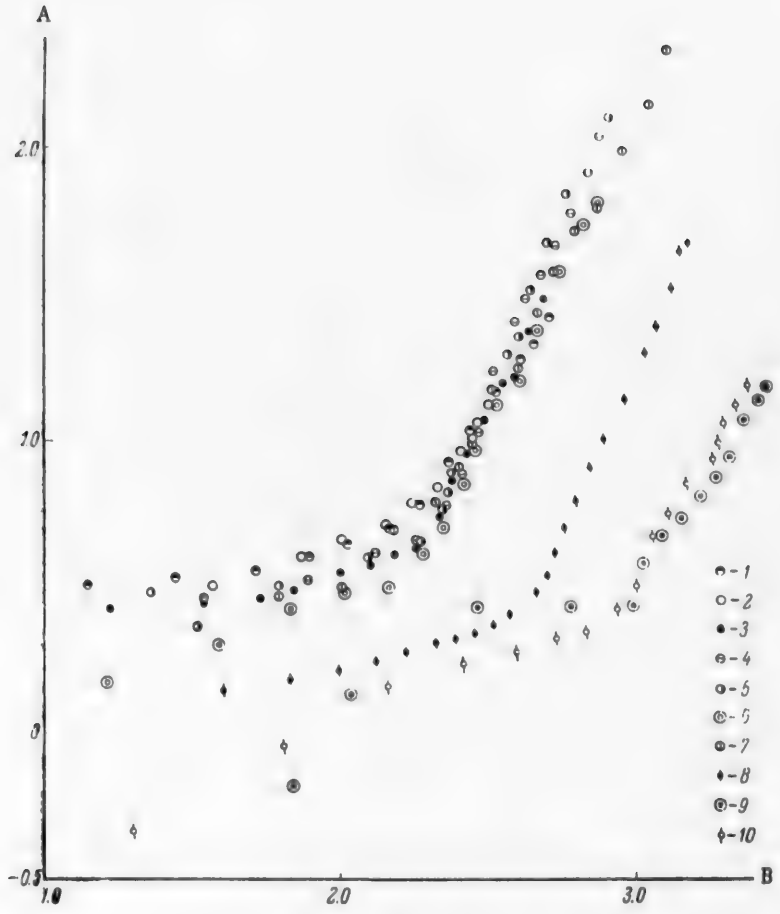

Fig. 5. Variation of the rate of gas formation with the pressure in the decomposition of nitroglycerin at 100° and at different values of m/v. A) Rate of gas formation $\log \frac{\Delta v}{\Delta \tau} \cdot 10^{-3}$ (in cc/g·min), B) log p mm Hg). Values of m/v ($\frac{g}{cc} \cdot 10^{-4}$) and induction period τ (minutes) respectively: 1) 23 and 20,000; 2) 31 and 10,500; 3) 70 and 8000; 4) 142 and 3800; 5) 155 and 3600; 6) 634 and 1100; 7) 1120 and 550; 8) 4780 and 580; 9) 13,700 and 370; 10) 14,500 and 360.

The nature of the $p = f(\tau)$ curves, and the time before rapid acceleration is reached, in presence of water depends on the water-vapor pressure and the value of m/v. As the pressure increases, the $p = f(\tau)$ curve shows an increasingly pronounced dip; the decrease and subsequent increase of the pressure become progressively sharper (Fig. 7). At moderate values of $m/v \approx 100 \cdot 10^{-4}$ g/cc and higher pressures of water vapor (above 500 mm) its effect becomes less pronounced. At low values of m/v the presence of a considerable amount of water even diminishes the acceleration of gas formation.

The effects of nitric and sulfuric acid on the decomposition of nitroglycerin were also studied. Addition of nitric acid to dry nitroglycerin accelerates gas formation and shortens the time before the sharp autoacceleration of the reaction begins. However, this effect is weaker than might have been expected. Thus, at $m/v = 100 \cdot 10^{-4}$ g/cc in presence of 1% nitric acid (the vapor pressure of nitric acid over the nitroglycerin at 100° was 63 mm) acceleration of gas formation began after 14 hours, whereas under the same conditions but in

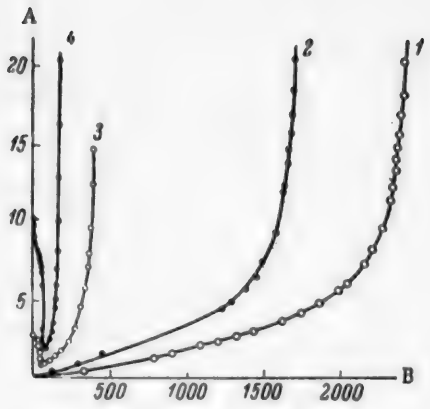

Fig. 6. Decomposition of nitroglycerin (m/v≈ $500 \cdot 10^{-4}$ g/cc) at 100° in presence of water vapor. A) Gas formation V (in cc/g), B) time τ (minutes). Pressure of water vapor at 100° (in mm Hg): 1) 0, 2) 8, 3) 158, 4) 526.

absence of acid the decomposition of nitroglycerin began to accelerate sharply after 90 hours. Sulfuric acid has a stronger accelerating effect than nitric, which may be to some extent due to its lower volatility. Little can be said as yet about the mechanism of the influence of water on the decomposition of nitroglycerin and about the physical meaning of the $p = f(\tau)$ curve in the presence of water. It seems reasonable to assume that the action of water is hydrolytic and that the reaction is autocatalytic, since it gives rise to acids* which accelerate hydrolysis. There is no doubt, however, that the matter does not end in hydrolysis, but an exothermic oxidation–reduction begins between the hydrolysis products, which may lead to thermal explosion.

It has not yet been established which is the determining reaction in the decomposition of nitroglycerin in presence of water.

Two possibilities may be considered. 1) The same reaction takes place in presence of water as in its absence. This reaction gives rise to NO_2, which forms acid with water. In presence of acid which catalyzes the hydrolysis, water induces a rapid and self-accelerating hydrolytic reaction. 2) If the rate of hydrolysis, even of neutral nitroglycerin, is considerably greater than the rate of decomposition in absence of water, then hydrolysis, i.e., water, is the source of the acid, and therefore the cause of the acceleration of decomposition.

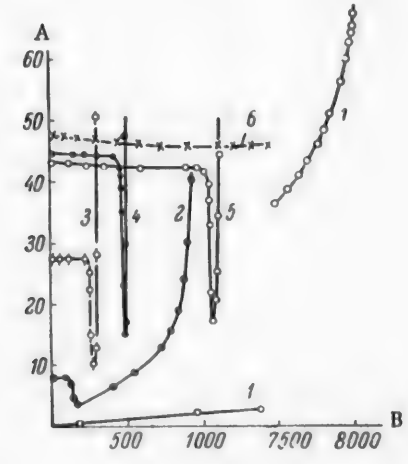

Fig. 7. Decomposition of nitroglycerin (m/v≈ $100 \cdot 10^{-4}$ g/cc) in presence of water vapor at 100°. A) Gas formation V (in cc/g), B) time τ (minutes). Pressure of water vapor at 100° (in mm Hg): 1) 0, 2) 116, 3) 328, 4) 447, 5) 467, 6) 471.

If the second alternative is correct – and the few available experimental facts are in its favor – then the stability of nitroglycerin made by the usual process is determined not so much by the characteristics of the thermal decomposition of anhydrous nitroglycerin, as by its water content and the hydrolytic action of the latter.

It was shown earlier that acceleration of the decomposition of nitroglycerin takes place even if the latter did not initially contain water. It seems that water is formed during the decomposition, but a considerable time is required. The great importance of water in this case is indicated by the results of experiments on the decomposition of nitroglycerin, with a bulb containing phosphorus pentoxide sealed to the vessel. This caused a sharp retardation of gas formation.**

The suggestion that the rapid acceleration of the decomposition of nitroglycerin is caused by the combined action of water and acid may be confirmed by direct experiments with addition of these substances to nitroglycerin.

* Nitroglycerin decomposed in presence of water has considerable acidity when the pressure has fallen to the minimum.

** It must be noted, however, that phosphorus pentoxide absorbs nitrogen dioxide as well as water.

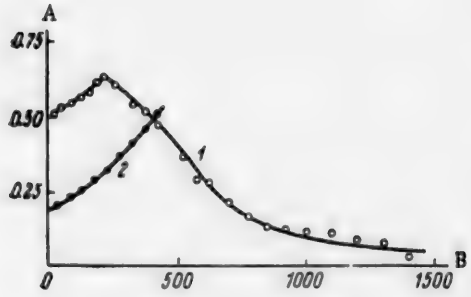

Fig. 8. Rate of decomposition of nitroglycerin at 140° in the vapor and liquid states. A) Decomposition rate $\frac{\Delta v}{\Delta \tau}$ (cc/g·min), B) time τ (minutes). Values of m/v (in g/cc): 1) $4.1 \cdot 10^{-4}$, 2) $46 \cdot 10^{-4}$

The induction period becomes much shorter as a result. Thus, if the nitroglycerin ($m/v = 100 \cdot 10^{-4}$ g/cc) containing 1% HNO_3 water is added in such quantity that the total vapor pressure of water and acid over the nitroglycerin is 340 mm, rapid acceleration begins after 40 minutes, whereas in the case of nitroglycerin without acid, under the same pressure of water vapor, acceleration of gas formation does not begin for 250 minutes or more.

Decomposition of nitroglycol and nitrocellulose. The foregoing relationships were determined for nitroglycerin. However, studies of the decomposition of nitroglycol [3] and nitrocellulose [6] show that they are largely typical for nitrate esters in general. For example, nitroglycol, which decomposes much more slowly in the vapor phase at high temperatures than nitroglycerin (at 1/5 the rate at 140°) has, like nitroglycerin, a considerably higher rate of gas formation at the start of decomposition in the vapor state than in the liquid state (Fig. 8).

In contrast to nitroglycerin, nitroglycol decomposes with some acceleration even in the vapor phase This acceleration is even more pronounced in the liquid phase. Moreover, the temperature coefficient of the gas formation rate is considerably lower for nitroglycol than for nitroglycerin, and therefore E and B in the expression for the rate constant $K = Be^{-E/RT}$ have normal values; for the vapor phase at the initial stage of decomposition $K = 10^{14.3} \cdot e^{-30000/RT}$; the temperature coefficient is greater for the liquid. The curve for liquid nitroglycol in presence of water is similar to Curve 3 in Fig. 7 for nitroglycerin under similar conditions. Water has no significant influence on the decomposition rate of nitroglycol in the vapor phase.

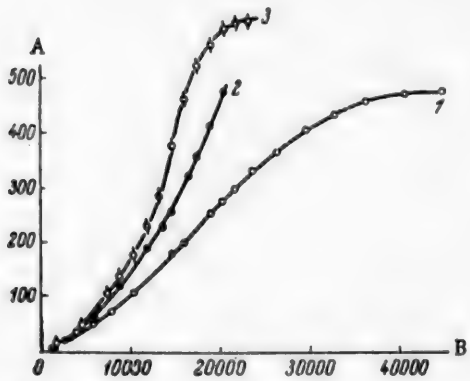

Fig. 9. Decomposition of nitrocellulose at 120°, without evacuation of the decomposition products, at different values of m/v. A) Gas formation V (cc/g), B) time (minutes). Values of m/v (in $\frac{g}{cc} \cdot 10^{-4}$): 1) 7.5, 2) 13, 3) 19.

The decomposition of nitrocellulose (pyroxylin No. 1) without removal of the reaction products proceeds with appreciable acceleration, which is greater at higher values of m/v (Fig. 9). However, even if the gaseous products are removed as completely as possible (by decomposition in vacuum, under pressures not exceeding 10^{-3} mm) the decomposition still proceeds over a considerable region with some increase of the absolute rate, in so far as the rate can be judged (Fig. 10) from the rate of gas formation or from the loss in weight (by means of the McBain balance). In this case the rate, even at these low pressures, is only 1/3 or 1/4 of the rate under pressure of the gaseous products, which reaches a maximum of 500 mm. This suggests that the autoacceleration of the decomposition under the influence of the gaseous reaction products should not be regarded as autocatalysis, but rather as interaction of the reactive components with the condensed decomposition products. This view is also supported by the fact that acceleration of gas formation is also observed if the decomposition is performed at a low (10 mm) quasiconstant pressure, by periodic evacuation of the gases.

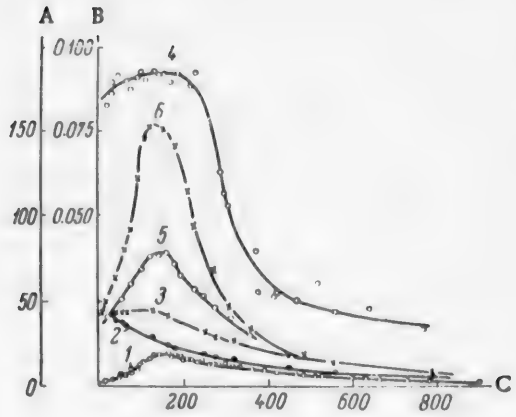

Fig. 10. Decomposition of nitrocellulose at 160°. A) Rate of gas formation $\frac{\Delta v}{\Delta \tau}$ (cc/g·hour), B) values of $\frac{\Delta m}{\Delta \tau}$ (g/g·hour), C) time τ (minutes).

Decomposition: in vacuum, with evacuation of 1) uncondensing gases, 2) condensing gases, 3) total gases; 4) weight loss; 5) under quasiconstant pressure; 6) without evacuation of the decomposition products ($m/v = 14 \cdot 10^{-4}$ g/cc).

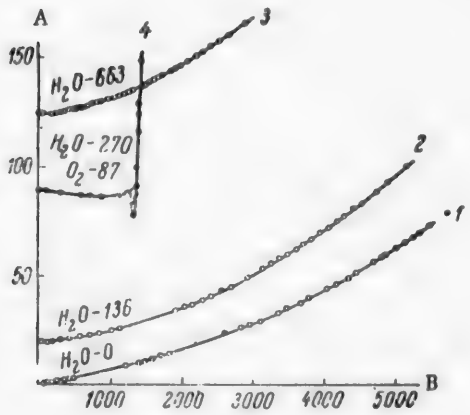

Fig. 11. Decomposition of nitrocellulose at 120° in presence of water and oxygen. A) Gas formation V (in cc/g), B) time τ (minutes). Values of $m/v \cdot 10^{-4}$ (in g/cc): 1) 57, 2) 67, 3) 49, 4) 38.

It must be added that if the gas formed during decomposition in vacuum is passed through a trap containing liquid nitrogen, and the condensed and uncondensed volumes are measured separately, the rate of formation of the uncondensing gases increases considerably (6 to 8-fold) with time. This is easily explained if a condensed intermediate product, which reacts with the formation of uncondensing gases, is formed during the decomposition.

The presence of water in the decomposition of nitrocellulose results in a relatively small increase of the rate of gas formation; the nature of the $p = f(\tau)$ curve remains unchanged (Fig. 11). A different result is obtained if acids or oxygen are present together with water. In such cases the $p = f(\tau)$ curve is of the same form as the curve for nitroglycerin or nitroglycol in presence of water. It seems that in the decomposition of nitrocellulose the reduction of NO_2 to NO proceeds relatively rapidly, and the acid which could intensify the hydrolytic action of water is not formed. Oxygen rapidly converts NO into NO_2, which forms acids with water. In the case of nitroglycerin the reduction of NO_2 is slower; however, in this case also the presence of oxygen shortens the time before rapid acceleration begins.

As already stated, acids greatly accelerate the decomposition of nitrocellulose, especially in presence of water. Sulfuric acid has a stronger effect than nitric. The accelerating effect of nitric acid in conjunction with water depends on their relative proportions; dilute and concentrated acids are relatively less effective. Dry nitrogen dioxide at low concentrations accelerates decomposition relatively slightly; the decomposition is also accelerated by nitric oxide, but only at high concentrations.

SUMMARY

The decomposition of nitroglycerin at high temperatures in absence of impurities is a complex homogeneous–heterogeneous reaction at the initial stage; in the vapor phase this reaction proceeds without acceleration of gas formation, while in the liquid phase there is a slight acceleration. The gas formation accelerates sharply after a certain pressure of the gaseous products has been reached, with a corresponding concentration of these products in the liquid. A similar acceleration of gas formation takes place when water, and especially water together with acids, is added to nitroglycerin; it follows that acceleration of gas formation in both cases is due to a hydrolytic reaction followed by interaction of the hydrolysis products. The decomposition of nitroglycol and nitrocellulose is in general similar to the decomposition of nitroglycerin.

LITERATURE CITED

[1] R. Robertson, J. Chem. Soc. 95, 1241 (1909).

[2] S. Z. Roginskii and L. M. Sapozhnikov, Zhur. Fiz. Khim. 2, 80 (1931); Sow. Phys. 1, 640 (1932); A. Ia. Lukin, Zhur. Fiz. Khim. 3, 406 (1932).

[3] K. K. Andreev and A. P. Glazkova, DAN SSSR 105, 286 (1955).

[4] N. M. Emanuel', in the book: Questions of Chemical Kinetics, Catalysis, and Reactivity* (Izd. AN SSSR, 1955) p. 117.

[5] A. Ia. Apin, O. M. Todes and Iu. B. Kharlton, Zhur. Fiz. Khim. 8, 866 (1936); J. B. Levy, J. Am. Ch. Soc. 76, 3254, 3790 (1954); F. H. Pollard, A. E. Pedler and C. I. Hardy, Nature 20, 979 (1954).

[6] K. K. Andreev and B. S. Samsonov, Proc. Acad. Sci. USSR 114, 815 (1957).**

Received July 3, 1957

*In Russian.

**Original Russian pagination. See C. B. Translation.

BRIEF COMMUNICATIONS

PRODUCTION TRIAL OF THE EXTRACTION OF GOLD FROM SPENT ELECTROLYTIC SOLUTIONS BY MEANS OF ION EXCHANGE

A. B. Davankov, V. M. Laufer, and N. E. Razgil'deev

The success of a number of studies of sorption processes with the use of ion-exchange resins [1, 2] prompted us to perform certain trials under industrial conditions. Trials of the extraction of gold from spent electrolytes, after replacement by fresh solutions of potassium auricyanide in the electrolytic cells, were performed at the Moscow Mint.

The aim of the investigation was the development of a simple, rapid, and economically advantageous process for the extraction of gold from spent solutions and its return to the production cycle. It was necessary to find a suitable range of ion exchangers, with sufficiently pronounced selective adsorption of complex gold anions, and inert toward simple anions of other salts, the concentration of which in spent electrolytes is hundreds of times that of the gold salts. Moreover, the contents of caustic alkalies and alkali carbonates in these solutions reach 100 g/liter, so that the conditions are very unfavorable for the use of anion-exchange resins of a weakly and moderately basic character.

Acidification of the gold cyanide solutions in order to lower the solution pH to 2-3 and thereby to create more favorable conditions for anion exchange was difficult because of the possibility that hydrocyanic acid would be evolved by decomposition of residual potassium cyanide in the solutions.

The resin chosen for extraction of complex gold anions from these solutions was "N—O" anion-exchange resin, which had been tested previously, together with other resins synthesized by us, for the sorption of suspended (colloidal) particles of gold from production wastes obtained in the polishing of gold and glided articles [3].

The successful operation of anion-exchange units in gold-processing plants during the past 2 years suggests that ion exchangers might be used in the near future in the hydrometallurgy of gold and other precious metals.

It is known that the value of modern synthetic ion exchangers lies not only in their high adsorptive capacity for various elements or complex chemical compounds, but also in their stability for separation of complex mixtures into their constituents, either by selective adsorption or by consecutive (fractional) desorption from the resins.

Ion exchangers may be of particular importance for separation of complex compounds, such as those formed by metal salts with nitrogen compounds (ammoniates, ammines, etc.).

If, moreover, it is remembered that methods are now known for concentration and accumulation of precious metals on adsorbents in amounts considerably exceeding the total exchange capacity (over 100% of the adsorbent weight) [4], the technological significance and advantages of adsorption processes effected on ion-exchange resins over other methods now used in industry and laboratory practice become evident. These advantages apply to the extraction of gold from spent industrial electrolytes, the treatment of which by methods other than ion exchange proved extremely difficult and impracticable in plant conditions.

The choice of the highly porous "N—O" anion-exchange resin, which had earlier proved effective both in molecular and ion-exchange sorption, for this purpose was found to be justified. In tests under plant conditions it gave almost complete (100%) extraction of gold from spent electrolytes, highly contaminated with mineral salts and alkali. The technical characteristics of such electrolytes are given in Table 1.

TABLE 1

Characteristics of Spent Gold Cyanide Electrolytes Passed Through Adsorption Columns Packed with "N–O" Anion-Exchange Resin

Electrolytic cell No.	Amount of spent electrolyte (liters)	Au conc. in electrolyte, calc. as metal (g/liter)	Total Au content of solution (g)	KCN content (g/liter)	Alkali content (g/liter)	Au isolated after combustion of resin	
						in g	% of the amount present in solution
1	47.40	3.08	145.99	1.04	64.5	636.52	99.81
2	40.20	8.5	341.70	0.2	119.7		
3	10.0	15.0	150.00	Not determined			

The fears that the extraction of $Au(CN)_2^-$ anions from strongly alkaline solutions might be incomplete owing to possible desorption of the anions from the resin proved unfounded. This was confirmed by the first exploratory experiment in a small unit containing 300 g of resin of 60% moisture content. After one liter of spent industrial electrolyte, containing 4.8 g of gold, had been passed through it, all the gold was recovered from the ash after combustion of the adsorbent.

The subsequent experiments on the extraction of gold were performed in a large unit consisting of two vinyl plastic columns in series, each 1665 mm high and 73 mm in diameter. Each was packed with 3.5 kg of anion-exchange resin containing 64-68% moisture, of grain size 2-2.5 mm. The gold-containing solution was fed by gravity into the adsorption columns from a vinyl plastic header tank 30-40 liters in capacity. The rate of percolation through the resin was regulated by means of stopcocks at the header tank and the columns. A special head and outlet tube of transparent plastic was fitted to the top of each column, for observations of the course of the process and for release of any gases formed.

In the first experiment the solution was fed into only one of the adsorption columns, and flowed out at a rate of 1.5-2 liters/hour.

According to the plant laboratory data, each liter of the solution contained 3.17 g of gold (reckoned as the metal), 0.26 g of potassium cyanide, 102.16 g of mineral salts, and 93.8 g of caustic and carbonate alkali. Nineteen liters of solutions with a total gold content of 60.23 g was passed through the adsorption column. No breakthrough of gold ions into the filtrate was detected, so that the extraction of gold from the solution was complete; neither was any gold found in the 5 liters of wash water used for washing out residual mineral salts from the adsorbent.

In the next experiment several production batches of spent gold electrolytes, the composition of which is given in Table 1, were combined; the mixed solution was passed through 2 columns in series at 10 liters/hour.

The sorption of the complex gold ions was rapid and complete.

As the "N–O" anion-exchange resin was used in the chloride form (after treatment with 5% HCl solution), gases were evolved at the beginning of the experiments, probably as the result of decomposition of carbonates present in the original solution. As the Cl^- ions in the resin became replaced by other anions, gas evolution decreased and finally ceased entirely. 97.6 liters of gold-containing solutions, consisting of contaminated electrolytes from 3 cells, was passed through the adsorption columns; the color of the solutions was yellow-green, with clear signs of copper salts; the total gold content of the solution, according to the plant laboratory data, was 637.69 g.

To check that the extraction of gold from the solutions by treatment with "N–O" anion-exchange resin was complete, samples were taken from each 3-5 liters of filtrate and tested qualitatively for gold ions by means of benzidine acetate; gold was also determined quantitatively in three samples by the usual method. "Breakthrough" of gold ions occurred after 74.4 liters of solution had been passed through the resin. When the concentration of gold ions in the filtrate reached 2.25 g/liter, the supply of the gold-containing solution to the

adsorption columns was stopped. The rest of the spent electrolyte together with the filtrate in which gold was detected was passed through the same columns charged with fresh "N–O" resin. All the gold was held in the resin, and no gold ions were detected in the filtrate.

The resin was washed with 10 liters of water, dried, and burned together with the two portions of resin removed from the columns after "breakthrough" of $Au(CN)_2^-$ ions into the filtrate. This gave 1247 g of ash, which was analyzed and found to contain 630.02 g of pure gold, or 50.5% of the weight of the ash. 1219.08 g of the ash, ground in a ball mill and passed through a fine screen, was sent to the Moscow Assay Laboratory, where it was analyzed and subjected to additional treatment. When the ash was calcined in a ceramic vessel in presence of atmospheric oxygen, its weight decreased by 38.8% (owing to combustion of residual carbon), and its gold content increased to 73%.

The gold was melted by portions in a small graphite crucible which was heated in a high-frequency furnace. Five gold ingots were cast, and were found to contain, by analysis, 607.49 g of pure gold.*

The conditions and results of one experiment on the treatment of the auriferous ash obtained by combustion of the resin are given in Table 2.

TABLE 2

Extraction of Gold from the Residual Ash after Combustion of the Adsorbent

Sample No.	Weight of ash (g)	Gold content of ash samples		Wt. of ash after additional calcination (g)	Weight of Au + Ag + Cu ingot (g)	Purity of ingot	Gold content (g)
		%	g				
1	250.00	50.5	126.25	172.2	147.4	857.0	126.32
2	250.00	50.5	126.25	172.2	148.5	852.7	126.63
3	250.00	50.5	126.25	174.8	147.6	856.2	126.38
4	279.75	50.5	141.27	193.8	164.2	860.3	141.26
5	172.63	50.45	87.09	118.1	99.6	—	86.90
Total . . .	1202.38	50.5	607.11	831.1	707.3	—	607.49

In the second experiment on the extraction of gold, performed at the Moscow Mint, several samples of electrolyte, with a total gold content of 6.28 g, were taken for analysis, and 45.06 g of ash containing 22.75 g of pure gold was left for the tests. Thus the total amount of gold extracted from 97.6 liters of solution was 636.52 g, or 99.81% of the original content in the electrolytes.

In addition to these experiments on the extraction of gold from spent gold electrolytes, an experiment was also carried out on the extraction of metallic gold particles present in suspended form in the wash waters obtained as wastes in the grinding and polishing of gold articles. 250 liters of water, containing 16.5 g of metallic gold, was acidified and agitated mechanically with 2.5 kg of finely-divided "N–O" resin for 30 minutes; after separation of the resin by filtration, gold could not be detected in the water, which shows that the gold particles were completely held by the adsorbent.

SUMMARY

1. In studies of methods for the extraction of gold from spent gold electrolytes by means of anion exchangers it was found that "N–O" anion-exchange resin completely extracts gold anions from strongly alkaline electrolytes contaminated with large amounts of mineral salts.

2. The gold can be recovered quantitatively from the adsorbent if the combustion of the resin is correctly performed and the proper conditions in the melting of the gold from the residual ash are maintained.

*Workers of the Moscow Assay Inspection Department, V. P. Tarusin, O. E. Neginskii, and M. S. Ruzhnikov, took part in the work on analysis of the auriferous ash and extraction of gold from it.

3. This method for the extraction of gold from production wastes can be recommended for industrial use.

LITERATURE CITED

[1] A. B. Davankov and V. M. Laufer, J. Appl. Chem. 28, 952 (1956);* 29, 1029 (1956).*

[2] A. B. Davankov and V. M. Laufer, Tsvetnye Metal 11, 1 (1956).

[3] A. B. Davankov and V. M. Laufer, Authors' Certif. No. 101986, August 21, 1954.

[4] A. B. Davankov, V. M. Laufer and L. A. Shits, J. Appl. Chem. 30, 839 (1957).*

Received December 28, 1956

*Original Russian pagination. See C. B. Translation.

STUDY OF THE RATE OF SOLUTION OF THE OXIDE FILM ON ALUMINUM

N. P. Fedot'ev and I. Kosha-Shomodi

Electrolytic anodizing of aluminum is one of the main methods for protecting aluminum against corrosion. The principal processes taking place in the anodizing of aluminum are the formation of an oxide film, solution of a part of the film formed under the action of the electrolyte, evolution of gases, and adsorption of molecules and ions from the electrolyte.

The nature of the oxide film formed depends mainly on the type of electrolyte. If the electrolyte has no solvent action on aluminum oxide, a compact film without pores is formed. The film thickness depends on the voltage used. Electrolytes of another group used in anodizing dissolve the film appreciably during its formation. A porous film is formed, and its thickness does not depend on the voltage.

Therefore considerable interest attaches to studies of dissolution of the film in relation to investigations of the anodizing of aluminum, since the effectiveness of the anodizing treatment and the properties of the film greatly depend on the solvent power of the electrolyte. This process must also be taken into account in compilation of energy and material balances for the anodizing process.

The influence of various factors on the solution rate of a porous oxide film on aluminum was studied in the present investigation. The solution rates were determined, both without polarization of the oxide film, and directly during its electrochemical formation.

EXPERIMENTAL

A sulfuric-acid electrolyte was used, as this is the most important industrial electrolyte. The aluminum oxide films the solution rates of which were studied without polarization were obtained by electrolytic surface oxidation of pure aluminum in 10% sulfuric acid solution. Sheet aluminum of the following composition • (in %) was used Al 99.93, Si 0.035, Fe 0.03, Cu 0.002.

The experiments on the solution rates of aluminum oxide during electrolytic oxidation were performed both with and without internal cooling. In the experiments with internal cooling the aluminum was oxidized on one side only, while heat was removed from both sides of the specimen. The apparatus [1, 2] shown in Fig. 1, was used for the experiments with internal cooling.

For determination of the amount of oxide formed, the samples of oxidized aluminum were treated with a solution containing 20 g of chromic anhydride and 35 g of orthophosphoric acid (sp.gr. 1.52) per liter.

This solution is widely used for removal of surface oxide [2, 3], as it has no action on metallic aluminum.

The quantity of electricity used in the formation of the aluminum oxide was found from the difference in weight of the specimen before oxidation and after removal of the film. The result could be used for calculation of the theoretical amount of oxide which should be formed if the oxide film did not dissolve in the electrolyte used for the oxidation.

The use of aluminum as a peculiar form of coulometer is described in the literature [4]. A copper coulometer is less convenient to use in this instance, because a certain amount of oxygen is liberated during the oxidation, and this would necessitate the introduction of a correction in calculation of the amount of oxide.

• The spectroscopic analysis was performed in the All-Union Institute of Aluminum and Magnesium.

The temperature was kept constant to the nearest ± 0.1°.

As is known, a compact nonporous layer is formed during the first few seconds of oxidation, and the thickness of this layer can be found from the quantity of electricity passed. Films formed in 10 seconds in 10% sulfuric acid at 20° and current density 4 amps/dm^2 were separated from the aluminum by the amalgamation method used in the preparation of oxide films in electron microscopy [5], and dissolved completely in 10% sulfuric acid. The solution was stirred at a rate of 60 revolutions/minute. Division of half the film thickness by the time required for complete dissolution gives the rate of solution of the film in A/minute.

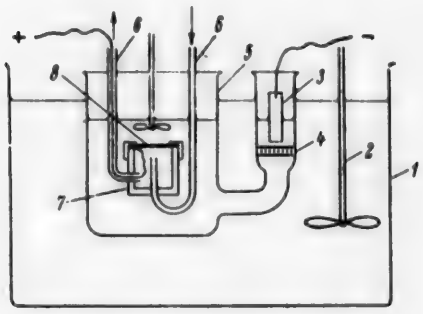

Fig. 1. Apparatus for anodizing with internal cooling. 1) Thermostat, 2) thermostat stirrer, 3) lead cathode, 4) glass filter, 5) anodizing cell, 6) inlet and outlet tubes for cooling liquid, 7) holder with anodized specimen, 8) aluminum cathode.

As was to be expected, the logarithm of the solution rate of the oxide film is a linear function of the electrolyte temperature. A plot of the solution rate as a function of the temperature, in semilogarithmic coordinates, is therefore linear (Fig. 2).

The results yield the following equation for the solution rate of the oxide film as a function of the temperature:

$$\log v = 0.06t - 1.2, \qquad (1)$$

where: v is the solution rate of the film (in A/minute per unit true surface area), t is the electrolyte temperature.

If the solution rate is expressed in mg/min · dm^2, Equation (1) becomes:

$$\log v' = 0.06t - 3.723 \qquad (1a)$$

It follows from Equation (1a) that the solution rate of an oxide film in 10% sulfuric acid is increased 10-fold when the electrolyte temperature is raised by 16.6°. Equation (1a) can be used for determination of the true surface area of any anodized aluminum specimen. It is clear that differences between the solution rates for specimens with the same apparent surface areas are due to differences in their true surface areas. It is assumed that the rate of solution is the same on the surface as within the pores. Variations of the true surface area of the oxide film with the anodizing time are plotted in Fig. 3. It is seen that the true area of the film increases linearly with the time.

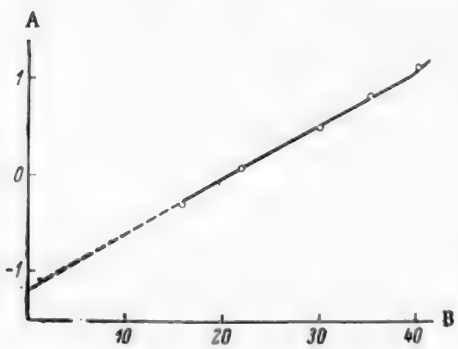

Fig. 2. Variation of the logarithm of the solution rate of the oxide film on aluminum in 10% sulfuric acid, as a function of the temperature. A) Log v, B) temperature (°C).

Variations of the solution rate of the oxide film with the electrolyte concentration are plotted in Fig. 4; it is seen that 20% sulfuric acid has the greatest solvent power. The temperature is the most important of the factors which influence the solution rate. The electrolyte concentration has much less influence on the solution rate, and its effect can be counteracted by slight variations of the temperature.

Rate of solution of the oxide during its formation. A number of workers have shown [4, 6, 7] that accumulation of aluminum salts in the electrolyte is the consequence of secondary dissolution of the oxide film. Hence it follows that during the anodizing the aluminum is oxidized fully according to the equation

$$2Al + 3H_2O + 3SO_4^{--} - 6e = Al_2O_3 + 3H_2SO_4.$$

Determination of the actual weight of oxide presents no difficulties. The solution rate of the film during the anodizing process can be found from the difference between the calculated and the actual weights of the oxide.

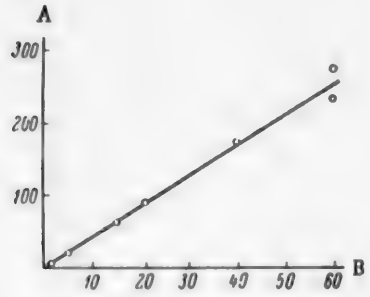

Fig. 3. Variation of the true area of the oxide film with the anodizing time in 10% sulfuric acid at current density 1 amp/dm^2 and 20°. A) Ratio of true area of film to the apparent area (dm^2/dm^2), B) anodizing time (minutes).

The amount of oxide dissolved can also be found by direct analysis, from the amount of aluminum present in the electrolyte after the anodizing. The two methods give the same results if account is taken of the SO_4^{--} content in the film. The amount of SO_4^{--} depends on the anodizing conditions. In our experiments it was about 17% on the weight of the film. Similar contents of SO_4^{--} in the films were found by Liechti [8] and Mason [9].

If the solution rate of compact nonporous films is known, it is possible to determine the true surface area of films obtained after prolonged anodizing, and having appreciable porosity. It is assumed that the oxide dissolves at the same rate within the pores as in nonporous films. With data available on the true surface area of films obtained under particular conditions of anodizing, and on the current efficiency under the same conditions, it is easy to calculate the average temperature within the pores. Equation (1a) is used for this purpose.

The source of heat in the anodizing process lies on the inner side of the film; therefore the temperature must be highest at the bottom of the pores, gradually decreasing to the electrolyte temperature at the outer surface of the film. Therefore the temperature calculated from the solution rate of the film is the average temperature in the pores. Variations of the average electrolyte temperature in the pores during anodizing are plotted in Fig. 5.

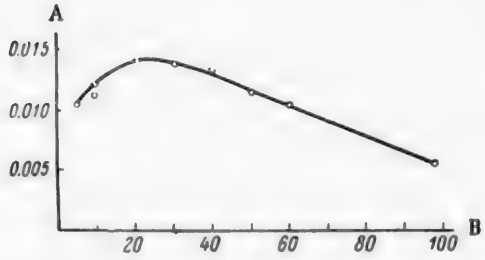

Fig. 4. Variation of the rate of solution of the oxide film with the concentration of sulfuric acid at 30°. A) Solution rate (in mg/min·dm^2), B) H_2SO_4 concentration (%).

During the first few seconds of the process the pore length is still very small, and the external surface is hotter than the electrolyte; therefore the average temperature determined by the method described should be approximately equal to the temperature at the bottom of the pores. As Fig. 5 shows, at this stage of the process the average temperature of the electrolyte in the pores reaches 75°, whereas the electrolyte temperature in the cell is 20°. It is interesting to note that at this temperature the rate of solution of the film at the bottom of the pores is approximately equal to the rate of its formation; this is easily seen if the rate of film formation at the given current density is substituted for the rate of solution in Equation (1a). The fact that film is formed and dissolved at the same rate at the bottom of the pores evidently accounts for the constant thickness of the so-called barrier layer.

Experiments showed that internal cooling does not alter the temperature at the bottom of the pores.

It follows from a consideration of these results that the decrease in the rate of film formation with increasing thickness is caused by an increase of its true surface area, and not by an increase of the electrolyte temperature in the pores.

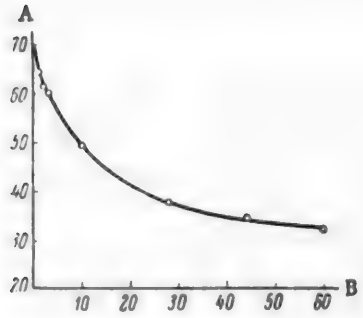

Fig. 5. Variation of the average temperature in the film pores with the anodizing time at current density 2 amps/dm^2 and cell electrolyte temperature 20°. A) Average temperature in the film pores (°C), B) anodizing time (minutes).

SUMMARY

The solution rate of the oxide film on aluminum increases logarithmically with the electrolyte temperature.

The true surface area of the film increases linearly with the anodizing time. Increase of the true area is the main factor which decreases the rate of oxide formation.

The rate of solution of the oxide film on aluminum during the anodizing process is considerably higher than is to be expected at the cell electrolyte temperature.

The average temperature of the electrolyte in the pores was calculated from the rate of solution of the film during the anodizing process. It was found that this temperature decreases in the course of the process.

LITERATURE CITED

[1] N. D. Tomashov and A. V. Bialobzheskii, Tr. Inst. Fiz. Khim. Akad. Nauk SSSR 4, 99 (1955).

[2] N. D. Tomashov and A. V. Bialobzheskii, Tr. Inst. Fiz. Khim Akad. Nauk SSSR 1, 136 (1951).

[3] B. Chanda, Trans. Indian Inst. Chem. Engrs. 1, 67 (1947-1948).

[4] M. Tosterud and R. B. Mason, Trans. Electroch. Soc. 90, 221 (1946).

[5] N. G. Sushkin, The Electron Microscope* (Gos. Izd. Tekhn.-Teor. Inst. Moscow–Leningrad, 1949) 228.

[6] N. D. Tomashov and A. V. Bialobzheskii, Trans. Inst. Fiz. Khim. Akad. Nauk SSSR 4, 114 (1955).

[7] W. Machu and M. Kamal Hussein, Werkstoffe und Korr. 5, 49 (1954).

[8] F. Liechti and W. D. Treadwell, Helv. Chim. Acta 30, 1204 (1947).

[9] R. B. Mason, J. Electroch. Soc. 102, 671 (1955).

Received March 2, 1957

* In Russian.

SOLUBILITY OF CHLORINE IN BENZENE*

F. F. Krivonos

The literature contains no data on the solubility of chlorine in benzene at different temperatures and pressures. Nevertheless, this question is of primary importance in relation to the chlorination of benzene, with regard both to the type of addition and the type of substitution. For example, it has been shown by Vorozhtsov and Travkin [1] that chlorination of benzene in presence of metallic iron is a homogenous catalytic process. This question is specially important in relation to the production of hexachloran. The present investigation was performed in order to obtain data on the solubility of chlorine in benzene, required in relation to studies of the kinetics of hexachloran formation.

Bezobrazov and Molchanov [2] presented approximate data on the solubility of chlorine in the reaction mixture at various temperatures. For example, it is stated that 4.8% chlorine dissolves at 20° in a reaction solution containing 4.6% hexachloran and 95.4% benzene. Since these data refer to the reaction solution and not to pure benzene, and the partial pressure of chlorine is not given, it is impossible to derive the values of the solubility (absorption) coefficient from them.

The difficulty here lies in the fact "that chlorine is dissolved, not in an inert solvent such as carbon tetrachloride, but in a chemically active solvent which reacts with chlorine" [2]. It must also be remembered that the method commonly used for determination of the solubility of gases in liquids [3] is not only cumbersome and complex, but is also unsuitable for use with chlorine, as the determination is performed over a layer of mercury, with which chlorine reacts chemically.

The principle of our method for the determination of solubility of chlorine in benzene is that a definite reduction of pressure is created in a hermetically sealed vessel owing to the solution of part of the chlorine in benzene. If this pressure reduction is measured by means of a manometer, the data necessary for calculation of the solubility can be obtained. Because of its simplicity and the ready availability of the apparatus needed, this method can be recommended as a general method for determination of the solubility of gases in liquids.

EXPERIMENTAL

A glass round-bottomed flask of known volume was used for the experiments. The flask was closed by means of a rubber bung with two holes with two glass tubes inserted: one long tube, reaching almost to the bottom of the flask, and a short tube, terminating near the bung. Well-ground glass stopcocks were fitted at the top of each tube. Rubber tubes with inserted glass rods may be used instead of glass stopcocks. The flask was weighed at known room temperature and atmospheric pressure determined at that instant. The stopcocks were then opened and the flask was filled, under the same conditions, with chlorine through the long tube. The flask was then closed and weighed again. The difference in weight gave the amount of chlorine introduced into the flask, together with residual air. The flask was then connected by means of a rubber tube and the tube used for the chlorine inlet to a mercury manometer. To prevent contact between the mercury and chlorine, a widened glass tube containing a special thin elastic rubber membrane was attached to the manometer (a medical finger stall can be used for this purpose). The flask was then thoroughly darkened. The short glass tube was connected, by a piece of rubber tube, to a buret with a glass stopcock. A definite quantity of benzene was introduced into the flask from the buret. To avoid leakage, the rubber tube was closed by a screw clip, the buret was detached, and a glass rod inserted in its place.

*Communication I in the series on the production of hexachloran (benzene hexachloride).

After addition of the benzene, the flask was immersed in a glass bath at a definite temperature (a thermostat). When equilibrium was reached, the manometer reading was taken and the solubility of chlorine in benzene was calculated from the experimental data. The apparatus is not dismantled, but the thermostat is merely filled with water at a different temperature, and the solubility is then determined at that temperature. The solubilities at 10, 20, 30, 40, and 50° were determined in a single experiment in this manner.

The water in the thermostat was then gradually cooled and the solubilities were determined again in the reverse sequence. It was thereby confirmed that the benzene had not reacted to any appreciable extent with chlorine in the dark.

Example 1. A round-bottomed flask 725 ml in capacity was taken. The difference in weight between the empty flask (containing air) and the flask filled with chlorine was 1.02 g. The weighing was performed at 17° and 755 mm Hg pressure. We now calculate the amounts of chlorine and air in the flask. If the flask contained chlorine only, its weight would be $\frac{755 \cdot 725 \cdot 70.9^{\bullet\bullet}}{760 \cdot 0.0808^{\bullet} \cdot 290} = 2.17$ g. The weight of the same volume of air is $\frac{755 \cdot 725 \cdot 29^{\bullet\bullet}}{760 \cdot 0.082 \cdot 290} = 0.875$ g. The difference between the weights of chlorine and air is $2.17 - 0.875 = 1.295$ g. The mixture of chlorine and air actually weighs $1.02 + 0.875 = 1.895$ g.

The difference between the weight of chlorine and the actual weight of the mixture in the flask is $2.17 - 1.895 = 0.275$ g. Hence we find the percentage content of air in the flask: $\frac{100 \cdot 0.275}{1.295} = 21.2\%$ (by volume).

The difference between the weights of chlorine and of air of a given volume depends on the difference between their densities. Consequently, this difference indicates the ratio of their volumes. However, the volume ratio also represents the ratio of the partial gas pressures. Hence the partial pressure of air is also 21.2% of the total pressure, and is $755 \cdot 0.212 = 160$ mm Hg. The partial pressure of chlorine is $755 - 160 = 595$ mm Hg (at 17°).

The above calculation may be presented in the general form

$$P_{air} = \frac{P(m_{Cl_2} - m_{mixture})}{m_{Cl_2} - m_{air}}$$

where P_{air} is the partial pressure of air, m_{air} and m_{Cl_2} are the calculated weights of air and chlorine corresponding to the flask volume, $m_{mixture}$ is the actual weight of the air–chlorine mixture in the vessel, and P is the barometric pressure during the experiment.

If the correction for the molecular volume of chlorine is neglected, a simplified formula can be used for determination of the partial pressure of chlorine:

$$P_{Cl_2} = \frac{\Delta RT}{V(M_{Cl_2} - M_{air})},$$

where R is the universal gas constant, T is the temperature of the experiment on the absolute scale, P is the barometric pressure, V is the volume of the vessel, M_{Cl_2} and M_{air} are the molecular weights of chlorine and air respectively, and Δ is the difference in weight between the flask containing air and the flask filled with chlorine.

• The weight of chlorine in 1 liter = 3.214 g. Hence the molecular volume is $\frac{70.9}{3.214} = 22.06$. Therefore $R = \frac{PV}{T} = \frac{1 \cdot 22.06}{273} = 0.0808$. This correction must be applied in exact calculations.

•• R is here in liter-atmospheres, and volume in ml, but the error due to this inconsistency is corrected in the final result.

For Example 1, the partial pressure of chlorine is

$$P_{Cl_2} = \frac{1.02 \cdot 0.082 \cdot 290}{0.725 \cdot 42} = 0.8 \text{ atm., or } 0.8 \cdot 760 = 608 \text{ mm Hg}$$

(instead of 595), i.e., the deviation is about 2%.

At the experimental temperature (20°) the chlorine content corresponds to $\frac{595 \cdot 293}{290} = 600$ mm Hg, and the air content, to $\frac{160 \cdot 293}{290} = 162$ mm Hg.

After the addition of 10 ml of benzene into the flask, the manometer reading was 218 mm Hg. Hence the total pressure of the mixture of chlorine, air, and benzene vapor at 20° was 755−218 = 537 mm Hg. Since the vapor pressure of benzene at 20° is 74.4 mm [4], the partial pressure of chlorine is 537−(162+ 74.7) = 300.3 mm Hg. Hence the amount of chlorine dissolved corresponds to 600−300.3 = 299.7 mm Hg.

The amount of benzene evaporated at 20° is $\frac{74.7 \cdot 725 \cdot 78}{760 \cdot 0.0808 \cdot 293} = 0.23$ g, which is equivalent to $\frac{0.23}{0.88} =$ = 0.26 ml. The amount of benzene remaining in the liquid state is 10−0.26 = 9.74 ml. These data are used to calculate the absorption coefficient by the usual method [5]. With partial pressure of chlorine 300.3 mm Hg, the amount of chlorine dissolved in 9.74 ml of benzene at T = 293° is equivalent to 299.7 mm Hg, which, for a 725 ml flask under 755 mm barometric pressure is equivalent to a volume of $\frac{299.7 \cdot 725}{755} = 288$ ml. Calculation for normal conditions, for a partial pressure of chlorine of 760 mm Hg, the amount of chlorine dissolv- in 1 ml of benzene is $\frac{288 \cdot 760 \cdot 273}{300.3 \cdot 293 \cdot 9.74} = 69$ ml of chlorine; i.e., the absorption coefficient is 69.

It follows from this example that the determination of the solubility of chlorine in benzene involves rather laborious calculations, and it was therefore desirable to confirm the validity of the results by chemical analysis.

Example 2. A round-bottomed flask 685 ml in capacity was filled with chlorine at 15° under barometric pressure of 758 mm Hg. The increase in weight of the flask when filled with chlorine was 0.83 g. Calculations by the above method showed that the chlorine in the flask corresponds to 500 mm Hg, or $\frac{500 \cdot 685 \cdot 709^*}{760 \cdot 0.0808 \cdot 288} =$ 137 g.

After addition of potassium iodide solution into the flask, back titration of the liberated iodine required 362 ml of 0.1043 N thiosulfate solution, corresponding to 1.335 g of chlorine. The difference from the calculated value is about 2.6%.

In the presence of benzene, iodometric determination of chlorine would not give correct results as both iodine, and chlorine in presence of iodine, react chemically with benzene. In this case it is easy to determine only the free chlorine present in the gaseous mixture (the partial pressure) from the decrease in pressure in the closed vessel after addition of potassium iodide solution. The addition of potassium bromide (rather than potassium iodide) gives even better results.

In general, however, chemical analysis cannot replace the calculations described above, as only one determination can be made. With the calculation method, numerous determinations can be performed, as described above, by variation of the temperature in the thermostat.

Example 3. A flask 725 ml in capacity was filled with chlorine at 15° under barometric pressure 757 mm Hg. The weight increase after addition of the chlorine was 1.115 g. After addition of 10 ml of benzene, the manometer reading was 246 mm Hg (at 20°). Calculation shows that the partial pressure of chlorine in the flask was 319.3 mm Hg. Potassium iodide solution was then introduced into the flask under hermetic conditions. The manometer reading at equilibrium was 575 mm Hg. Hence the decrease of pressure was 575−246 = 329 mm Hg, instead of the calculated value of 319.3. The error was about 3%.

The results obtained in determinations of the solubility of chlorine in benzene are given below:

*R is here in liter-atmospheres, and volume in ml; 709 should be 70.9. The final result should be 1.37 g.

Solubility of chlorine in benzene

Temperature (°C)	Absorption coefficient
10	95
20	69
30	57
40	49
50	42

In view of the fact that in the production of hexachloran the liquid at the end of the reaction consists of a solution of hexachloran in benzene, and not of pure benzene, experiments (approximate so far) were performed to determine the solubility of chlorine in a saturated solution (approximately 20%) of hexachloran in benzene. The coefficients of absorption at 10, 20, 30, 40, and 50° were found to be 79, 55, 44, 38, and 37 respectively.

The absorption coefficient can be used to calculate the solubility of chlorine in benzene in any other units. For example, the solubility at 10° is $\frac{95}{22.06}$ = 4.2 mole/liter or 4.2 · 71 = 298 g/liter. Expressed as a percentage, the solubility is $\frac{298}{298+880}$ = 25.2%.

In practice it is often necessary to find the solubility of chlorine in benzene at various temperatures, as maximum saturation in a vessel communicating with the external atmosphere. In this case the pressure over the benzene is about 760 mm, and therefore the partial pressure of chlorine is always less than atmospheric by an amount equal to the vapor pressure of benzene at the given temperature. For example, at 10° 1 ml of benzene dissolves not 95, but $\frac{95 \cdot (760-75.4)}{760}$ = 89.5 ml of chlorine; a 24.7% solution is formed. It follows from this example that at low temperatures, and therefore at low pressures of benzene vapor, the difference between the solubility at complete saturation of benzene with chlorine in an open vessel and the solubility calculated from the absorption coefficient is not large. With increase of temperature, however, this difference becomes very appreciable and at 60° the solubility is approximately halved, as the vapor pressure of benzene at 60° is 388.6 mm Hg.

The maximum solubilities of chlorine in benzene at atmospheric pressure, calculated for different temperatures, are given below.

Maximum solubility of chlorine in benzene in an open vessel

Temperature (°C)	Solubility	
	In moles/liter	In %
10	3.97	24.7
20	2.86	18.5
30	2.14	14.7
40	1.65	11.8
50	1.2	8.86

Data on the maximum solubility of chlorine in benzene attainable in practice are important in the development of a procedure for the production of hexachloran, and are generally useful in studies of the chlorination of benzene.

LITERATURE CITED

[1] Proc. Acad. Sci. Conference on Cyclic Raw Materials (in Russian) (Izd. AN SSSR, 1936) p. 186.

[2] Iu. N. Bezobrazov and A. V. Molchanov, Hexachloran (in Russian) (Goskhimizdat, 1949) p. 52.

[3] B. E. Eremina, Gas Analysis (in Russian) (1955) p. 349.

[4] F. Getman and F. Daniels, Outlines of Physical Chemistry (Russian translation) (1941) p. 42.

[5] I. F. Fedulov and V. A. Kireev, Text Book of Physical Chemistry (in Russian) (1952) p. 213.

Received August 3, 1956

INVESTIGATION OF THE FATTY OIL OF SILYBUM MARIANUM GAERTN.

G. V. Pigulevskii and S. B. Rzaeva

Silybum marianum (kangal) is common all over Transcaucasia and in Dagestan. It occurs in considerable quantities in the steppes of Azerbaidzhan. The seeds of the plant ripen early June to July. They contain up to 30% fat.

More detailed study of the composition of the oil is desirable in view of its possible technical utilization. The material for the study was gathered at the end of July in the Mil'skaia steppe of Azerbaidzhan. The oil had the following constants: d_4^{20} 0.9134, acid number 3.4, saponification number 195.5, Hübl iodine number 113, thiocyanate number 82.2; unsaponifiables 0.7%. Investigation of the acid composition of the oil revealed the presence of 17.8% of saturated acids, consisting entirely of stearic acid. Investigation of the unsaturated acids by bromination and by oxidation with $KMnO_4$ by Zaitsev's method revealed the presence of linoleic and oleic acids.

The next task was determination of the structure of the mixed triglycerides. The method proposed by one of us jointly with Starostina [1] was used for this purpose. The procedure is as follows. The oil is oxidized by acetyl hydroperoxide, and the oxides of the mixed triglycerides are hydrogenated in presence of palladium catalyst, being converted into triglycerides of hydroxystearic acids. By subsequent crystallization it is possible to isolate individual compounds, the structure of which gives an indication of the nature of the original triglyceride. In the present instance oxidation by acetyl hydroperoxide and subsequent hydrogenation of the oxide yielded a triglyceride with m. p. 66.5° [2].

Analysis of the triglyceride showed that it had the molecular formula $C_{57}H_{110}O_9$. The saponification products of the triglyceride were found to contain only hydroxystearic acid with m. p. 80.5-81.5°. Hence the triglyceride has the following structural formula [2]

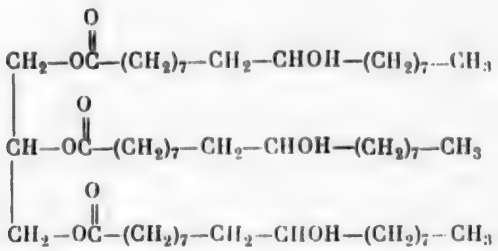

This leads to the conclusion that one of the components of kangal oil is triolein. The question of the nature of the other triglycerides remains open.

EXPERIMENTAL

The oil was extracted from 10 kg of seeds by cold pressing followed by extraction of the cake with ether. The yield of oil was 2.6 kg.

Investigation of the acid composition of the oil. One hundred g of the oil was saponified by treatment with 2% alcoholic KOH solution for 2 hours. 40% sulfuric acid was added to the solution of the potassium salts, diluted with water. The liberated fatty acids were extracted in ether. The ether solution was dried over Na_2SO_4 and ether was then evaporated off. The fatty acids so obtained were used in the subsequent investigations.

Determination of acids by the Bertram method gave 17.8% of saturated acids. The melting point of the saturated acids after recrystallization was 71.5°. Further attempts to separate the magnesium salts by fractional crystallization into fractions differing in properties were not successful.

Determination of the neutralization number

Sample 0.2212 g; took 43.43 mg KOH.
Sample 0.2160 g; took 42.52 mg KOH.
Found: neutralization number 196.3, 196.9.
$C_{18}H_{36}O_2$. Calculated: neutralization number 197.37.

A mixed sample with stearic acid gave no melting point depression.

Bromination of the fatty acids. 7.36 g of the fatty acid mixture was dissolved in a 10-fold quantity of ethyl ether. Bromine was added dropwise to the solution to a permanent yellow color. The bromination was performed at a low temperature (−5°). The precipitate was filtered off, washed with cold ether, and recrystallized from alcohol. The m. p. was 113-114°, characteristic of tetrabromolinoleic acid. The hexabromide was not found in these experiments.

Oxidation of the fatty acid mixture by potassium permanganate. Thirty g of the acids isolated from the oil was placed in a flask fitted with a stirrer, and dissolved in 36 ml of 2 N caustic potash. Two liters of water was added to the solution of the salts. The reaction mixture was then cooled to 0° and 1 liter of aqueous $KMnO_4$ solution (22.3 g) was added during 30 minutes. The reaction mixture was stirred continuously, and its temperature was not allowed to rise above −5°. The manganese dioxide formed was dissolved by treatment with sulfur dioxide. Hydroxy acids were isolated from the solution of the salts of the oxidized acids, by addition of dilute sulfuric acid. The hydroxy acids were washed with water, dried in air, and treated with ligroine to remove saturated acids, unoxidized unsaturated acids, and their decomposition products. The total yield of hydroxy acids was 20.21 g. These hydroxy acids were extracted by means of ethyl ether in a Soxhlet apparatus. A total of 3.1 g of presumed dihydroxystearic acid was extracted; after recrystallization from alcohol it had m. p. 131-132°.

Determination of the neutralization number of the hydroxy acid with m. p. 131-132°

Sample 0.1176 g; took 20.70 mg KOH.
Sample 0.1170 g; took 20.70 mg KOH.
Found : neutralization number 176.1, 176.9.
$C_{18}H_{34}(OH)_2O_2$. Calculated : neutralization number 177.0.

13.1 g of acids which did not dissolve in ether was then treated stepwise with boiling water. Six fractions were isolated. The melting point of the first two fractions after recrystallization from water was 156-157°; the melting point of the other fractions was 157-158°. The total yield of the hydroxy acids was 1.916 g.

Determination of the neutralization number of the hydroxy acids with m. p. 157-158°

Sample 0.1150 g; took 17.73 mg KOH.
Found: neutralization number 154.2.
$C_{18}H_{32}(OH)_4O_2$. Calculated: neutralization number 160.8.

Oxidation of the oil by acetyl hyderperoxide. • 200 g of the oil dissolved in 400 ml of dry ether was put into a 2 liter flask. 355 ml of an ether solution of acetyl hydroperoxide (134.4 ml) was then added. Acetyl peroxide was taken in excess (15%). The reaction mixture was cooled in water to prevent overheating. At the end of the addition, when the temperature became constant at near the room level, the flask was left to stand for some time, the course of the oxidation being examined at intervals. The reaction was complete on the 38th

• 95% acetyl hydroperoxide was used.

day. The reaction product was washed with water and sodium carbonate solution until neutral. The solution was dried over sodium sulfate and the ether was then evaporated off. The residue was a very viscous liquid with iodine number 0.

Catalytic hydrogenation of the oxidized product. Five g of the hydroxy acid triglycerides, 0.5 g of Pd, and 40 ml of acetic acid was taken. The total volume of hydrogen absorbed was 381 ml (19°, 761 mm); the calculated volume is 496 ml.

The acetic-acid solution of the hydrogenated product was separated from palladium black by decantation and treated with water. The white precipitate formed was extracted with ether. The ether solution was washed with water and dried over sodium sulfate. After removal of ether, the residue in the form of a white powder was repeatedly recrystallized from alcohol. The melting point of the purified substance was 66.5°, yield 5 g.

Elementary analysis;

Sample 11.41 mg; 30.51 mg CO_2, 11.92 mg H_2O.
Sample 12.36 mg; 32.91 mg CO_2, 12.78 mg H_2O.
Found %: C 72.90, 72.61; H 11.67, 11.57.
$C_{57}H_{110}O_9$. Calculated %: C 72.93; H 11.72.

Determination of molecular weight;

Sample 0.7672 g: took 140.2 mg KOH.
Sample 0.7124 g: took 129.0 mg KOH.
Found M: 921.5, 929.3.
$C_{57}H_{110}O_9$. Calculated M: 938.

Determination of the structure of the triglyceride of formula $C_{57}H_{110}O_9$. Five g of the triglyceride, dissolved in 52 ml of 0.5 N alcoholic KOH solution, was saponified. The alcoholic solution of the potassium salts was diluted with water and sulfuric acid was added to liberate the acids. The acids were fractionally crystallized from ligroine and alcohol. Recrystallization yielded a compound with m. p. 80.5-81.5° [2].

Elementary analysis;

Sample 13.32 mg: 35.13 mg CO_2, 14.81 mg H_2O.
Sample 13.82 mg: 35.96 mg CO_2, 14.86 mg H_2O.
Found %: C 71.96, 71.72; H 11.91, 12.02.
$C_{18}H_{36}O_3$. Calculated %: C 72.00; H 12.03.

Determination of the neutralization number;

Sample 0.1248 g: took KOH 22.30 mg.
Sample 0.1872 g: took KOH 13.34 mg.•
Found: neutralization number 178.6, 178.6.
$C_{18}H_{36}O_3$. Calculated: neutralization number 186.6.

LITERATURE CITED

[1] G. V. Pigulevskii and T. A. Starostina, Doklady Akad. Nauk SSSR 79, 261 (1951).

[2] G. V. Pigulevskii and A. E. Saprokhina, J. Appl. Chem. 30, 7, 1104 (1957).••

Received October 26, 1957

• As in original – Publisher's note.
•• Original Russian pagination. See C. B. Translation.

PREPARATION OF OCTACHLORO-1,3-PENTADIENE

L. M. Kogan, N. M. Burmakin, N. P. Ignatova, and N. V. Cherniak

Octachloro-1,3-pentadiene is a transparent colorless liquid with b. p. 139-140° (10 mm), d_4^{20} 1.7723, n_D^{20} 1.5725 [1]. Chemically, it is a chlorinated hydrocarbon with conjugated double bonds; its reactivity is low owing to the shielding influence of the chlorine atoms. Octachloro-1,3-pentadiene does not add on chlorine either in the liquid or in the vapor phase at temperatures up to 500°. At high temperatures it tends to decompose into chlorinated hydrocarbons containing fewer carbon atoms, and also to undergo cyclization. Octachloro-1,3-pentadiene can be used for vulcanization of synthetic rubber to give vulcanizates with increased heat resistance [2].

Open-chain unsaturated chlorinated hydrocarbons with more than 2 carbon atoms in the chain can be prepared by the Prins reaction [3]. This method consists of a stepwise increase of the carbon chain length by reactions of the chlorinated hydrocarbons with each other, alternating with dehydrochlorination of the compounds formed. This is the only method for the preparation of octachloro-1,3-pentadiene. One version of the preparation of octachloro-1,3-pentadiene by the Prins method is represented by the following reaction scheme:

$$CHCl{=}CCl_2 \xrightarrow{+CCl_4} CCl_3{-}CHCl{-}CCl_3 \xrightarrow{-HCl} CCl_2{=}CCl{-}CCl_3 \xrightarrow{+CHCl=CCl_2}$$
$$\rightarrow CCl_2{=}CCl{-}CCl_2{-}CHCl{-}CCl_3 \xrightarrow{-HCl} CCl_2{=}CCl{-}CCl{=}CCl{-}CCl_3.$$

All the reactions take place at slightly elevated temperature and normal pressure. The condensation reactions are effected in presence of aluminum chloride, and the dehydrochlorination takes place in presence of aluminum chloride or by the action of alcoholic alkali.

The disadvantage of this method for the preparation of octachloro-1,3-pentadiene is the multistage nature of the process, so that the total yield of the product from the starting materials is low. This would still be the case if the yield at each stage was high. For example, with 85% yield in each reaction the total yield of octachloro-1,3-pentadiene calculated on the calcium carbide required for the production of the trichloroethylene is about 30%.

The formation of dienes by dehydrochlorination was studied by Tishchenko [4] and others.

We have devised a method for the preparation of octachloro-1,3-pentadiene from chlorine and polychloropentanes. The method consists of the catalytic interaction of these substances at 300-400° and under normal pressure in presence of octachlorocyclopentene. The processes which take place are

$$C_5H_{12-n}Cl_n + (10-n)\,Cl_2 \longrightarrow C_5H_2Cl_{10} + (10-n)\,HCl$$

and

$$C_5H_2Cl_{10} \longrightarrow C_5Cl_8 + 2HCl.$$

The catalyst is infusorial earth. The octachlorocyclopentene in the reaction mixture prevents or restricts the cyclization of the octachloro-1,3-pentadiene formed.

We showed earlier [5] that when polychloropentanes are chlorinated under the identical conditions, but without addition of octachlorocyclopentene, the principal reaction products are hexachlorocyclopentadiene and octachlorocyclopentene. Octachloro-1,3-pentadiene is obtained in low yield (up to 15%), since it is the intermediate compound in the conversion of polychloropentanes into the above-named compounds. It was found in special experiments that if octachlorocyclopentene is brought in contact with infusorial earth under the same conditions, but in absence of polychloropentanes, dechlorination takes place with formation of hexachlorocyclopentadiene. The reaction products did not contain octachloro-1,3-pentadiene; this is consistent with the low probability of ring opening under these conditions.

In the preparation of octachloro -1,3-pentadiene by the proposed method, octachlorocyclopentene can be introduced into the system in different ways; it can be fed into the process together with the raw material, introduced previously into the catalyst, or formed on the catalyst in the reaction between chlorine and polychlorocyclopentahes. In the latter two cases the catalyst is subjected to special treatment which results in adsorption of octachlorocyclopentene on its surface. The yield of octachloro-1,3-pentadiene from polychloropentanes is about 30%, and may be increased considerably by suitable choice of conditions. The above method for the preparation of octachloro-1,3-pentadiene is considerably simpler than the process based on the Prins reactions, as the product is formed directly from chlorine and pentane in two stages through polychloropentanes, without expenditure of other reagents.

EXPERIMENTAL

Polychloropentanes were prepared by photochemical chloronation of n-pentane of b. p. 36-37°, n_D^{20} 1.3750 and d_4^{20} 0.6252. The chlorine was taken from a cylinder. Octachloro-1,3-pentadiene was prepared in the usual type of flow apparatus. A quartz tube 20 mm in diameter and 300 ml in volume was packed with infusorial earth and placed in an electrical resistance furnace. The required compound was isolated by distillation of the liquid reaction products.

Experiment 1. Ninety-three g of polychloropentanes (n_D^{20} 1.5375, d_4^{20} 1.6554, chlorine content 78%) and 79 g of octachlorocyclopentene (n_D^{45} 1.5680, d_4^{45} 1.812) was passed together with 115 g of chlorine at 350° through the reaction tube, the feed rate of the organic compounds being 42 g/hour.

Thirty-seven g of octachloro-1,3-pentadiene was isolated from the reaction products (yield 34%); n_D^{20} 1.5711, d_4^{20} 1.7706.

Experiment 2. A mixture of chlorine and polychlorocyclopentanes was passed through the reaction tube, the feed rate of the polychlorocyclopentanes being 100 g/hour. This treatment of the catalyst was continued for 3 hours. After removal of the residual vapors of the cyclic compounds in a stream of chlorine the catalyst was ready for use. 170 g of polychloropentanes (n_D^{20} 1.5455, d_4^{20} 1.6903, chlorine content 80%) and 227 g of chlorine was passed through the reaction tube containing the prepared catalyst. The feed rate of the polychloropentanes was 66 g/minute. Sixty-one g octachloro-1,3-pentadiene (yield 34%) was isolated from the reaction products.

The duration of the catalyst pretreatment can probably be shortened. The service life of the catalyst must be determined experimentally.

SUMMARY

A method is proposed for the production of octachloro-1,3-pentadiene from polychloropentanes and chlorine in presence of cyclic compounds.

LITERATURE CITED

[1] J. A. Krynitsky and R. W. Bost, J. Am. Chem. Soc. 69, 1918 (1947).

[2] B. M. Sturgis, A. A. Baum and J. H. Trepagnier, Ind. Eng. Ch. 39, 64 (1947).

[3] H. J. Prins, Rec. trav. Chim. 69, 1003 (1950).

[4] D. V. Tishchenko, Zhur. Obshchei Khim. 17, 460 (1947).

[5] L. M. Kogan, N. M. Burmakin and N. V. Cherniak, J. Gen. Chem. 28, 1, 27 (1958).*

*Original Russian pagination. See C. B. Translation.

Received February 19, 1957

DISTRIBUTION OF ACETIC ACID BETWEEN TWO COEXISTING PHASES – NONAQUEOUS AND AQUEOUS

V. N. Kozlov and B. I. Smolenskii

Wood Chemistry Laboratory, the Urals Institute of Wood Technology

The methods now used in industrial production of organic substances for the isolation of dissolved substances in concentratd form from dilute aqueous solutions include extraction, absorption, and azeotropic distillation.

In the separation of, say, acetic acid from dilute aqueous solution the extraction solvents used are diethyl ether, ethyl acetate, etc.; absorbents used include wood tar oils, and the withdrawing agents are wood alcohol oils, dichloroethane, butyl acetate, etc.

For calculations relating to the extraction and distillation of dilute acetic acid and its homologs in presence of withdrawing agents, it is necessary to have data on the distribution of the total acid concentrations between two coexisting phases – nonaqueous and aqueous.

In this paper we present the derivation of the law governing the distribution of a solute between two coexisting phases (nonaqueous and aqueous) when the dissociation constant of the solute in the aqueous phase is zero.

It is assumed in the derivation that the following laws are valid over a certain range of the total concentrations of the solute in the nonaqueous and aqueous phases: the Nernst distribution law [1]

$$\frac{x_1}{y} = \bar{K}, \tag{1}$$

and the law of mass action

$$\frac{x_1^n}{x_0 - x_1} = \bar{K}_0, \quad 0 < n \neq 1. \tag{2}$$

In Equations (1) and (2): $\bar{K}$, K_0, n are constants, although in reality $\bar{K}$ and n may vary with variations of the concentrations of the solute in two coexisting phases; x_1 is the concentration of simple molecules in the nonaqueous phase; y is the total concentration of the solute in the aqueous phase (in the present instance, in absence of electrolytic dissociation, y is the concentration of simple molecules); x_0 is the total concentration of the solute in the nonaqueous phase.

From Equations (1) and (2) it is easy to derive the law for the distribution of the total concentrations x_0 and y of the solute between the nonaqueous and aqueous phases. In parametric form, this law is given by the system of equations

$$\left.\begin{aligned} x_0 &= x_1 + \frac{x_1^n}{\bar{K}_0} \\ y &= \frac{x_1}{\bar{K}} \end{aligned}\right\} \tag{3}$$

We eliminate x_1 from the Equations (3) to find the equation for the curve for the distribution of total concentrations, in Cartesian coordinates, if x_0 and y are regarded as the running coordinates of a point on a plane in a system of rectangular Cartesian coordinates

$$x_0 = \overline{K}y + by^n, \tag{4}$$

where

$$b = \frac{\overline{K}^n}{\overline{K}_0}.$$

Discarding by^n from Equation (4), we have

$$\frac{x_0}{y} \approx \overline{K}. \tag{5}$$

It also follows from Equation (4) that

$$\frac{x_0}{y^n} = \frac{\overline{K}}{y^{n-1}} + b.$$

Discarding $\frac{\overline{K}}{y^{n-1}}$ from the above, we obtain Shilov's equation [2]

$$\frac{x_0}{y^n} \approx b. \tag{6}$$

The use of the approximate Equations (5) and (6) involves the following errors:

$$\varepsilon_5 = by^{n-1}, \quad \varepsilon_6 = \frac{\overline{K}}{y^{n-1}}.$$

It follows from $\frac{dx_0}{dy}$ and $\frac{d^2x_0}{dy^2}$ derived from Equation (4) that x_0 increases with increase of y.

When $n > 1$, the curve for Equation (4) is convex toward the abscissa axis. When $n < 1$, the curve is concave toward the abscissa axis (see Figure).

Let us apply Equation (4) to the system acetic acid – diethyl ether – water.

In the extraction of acetic acid from aqueous solutions under industrial conditions, the concentration of acetic acid in the exit water from the extractor is 0.2 to 0.3%. The degree of electrolytic dissociation of acetic acid is assumed to be small, and is disregarded.

The distribution of acetic acid between diethyl ether and water at 15° is given in the Table.

In this table x and y are the total concentrations of acetic acid in the nonaqueous and aqueous phase respectively. The parameters $\overline{K}$, b, and n in Equation (4) are best determined by the method of least squares with the use of all the values of x and y given in the Table. Since the use of the method of least squares in the case of the three parameters in Equation (4) is very cumbersome, we do not use it, since satisfactory results are obtained in this instance by the method of three selected points. We take the following three points from the data in the Table:

$$\begin{aligned} x_1 &= 1.25, \quad y_1 = 2.40, \\ x_3 &= 29.80, \quad y_3 = 30.1, \\ x_2 &= 7.60, \quad y_2 = 10.70. \end{aligned} \tag{7}$$

From Equation (4)

$$x_1 = \bar{K}y_1 + by_1'',$$
$$x_2 = \bar{K}y_2 + by_2'', \qquad (8)$$
$$x_3 = \bar{K}y_3 + by_3''.$$

From the System (8)

$$K = \frac{x_1y_2'' - x_2y_1''}{y_1y_2'' - y_2y_1''}, \qquad (9)$$

$$b = \frac{x_2y_1 - x_1y_2}{y_1y_2'' - y_2y_1''}. \qquad (10)$$

$$(x_2y_1 - x_1y_2)\,y_3'' + (x_1y_3 - y_1x_3)\,y_2'' + (x_3y_2 - y_3x_2)\,y_1'' = 0. \qquad (11)$$

Water layer (% by weight)			Ether layer (% by weight)		
acetic acid, y	ether	water	acetic acid, x	ether	water
0.84	6.66	92.50	0.40	98.36	1.24
2.40	7.30	90.30	1.25	97.23	1.52
3.55	7.15	89.30	1.95	96.30	1.75
5.52	8.05	86.43	3.30	94.45	2.25
8.00	9.03	82.97	5.20	92.05	2.75
10.70	9.55	79.75	7.60	88.70	3.70
13.33	10.15	76.52	10.00	85.30	4.70
22.22	12.10	65.68	20.00	69.60	10.40
26.32	18.50	55.18	25.00	59.60	15.40
30.1	25.10	44.80	29.80	44.40	25.80
30.35	37.95	31.70	30.35	37.95	31.70

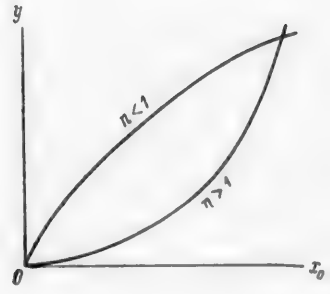

Plot of the law for the distribution of the total concentrations of a solute between a nonaqueous and an aqueous phase. Explanations in text.

After substitution of the coordinates (7) of the three chosen points, Equation (11) takes the form

$$0.973c_2'' - 6.779c_1'' + 18.02 = 0, \qquad (12)$$

where:

$$c_2 = \frac{y_3}{y_1} = \frac{301}{24}, \quad c_1 = \frac{y_2}{y_1} = \frac{107}{24}; \qquad (13)$$

$$n \approx 1.614. \qquad (14)$$

Equation (12) has two positive roots (the proof is not given here), of which one is unity, and does satisfy the condition (2); the second is found by the method of "chords and tangents."

From Equations (9) and (10)

$$\bar{K} \approx 0.39485, \qquad (15)$$
$$b \approx 0.07360. \qquad (16)$$

For the system acetic acid – diethyl ether – water, Equation (4) has the form

$$x_0 = 0.39485\, y + 0.07360\, y^{1.614}, \tag{17}$$

where y is in the range

$$0 \leq y \leq 30.35. \tag{18}$$

Let the variable y have the values given in the Table; we then calculate the corresponding values of x_0 from Equation (17) and compare them with the experimental values of x in the Table. The calculation results are given below.

y	x	x_0	Absolute value of the relative error of x_0 (in %)
0.84	0.40	0.39	2.6
2.40	1.25	1.25	0
3.55	1.95	1.97	1.0
5.52	3.30	3.34	1.2
8.00	5.20	5.27	1.3
10.70	7.60	7.60	0
13.33	10.00	10.08	0.8
22.32	20.00	19.75	1.3
26.32	25.0	24.82	0.7
30.1	29.80	29.80	0
30.35	30.35	30.14	0.7

These results show that Equation (17) conforms quite satisfactorily to the experimental data over the whole range of acetic acid concentrations in the aqueous phase.

Investigations of the distribution of propionic acid between toluene and water showed that the distribution law (4), in the form of the equation

$$x_0 = 0.147y + 0.334y^{1.90}, \tag{19}$$

is obeyed to a satisfactory degree of accuracy for variations of the propionic acid concentration in the range

$$0 \leq y \leq 1.67.$$

The experimental data (x) and the values calculated from the equation (x_0) are compared below.

y	x	x_0	y	x	x_0
0.25	0.05	0.06	1.06	0.54	0.53
0.39	0.11	0.11	1.27	0.73	0.72
0.53	0.17	0.17	1.47	0.93	0.93
0.66	0.24	0.24	1.67	1.13	1.17
0.84	0.36	0.36			

On further increase of the propionic acid concentration in the two phases, Equation (19) begins to show deviations from the experimental data.

Similar investigations of the system ethyl alcohol – water – diethyl ether showed that the experimental results cannot be represented in the form of Equation (4), either over the entire range of ethyl alcohol concentrations in the aqueous phase

$$0 \leq y \leq 28.4,$$

or over narrower ranges.

LITERATURE CITED

[1] W. Nernst, Z. phys. Ch. 13, 531 (1894).

[2] N. A. Shilov and L. K. Lepin', Vesta. Lomonos Fiz. Khim Obshch. 1-2 (1930).

Received July 20, 1956

A NEW METHOD FOR THE ISOLATION OF LEVOPIMARIC ACID FROM MIXTURES OF RESIN ACIDS

I. I. Bardyshev, Kh. A. Cherches, and L. I. Ukhova

Levopimaric acid has usually been isolated from mixtures of resin acid by fractional crystallization of aqueous solutions of the sodium salts [1].

Later [2] this method was improved somewhat,, and made more rapid. A more convenient and efficient method for the isolation of levopimaric acid was proposed by Harris [3]. The method consisted of the recrystallization of the butanolamine salt of levopimaric acid from acetone, followed by decomposition of the salt by means of boric acid.

Our proposed new method for the isolation of levopimaric acid from mixtures of resin acids consists of the crystallization of bornylamine salts from alcohol [4]. Either pure bornylamine or its mixtures with neobornylamine can be used for the purpose; the salts can be conveniently prepared by the mixing of ether solutions of the amines with mixtures of the resin acids (a filtered ether solution of the resin can be used).

The precipitated salts were washed on the filter with large amounts of ether. The residue remaining on the filter consisted mainly of the bornylamine salt of levopimaric acid. This salt was decomposed by boric acid or 1% aqueous acetic acid solution. After 2-3 recrystallizations of the free acid from alcohol, a sample of levopimaric acid was obtained with a higher degree of purity than the samples reported in the literature [5-8].

The proposed method was tested for the isolation of levopimaric acid from samples of resins from the conifers Pinus silvestris, Picea excelsa Lk, Pinus Pallasiana Lamb, and gave good results.

TABLE 1

Data on the Isolation of Levopimaric Acid by the 1st Method

Substances	Weight (g)	Melting point (°C)	$[\alpha]_D$ (in alcohol)
Mixture of resin acids	140	118—130	— 99
Amine salts of mixed acids	80	179—182	—158
Acid after crystallizations:			
First	43	138—148	—268
Second	23	151.5—152	—287
Third	—	151.5—152	—288
Fourth	—	151.5—152	—288

EXPERIMENTAL

The resin acids, isolated from the resin by the usual method [1] (the resin itself, dissolved in ether and free from dirt, may be used) were dissolved in ether and neutralized with an ether solution of bornylamine or a mixture of bornylamine and neobornylamine in 1 : 1 molar ratio (confirmed by a drop test with phenolph-

thalein). The mixture was stirred vigorously. After some time (sometimes immediately) the amine salts were precipitated. The solution became somewhat warm in the process. The salts were washed on the filter with a large amount of ether. Further purification of the crystals can be effected by either of two methods.

TABLE 2

Data on the Isolation of Levopimaric Acid by the Second Method

Substances	Weight (g)	Melting point (°C)	$[\alpha]_D^{20}$ (in alcohol)
Mixture of resin acids from Picea	140	118—130	—
Amine salts of mixed acids	100	159—160	— 84
Amine salts after crystallizations:			
First	25	175—178	—159
Second	16	181—183	—167
Third	4.2	186—187	—179
Acid from salt of the 3rd crystallization, after single crystallization from alcohol	—	147—148	—272
Amine salt obtained from 200 g of Pinus silvestris resin	150	—	—
Amine salts after crystallizations:			
First	22	168—174	—152
Second	—	174—179	—172
Third	—	179—183	—178
Fourth	2.6	182—185	—179
Acid from salt of the 4th crystallization, after single recrystallization from alcohol		147—148	—267

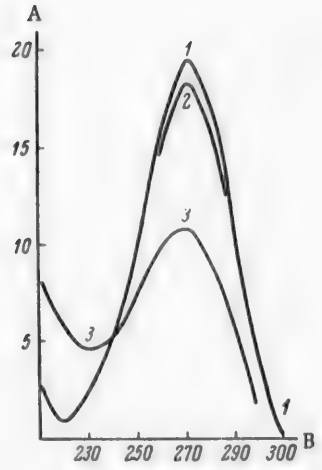

Absorption coefficient α as a function of the wave length for different samples of levopimaric acid. A) Absorption coefficient α, B) wave length (mμ). Samples isolated: 1) by the first method, 2) by the second method, 3) by the second method (the original bornylamine salt was obtained directly from the resin). Salts of bornylamine and levopimaric acid obtained after the 4th crystallization.

1st Method. The finely powdered salt was suspended in ether and decomposed by an excess of an aqueous suspension of boric acid or 1% aqueous acetic acid solution. The ether solution of the resin acids was washed with water, the ether was driven off, and the acids were recrystallized from alcohol. Data on the isolation of levopimaric acid from the resin of Picea are presented in Table 1. The diagram shows curves for the absorption coefficients α in the ultraviolet region of the spectrum, for different samples of levopimaric acid.

2nd Method. Relatively pure samples of levopimaric acid can be prepared by repeated crystallization, from alcohol, of the salts of resin acids and bornylamine or salts of resin acids with a mixture of bornyl- and neobornylamines, followed by treatment by the 1st method. It must be pointed out, however, that the yield of pure levopimaric acid obtained in this way is a little more than 1/10 of the yield obtained by the first method (Table 2).

It is clear from the data in Tables 1 and 2 and the diagram that the sample of levopimaric acid obtained by the first method was purer than the samples obtained by the second method or described in the literature [3]. The pure sample of levopimaric acid shows almost no absorption in the 218 mμ region of the spectrum. It

is interesting to note that if the resin acids are neutralized by a mixture of two diastereoisomeric amines – bornylamine and neobornylamine – then the levopimaric acid forms a salt with bornylamine, and abietic acid, with neobornylamine [9-10]. These salts may be isolated pure by consecutive crystallizations from alcohol. Therefore our proposed methods for the isolation of levopimaric and abietic acid can also serve as methods for separation of mixtures of amines of similar structure in the terpene series.

SUMMARY

A new method for the isolation of levopimaric acid from its mixtures with other resin acids has been developed. The levopimaric acid prepared by this method has melting point 151.5-152° $[\alpha]_D^{20}$ – 288° (in alcohol), absorption coefficient α at 272-273 mμ – 19.6, and at 218 mμ – 0.8.

LITERATURE CITED

[1] V. N. Krestinskii, S. S. Malevskaia, N. F. Komshilov and E. V. Kazeeva, Zhur. Prik. Khim. 12, 1839 (1939).

[2] S. Palkin and T. H. Harris, J. Am. Chem. Soc. 55, 3677 (1933).

[3] G. C. Harris and T. S. Sanderson, J. Am. Chem. Soc. 70, 334 (1948).

[4] V. N. Krestinskii and I. I. Bardyshev, Zhur. Obshchei Khim. 10, 1894 (1940).

[5] L. Fieser and M. Fieser, Natural Products Related to Phenanthrene (Russian translation) (Moscow–Leningrad, Goskhimizdat, 1953).

[6] J. Simonsen, The Terpenes (Cambridge, 1952).

[7] S. S. Malevskaia, Primary Resin Acids from the Resin of Pinus silvestris (in Russian) (Main Administration of Educational Institutions, People's Commissariat of the Forest Industry USSR, Leningrad, 1941).

[8] N. F. Komshilov, Composition of Rosin and the Structure of the Resin Acids of Spruce and Pine (in Russian) (Izd. AN SSSR, 1955).

[9] I. I. Bardyshev and L. I. Ukhova, Proc. Acad. Sci. USSR 109, 1, 86 (1956).*

[10] I. I. Bardyshev and Kh. A. Cherches, J. Appl. Chem. 29, 1888 (1956).*

Received February 16, 1957

*Original Russian pagination. See C. B. Translation.

SOME COMMENTS ON THE PAPER BY V. N. KRYLOV AND A. S. POLUBELOVA: "THE DEHYDRATION OF BAUXITES OF DIFFERENT ORIGINS" (J. APPL. CHEM. 29, No. 5, 698-704, 1956)*

S. I. Beneslavskii and L. A. Pashkevich

We cannot agree with the authors' view that variations of the mineralogical composition of bauxites during heat treatment are inadequately considered in the literature. Numerous papers by Soviet and foreign investigators deal with this question. There are even more papers describing the primary mineralogical composition of bauxites, including those studied by the authors cited.

The absence of references to at least the most important papers (by Academicians A. D. Arkhangel'skii and D. S. Beliankin, and the geologists S. F. Mallavkin, A. K. Gladkovskii, and S. G. Vishniakov) suggests that these papers were unknown to the authors.

V. N. Krylov and A. S. Polubelova, without finding out what had been done before them in the study of Urals and Tikhvin bauxites, attempted to determine the mineral form of the alumina in them from the results obtained by thermal analysis and hygroscopicity studies only, ignoring such convincing and widely used methods as optical crystallography and x-ray analysis.

As a result, they reached entirely erroneous conclusions, which contradict the results of earlier investigations and industrial experience, especially that of the Tikhvin and Urals aluminum plants.

For example, they state that Tikhvin bauxites belong to the gibbsite–diaspore type, whereas it is well known to geologists studying the composition of Tikhvin bauxites, and to workers in plants converting these bauxites into alumina, that Tikhvin bauxites belong to the gibbsite–boehmite type. The causes of these errors lie in incorrect experimental procedure.

The authors determined the mineralogical form of alumina from the results of studies of the hygroscopicity of bauxites ignited at various temperatures. It is difficult to understand why they chose such a lengthy, laborious, and unconvincing method. At times they were themselves incapable of using their own method correctly. Thus, on p. 702 (Tp. 762) they state that the maximum hygroscopicity is found in bauxites heated at 300-400°. However, Fig. 2 (IV) shows that the bauxite heated at 300° has the minimum hygroscopicity. The maximum is found for samples heated at 600°.

It is also puzzling why, in the case of Tikhvin bauxites containing gibbsite, the authors used their method for determination of the form of alumina by the presence of the γ form of Al_2O_3, when the latter is formed from gibbsite, which on heating is converted first into boehmite and then into γ-Al_2O_3.

It is stated in the text on p. 701. (T.p. 761) that a dehydration temperature of 600° produces the maximum hygroscopicity, but Fig. 2 (I) to which the authors refer does not show this; the maximum corresponds to a dehydration temperature of 750°.

It is quite incomprehensible why the authors express hygroscopicity as a percentage of the weight loss when the original bauxite is heated, thereby comparing water of crystallization and hygroscopic water, which differ in the manner of their binding.

*Original Russian pagination. See C. B. Translation.

The arrangement of the bauxites in order of their desiccating properties is also incomprehensible. The sequence given by the authors is: South Urals, North Urals, Hungarian, and Tikhvin; in reality, this sequence should be completely reversed.

The hygroscopicity experiments are dubious, because the points on the graphs (Fig. 2) are really incomplete, since they were determined not for constant weight increases, but after different arbitrary times of exposure, not comparable for different bauxites.

Krylov and Polubelova's assertion concerning the boehmite composition of the Urals bauxites is also wrong; during a period of over 10 years of study of Urals bauxites we never found monoboehmitic bauxites, and did not find any reports to that effect in the literature or manuscripts. It is known that the principal industrial varieties of North Urals bauxites consist mainly of diaspore, while boehmite is present in them only as an impurity. The authors should have stated the locality from which their bauxites were taken, as there are dozens of such localities in the Urals.

The experimental procedure itself is very dubious. For example, in the dehydration experiments the bauxite was heated in large lumps 20-40 mm in size in muffle furnace for 1 hour. It is known, however, that the system hydrate–water reaches equilibrium very slowly, and when dehydration curves are recorded finely divided specimens must be held at each temperature to constant weight. In our opinion it was because of the incorrect experimental procedure that the dehydration temperatures of bauxites determined by these experiments were higher than those given by the heating curves, when in reality the reverse should be the case.

The conclusions concerning the influence of grain size on the dehydration temperature are unconvincing, as they were reached by comparison of dehydration temperatures determined under different conditions – from heating curves and from dehydration experiments. Such comparisons are inadmissible, because in the former case the water is lost in dynamic and in the second case in static conditions. The temperature halts on the heating curves always lag behind those on the dehydration curves, the difference reaching 100° and over.

In conclusion it must be pointed out that the authors did not achieve their intended aim – to shed light on the nature of the bonds between water molecules and alumina in bauxites, and to clarify a number of questions related to their dehydration. Their suggestions are not confirmed by experimental data, and in some cases reduce to facts which have long been known. We therefore considered it appropriate to dispel the incorrect ideas on the composition of bauxites which are conveyed by this article by V. N. Krylov and A. S. Polubelova.

ORGANIZING COMMITTEE OF THE VIIIth MENDELEEV CONGRESS ON GENERAL AND APPLIED CHEMISTRY

ANNOUNCEMENT

The Organizing Committee of the VIIIth Mendeleev Congress informs all chemists of the Soviet Union that the VIIIth Mendeleev Congress on general and applied chemistry will be held December 8-13, 1958 in Moscow.

In addition to the plenary sessions, at which communications on the principal problems of modern chemistry will be presented, scientific communications will be presented and discussed in the following sections: 1) inorganic chemistry and technology (including the rare elements), 2) organic chemistry and technology, 3) analytical chemistry, 4) physical chemistry, 5) colloid chemistry, 6) polymer chemistry and technology, 7) chemistry of natural compounds and biochemistry, 8) agronomic chemistry, 9) chemistry and chemical technology of fuel, 10) chemistry and technology of food products, 11) chemistry and technology of silicates, 12) radiochemistry and isotope chemistry, 13) theoretical and applied electrochemistry, 14) chemistry of metals and alloys, 15) economics, planning, and organization of chemical industries, 16) the main processes and equipment of chemical technology, and 17) history of chemistry and chemical technology.

In addition, there will be a symposium on higher chemical education. The Congress will be attended by delegates elected by the branches of the D. I. Mendeleev All-Union Chemical Society, and invited personally by the Organizing Committee.

Other persons, including young specialists and students, may take part in the work of the Congress as guests.

The personal expenses of delegates arriving from other towns must be paid by the institution or undertaking at which the given delegate is employed, or by the D. I. Mendeleev All-Union Chemical Society.

Each particpant may present one paper at the meetings of his section.

Papers at the sections may be of two kinds:

a) Papers containing details of new unpublished investigations of theoretical or experimental nature. In distinction from scientific communications presented at conferences and congresses on individual problems, these papers must be of more general significanee for science and practice. The time limit for such communications is 15 minutes.

b) Brief communications, principally for young chemists, which deal only with new facts, new observations, or theoretical concepts; the time for such communications must not exceed 5 minutes.

Those wishing to present a paper or a brief communication at a meeting of a section of the Congress must inform the Organizing Committee and send a signed summary and also the prescribed form of questionnaire not later than April 15, 1958.

The summary must be typed on one side of the paper, in 2 copies, and the text must not exceed 3 typed pages, with double spacing, including spaces for tables and diagrams. Texts requiring the preparation of complex blocks should be avoided.

The summary of the paper must be approved by a teaching or scientific institution, industrial undertaking, or a Branch of the D. I. Mendeleev All-Union Chemical Society. The application sent to the Organizing Committee must have the signature of the manager of the institution or undertaking. Summaries of the papers and communications accepted by the Organizing Committee will be available in printed form at the Congress.

Correspondence concerning the Congress must be addressed as follows: Moscow V-71, Leninskii Prospect, 14, Division of Chemical Sciences Academy of Sciences USSR, Chief Scientific Secretary of the Organizing Committee of the VIIIth Mendeleev Congress Prof. V. V. Kozlov.

The Organizing Committee, VIIIth Mendeleev Congress

QUESTIONNAIRE

for a delegate to the VIIIth Mendeleev Congress
on General and Applied Chemistry in Moscow.

1. Surname, first name and patronymic. 2. Year of birth. 3. Scientific degree and title. 4. Speciality. 5. Where employed. 6. Section which it is proposed to attend.

Home address and telephone number

Signature.

SIGNIFICANCE OF ABBREVIATIONS MOST FREQUENTLY ENCOUNTERED IN SOVIET PERIODICALS

FIAN	Phys. Inst. Acad. Sci. USSR.
GDI	Water Power Inst.
GITI	State Sci.-Tech. Press
GITTL	State Tech. and Theor. Lit. Press
GONTI	State United Sci.-Tech. Press
Gosenergoizdat	State Power Press
Goskhimizdat	State Chem. Press
GOST	All-Union State Standard
GTTI	State Tech. and Theor. Lit. Press
IL	Foreign Lit. Press
ISN (Izd. Sov. Nauk)	Soviet Science Press
Izd. AN SSSR	Acad. Sci. USSR Press
Izd. MGU	Moscow State Univ. Press
LEIIZhT	Leningrad Power Inst. of Railroad Engineering
LET	Leningrad Elec. Engr. School
LETI	Leningrad Electrotechnical Inst.
LETIIZhT	Leningrad Electrical Engineering Research Inst. of Railroad Engr.
Mashgiz	State Sci.-Tech. Press for Machine Construction Lit.
MEP	Ministry of Electrical Industry
MES	Ministry of Electrical Power Plants
MESEP	Ministry of Electrical Power Plants and the Electrical Industry
MGU	Moscow State Univ.
MKhTI	Moscow Inst. Chem. Tech.
MOPI	Moscow Regional Pedagogical Inst.
MSP	Ministry of Industrial Construction
NII ZVUKSZAPIOI	Scientific Research Inst. of Sound Recording
NIKFI	Sci. Inst. of Modern Motion Picture Photography
ONTI	United Sci.-Tech. Press
OTI	Division of Technical Information
OTN	Div. Tech. Sci.
Stroiizdat	Construction Press
TOE	Association of Power Engineers
TsKTI	Central Research Inst. for Boilers and Turbines
TsNIEL	Central Scientific Research Elec. Engr. Lab.
TsNIEL-MES	Central Scientific Research Elec. Engr. Lab.–Ministry of Electric Power Plants
TsVTI	Central Office of Economic Information
UF	Ural Branch
VIESKh	All-Union Inst. of Rural Elec. Power Stations
VNIIM	All-Union Scientific Research Inst. of Meteorology
VNIIZhDT	All-Union Scientific Research Inst. of Railroad Engineering
VTI	All-Union Thermotech. Inst.
VZEI	All-Union Power Correspondence Inst.

Note: Abbreviations not on this list and not explained in the translation have been transliterated, no further information about their significance being available to us. – Publisher.

DENDRITIC CRYSTALLIZATION

by **D. D. SARATOVKIN**

2nd Edition,
Revised and Enlarged

Translated from Russian

THIS SIGNIFICANT volume has been extensively revised by the author from the 1953 edition; in particular with *fresh material derived from observations under the stereoscopic microscope.*

The first section deals briefly with some general concepts on crystallization, drawing an important distinction between *genetic* and *structural* types of crystals, including some aspects of the *defect crystal state.* The second section covers at length the illuminating ideas and observations of the 19th-century Russian metallurgist D. K. Chernov, who proposed many of the basic ideas of dendritic crystallization. The third section is an extended survey of current views on dendritic crystallization, in which the ideas of many Soviet and other scientists are briefly summarized and criticized. Section four presents the growth forms of real crystals; all types are reviewed, but only dendritic or closely related forms are selected for subsequent investigation.

Following sections discuss the causes and forms of crystal growth, with *detailed applications* to certain substances that have been extensively studied *(particularly the ammonium halides)*, and to eutectics in metal and organic systems; an extensively revised presentation on steel castings which provides a lucid explanation of how the various structures found in real castings can be fitted into the author's theory of dendritic crystallization. Nearly all the concepts developed earlier in the book are utilized in this final section.

The main bulk of the volume contains many *original* and *unpublished* ideas and observations, and is an excellent example of the modern macroscopic approach to the crystalline state by an experienced worker concerned with the infinite variety of real crystals—all of which is enhanced by a *profusion of explanatory line diagrams and sets of stereoscopic photographs.*

CB translations are by bilingual scientists, and include all photographic, diagrammatic and tabular material integral with the text.

CONTENTS

Cloth-bound; 126 pp., illustrated; $6.00

CONSULTANTS BUREAU, INC.

227 WEST 17TH STREET, NEW YORK 11, N. Y

BULLETIN OF THE ACADEMY OF SCIENCES OF THE USSR

(Division of Chemical Science)

in complete English translation

Contains outstanding work by the leading members of the Academy of Sciences, making it one of the most significant journals. A broad survey of Soviet chemical research, covering the general and inorganic, as well as the organic and biological fields.

SAMPLE PAPERS: Isomerizations of cycloalkanes; preparation and properties of N-oxides of nicotine; synthesis and polymerization of methyl p-vinylbenzoate; transarylation of diphenylmethane; peculiar features of the oxidation of cellulose with sodium periodate and with sodium chlorite; copolycondensation in the systems 1,2-dichloroethane-benzene-fluorobenzene and 1,2-dichloroethane-chlorobenzene-fluorobenzene.

Annual subscription, 12 issues, approx. 1500 pp: $45.00 in the U.S. and Canada; $50.00 elsewhere. (Special price for libraries of non-profit academic institutions: $15.00 in the U.S. and Canada; $20.00 elsewhere.

CONSULTANTS BUREAU, INC.
227 W. 17th St., NEW YORK 11, N.Y.